MODELING AND EXPERIMENTAL EVALUATION OF VARIABLE SPEED PUMP AND VALVE CONTROLLED HYDRAULIC SERVO DRIVES

A THESIS SUBMITTED TO
THE GRADUATE SCHOOL OF NATURAL AND APPLIED SCIENCES
OF
MIDDLE EAST TECHNICAL UNIVERSITY

BY

HAKAN ÇALIŞKAN

IN PARTIAL FULFILLMENT OF THE REQUIREMENTS
FOR
THE DEGREE OF MASTER OF SCIENCE
IN
MECHANICAL ENGINEERING

SEPTEMBER 2009

Approval of the thesis:

MODELING AND EXPERIMENTAL EVALUATION OF VARIABLE SPEED PUMP AND VALVE CONTROLLED HYDRAULIC SERVO DRIVES

submitted by **HAKAN ÇALIŞKAN** in partial fulfillment of the requirements for the degree of **Master of Science in Mechanical Engineering Department, Middle East Technical University** by,

Prof. Dr. Canan Özgen ________________
Dean, Graduate School of **Natural and Applied Sciences**

Prof. Dr. Suha Oral ________________
Head of Department, **Mechanical Engineering**

Prof. Dr. Tuna Balkan ________________
Supervisor, **Mechanical Engineering Dept., METU**

Prof. Dr. Bülent E. Platin ________________
Co-Supervisor, **Mechanical Engineering Dept., METU**

Examining Committee Members:

Prof. Dr. Metin Akkök ________________
Mechanical Engineering Dept., METU

Prof. Dr. Tuna Balkan ________________
Mechanical Engineering Dept., METU

Prof. Dr. Bülent E. Platin ________________
Mechanical Engineering Dept., METU

Asst. Prof. Dr. Yiğit Yazıcıoğlu ________________
Mechanical Engineering Dept., METU

Prof. Dr. Yücel Ercan ________________
Mechanical Engineering Dept., TOBB ETU

Date: 11.09.2009

I hereby declare that all information in this document has been obtained and presented in accordance with academic rules and ethical conduct. I also declare that, as required by these rules and conduct, I have fully cited and referenced all material and results that are not original to this work.

Name, Last name : Hakan ÇALIŞKAN

Signature :

ABSTRACT

MODELING AND EXPERIMENTAL EVALUATION OF
VARIABLE SPEED PUMP AND VALVE CONTROLLED HYDRAULIC
SERVO DRIVES

Çalışkan, Hakan
M.S., Department of Mechanical Engineering
Supervisor: Prof. Dr. Tuna Balkan
Co-Supervisor: Prof. Dr. Bülent E. Platin

September 2009, 209 pages

In this thesis study, a valveless hydraulic servo system controlled by two pumps is investigated and its performance characteristics are compared with a conventional valve controlled system both experimentally and analytically. The two control techniques are applied on the position control of a single rod linear actuator. In the valve controlled system, the flow rate through the actuator is regulated with a servovalve; whereas in the pump controlled system, two variable speed pumps driven by servomotors regulate the flow rate according to the needs of the system, thus eliminating the valve losses.

To understand the dynamic behaviors of two systems, the order of the differential equations defining the system dynamics of the both systems are reduced by using the fact that the dynamic pressure changes in the hydraulic cylinder chambers become linearly dependent on leakage coefficients and cylinder chamber volumes above and below some prescribed cut off frequencies. Thus the open loop speed response of the pump controlled and valve controlled systems are defined by second order transfer functions. The two systems are modeled in MATLAB Simulink environment and the assumptions are validated.

For the position control of the single rod hydraulic actuator, a linear state feedback control scheme is applied. Its state feedback gains are determined by using the linear and linearized reduced order dynamic system equations. A linear Kalman filter for pump controlled system and an unscented Kalman filter for valve controlled system are designed for estimation and filtering purposes.

The dynamic performances of both systems are investigated on an experimental test set up developed by conducting open loop and closed loop frequency response and step response tests. MATLAB Real Time Windows Target (RTWT) module is used in the tests for application purposes.

Keywords: Fluid Power Control, Variable Speed Pump Control, Energy Efficient, Valve Control, State Feedback, Kalman Filtering, Unscented Kalman Filter.

ÖZ

DEĞİŞKEN DEVİRLİ POMPA VE VALF DENETİMLİ SERVO HİDROLİK SİSTEMLERİN MODELLENMESİ VE DENEYSEL DEĞERLENDİRİLMESİ

Çalışkan, Hakan
Yüksek Lisans, Makina Mühendisliği Bölümü
Tez yöneticisi: Prof. Dr. Tuna Balkan
Yardımcı tez yöneticisi: Prof. Dr. Bülent E. Platin

Eylül 2009, 209 sayfa

Bu tez çalışması kapsamında iki pompa denetimli valfsiz bir hidrolik sistem incelenmiş ve geleneksel valf denetimli hidrolik sistem ile deneysel ve analitik olarak karşılaştırılmıştır. Bu iki kontrol tekniği tek milli bir hidrolik eyleyicinin konum denetiminde uygulanmıştır. Tez kapsamında kurulan valf denetimli sistemde eyleyiciye giden debi bir servo valf ile ayarlanırken, pompa denetimli sistemde sistemin gerek duyduğu debi pompa hızı değiştirilerek ayarlanmakta böylelikle valf kayıpları elenmektedir.

Sistemlerin dinamik davranışlarını anlamak için her iki sistemi tanımlayan türevsel denklemlerin mertebesi eyleyici oda basınçlarının belirli kesim frekanslarından önce ve sonra sızıntı katsayıları ve silindir oda hacimleriyle doğru orantılı olarak değiştiği gösterilerek azaltılmıştır. Böylelikle iki sistemin açık döngü hız tepkileri ikinci mertebeden bir aktarım fonksiyonu ile ifade edilebilmiştir. Her iki sistem MATLAB Simulink ortamında modellenerek yapılan varsayımlar doğrulanmıştır.

Tek milli hidrolik eyleyicinin konum denetimi için doğrusal durum geri beslemesi uygulanmıştır. Durum geri beslemesi katsayıları mertebesi düşürülmüş doğrusal ve doğrusallaştırılmış dinamik sistem denklemleri kullanılarak hesaplanmıştır. Durum tahmini ve filtreleme amacı ile pompa denetimli sistemde doğrusal Kalman filtre ve valf denetimli sistemde doğrusal olmayan Kalman filtre uygulanmıştır.

Her iki sistemin dinamik performansı tez kapsamında kurulan test düzeneğinde açık döngü ve kapalı döngü frekans tepkisi ve basamak girdi testleri yapılarak incelenmiştir. Testlerde denetim uygulamasında MATLAB yazılımının Real Time Windows Target (RTWT) modülü kullanılmıştır.

Anahtar kelimeler: Akışkan Gücü Kontrolü, Değişken Devirli Pomp Denetimi, Valf Denetimi, Enerji Verimliliği, Durum Geri Beslemesi, Kalman Filtre, Doğrusal Olmayan Kalman Filtre

To my country…

ACKNOWLEDGEMENTS

I would, first of all, like to thank to Prof. Dr. Tuna Balkan and Prof. Dr. Bülent E. Platin for their guidance, suggestion and support throughout the thesis study.

I would specially like to thank to Suat Demirer for his financial and technical support and suggestions, also I would like to thanks to all the employees of Demirer Teknolojik Sistemler Inc. for their support and friendship during the production of the test set up.

I would like to thank to my colleagues for their useful discussions, support and friendship.

I would, sincerely, like to thank to my family for their patience support and love.

TABLE OF CONTENTS

ABSTRACT iv

ÖZ vi

ACKNOWLEDGEMENTS ix

TABLE OF CONTENTS x

LIST OF FIGURES xiviv

LIST OF TABLES xx

LIST OF SYMBOLS xxii

CHAPTERS

1. INTRODUCTION 1

1.1 Background and motivations 1

1.2 Literature Survey 4

1.3 Objective of the Thesis 9

1.4 Thesis Outline 10

2 HYDRAULIC POWER SYSTEMS 12

2.1 Conventional Valve Controlled Hydraulic Power Systems 12

2.2 Energy Efficient Hydraulic Power Systems 22

2.2.1 Energy Efficiency in Valve Controlled Circuits 22

2.2.2 Variable Displacement Pump Controlled Systems 26

2.2.3 Variable Speed Pump Controlled Systems 30

3. SYSTEM MODELING AND SET UP CONFIGURATION 35

3.1 Experimental Test Set-up 35
3.2 Pump Controlled System 44
3.2.1 Principle of the Hydraulic Circuit 44
3.2.2 Mathematical Modeling of the System 46
3.2.2.1 Pump Model 47
3.2.2.2 Hydraulic Actuator Model 54
3.2.2.3 Load Model 57
3.2.3 Steady State Characteristics of the System 58
3.2.4 Dynamic Characteristics of the System 61
3.3 Valve Controlled System 71
3.3.1 Mathematical Modeling of the System 71
3.3.1.1 Valve Model 72
3.3.2 Steady State Characteristics of the System 74
3.3.3 Linearized Valve Coefficients 76
3.3.3.1 Extension Case 77
3.3.3.2 Retraction Case 79
3.3.4 Dynamic Characteristics of the System 81
4. CONTROLLER DESIGN AND IMPLEMENTATION 91
4.1 State Space Representation of Pump Controlled System 91
4.1.1 4^{th} Order State Space Representation of Pump Controlled System 92
4.1.2 Reduced 3^{th} Order State Space Representation of Pump Controlled System 94
4.2 State Space Representation of Valve Controlled System 95
4.2.1 4^{th} Order State Space Representation of the Valve Controlled System 96

4.2.2 Reduced 3rd order state space representation of valve controlled system 97

4.3 Controller Design for the Pump System 98

4.4 Controller Design for the Valve System 105

4.5 Kalman Filter Theory and Design 111

4.5.1 Discrete Kalman Filter 112

4.5.2 Application in Pump Controlled System 117

4.5.3 Unscented Kalman Filter 118

4.5.4 Application in Valve Controlled System 123

4.5.5 Filter Tuning 124

4.5.5.1 Pump Controlled System 126

4.5.5.2 Valve Controlled System 132

5. PERFORMANCE TESTS OF THE SYSTEM 133

5.1 System Identification 135

5.1.1 Hydraulic Pump Leakage Coefficients 135

5.1.2 Hydraulic Cylinder Friction 139

5.2 Step Response of Pump Controlled System 144

5.3 Step Response of Valve Controlled System 147

5.4 Frequency Response Test 152

5.4.1 Test Signal 153

5.4.2 Open Loop Frequency Response of Pump Controlled Hydraulic System 153

5.4.3 Close Loop Frequency Response of Pump Controlled Hydraulic System 156

5.4.4 Open Loop Frequency Response of Valve Controlled Hydraulic System 165

5.4.5 Closed Loop Frequency Response of Valve Controlled Hydraulic System 167
5.5 Comparison of Two Systems 174
6. DISCUSSIONS, CONCLUSIONS AND RECOMMENDATIONS 179
6.1 Outline of the Study and Discussions 179
6.2 Conclusions 182
6.3 Recommendations for Future Work 184
REFERENCES 187
APPENDICES
A. TRANSFER FUNCTION DERIVATION FOR PUMP CONTROLLED SYSTEM 191
B. TRANSFER FUNCTION DERIVATION FOR VALVE CONTROLLED SYSTEM 197
C. MATLAB FILES 202
D. DRIVERS AND DAQ CARD CONNECTIONS 207

LIST OF FIGURES

FIGURES

Figure 1-1 The Circuit Operation and Sum Pressure Principle [19]........ 8

Figure 2-1 Conventional Valve Controlled Hydraulic Circuit.............. 13

Figure 2-2 Constant Pressure Valve Controlled Hydraulic Circuit 15

Figure 2-3 Valve Characteristic Curves for Different Valve Openings. 17

Figure 2-4 Valve Losses of a Constant Pressure Valve Controlled Circuit for Maximum Energy Efficiency 18

Figure 2-5 Pressure Compensated Pump [23]...................................... 23

Figure 2-6 Load Sensing Pump Schematic [23] 24

Figure 2-7 Electro-Hydraulic Load Sensing System with Constant Displacement Pump [8].. 24

Figure 2-8 Individual Meter In Meter Out Valve Control System [24]. 25

Figure 2-9 Variable Displacement Pumps 26

Figure 2-10 Hydrostatic Transmission System with Variable Displacement Pump Control Technique 27

Figure 2-11 Single Rod Symmetric Linear Actuator [25] 28

Figure 2-12 Displacement Controlled Drive with Single Rod Cylinder in Position Control [7].. 29

Figure 2-13 Constant Displacement Pump Types a) Screw Type, b) External Gear, c) Internal Gear 30

Figure 2-14 Electro Hydraulic Actuation System of Habibi and Goldenberg with Symmetric Actuator [3]........................... 31

Figure 2-15 Two Pump Control Circuit Configurations.......................... 32

Figure 3-1 A photograph of the Experimental Test Set-Up.................. 36

Figure 3-2 Schematic Diagram of the Experimental Test Set-Up 37

Figure 3-3 Servovalve Frequency Response Diagram [27].................. 41

Figure 3-4 Flow Rate versus Valve Spool Position Signal of the Servo Solenoid Valve [27] 42

Figure 3-5 Variable Speed Pump Control Circuit................................ 45

Figure 3-6 Hydraulic Pump Operation in 4 Quadrants......................... 48

Figure 3-7 Representation of Flow Losses in Hydraulic Pumps and Motors [28]... 50

Figure 3-8 Flow Rates of the Hydraulic Cylinder and Pumps.............. 53

Figure 3-9 MATLAB Simulink Model of the Hydraulic Pump/Motor Unit... 54

Figure 3-10 MATLAB Simulink Model of the Hydraulic Actuator........ 56

Figure 3-11 MATLAB Simulink Model of the Hydraulic Cylinder Chamber Volumes.. 57

Figure 3-12 MATLAB Simulink Model of the Overall System.............. 58

Figure 3-13 Electrical Analogy of the Pump Leakage Flow Rates.......... 59

Figure 3-14 Representation of the Hydraulic Pump Leakages with Additional External Leakages 65

Figure 3-15 Block Diagram Representation of the Open Loop Position Response of the Variable Speed Pump Controlled System.. 68

Figure 3-16 Pump Dynamic Chamber Pressure Change Relations 69

Figure 3-17 Schematic Representation of the Valve Controlled System. 72

Figure 3-18 MATLAB Simulink Model of the Proportional Valve with Zero Lap ... 74

Figure 3-19 Schematic Representation of the Valve Spool Opening for Extension ... 77

Figure 3-20 Schematic Representation of the Valve Spool Opening for Retraction ... 80

Figure 3-21 Dynamic Pressure Change Ratios ... 85

Figure 3-22 Block Diagram Representation of the Valve Controlled System for the Extension Case ... 87

Figure 4-1 Block Diagram Representation of the Close Loop Pump Controlled System ... 100

Figure 4-2 MATLAB Simulink Model of the Closed Loop Pump Controlled Position Control System ... 104

Figure 4-3 Block Diagram Representation of the Closed Loop Valve Controlled System ... 105

Figure 4-4 MATLAB Simulink Model of the Closed Loop Valve Controlled Position Control System ... 111

Figure 4-5 Kalman Filter Block Diagram ... 113

Figure 4-6 Kalman Filter Algorithm ... 116

Figure 4-7 MATLAB Simulink Kalman Filter Model for the Variable Speed Pump Controlled System ... 118

Figure 4-8 Unscented Kalman Filter Algorithm ... 123

Figure 4-9 Position Transducer Measurement for Zero Reference Input ... 127

Figure 4-10 Hydraulic Cylinder Chamber B Pressure Transducer Measurement for Zero Speed ... 127

Figure 4-11 Hydraulic Cylinder Chamber A Pressure Transducer Measurement for Zero Reference Signal ... 128

Figure 4-12 Kalman Filter Position Filtering Performance 130

Figure 4-13 Kalman Filter Pressure Filtering Performance.................. 130

Figure 4-14 Kalman Filter Performance Load Pressure 131

Figure 5-1 MATLAB Simulink RTWT Controller of the Pump Controlled System 134

Figure 5-2 MATLAB Simulink RTWT Controller of the Valve Controlled System 135

Figure 5-3 Steady State Chamber Pressures 137

Figure 5-4 Steady State Cylinder Position for the Given Offset Pump Speeds... 138

Figure 5-5 Friction Test Signal and System Response 140

Figure 5-6 Friction Force vs Cylinder Velocity................................. 142

Figure 5-7 Mean Friction Force vs Cylinder Velocity........................ 142

Figure 5-8 Body Force due to Acceleration....................................... 143

Figure 5-9 Step Response of the Pump Controlled System with Dominant Desired Closed Loop Pole Located at -2.2π rad/s............ 145

Figure 5-10 Step Response of the Pump Controlled System with Dominant Desired Closed Loop Pole Located at -10.2π rad/s 147

Figure 5-11 Step Response of the Valve Controlled System with Dominant Desired Closed Loop Pole Located at -2.2π rad/s............ 149

Figure 5-12 Step Response of the Valve Controlled System with Dominant Desired Closed Loop Pole Located at -10.2π rad/s......... 150

Figure 5-13 Real System Valve Spool Position Command and Simulink Model Spool Position Command 151

Figure 5-14 Pump Controlled System Open Loop Frequency Response Test Signal... 154

Figure 5-15 Experimental and Theoretical Open Loop Frequency Response of the Pump Controlled System 154

Figure 5-16 Hydraulic Cylinder Position in Open Loop Tests 155

Figure 5-17 Position Response of Pump Controlled System................ 157

Figure 5-18 Detailed View of Position Response of Pump Controlled System 158

Figure 5-19 Error Between the Measured and Filtered Position Signal 159

Figure 5-20 Pressure Response 160

Figure 5-21 Servomotor Response... 161

Figure 5-22 Load Pressure 162

Figure 5-23 Magnitude Plot of the Experimental and Theoretical Frequency Response of Pump Controlled System with Desired Dominant Pole Located at -5.2π rad/s............................. 163

Figure 5-24 Phase Plot of the Experimental and Theoretical Frequency Response of Pump Controlled System with Desired Dominant Pole Located at -5.2π rad/s... 164

Figure 5-25 Test Signal for Valve Controlled System Open Loop Frequency Response... 165

Figure 5-26 Magnitude Plot of the Experimental and Theoretical Open Loop Frequency Response of the Valve Controlled System166

Figure 5-27 Phase Plot of the Experimental and Theoretical Open Loop Frequency Response of the Valve Controlled System 167

Figure 5-28 Valve Controlled System Position Response 169

Figure 5-29 Valve Controlled System Error Between the Measured and Filtered Position Signal 170

Figure 5-30 Valve Controlled System Hydraulic Cylinder Chamber Pressure Response 171

Figure 5-31 Valve Controlled System Load Pressure Response 172

Figure 5-32 Experimental and Theoretical Frequency Response of Valve Controlled System with Desired Dominant Pole Located at -5.2π rad/s 173

LIST OF TABLES

TABLES

Table 3-1 Hydraulic Oil Properties 38

Table 3-2 Hydraulic Pump/Motor Unit Properties 39

Table 3-3 Hydraulic Actuator Properties 40

Table 3-4 Servovalve Properties 41

Table 3-5 Pole and Zero Comparison of Reduced and Full Order Transfer Functions 71

Table 3-6 Pole and Zero Comparison of Reduced and Full Order Transfer Functions 89

Table 3-7 Numerical Values of the System Parameters 90

Table 5-1 Pump Controlled System Step Response Test-1 Data 144

Table 5-2 Pump Controlled System Step Response Test-2 Data 146

Table 5-3 Valve Controlled System Step Response Test-1 Data 148

Table 5-4 Valve Controlled System Step Response Test-2 Data 150

Table 5-5 Pump Controlled System Frequency Response Test Data 157

Table 5-6 Valve Controlled System Frequency Response Test Data 168

LIST OF SYMBOLS

SYMBOLS

b	Viscous friction force coefficient
$\mathbf{e}^{-}_{k}$	Priori state estimate error
$\mathbf{e}_{k}$	Posteriori state estimate error
f_L	Force applied on the load
f_f	Friction force
$\mathbf{f}[\ldots]$	Non-linear process model
g	Gravitational acceleration
$\mathbf{h}[\ldots]$	Non-linear observation model
m	Mass
n_P	Pump drive speed
n_1	Dynamic drive speed of pump 1, output of the position control loop
n_2	Dynamic drive speed of pump 2, output of the position control loop
n_{1o}	Offset drive speed of pump 1, output of the pressure control loop
n_{2o}	Offset drive speed of pump 2, output of the pressure control loop
n_{1t}	Total drive speed of pump 1
n_{2t}	Total drive speed of pump 2
Δp	Pressure differential
p_A	Cap end hydraulic cylinder chamber pressure
p_{A_ss}	Steady state cap end hydraulic cylinder chamber pressure

$p_{A\_ss\_ext}$ Steady state cap end side cylinder chamber pressure while extending

$p_{A\_ss\_ret}$ Steady state cap end side cylinder chamber pressure while retracting

p_B Hydraulic cylinder rod end side chamber pressure

p_{B_ss} Steady state rod end side hydraulic cylinder chamber pressure

$p_{B\_ss\_ext}$ Steady state rod end side cylinder chamber pressure while extending

$p_{B\_ss\_ret}$ Steady state rod end side cylinder chamber pressure while retracing

p_L Load pressure

p_{L_s} Static load pressure

$\bar{p}_L$ Non dimensional load pressure

p_s Supply pressure of the valve controlled hydraulic system

p_{sum} Sum of the hydraulic cylinder chamber pressures

p_t Hydraulic oil tank pressure

q Flow rate

q_1 Flow rate through valve orifice opening 1

q_2 Flow rate through valve orifice opening 2

q_3 Flow rate through valve orifice opening 3

q_4 Flow rate through valve orifice opening 4

q_A Flow rate entering the cap end side of the hydraulic cylinder

q_{A_ss} Steady state flow rate entering the cap end of the hydraulic cylinder

q_B Flow rate exiting from the rod end side of the hydraulic cylinder

q_{B_ss} Steady state flow rate exiting from the rod end of the hydraulic cylinder

q_a Flow rate of a general hydraulic pump input (suction) port

q_b	Flow rate of a general hydraulic pump output port
q_{a_m}	Flow rate of a general hydraulic motor output port
q_{b_m}	Flow rate of a general hydraulic motor input port
q_{ca}	Compressibility flow losses of a general hydraulic pump/motor port a
q_{cb}	Compressibility flow losses of a general hydraulic pump/motor port b
q_{ea}	External leakage flow losses from hydraulic pump/motor port a
q_{eb}	External leakage flow losses from hydraulic pump/motor port b
q_i	Internal (cross-port) leakage flow of a general hydraulic pump/motor
q_t	Theoretical hydraulic pump / motor flow rate
q_{p2A}	Flow rate of the pump 2 outlet port (hydraulic cylinder cap end side)
q_{p2B}	Flow rate of the pump 2 inlet port (hydraulic cylinder rod end side)
q_{p1A}	Flow rate of the pump 2 outlet port (hydraulic cylinder cap end side)
q_L	Load flow rate
$\overline{q}_L$	Non dimensional load flow rate
$q_{\max}$	Maximum flow rate of the valve
$\mathbf{q}_k$	Kalman filter state vector at time step k
$\hat{\mathbf{q}}_k^-$	Priori state estimate vector
$\hat{\mathbf{q}}_k$	Posteriori state estimate vector
t	Time
u	Reference valve spool position signal in terms of voltage
u_v	Valve spool position
$u_{\max}$	Maximum valve spool position

u_{ext}	State feedback control signal for the extension of the hydraulic cylinder
u_{ret}	State feedback control signal for the retraction of the hydraulic cylinder
$\mathbf{u}$	Control input vector
x	Hydraulic cylinder position
$\dot{x}$	Hydraulic cylinder velocity
$\ddot{x}$	Hydraulic cylinder acceleration
x_{ref}	Reference hydraulic cylinder position
$\mathbf{x}$	State vector
$\mathbf{y}$	Output vector
$\mathbf{v}$	Process noise vector
$\mathbf{w}$	Measurement noise vector
w_o	Valve orifice perimeter
$\mathbf{z}_k$	Discrete output vector
$\mathbf{A}$	System matrix
$\mathbf{A}_{ext}$	System matrix for the extension of hydraulic cylinder
$\mathbf{A}_{ret}$	System matrix for the retraction of hydraulic cylinder
A_A	Hydraulic cylinder cap end side area
A_B	Hydraulic cylinder rod end side area
$\mathbf{B}$	Input matrix
$\mathbf{B}_{ext}$	Input matrix for the extension of hydraulic cylinder
$\mathbf{B}_{ret}$	Input matrix for the retraction of hydraulic cylinder
$\mathbf{C}$	Output matrix
C_d	Valve orifice discharge coefficient
C_i	Internal leakage coefficient of hydraulic pump
$C_{ie_{Ratio}}$	Pump internal and external leakage ratio

C_{Aext} Artificial external leakage coefficient of hydraulic cylinder cap end side

C_{Bext} Artificial external leakage coefficient of hydraulic cylinder rod end side

C_{Leak} Equivalent leakages coefficient of the pump controlled system

C_{ea} External leakage coefficient of hydraulic pump port a

C_{eb} External leakage coefficient of hydraulic pump port b

$\mathbf{D}$ Feed forward matrix

D_P Pump displacement

E Hydraulic oil bulk modulus

$\mathbf{G}$ Input matrix in discrete time domain

$\mathbf{H}$ Measurement matrix in discrete time domain

I Identity matrix

K_v Valve flow gain

$\mathbf{K}$ State feedback gain vector

$\mathbf{K}_k$ Kalman gain matrix

$\mathbf{K}_{ext}$ State feedback gain vector for the extension of the hydraulic cylinder

$\mathbf{K}_{ret}$ State feedback gain vector for the retraction of the hydraulic cylinder

K_{u2_ext} Linearized valve spool position gain of orifice 2 for extension

K_{u4_ext} Linearized valve spool position gain of orifice 4 for extension

K_{p2_ext} Linearized valve pressure gain of orifice 2 for extension

K_{p4_ext} Linearized valve pressure gain of orifice 4 for extension

K_{u1_ret} Linearized valve spool position gain of orifice 1 for retraction

K_{u3_ret} Linearized valve spool position gain of orifice 3 for retraction

K_{p1_ret} Linearized valve pressure gain of orifice 1 for retraction

K_{p3_ret} Linearized valve pressure gain of orifice 3 for retraction

$\mathbf{M}$	Controllability matrix
$\mathbf{M}_{ext}$	Controllability matrix for the extension of hydraulic cylinder
$\mathbf{M}_{ret}$	Controllability matrix for the retraction of hydraulic cylinder
$\mathbf{P}^{-}_{k}$	Priori state estimate error covariance matrix
$\mathbf{P}_{k}$	Posteriori state estimate error covariance matrix
$\overline{P}$	Non dimensional power transmitted to the system over valve
$\overline{P}_{\max}$	Maximum non dimensional power transmitted to the system
$\overline{P}_{loss\_RV}$	Non dimensional power lost on the relief valve
$\overline{P}_{loss\_FCV}$	Non dimensional power lost on the flow control valve
$\mathbf{Q}$	Process noise covariance matrix
$\mathbf{R}$	Measurement noise covariance matrix
$\mathbf{T}$	Transformation matrix
$\mathbf{T}_{ext}$	Transformation matrix for extension of hydraulic cylinder
$\mathbf{T}_{ret}$	Transformation matrix for retraction of hydraulic cylinder
V_A	Hydraulic cylinder cap end side volume
V_B	Hydraulic cylinder rod end side volume
α	Hydraulic cylinder chambers volume ratio for a fixed cylinder position
β	Offset pump speed ratio
γ	Hydraulic cylinder area ratio
φ	Dynamic pressure change ratio of the hydraulic cylinder chambers
λ	Non dimensional valve spool opening
ρ	Hydraulic oil density
ω_n	Natural frequency
ξ	Damping ratio
$\mathbf{\Phi}$	Discrete state transition matrix
Ψ	Conversion factor between the hydraulic cylinder chamber pressures sum and pump 2 speed

CHAPTER 1

INTRODUCTION

1.1 Background and Motivations

The history of fluid power transmission dates back to 1795 where a patent was granted for a hydraulic press to transmit and amplify force by using a hand pump [1]. In 1850's there were many other cranes, winches, presses and extruding machines utilizing fluid power transmission. However control of these devices was open loop. The first closed loop fluid power system was patented by Brown in 1870, where a mechanical feedback from the rudder to position a valve controlled cylinder in a ship steering system [2]. The fluid power technology is boosted in 1940's by the demand for automatic fire control systems and military aircraft control, till that time the electro hydraulic servo systems appeared and developed steadily.

Today, in most of engineering fields the fluid power transmission is used extensively such as in heavy duty industrial robots, presses, mining and earthmoving machines, material handling, forestry and agricultural applications, manufacturing, construction and so forth. Some of the main reasons why they are used so extensively can be given as follows [3, 4].

- Comparatively small final actuator size,
- High power/mass ratio,
- Ability to apply high forces with high load stiffness,

- Easy heat dissipation of moving elements by means of hydraulic oil, also it acts as a lubricant,
- Long operation life even in harsh environments.

However, there exist many important drawbacks to use hydraulic actuators in engineering systems, which can be simply given as,

- Requirement for a bulky power system with large oil reservoir,
- Low efficiency, requirement of a constant supply pressure depending on application,
- Leakage,
- Noise,
- Environmental risks of the oil,
- Complex control strategies due to its non-linear nature.

Most conventional hydraulic control systems are based on valve controlled cylinders, in which valves located next to the actuator regulate the flow rate by changing their orifice areas. In spite of their high precision and fast dynamic behavior, a considerable amount of hydraulic energy is wasted as heat loss to the environment due to throttling in control valves, increasing the oil temperature. This is an important drawback for hydraulic systems.

In past, the power efficiency of hydraulic circuits was not an important factor; much attention has been oriented to their high system performance. However, in recent years, engineering systems are forced to be energy efficient due to limited and high-priced energy resources and the increasing environmental sense. For this reason, factors like the total energy usage, noise level, amount of oil used and oil replacement cost are becoming important performance criteria combined with the fast dynamic response.

Therefore, in today's hydraulic engineering, the energy efficiency becomes an important subject. The basic approach to improve the energy efficiency in hydraulic systems is to decrease or eliminate valve losses. To do so, several new valve control circuits are developed which utilize programmable valves to decouple the incoming and outgoing flow rate of the hydraulic cylinder and control them independently. This new technique has more complex controllers but the added control flexibility is used to significantly reduce the fluid power energy [5].

However, to eliminate the valve losses completely, the flow should be completely regulated according to the load requirements, Thus, the final control element of fluid power actuators and drives should be replaced with pumps and motors instead of valves. Hence, in energy efficient hydraulic systems, pump control techniques became the center of the focus [6].

There are mainly two methods to control the flow rate of a pump. In the first method, the flow rate is regulated by changing the pump displacement whereas in the second one, the flow rate is regulated by changing the drive speed of a constant displacement pump. Furthermore, the combination of these two methods that is changing the flow rate by both changing the displacement and drive speed of the pump can also be used.

There are many advantages of pump control techniques over the conventional valve control technique, which can be given as [7].

- improved utilization of energy,
- use of load and brake energy,
- smaller oil reservoir,
- less cooling power required,
- load independent system behavior,
- simpler systems, reduced number of interfaces and fittings,
- low filtration rate in main circuit,
- less fuel consumption and pollution.

Besides the numerous advantageous written above, the dynamic performance of the pump controlled systems are considered not to have as high as the valve controlled systems. This is due to the slow dynamic response of standard pumps. However, today with the developing technology, it is possible to have a fast dynamic response by utilizing specially designed hydraulic pump/motor units with electrical servomotor drives.

1.2 Literature Survey

In a conventional valve controlled hydraulic circuit, most of the energy transmitted to the system is converted into heat energy as a consequence of pressure losses across throttling valves. To decrease the valve losses, there exist several solutions utilizing the control of the power source without changing the final control element, that is the flow control valve. One way to achieve energy efficiency in valve controlled systems is to adjust the flow rate of the pump such that no excess flow rate is delivered to the system, in the mean time maintaining a constant supply pressure of the valve. These systems are called as "pressure compensated systems" and generally a variable displacement pump is utilized to regulate the flow rate.

Other type of energy efficient valve controlled systems is called “load sensing systems”. In these systems, the pump flow rate is adjusted such that the pressure drop across the flow control valve remains constant independent of the load pressure. Variable displacement pumps with a controller inside are utilized in these systems and they are favorable in mobile applications where the drive speed is constant. Nowadays there are also systems where the flow rate is adjusted by the drive speed of a constant displacement pump. These systems are called as "electro-hydraulic load sensing systems". They are generally used in stationary applications and the speed of the electric motor driving a constant displacement pump is controlled via a frequency converter [8, 9].

Furthermore, different from the control of the power source, a distinctive research area appears on the flow control valve itself nowadays. Instead of using a typical 4-way valve, four or five cartridge type valves are used to regulate the meter in and meter out flow rate of the hydraulic actuator. Here, the "meter-in" stands for the flow rate from power supply to the hydraulic actuator, and "meter-out" stands for the flow rate from the hydraulic actuator to the hydraulic tank. In this valve configuration, different from a typical 4-way flow control valve, the meter-in and meter-out flow rates are independent, as there is no mechanical connection between the valve orifice openings, this gives a tremendous control flexibility as well as ability to increase the energy efficiency if it is well utilized [5, 10].

In a valve controlled hydraulic circuit, whether it is pressure compensated or load sensing, the throttling losses are inevitable. To get rid of throttling losses completely the valve, as the final element of the hydraulic circuit, should be taken out from the circuit. One such circuit can be made up by using variable displacement pumps or variable speed pumps. In these circuits, the final control element that regulates the flow rate going through the hydraulic actuator is the pump itself. By adjusting the drive speed or the displacement of the pump, the flow rate going through the hydraulic actuator is fully adapted to the load requirements; thus, eliminating the throttling losses.

Using a pump as the final control element is not a new concept. The hydrostatic servomotor control circuits utilize variable displacement pumps. In these circuits, the speed and direction of the motor are adjusted by the swash plate angle of the variable displacement pump. These type of drives are often employed in machine tool control centers, tension control systems, gun turret drive, antenna drives, and ship steering systems [11]. In electric-hydrostatic drives, the same principle is applied by adjusting the drive speed of a constant displacement pump. They are suitable for stationary applications like injection molding machines. The position tracking control of the double rod clamping cylinder is accomplished by adjusting the speed of an asynchronous AC motor driving a constant displacement pump [12].

One important property of the hydrostatic systems is the use of symmetric actuators. Here, assuming the leakages are compensated, the input flow rate of the variable displacement pump or variable speed pump will be equal to the output flow rate of the actuator making the control very simple. However if an asymmetric single rod cylinder is used as the hydraulic actuator, then the flow entering the actuator will not be equal to the flow exiting from the actuator. To overcome this problem, a novel symmetric single rod actuator design is presented by Goldenberg and Habibi [3]. However, manufacturing of this new design necessitate more precision than the simple single rod cylinder and introduce more manufacturing cost.

To compensate the asymmetric flow rate of a single rod hydraulic actuator, hydraulic transformers are utilized. A hydraulic transformer converts an input flow at a certain given pressure to an output flow at any other pressure level. Here, the product of pressure and flow at the input is equal to the product of pressure of flow at the output. It can be compared to an electric transformer where the product of voltage and current in principle remains constant [13]. In 1988, Berbuer introduced a hydraulic transformer for the volume flow compensation of the single rod cylinder. The ratio of the transformer is designed according to the single rod cylinder area ratio [14].

In 1994, a closed circuit displacement control concept was patented. It utilizes a variable displacement pump and a low pressure charge line for compensating the difference in volumetric flow through the cylinder [15]. A 2-position 3-way valve is used to connect the charge line to the low pressure side of the cylinder. A similar concept was developed by Ivantysynova and Rahmfeld [7] which uses a variable displacement pump with differential flow compensation via a low pressure charge line and two pilot operated check valves. This concept is not only limited to variable displacement pumps, but also speed variable constant displacement pumps can be used. In literature, there are also studies utilizing the Rahmfeld's circuit solution with speed variable pumps [16].

Another way to balance the unequal flow rates entering and leaving the cylinder volumes is using the two pump control principle. In literature several solutions utilizing two pump working dependently or independently for the control of single rod cylinder. The pumps can be speed controlled or displacement controlled.

The energy efficiency of displacement controlled and speed controlled pump systems are compared by Helduser [17]. In this study, the total power usage of a plastic injection machine was measured for one hour experimentally for a predetermined duty cycle. It was seen that the speed controlled pump was more energy efficient than the displacement controlled pump system, to due its energy saving potential during the idling.

In the following two papers two variable speed pumps are utilized for the position control of a single rod hydraulic actuator.

Long and Neubert utilized speed variable pumps to implement closed loop differential cylinder control [18]. In the control circuit, two compound controlled speed variable pumps were used to control the non-symmetric flow of the differential cylinder. In their study, they used two control loops one for the control of the sum of the hydraulic cylinder chamber pressures, and one for the control of the hydraulic cylinder position. The proposed circuit scheme of the control strategy is shown in Figure 1-1. The aim of the pressure control loop is to maintain a constant hydraulic cylinder chamber pressure sum so that in case of a loading the dynamic pressure changes of the cylinder chambers are equal in magnitude but opposite in direction. They proposed that the sum pressure control strategy can automatically compensate the leakages of the pump and the cylinder and make the system have the same technology characteristics as the valve controlled circuit, where the sum of the hydraulic cylinder chambers are always equal to the supply pressure. However, it should be noted that, in valve controlled circuits, the sum of the hydraulic cylinder chambers is equal to supply pressure only when the actuator is symmetric. Hence, this is not true for single rod actuators with unequal cylinder areas. Long and Neubert used a PI controller for the pressure control loop and PID controller for the position control loop. After pressurizing the cylinder chambers and setting the position of the cylinder to a fixed value, they applied a 65 bar load pressure as a step input, and measured the chamber pressure changes, the chamber pressures vary toward opposite direction and with equal amplitude. In dynamic state the maximum value of the position error was observed as 2.5 mm while in steady state it was 0.6 mm.

In their latter study related to variable speed pump control circuit, Quan and Neubert reduced the double degree of control principle to one, by omitting the closed loop pressure control [20]. The new method is based on leakage compensation. The leakage flow losses of the system are compensated in an open loop manner, by driving the pumps with offset speeds. They showed mathematically that the pressure responses of cylinder chambers to preloading act as first order systems, where their time constants are determined by the bulk modulus of the oil and the volume of the individual chamber. They concluded that, as long as the speed loop is steady, the pressure response of each chamber will be steady, the disturbance as the outer load does not affect these time constants. They also concluded that the response speeds of the chamber pressures have hardly any influence on the controlling process of the position loop. Different from the sum pressure control principle, in this single loop circuit, the pressures in each chamber changes in opposite direction but not in equal amplitude. Then they presented a formula for the pressure changes of the chambers with respect to pump speed variations, and concluded that for a certain pump leakage coefficient ratio, the pressure change characteristics will be the same as the valve controlled system.

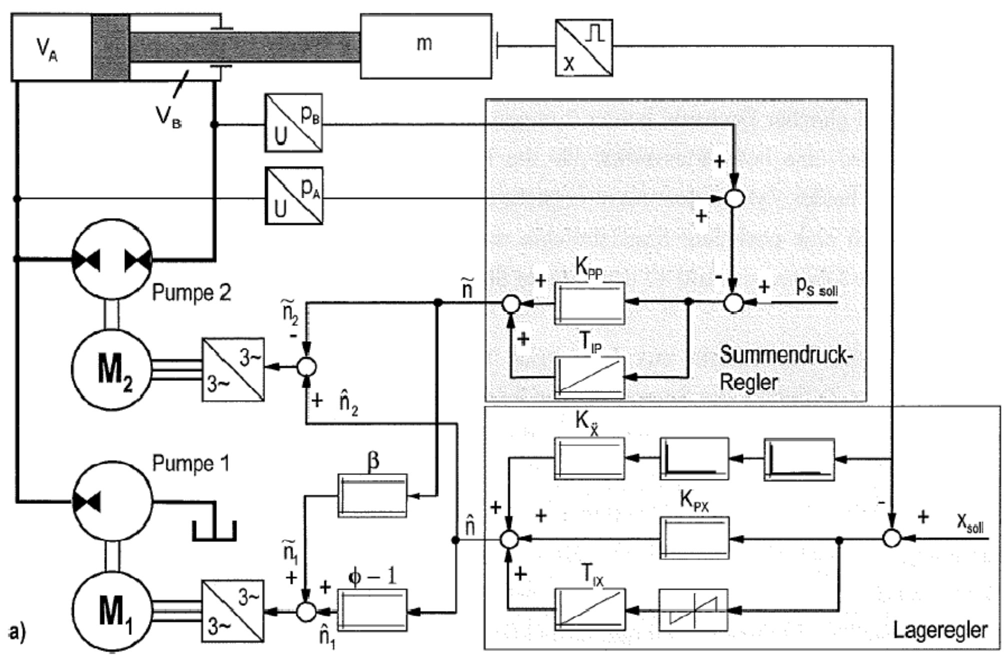

Figure 1-1 The Circuit Operation and Sum Pressure Principle [19]

1.3 Objective of the Thesis

The main objective of this thesis study is to investigate a valveless hydraulic servo system controlled by two independent servo pumps and compare it with the conventional valve controlled hydraulic system both experimentally and analytically. It is aimed to eliminate the valve losses without conceding from the dynamic performance [21].

To this end, because one of the objectives is analytical comparison, both valve and pump controlled systems are modeled mathematically. The novelty of this thesis is the reduced order system modeling. Different from the previous researches [18,20], in this thesis study, a transfer function between the hydraulic cylinder chamber pressures is derived and it is shown that; the chamber pressure changes become linearly dependent above and below some prescribed frequencies. Thus, it is possible to derive a second order transfer function defining the open loop speed response of the system indicating the system dynamics explicitly. Likewise, the same procedure is applied to the linearized valve controlled system equations and the two systems are compared mathematically.

For the objective of experimental comparison, an experimental test set-up including both valve and pump control techniques is constructed. A single rod or asymmetric hydraulic actuator with unequal cylinder area is utilized in the test set-up, because it is the most common actuator type in industrial applications due to its simple design and lower cost. Furthermore in the experimental test set-up, common industrial use low cost sensors and drivers are used.

The position control of the single rod hydraulic actuator is aimed in this thesis study. For this purpose, closed loop linear state feedback controllers are designed both for pump and valve controlled systems. The state feedback gains are calculated by using the reduced order linear and linearized dynamic system equations of the pump and valve controlled systems, for the identical desired close loop pole locations.

The other objective is to attenuate the highly noise on the measurement signals due to the low cost measurement system, and estimate the unknown state which is not measured and necessary for state feedback. For this purpose Kalman filtering is utilized. A linear Kalman filter is designed for the pump controlled system and an Unscented Kalman filter is designed for the valve controlled system. The two filters smooth feedback position and pressure signals while estimating the unmeasured actuator velocity.

To compare the performance of the two systems step response and open loop and closed loop frequency response tests are conducted on the constructed experimental test set-up.

1.4 Thesis Outline

This thesis study deals with the modeling, application and comparison of an energy efficient variable speed pump controlled hydraulic system with the conventional valve controlled hydraulic system. The thesis manuscript has three principal parts: the first part deals with the mathematical modelings of the pump controlled and valve controlled test systems, the second part deals with the controller design and Kalman filter design based on the modeled systems, and the third part concerns with the performance tests and the comparison of the two systems in term of their dynamic performance. These parts are organized as five chapters as summarized below.

In Chapter 2, some general features of hydraulic systems are investigated. Energy losses in the conventional valve controlled hydraulic systems are introduced and the proposed energy efficient hydraulic control systems are presented.

In Chapter 3, the experimental hydraulic set-up which consists of a variable speed pump controlled system and a valve controlled system is introduced. The mathematical model of the two systems are developed and explained in detail.

In Chapter 4, the state space representations of the pump controlled and valve controlled systems are given, and controller designs for the both systems are explained. The design of a Kalman filter for the linear pump controlled system and the design of an unscented Kalman filter for the non-linear valve controlled system are explained and its details are provided.

In Chapter 5, the unknown system parameters are found experimentally and the mathematical models of the two systems are validated with the test results. A series of step response and frequency response tests are performed for both systems and compared with their simulation results. At the end of this chapter, the performances of two systems are compared.

In Chapter 6, the whole performed study is summarized, the conclusions drawn from the investigations are presented, and the prospects for application and further developments are discussed.

CHAPTER 2

HYDRAULIC POWER SYSTEMS

The subject of this thesis study is to investigate an energy efficient hydraulic control system. Thus, to understand the importance of energy efficiency in hydraulic systems, it would be useful to discuss the conventional valve controlled hydraulic systems before investigating the variable speed pump controlled hydraulic systems. For this reason, this chapter is devoted to investigate the losses in conventional valve controlled hydraulic systems and introduce the solutions to increase the energy efficiency.

In Section 2.1, the theoretical energy losses in a conventional valve controlled hydraulic systems will be investigated. In Section 2.2 the methods to increase the efficiency of a valve controlled system and the recently developed valve technologies are introduced. In Sections 2.2.2 and 2.2.3, the control principles, which eliminate the throttling losses completely by omitting the valve and using the pump as the final control element will be introduced. In Section 2.2.3, several circuit solutions utilizing 2 pump control principle will be discussed and the circuit which is the subject of this thesis study is introduced.

2.1 Conventional Valve Controlled Hydraulic Power Systems

A conventional hydraulic control system represented in Figure 2-1 consists of the following components:

- Power source,
- Pump,

- Relief valve,
- Fluid reservoir,
- Control valve,
- Actuator

In the circuit illustrated in Figure 2-1, generally an AC electric motor or an internal combustion engine (especially for mobile applications) is used as the power source. The motor drives a positive displacement pump. It is a common practice to use fixed displacement pumps since they are cheaper than other types of pumps. The fixed displacement pump is driven in one direction with constant speed; it sucks oil from the oil reservoir and delivers a constant flow rate through the hydraulic cylinder. The direction of motion of the hydraulic cylinder and its velocity are controlled by a flow control valve, which can be a proportional or servovalve. This valve regulates the flow by changing its orifice area. Assuming that the pressure drop across the valve is kept constant, there is a linear relationship between the flow rate and the orifice area. To retard or decelerate the hydraulic cylinder, the orifice area decreases, but this time as the valve resistance increases the pump exit pressure increases.

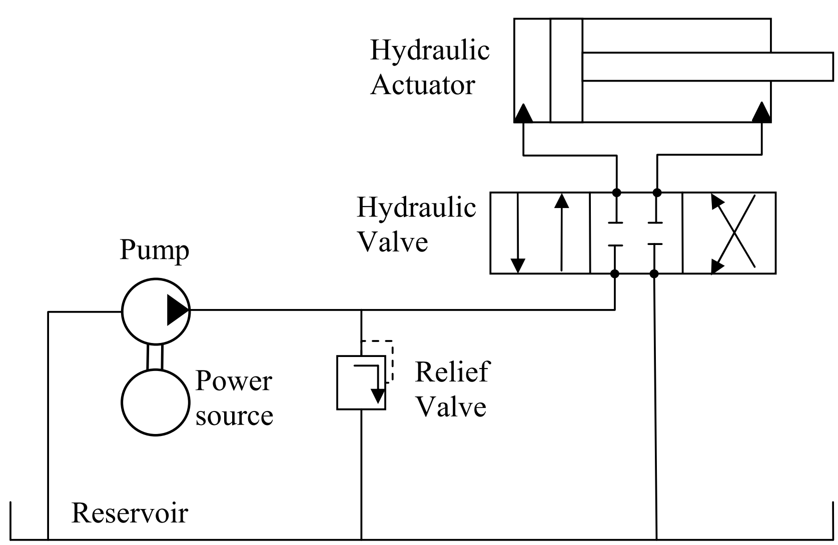

Figure 2-1 Conventional Valve Controlled Hydraulic Circuit

To have a constant pressure, a pressure relief valve is used at the pump outlet. This valve is normally closed, however, when the exit pressure of the pump reaches the set pressure of the relief valve, it opens and the excess flow returns to the oil tank through the relief valve. By this way, as long as an excess flow rate is delivered to the system, the relief valve will be always open limiting the pump exit pressure so that it does not affect by the changing valve orifices areas.

The circuit in Figure 2-1 is called as the "constant pressure (CP) valve controlled hydraulic system". The other type of the valve controlled hydraulic systems is the constant flow (CQ) systems. In constant pressure systems, the supply pressure to the control valve is kept constant whereas, in constant flow systems the rate of flow from the source through the control valve is kept constant. Therefore the supply pressure of the valve at any instant depends upon the conditions of operation at any time in CQ systems. The CP systems are the most popular one in hydraulic applications. Because the valve characteristics of CQ systems are highly non-linear compared with the CP systems, also with CQ systems it is not suitable to drive multi actuators from the same source [11].

The following discussion covers the theoretical power losses in simple CP valve controlled hydraulic systems. For simplicity, the hydraulic actuator is assumed to be double rod with equal areas at each side of the piston and the hydraulic servo/proportional valve is assumed to be zero lapped. In a zero lapped valve, there is no dead band when the spool is centered. The orifice opening is zero for the centered spool position and under constant pressure drop across the valve the valve flow gain is constant for every spool position. The hydraulic circuit representation of such a system is shown in Figure 2-2.

In Figure 2-2 only two of the arms are open at any time since the valve is zero lapped [11]. When $u_v > 0$ (extension of the hydraulic actuator), the pressurized oil from the supply passes trough orifice 2 to the hydraulic cylinder chamber A, and the oil in chamber B passes through the orifice 4 back to the oil reservoir. When $u_v < 0$ (retraction the hydraulic actuator), the pressurized oil coming from the supply passes through orifice 3 to the cylinder chamber B and the oil at chamber A passes through the orifice 1 back to the oil reservoir. This configuration corresponds to a simple series circuit as shown in Figure 2-2 and it simplifies the derivation of the characteristic equations.

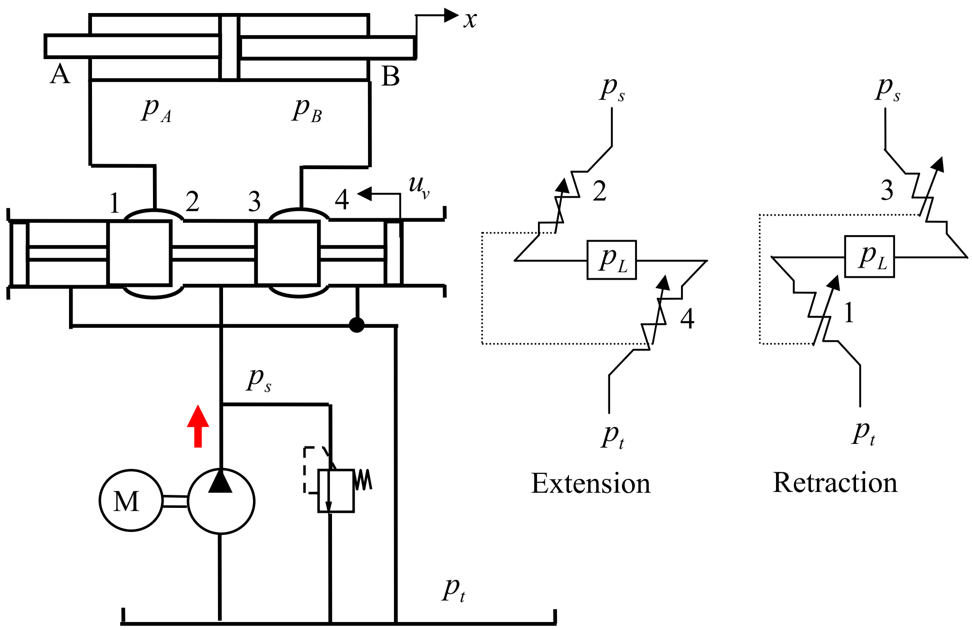

Figure 2-2 Constant Pressure Valve Controlled Hydraulic Circuit

Because the actuator has a double rod with equal areas, the flow rates passing through the orifices 2 and 4 for the extension and 1 and 3 for the retraction will always be the same. Moreover, because the valve is symmetric the orifice resistances are also identical. Therefore, in this series circuit, the pressure drop at each orifice will be the same and can be expressed as

$$\Delta p = \frac{p_s - p_t - p_L}{2} \tag{2.1}$$

where,

p_s represents the supply pressure,

p_t represents the hydraulic tank pressure,

p_L represents the load pressure; that is, the pressure drop across the load.

The hydraulic valve dynamics can be represented by the equations presented by Merritt [22]. The flow rate through a servovalve is proportional to the square root of the pressure drop across the port and the valve opening. The flow rate through the load q_L, is defined as,

$$q_L = C_d w_o u_v \sqrt{\frac{2}{\rho}\Delta p} = C_d w_o u_v \sqrt{\frac{2}{\rho}\frac{p_s - p_t - p_L}{2}} \tag{2.2}$$

where,

C_d represents the orifice discharge coefficient,

w_o represents the perimeter of the orifice,

u_v represents the orifice opening which is same as the spool position,

ρ represents the hydraulic oil density.

By taking the squares of each side and rearranging the Eq. (2.2), the expression for the load pressure is obtained as

$$p_L = p_s - p_t - \left(\frac{\rho}{C_d^{\,2}\, w_o^{\,2}\, u_v^{\,2}}\right) q_L^{\,2} \tag{2.3}$$

If Eq. (2.3) is nondimensionalized, the following non-dimensional load pressure expression is obtained.

$$\overline{p}_L = 1 - \frac{\overline{q}_L^{\,2}}{\lambda^2} \tag{2.4}$$

where,

$\overline{p}_L = \dfrac{p_L}{p_s - p_t}$ represents the non-dimensional load pressure,

$\overline{q}_L = \dfrac{q_L}{q_{\max}}$ represents the non-dimensional load flow rate,

$\lambda = \dfrac{u}{u_{v\_\max}}$ represents the non-dimensional valve spool opening,

$q_{\max}$ is the maximum flow rate,

$u_{v\_\max}$ is the maximum valve spool opening.

By using Eq. (2.4), valve characteristic curves for the constant pressure zero lapped valve control circuit can be drawn as in Figure 2-3.

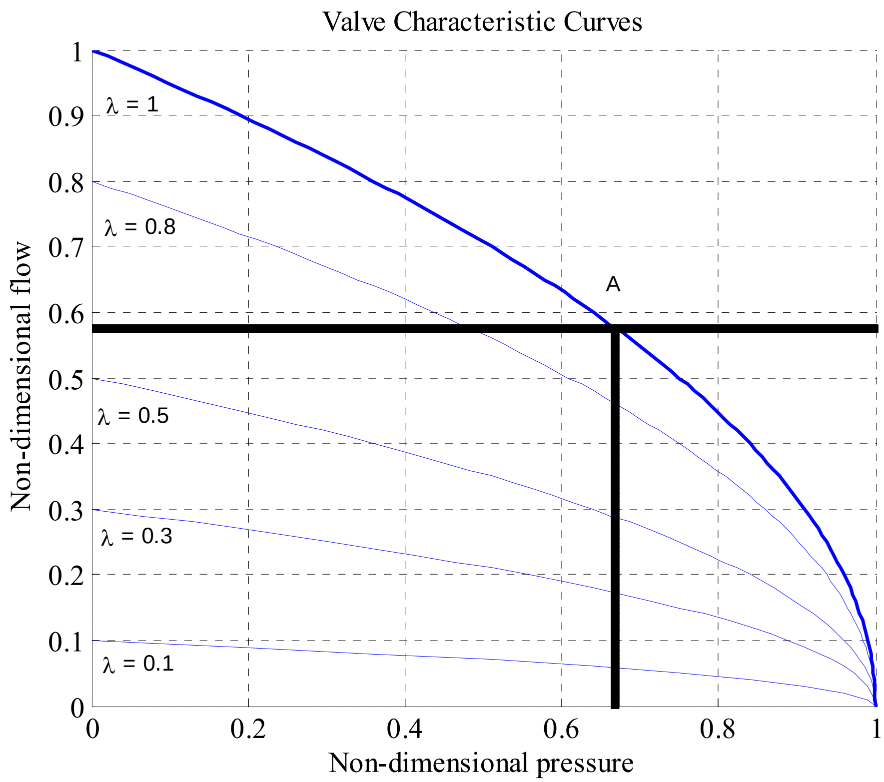

Figure 2-3 Valve Characteristic Curves for Different Valve Openings

In Figure 2-3, the nondimensional 1x1 area formed by the non-dimensional flow and pressure axes represents the total power supplied to the system by the pump. The area formed by drawing perpendicular lines from an arbitrary point A on the valve characteristic curve to the non-dimensional pressure and flow axes represents the power transmitted to the load by the valve. According to that graph for the valve to transmit the maximum power to the load for maximum efficiency, the point A should be on the curve drawn for maximum non-dimensional valve opening; that is, $\lambda = 1$.

Note that any characteristic curve of a drive whether it is an equivalent valve curve or any other, should enclose the load locus completely to perform the given operation fully [11]. The load locus is defined as the complete boundary of the region of the $\overline{q}_L$ - $\overline{p}_L$ plane that may be swept out by the load during its full cycle. It represents the pressure and flow requirement of the load. A load locus curve for a fictitious load is drawn in Figure 2-4.

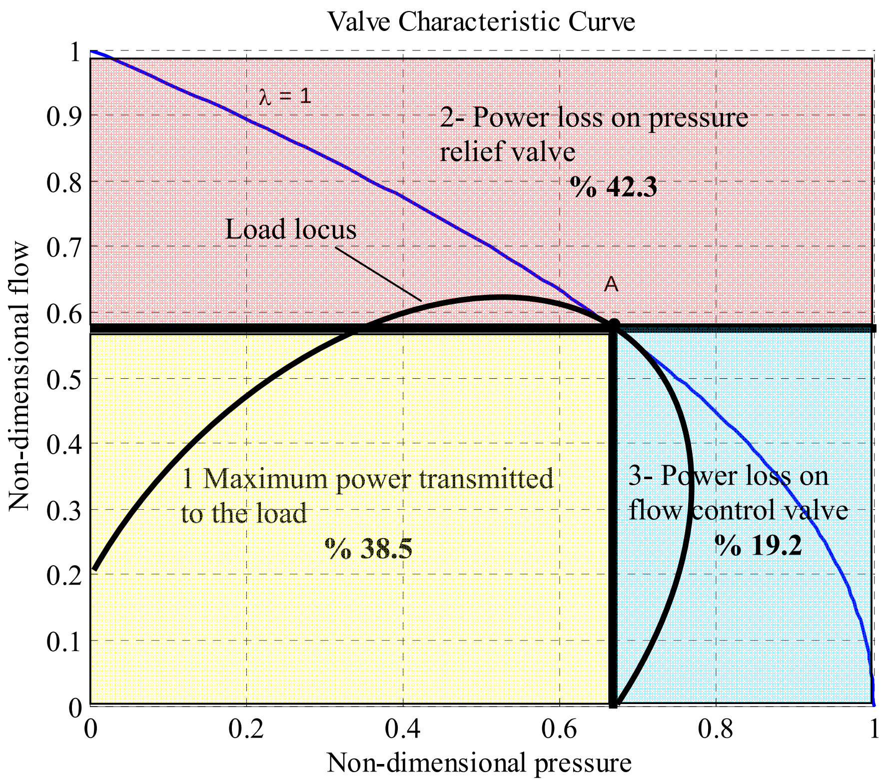

Figure 2-4 Valve Losses of a Constant Pressure Valve Controlled Circuit for Maximum Energy Efficiency

In Figure 2-4, the region covered by the drive curve but not by the load locus represents the uneconomical overdesign. For an efficient design, this load locus should be tangent to the drive curve at one or more points without yielding to any excessive points above the drive curve.

The point of tangency of a fictitious load locus and a valve drive curve is represented by point A in Figure 2-4. Now the problem is to determine the coordinates of point A which will represent the peak power requirement of the fictitious load is equal to the maximum power that can be transmitted by the valve. In other words, this point A will represent the maximum theoretical output power of an ideal constant pressure supply valve controlled circuit. This can be found by writing the non-dimensional power equation transmitted to the load, which is the area formed by drawing perpendicular lines to the axis.

The power transmitted to the load is

$$\overline{P} = \overline{q}_L \, \overline{p}_L \tag{2.5}$$

From the Eq. (2.4) for maximum spool opening $\lambda = 1$ Eq. (2.5) becomes,

$$\overline{P} = \overline{q}_L \left(1 - \overline{q}_L{}^2\right) \tag{2.6}$$

If the Eq. (2.6) differentiated with respect to non-dimensional flow $\overline{q}_L$ and set zero, the nondimensional flow rate required for maximum power output is found as follows,

$$\overline{P} = 1 - \frac{\overline{q}_L{}^2}{3} = 0 \tag{2.7}$$

$$\overline{q}_L = \sqrt{\frac{1}{3}} \tag{2.8}$$

and from Eq. (2.4) the corresponding non-dimensional pressure is found as,

$$\overline{p}_L = \frac{2}{3} \tag{2.9}$$

Hence the maximum theoretical nondimensional power output of the CP valve controlled system is found to be

$$\overline{P}_{\max} = \overline{q}_L \, \overline{p}_L = 0.385 \tag{2.10}$$

which is equal to the 38.5% of the total power supplied by the pump to the system.

The remaining power is lost on the pressure relief valve and the flow control valve. The excess flow rate of the pump which is equal to $1-\overline{q}_L$, returns to the tank through the pressure relief valve with a nondimensional pressure drop value of 1. Then, the power loss on the pressure relief valve can be found as

$$\overline{P}_{loss\_RV} = \left(1-\sqrt{\frac{1}{3}}\right)1 = 0.423 \tag{2.11}$$

The power loss on the flow control valve is equal to the multiplication of non-dimensional load flow rate by the non-dimensional pressure drop across the flow control valve which can be defined as

$$\overline{P}_{loss\_FCV} = \sqrt{\frac{1}{3}}\left(1-\frac{2}{3}\right) = 0.192 \tag{2.12}$$

All these losses are represented in Figure 2-4. Area 1 represents the maximum theoretical power that can be transmitted to the load. Area 2 represents the power loss on the relief valve and the area 3 shows the power loss on the flow control valve.

Note that all these calculations are carried out by assuming a fictitious load whose peak power requirement is equal to the maximum power output of the series valve circuit. Of course this is an unrealistic assumption as no load runs at its full load. The analysis above is to find the efficiency for an instant of time corresponding to the maximum power requirement of the load. During the duty cycle of the load the efficiency of the hydraulic circuit will be less than 38.5%. For example, the load locus of the fictitious load in Figure 2-4 is tangent to the valve curve only at one point at A, that is in all remaining times of its duty cycle the valve opening ratio λ, will be smaller than 1 so that decreasing the overall efficiency.

The overall efficiency of the system not only depends on the load and its duty cycle, but also on the nature of the power supply. As it can be understood from the Figure 2-4, most of the power is lost on the relief valve, due to the excess flow rate of the pump returning to the oil reservoir. Because the constant displacement pump is running at a constant speed there will be always an excess flow. However, the requirement of the hydraulic circuit is to obtain a constant valve supply pressure independent of the load flow rate. Therefore, while supplying a constant pressure, the flow rate supplied by the pump can be adjusted through changing its displacement or its driving speed according to load flow rate requirement. Theoretically, if the pump flow rate delivered to the system is adjusted so that there is no excess flow over relief valve, then at point A the maximum power output of the system will be 66.7%.

Another source of the power loss is the throttle losses on the zero lapped flow control valve which corresponds to 19.2% of the total power supplied to the system, at the instant of maximum power output. The valve used in the analysis is a zero lapped 4-way valve which is modeled as a series circuit, where only two ports of the valve remain open at any instant of time. As these two ports are mechanically connected, their resistance to flow is the same for any spool movement. Thus, half of the power lost is on the meter-in port, which is the port where the flow coming from the supply pressure passes through the hydraulic cylinder chamber, and the remaining half of the power is lost on the meter-out port where the flow coming from the hydraulic cylinder chamber passes through the tank. By utilizing mechanically decoupled meter-in and meter-out valves, the power lost on the flow control valve can be decreased as their resistance will not have to be the same and adjusted independently.

Remembering that the power loss in hydraulic circuits are absorbed by the hydraulic oil, an additional power is lost for the cooling necessities, which also increase the amount of the oil used, resulting in a bulky reservoir.

In the next sub-section, the solutions to power losses in hydraulic systems will be discusses in much more detailed manner and the hydraulic circuit which is the subject of the thesis will be introduced.

2.2 Energy Efficient Hydraulic Power Systems

There are several methods to increase the energy efficiency of a hydraulic circuit. To avoid any confusion, they are classified into three categories.

- Energy efficient valve controlled systems,
- Variable displacement pump control systems,
- Variable speed pump control systems.

In the first class of systems, the control principle is not changed; still the flow rate through the hydraulic actuator is controlled via flow control valve, but the system efficiency is increased by modifying circuit components. In the second and third class of systems, the control principle is completely changed. The flow rate going through the hydraulic actuator is not adjusted via valves, but the pump itself, thus eliminating all the throttle losses. In the following sub-section, the techniques used to increase the efficiency of valve control system will be discussed, in Section 2.2.2 the variable displacement pump control circuits will be introduced, and in Section 2.2.3 the variable speed pump control circuits will be introduced which is the subject of this thesis study.

2.2.1 Energy Efficiency in Valve Controlled Circuits

In Section 2.1 it is stated that most of the power supplied to the hydraulic system is lost on the relief valve in order to maintain a constant pressure at the valve intake. It is also discussed that this lost should be minimized if the excess flow passing through the relief valve is reduced by means of regulating the flow rate delivered by the pump.

In order to decrease the power losses on the relief valve, pressure compensated variable displacement pumps are used. This system is also referred as the "demand flow system" because the pump supplies only the required flow rate to minimize the excess flow passing through the relief valve. The schematic diagram of this type of pump is shown in Figure 2-5.

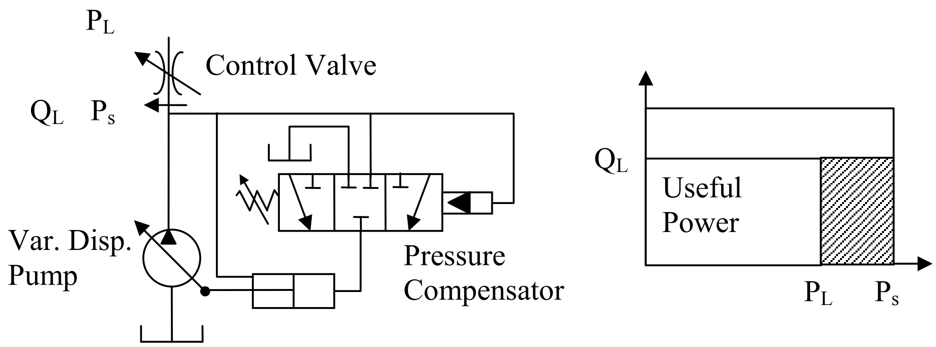

Figure 2-5 Pressure Compensated Pump [23]

In this system, the pump is running at a constant speed; however, the flow rate is adjusted by adjusting the pump displacement. When the pump output pressure comes to its regulated pressure, the pump decreases its pump displacement and supplies right amount of flow only to maintain the pump output pressure. When a flow is demanded by the load, it increases its displacement and supplies only the required rate of flow, without changing the pump output pressure. By this way, theoretically, the relief valve losses represented by the area 2 of the Figure 2-4 is eliminated totally, thus the new power losses of the system is only on the flow control valve and represented by the dashed area shown in Figure 2-5.

Another technique to increase the energy efficiency is to use load sensing pumps. Like the pressure compensated pump, the load sensing pump delivers only the required flow rate by the load but differently the pump output pressure changes according to the load pressure. In this system, not the valve supply pressure but the differential pressure across the valve is constant. The schematic diagram of load sensing pump is shown in Figure 2-6.

In this system, the load pressure is fedback to the pump compensator. The compensator control valve inside the pump adjusts the pump displacement to maintain a constant pressure drop across the flow control valve and in the mean time delivering the required flow rate. Because the valve supply pressure is not constant, but changes to maintain a constant pressure drop over the flow control valve, the power loss on the flow control valve, which was represented by the area 3 in Figure 2-4, is reduced and represented by the dashed area in Figure 2-6.

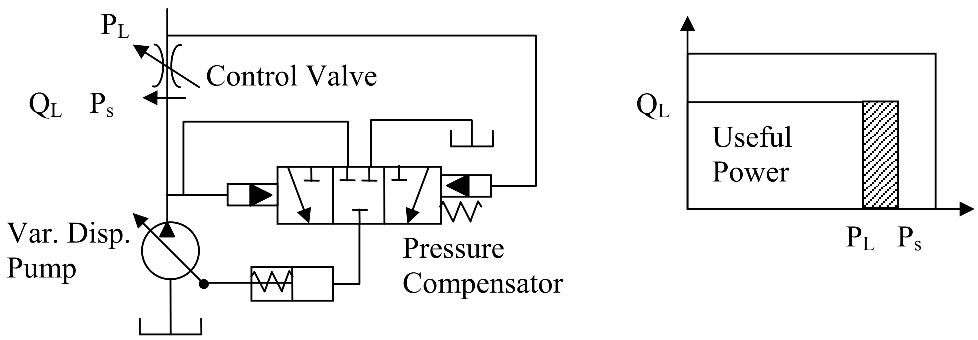

Figure 2-6 Load Sensing Pump Schematic [23]

There are also electro-hydraulic load sensing systems where the pump output pressure and the flow rate delivered to the system are adjusted by changing the drive speed of a constant displacement pump. Figure 2-7 shows the circuit diagram of an electro-hydraulic load sensing system circuit diagram.

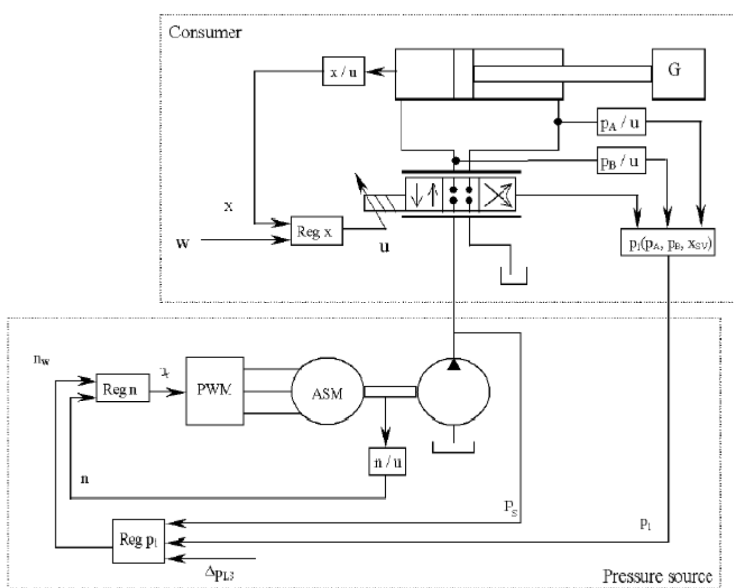

Figure 2-7 Electro-Hydraulic Load Sensing System with Constant Displacement Pump [8]

In Figure 2-7, the pump is driven by an AC asynchronous motor. The drive speed of the motor is controlled by a frequency converter according to the feedback pressure signals of the load pressure, pump output pressure, and the pump angular velocity [8,9].

Except for the relief valve, there occurs a considerable amount of power loss on the flow control valve itself. In recent years, a new valve technology is developed to reduce the power loss on the flow control valve, by mechanically decoupling the meter in meter out ports. The schematic diagram of the new valve control concept utilizing individual metering is shown in Figure 2-8. In the first circuit two 3/3 valves are used and in the second circuit four 2/2 valves are used.

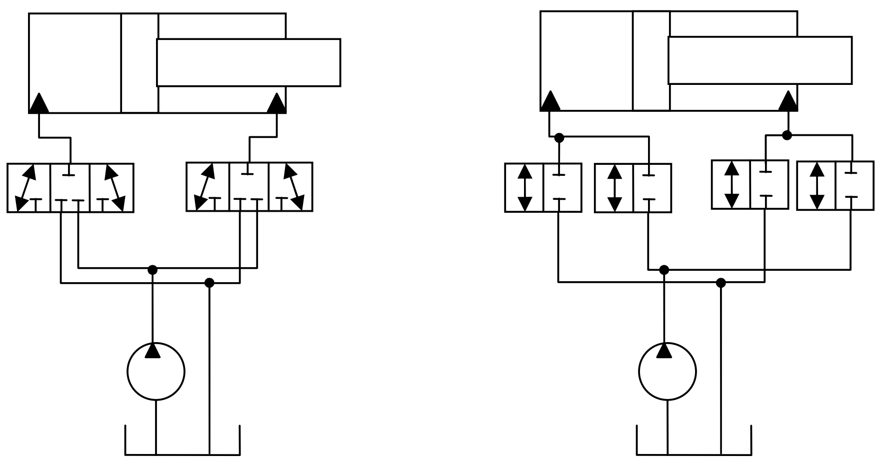

Figure 2-8 Individual Meter In Meter Out Valve Control System [24]

In a 4-way valve, the meter-in port and the meter-out port are mechanically linked together, so that their resistances to flow are also dependent. But in an individual meter-in meter-out valve, all ports are independent giving a control flexibility to improve system efficiency by adjusting the port resistances independently. For example, while extending the hydraulic cylinder with an opposing resistive load, the valve resistance of the meter-in port is adjusted to satisfy the velocity and force requirements. However, the resistance of the meter-out port is adjusted only to deliver the flow back to the oil reservoir. This provides a considerably energy saving as the power loss on the meter-out port will not be the same as the meter-in port but lesser.

The individual meter-in meter-out valve control concept is a developing research area; despite its complex control strategy it also allows energy regeneration and energy recuperation [24].

Note that in all three techniques discussed above, the final control element is the valve. Therefore, there is always a throttling loss to regulate the flow rate through the actuator. Of course, the most obvious way to get rid of throttling losses is not to use valves. In the next sections valveless hydraulic control systems are discussed.

2.2.2 Variable Displacement Pump Controlled Systems

A variable displacement pump is a positive displacement pump, where its displacement therefore the volume swept by the pump in one revolution can be changed. Shown in Figure 2-9 are two different types of variable displacement pump. The displacement of the vane type pump can be changed by changing the eccentricity ratio defined by "e" in the Figure 2-9-a and the displacement of the piston pump can be changed by changing the swash plate angle defined by "α" in Figure 2-9-b. Generally the variable displacement piston pumps are used in hydraulic applications as they are more suitable to work with high pressures.

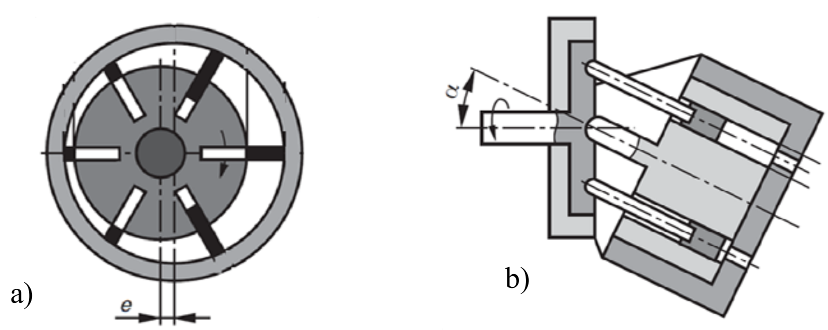

Figure 2-9 Variable Displacement Pumps a) Vane Pump, b) Piston Pump

The drive speed of the pump is kept constant; therefore, internal combustion engines as well as electric motors can be utilized as the pump driver. This feature makes them suitable especially for mobile applications.

Using the pump as the final control element is not a new concept. The variable displacement pumps are generally utilized in hydrostatic transmission systems, where the pump drives a hydraulic fixed displacement motor. The speed and direction of the motor is adjusted by the swash plate angle of the variable displacement pump. A simple circuit diagram of the hydro-static transmission system is shown in Figure 2-10, where an auxiliary constant displacement pump is utilized to keep a minimum pressure in each line and compensate the leakages of the system.

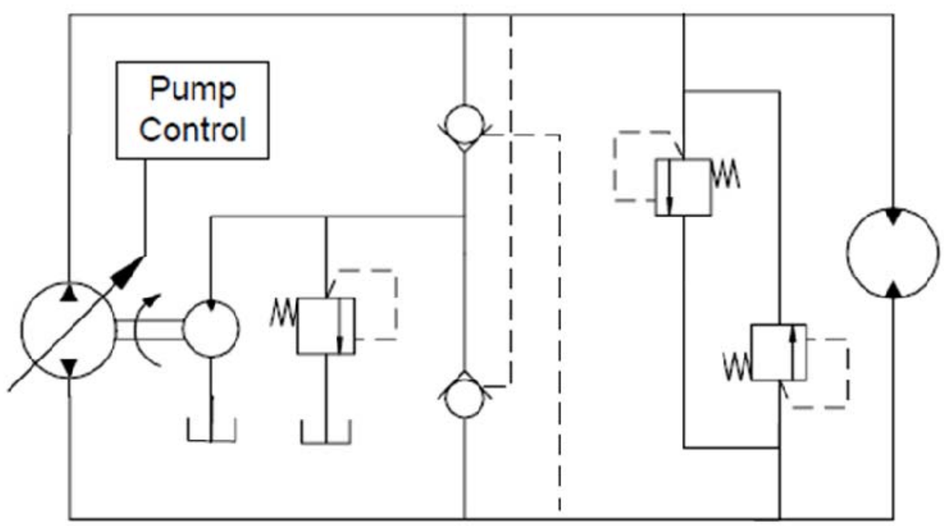

Figure 2-10 Hydrostatic Transmission System with Variable Displacement Pump Control Technique

Note that if the leakages are assumed to be zero, then the input flow rate of the variable displacement pump will be equal to the output flow rate of the actuator. This is due to the symmetric geometry of the hydraulic motor. The case will be the same if a double rod symmetric actuator is to be utilized as the hydraulic actuator.

However, in industrial applications, single rod actuators have a common use for space restriction reasons. This kind of asymmetric actuator cannot be controlled by a single variable pump without additional devices for balancing unequal flow. One solution to use of single rod actuator is presented by Goldenberg and Habibi [3]. They designed a single rod actuator, with equal effective pressure area as shown in Figure 2-11. As the ingoing and outgoing flow of the actuator is the same, the simple hydro-static circuit can be applied to this new type actuator.

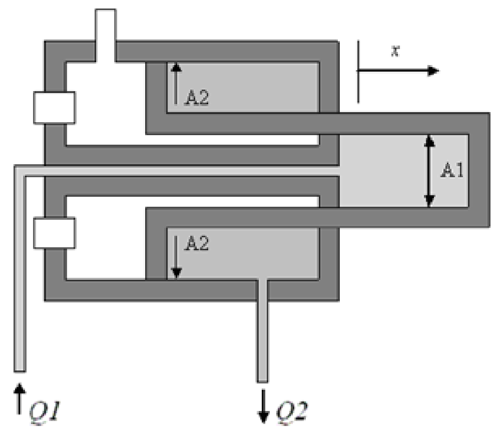

Figure 2-11 Single Rod Symmetric Linear Actuator [25]

The general use of single rod cylinders in industry is not only for space requirements but also for its compact simple design and mostly for its low price, however the design of Goldenberg and Habibi is not cost effective due to the increased precision of the actuator.

For the control of a standard asymmetric cylinder Rahmfeld and Ivantsysnova proposed a new circuit solution to control a differential cylinder as shown in Figure 2-12 [7]. In this circuit the variable displacement pump (1) is the final control element, a secondary pressure compensated pump (4) and a hydraulic accumulator (5) are used for compensation of the in going and outgoing flow of the cylinder chambers on the low pressure side. Two pilot operated check valves (3) are used to make sure that the low pressure side of the hydraulic cylinder (2) is always connected to the accumulator. Different from the conventional hydrostatic systems, this circuit uses an hydraulic accumulator as an energy storage element. When the load is working in motor mode, the low pressure side fills the accumulator.

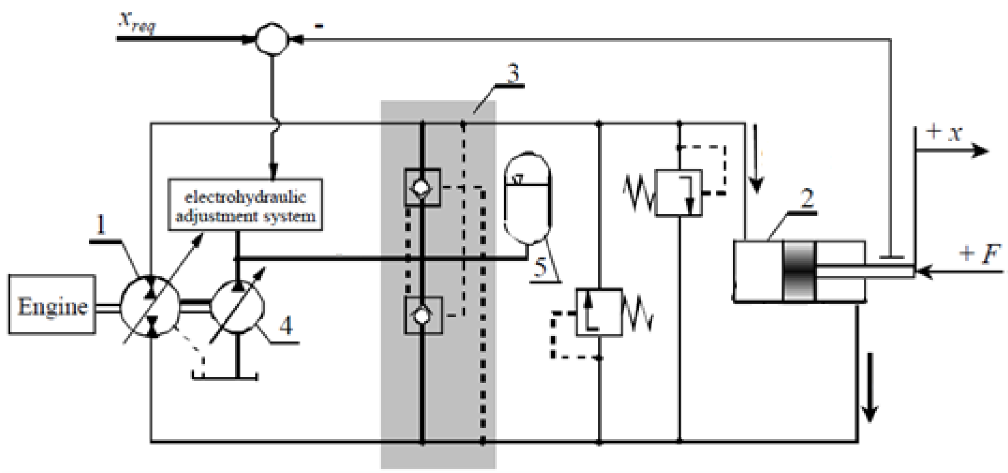

Figure 2-12 Displacement Controlled Drive with Single Rod Cylinder in Position Control [7]

Using pumps as the final control element offers the most energy efficient hydraulic control system, as all the throttling losses in the system are eliminated. Rahmfeld compared the energy efficiency of the displacement controlled drive with the load sensing system on a excavator. The load sensing system efficiency on the excavator was always smaller than 40% while the displacement controlled systems maximum efficiency was 70%.

Different from changing the pump displacement, the pump flow rate can also be regulated by changing pump drive speed. Then the same variable displacement pump control circuits can be used as the variable speed pump control circuits. In the next section, the variable speed pump control will be introduced.

2.2.3 Variable Speed Pump Controlled Systems

The variable speed pump control techniques utilize constant displacement pumps. Some types of constant displacement pumps are shown in Figure 2-13. The first one in Figure 2-13-is a screw type pump, the second and third one are internal and external gear pumps. Generally internal gear pumps are utilized as they are more suitable to work with high pressures.

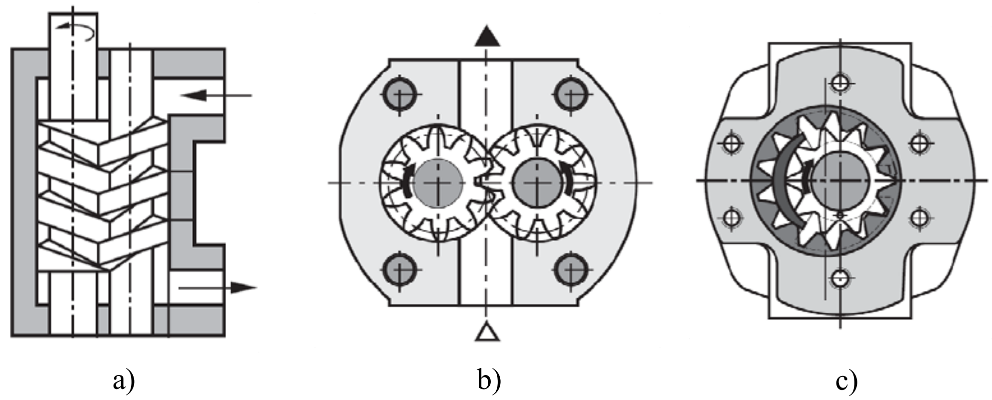

Figure 2-13 Constant Displacement Pump Types a) Screw Type, b) External Gear, c) Internal Gear

It should be noted that, according to the type of the application, these hydraulic pumps should be able to turn into reverse direction without a dead band at zero velocity also; hence, in many applications, they are operated under high pressure and nearly zero speed. This is a drawback of the speed controlled pump systems, because standard pumps are not designed to run around zero speed and the pump efficiency in component level around zero speed is very low. For this reason, specially designed pumps with equal resistance for the flow rate turning both directions should be used. Furthermore, they should be able to work as a hydraulic motor. They should not only transmit the energy from the electrical drives to the hydraulic system but also should be able to transmit the energy of the hydraulic system back to the electrical drives. For example, while braking an inertial load, some of the energy is dissipated by friction and the remaining is to be transmitted over the pump to an energy storage element like a hydraulic accumulator or to an energy dissipation or transformer element like the servomotor drives.

Different from the variable displacement pumps, as the drive speed of the pump is controlled to regulate the demanded flow rate of the system generally electrical drives are utilized as the pump drive elements. This is another drawback of variable speed pump control systems in mobile applications.

The variable speed pumps can be utilized in the hydrostatic circuits in place of variable displacement pumps. In Figure 2-14, where the hydrostatic circuit of Goldenberg and Habibi [15] is shown, a special symmetric single rod cylinder is used as the actuator. The circuit is the same with the classical hydro-static circuits, except a hydraulic accumulator is utilized to keep a minimum pressure in hydraulic lines and compensate the leakages. The hydraulic pump is driven by a 3-phase AC electrical motor. A high gain inner loop velocity controller is used for the electric motor to alleviate the effect of dead band of the hydraulic system [15]. It has demonstrated a high level of performance moving a load of 20 kg with an accuracy of 10 μm and a rise time of 0.2 seconds.

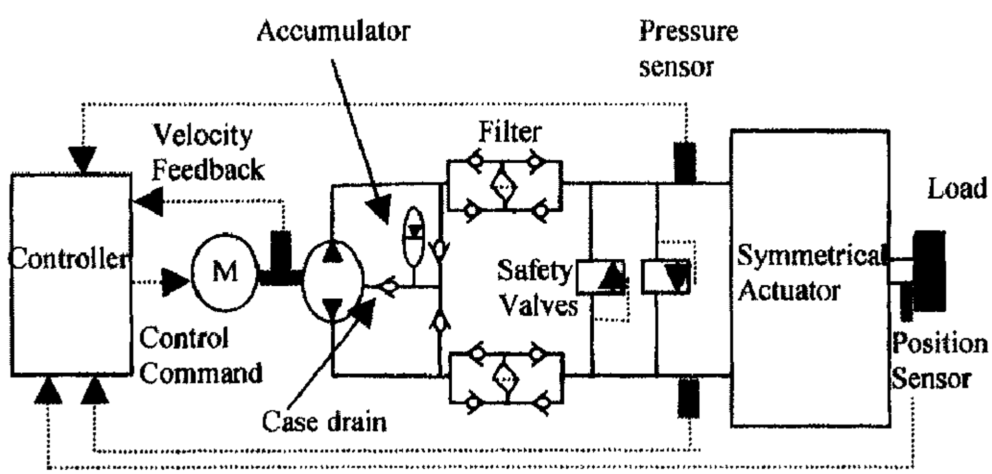

Figure 2-14 Electro Hydraulic Actuation System of Habibi and Goldenberg with Symmetric Actuator [3]

Not only the symmetric actuators but also the asymmetric actuators like single rod cylinder can be controlled by speed controlled pumps utilizing the same circuit solutions of the variable displacement pumps. However, they are not given here in order to avoid repeating similar points. Instead, different circuit configurations for the control of single rod hydraulic actuators are discussed below. They may be named as two pump control.

Shown in Figure 2-15 are the possible circuit schemes of two pump control method offered by many researchers [26, 19] for the control of asymmetric cylinder. The flow deviation of the inlet and outlet cylinder chambers due to area ratio is compensated by utilizing a second pump.

The first two circuit solutions have an open circuit configuration, and the last two have a closed circuit solution; that is, the oil returning from the hydraulic actuator directly goes through the pump inlet instead of returning to the oil reservoir. The open circuit solutions are advantageous to closed circuits, in terms of heat dissipation; because, the returning oil to the reservoir can be cooled there. This is a desired and mandatory process in valve controlled systems as much of the power is used to heat the hydraulic oil; however in pump controlled systems as there are no throttling losses cooling the hydraulic oil is not much of interest as in the valve controlled case. Furthermore, in the closed circuits proposed not only all the flow exiting from the cap end of the cylinder goes through the pump, but some of it returns to oil reservoir.

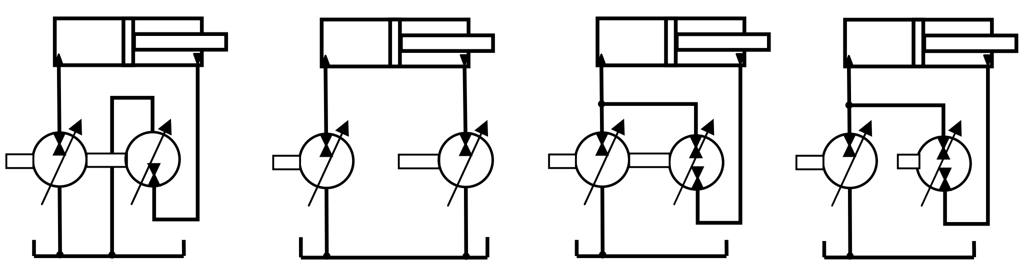

Figure 2-15 Two Pump Control Circuit Configurations

In Figure 2-15 the 1st and 3rd circuit solutions use one angular rotation source to actuate the both pumps, while in the 2nd and 4th circuit solutions use two independent drive sources to actuate the pumps. This is a big advantage in comparison as the number of power source directly affects the system's cost. However, these solutions are proposed both for variable displacement and variable speed pump control techniques. In variable displacement pump control technique, because the flow rate is adjusted via pump displacement, the actuation of the pumps from the same source is not much of interest. However in variable speed pump control, this means a reduction in control elements. It should be noted that in order to drive a load with a given speed and direction, one pump should deliver hydraulic oil to the one cylinder chamber and the other pump should suck hydraulic oil from the other cylinder chamber, assuming that they are turning in same direction. However, to pressurize the cylinder chambers without moving the load, both pumps should deliver hydraulic oil to the cylinder chambers, meaning that they should be turning in reverse directions. The 1st and 3rd circuit solution can accomplish both of these two missions if a variable displacement pump is used. However, they cannot do so if a variable speed pump technique is used as they will be forced to turn both in the same and in the reverse direction. Pressurizing the cylinder chambers without moving the load is a necessary operation, because to move a load one cylinder chamber pressure should is decreased while the other is increased. Then, before applying a dynamic load pressure change, two chambers should be pressurized at a static equilibrium in order not to be exposed to any negative pressure.

The 2nd and 4th circuit solutions with independent pump actuators remain to be convenient for the variable speed pump control technique. In the 2nd circuit scheme, the direction and the velocity of the hydraulic cylinder are determined by both pumps. However, in the second circuit solution, the velocity and direction of the cylinder are determined by only one pump which is connected between the cylinder chambers whereas the other pump connected to the hydraulic tank and cap end of the cylinder only compensates the flow rate difference due to the area ratio. This can be well understood if the cylinder areas are assumed to be constant, then without any leakage only the pump connected to both cylinder chambers is to be able to drive the load, resembles the hydrostatic circuit. Furthermore, in the open circuit scheme, the two pumps work in 2-quadrant; the direction of flow of the pumps change but the direction of load pressure on the pumps are fixed. However, in the closed circuit scheme, the pump connected between the two chambers of the hydraulic cylinder, work in 4-quadrant while the other pump works in 2 quadrant.

In this thesis, the closed loop hydraulic circuit solution utilizing two pumps with independent actuators (circuit scheme 4) is adopted for the position control of a hydraulic differential cylinder. In the next chapter, the constructed test set up is explained, the working principle of the circuit and control scheme are presented in detail, and the mathematical modeling of the whole system is given in depth.

CHAPTER 3

SYSTEM MODELING AND SET UP CONFIGURATION

In this chapter a detailed analysis and a description of the physical model of the experimental test set-up and its components will be stated. In Section 3.1 the test set-up components both for pump controlled and valve controlled system are to be introduced. In Section 3.2 the mathematical model of the variable speed pump controlled system and in Section 3.3 the mathematical model of the valve controlled system is to be obtained.

3.1 Experimental Test Set-up

An experimental test set-up is constructed to test the two different; pump controlled and valve controlled, control techniques. Because there will be a comparison, all the components of the experimental test set up, that is the plant, actuators, sensors, hardware and software are kept the same except for the control elements. In the valve controlled system, the final control element is the servo solenoid valve whereas in the pump controlled system the final control element is the variable speed constant displacement pump units. Test set up is constructed in such a flexible way that the same load is actuated with the same actuator, but with different control element after changing the actuator connections.

A photograph of the constructed experimental test set-up is shown in Figure 3-1, and the schematic diagram of the experimental set up is represented in Figure 3-2. The blue lines represent the variable speed pump controlled circuit, and the dashed red lines represent the valve controlled circuit. Switching between the valve controlled and pump controlled circuits are accomplished by changing the coupling connections 1, 2, 3.

In Figure 3-2, it is seen that the variable speed pump control system is composed of three main parts; a hydraulic actuator, two constant displacement pumps, and two servomotors to drive the pumps independently. The position of the differential cylinder is controlled without any throttling elements by adjusting the flow rates of the pumps via controlling the drive speeds of the servomotors. Both pumps can rotate in both directions, according to the flow need of the system.

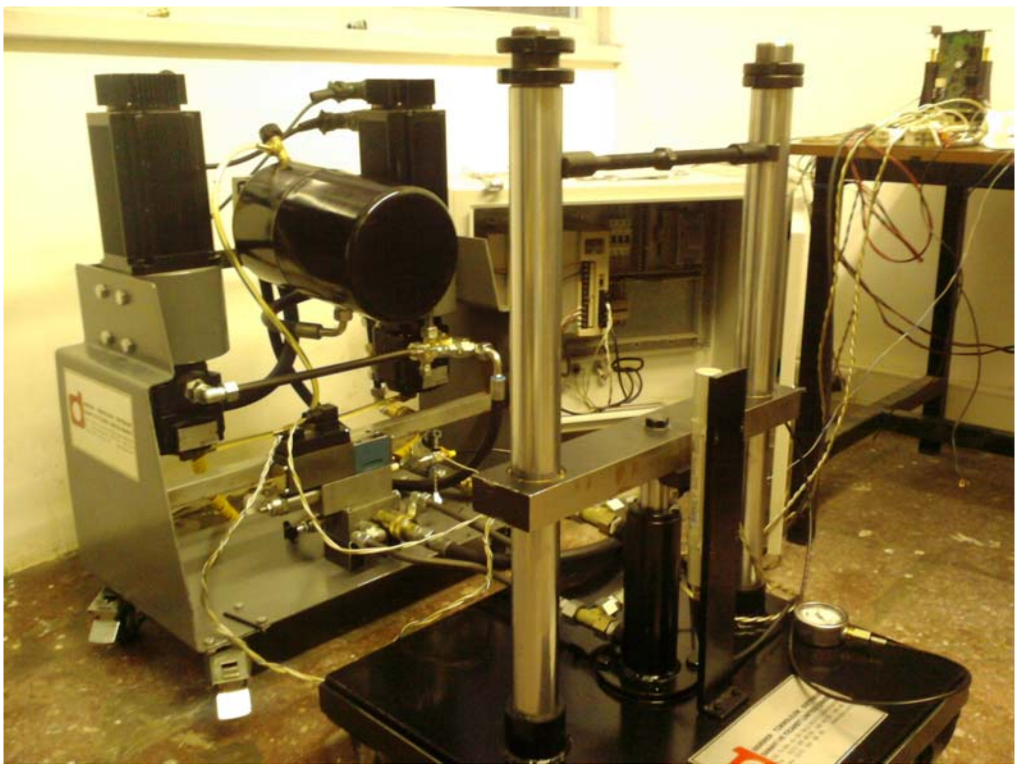

Figure 3-1 A photograph of the Experimental Test Set-Up

The two check valves shown in Figure 3-2 are for safety reasons of the pump controlled circuit. The check valves permit flow in one direction, from tank to the cylinder chambers A or B, and block the flow to the opposite direction. In normal operation conditions, the check valves remain close as both the hydraulic cylinder chambers are pressurized. In case of an unexpected pressure drop (negative pressure) where the pressure differential across the valve is greater than the cracking pressure, the check valve opens and a passage occurs between the chamber lines A/B and the tank. Thus, the suction of the pump is done through the check valve and the possibility of cavitations is prevented.

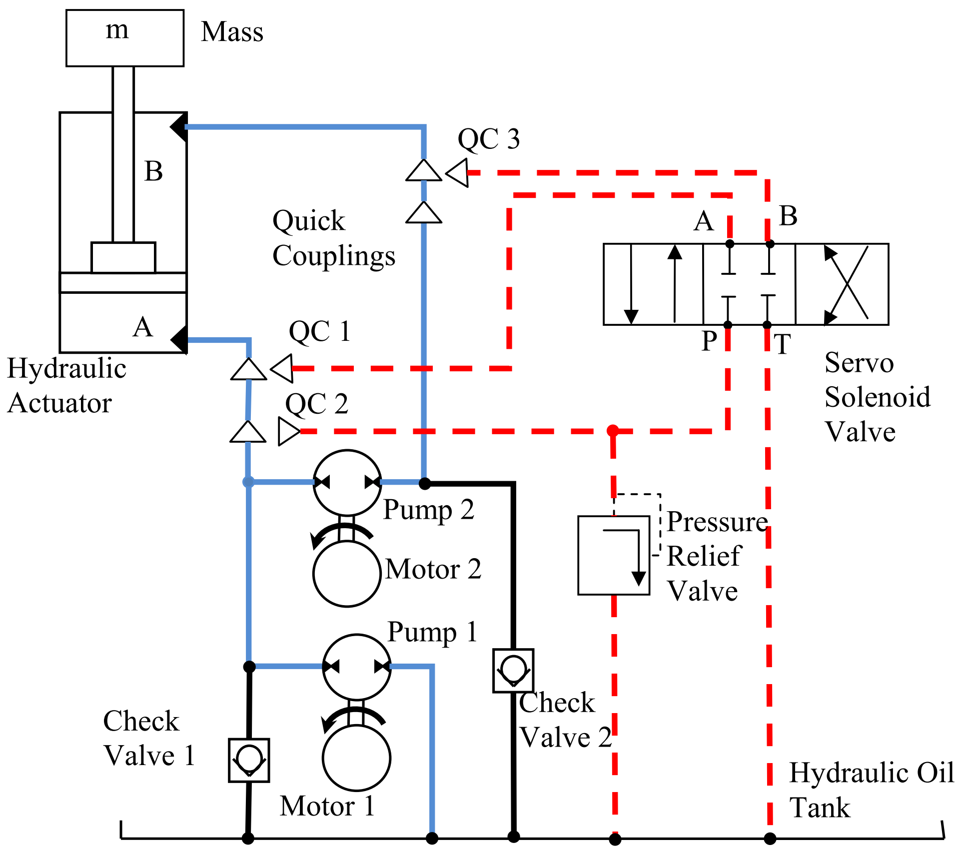

Figure 3-2 Schematic Diagram of the Experimental Test Set-Up

Valve controlled circuit is a conventional common use circuit. It is the same that is investigated in Section 2.1 and represented in Figure 2-2. During the valve control operation the pumps drive speeds and directions are constant. The two pump both suck oil from the tank and deliver flow to the servovalve inlet. In order to not to add any additional hoses to the system, the suction of the servo pump 2 is kept the same; thus, it sucks oil through the check valve 2. At the pump outlet, there stays a pressure relief valve, it is used to limit the supply pressure of the pump. The servo solenoid valve in the circuit serves as the final control element, the direction and magnitude of the flow rate going through the hydraulic cylinder is controlled by adjusting the servo solenoid valve spool position.

The experimental test set-up components are,

- Hydraulic oil,
- Hydraulic pumps (internal gear pump/motor unit),
- Hydraulic actuator,
- Transmission line elements,
- Load,
- Servo proportional valve and valve driver,
- Servomotors and motor drivers,
- Sensory elements,
- Computer environment and DAQ card.

Hydraulic Oil

Hydraulic oil is the main element of a hydraulic system as it serves as the power transmission medium. Shell Tellus 37 type mineral hydraulic oil is used in the experimental test set up. This oil is chosen due to its general use in most of the industrial hydraulic applications because its very low viscosity variation with temperature, high shear stability, outstanding anti-wear performance, and oxidation resistant and corrosion protection properties. The physical properties of the hydraulic oil are listed in Table 3-1.

Table 3-1 Hydraulic Oil Properties

Manufacturer and type	Shell Tellus 37
Kinematic viscosity at 20 °C	100 mm^2/s
Density at 15 °C	875 kg/m^3
Pour Point	-33 °C
Flash Point	207 °C
Bulk Modulus	1300 MPa

Hydraulic Pump

Two Bucher Hydraulics QXM series internal gear pumps are used in the experimental test rig. The pumps used in this project differ from the standard pumps. Due to their symmetric design, these pumps can operate both as a hydraulic pump or as a hydraulic motor and direction of rotation is not restricted. This is called 4-quadrant operation. Some properties of the hydraulic pump/motor unit is listed in Table 3-2.

Table 3-2 Hydraulic Pump/Motor Unit Properties

Manufacturer and Type	Bucher Hydraulics QXM32-016
Fluids	HLP mineral oils to DIN51524 HFB, HFD and HFC fluids to VDMA 24317
Min. fluid cleanliness level	NAS 1638, class 9 or ISO 4406
Minimum inlet pressure	0.85-2 bar.
Nominal and Effective Displacements	16 -15.6 cm^3/rev
Maximum Speed	3900 rpm as a pump 5500 rpm as a motor
Continuous / Intermitted Pressure	210 / 250 bar
Torque	52.0 N.m

Because the pumps can operate both as a pump and as a motor, they are named as QXM drive unit by the manufacturer, but throughout the thesis they will be named as just "pump".

Hydraulic Actuator

Due to their compact design, low cost and ease of manufacture in most of the industrial applications like presses, injection molding machines, cranes, single rod hydraulic actuators are used. In the experimental test set up a differential cylinder with an area ratio 1.96 is used. The hydraulic actuator at produced in OSTIM Ankara.

Table 3-3 Hydraulic Actuator Properties

Rod diameter	35 mm
Piston diameter	50 mm
Stroke	100 mm

Transmission Line Elements

The transmission line elements consist of hoses, couplings, and fittings. SEMPERPAC 2SNK .DIN 12 ½" W24 X oil resistant synthetic rubber hoses are used in the low pressure lines of the hydraulic system. Since elastic hoses may act as an accumulator and affect the system dynamics when building up pressure, 12 mm and 15 mm steel tubes are used in the high pressure lines of the system to minimize their effects.

Load

A steel plate of mass 11.6 kg is used as the load element. However the total mass of the load is 12.3 kg if the hydraulic cylinder piston mass is to be added. The steel plate is fixed to the hydraulic cylinder via an M16 screw. To restrict the rotation of the plate it is supported with two sliders at each end. The cylinder and load are positioned in the vertical direction to the ground for the purpose of simple construction.

Servo Proportional Valve and Valve Driver

BOSCH 4WRPH type servo solenoid valve with an electrical position feedback is used as the flow control valve. The valve driver is occupied with spool position feedback from the servo proportional valve LVDT, and receives its reference spool position command and other parameters via an DAQ card interface. The valve drive is able to return current spool position and diagnostic information. The properties of the servo solenoid valve used in the test set-up are listed in Table 3-4. The cable connections of the valve driver are given in Appendix D.

Table 3-4 Servovalve Properties

Type	4WRPH 6 C4B24L –2X/G24Z4 /M
Material no	0 811 404 038
Nominal Flow Rate	24lt/min under 70bar valve pressure difference (35bar/metering notch)
Reference Spool Position Command	±10 V
Working Hydraulic Oil	Mineral oil (HL, HLP) to DIN 51524
Power Supply	24V DC

The valve is a single stage proportional valve; however, the position feedback of the valve spool to its drive makes it a high a performance servovalve. The bandwidth of the servovalve for 100% spool is given as 70 Hz, the frequency response (Bode) diagram of the servo proportional valve is shown in Figure 3-3.

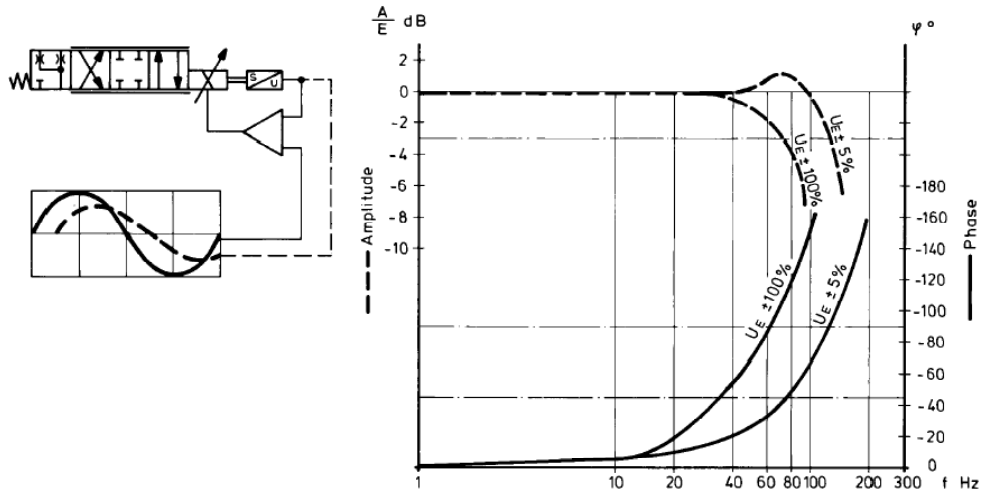

Figure 3-3 Servovalve Frequency Response Diagram [27]

The valve used in the experimental set up is a zero lapped valve; this means that there exists zero orifice opening when the valve is in center position. Therefore, under constant pressure, the differential the valve gain, which is the ratio between the input reference spool position voltage and the valve flow rate, is constant and does not change with valve spool position. The valve flow gain with respect to spool position under 7 MPa pressure differential is shown in Figure 3-4. It is seen that the slope of the line is constant revealing that the valve is zero lapped. It should be strictly noted that while finding the valve flow gain, not the valve pressure differential but the pressure drop at the orifice, which is half of the valve pressure differential for zero lapped valves, should be considered.

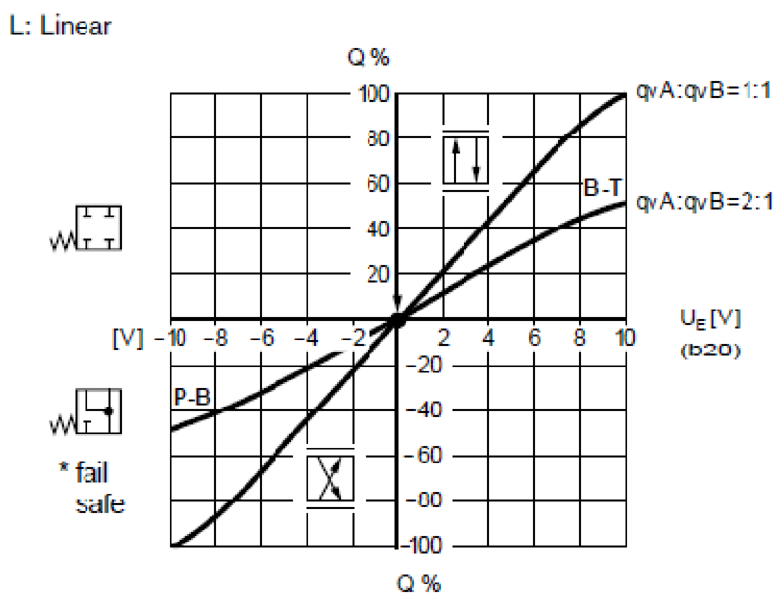

Figure 3-4 Flow Rate versus Valve Spool Position Signal of the Servo Solenoid Valve [27]

Servomotors and Motor Drivers

TECO 9300 JS DA 30 AC servomotors are used as the pump driver. The servomotors are driven with single phase 220 V AC source. The nominal power of the servomotor is 1 kW. The servomotor driver has analog velocity or torque output.

Position Transducer

Balluf BTL series contactless linear position transducer is utilized to measure the position of the steel plate. The stroke of the transducer is 0-100 mm and the resolution is 10 microns. The transducer has a 0-10 V analog output and the supply voltage is 24 V DC.

Pressure Transducer

Stauff SPT B0400 series pressure transmitters are utilized to measure the hydraulic cylinder chamber pressures. The operating range of the transducer is 0-400 bar and the resolution is 4 bar. The output of the transducer is 4-20 mA. The current is converted to 0-10 V analog output via Weidmuller WAS4 series converter. The supply voltage of the pressure transducer and current to voltage converter are 24 V DC.

Computer Environment and DAQ Card

MATLAB R2008b and Simulink software is used for modeling and controller design purposes. The real time control of the system is performed by using the MATLAB xPC Real Time Windows Target module. The discrete solver is used in all real time control applications with a sampling frequency of 1,000 Hz.

National Instruments 6025E type data acquisition card is utilized in the test set up. The card has 16 analog input channels and 2 analog output channels. The analog input channels of the card are utilized to interface with the pressure and position transducer and the analog outputs channels are utilized to interface with the servomotor and servovalve drives.

All the connections of the data acquisition card for valve the valve controlled and pump controlled system are shown in Appendix D.

A SCB 100 shielded connector block with 100 screw terminals is utilized to interface between the transducer and drives signal cables and the data acquisition card.

A standard desktop PC is utilized as a target PC.

Pressure Relief Valve

Bucher Hydraulics DVPA 10 HM series pressure relief valve is used to limit the pump exit pressure. The pressure range of the relief valve is 10-210 bar. The cracking pressure is set with a screw adjuster.

3.2 Pump Controlled System

In Section 3.2.1 a brief explanation of the variable speed pump controlled system operation is given. In Section 3.2 the mathematical model of the pump controlled hydraulic position system is obtained; the steady state characteristics of the system is investigated; the relation between the steady state pumps speeds, which are required to pressurize cylinder chambers and compensate for the leakages, are obtained; the dynamic characteristics of the systems is investigated and a transfer function between the second pump speed and hydraulic cylinder rod velocity is derived.

3.2.1 Principle of the Hydraulic Circuit

Figure 3-5 shows a variable speed pump controlled differential cylinder position control system. The system consists of two independent control loops; namely, the pressure and position control loops. The inputs to the system are x_{ref} which is the reference position and p_{sum}, which is the desired value of the chamber pressure sum at steady state given as

$$p_{sum} = p_{A\_ss} + p_{B\_ss} \tag{3.1}$$

The pressure control loop is an open loop static process, aiming to pressurize the cylinder chambers to a predetermined value and to assure a static force balance. At steady state, the cylinder chambers are pressurized to compensate for the pump leakages; if not, the hydraulic cylinder will not be stable and move freely under any disturbance due to pump leakages. Pump 2 turns in negative direction and supply flow to the cylinder chamber B. Some of the oil is compressed to form p_B and some to compensate the internal and external leakages of the chamber B. Pump 1 turns in positive direction some of the flow rate supplies the need of pump 2, some of the flow is compressed to form p_A and remaining is used to compensate the leakages of chamber A.

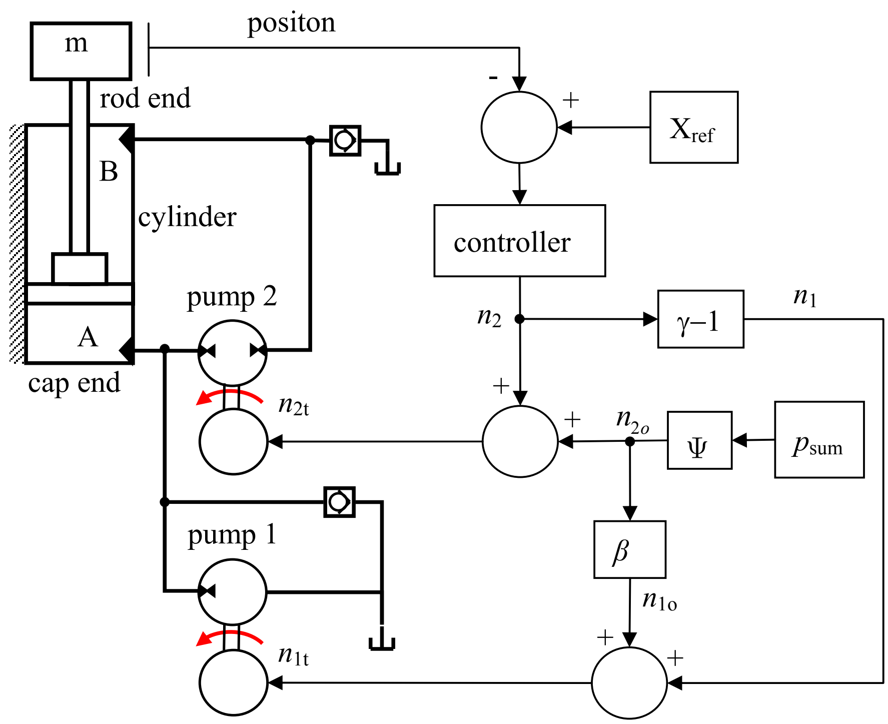

Figure 3-5 Variable Speed Pump Control Circuit

It is important to note that the revolutions of pump 1 and 2 are not independent. As the static balance of the cylinder is aimed, there exist a ratio β which completely depends on the leakage characteristics of the system and assures a stationary hydraulic cylinder. The definition of β is given as

$$n_{1o} = \beta n_{2o} \tag{3.2}$$

where n_{1o} and n_{2o} represent the offset pump speeds of pumps 1 and 2, respectively. Note that since directions of rotations of the pumps is opposite, the β

constant has a negative value. The other constant in the pressure control loop is Ψ which determines the relation between desired sum pressure and the pump 2 speed. The constants β and Ψ can be found from the system continuity equations at steady state.

The position control loop is a closed loop dynamic process. The position of the hydraulic cylinder is measured and feedback to the controller. After comparing with the reference position signal the controller creates manipulated input signal n_2 and sends to the servomotor drivers.

Assuming all the leakages of the system are compensated, if the hydraulic actuator is a double rod actuator having equal cylinder areas, then pump 2 will be adequate to control the direction and the velocity of the actuator. However the hydraulic actuator used in this thesis study is a single rod differential cylinder, with an area ratio greater than one and defined by Eq. (3.3).

$$\gamma = \frac{A_A}{A_B} > 1 \tag{3.3}$$

Therefore, the output flow of the chamber 2 is not equal to the inlet flow rate of the chamber B due to the area difference of the differential cylinder for a given cylinder speed. To compensate this asymmetric flow rate, there is a ratio between the dynamic pump speeds determined by the area ratio and defined by Eq. (3.4)

$$n_1 = (\gamma - 1) n_2 \tag{3.4}$$

By this way, pump 2 controls the direction and speed of the actuator while pump 1 compensates the asymmetric flow rate due to the difference in areas on two sides of the piston. During the extension, pump 1 provides the lacking flow for the cap end and during the retraction it absorbs the excess flow of pump 2.

3.2.2 Mathematical Modeling of the System

The pump controlled hydraulic position system consists of four main parts:

- Hydraulic pumps,
- Hydraulic differential cylinder,
- Servomotors,
- Transmission line elements.

Here, the mathematical modeling of the hydraulic pumps and the hydraulic cylinder is explained in detail. The servomotors are not modeled and are assumed to be ideal angular velocity sources, as each has a controller inside and both have higher dynamics than the hydraulic system. Furthermore, all hydraulic transmission lines are assumed to be lossless and not modeled. However, the hydraulic capacitances constituted by the transmission line volumes which affect the dynamics of the system heavily, are lumped into the associated hydraulic cylinder chamber volumes. The mathematical models of the remaining parts of the system are given below.

3.2.2.1 Pump Model

Two identical internal gear pumps are used in this application. The pumps used in this project differ from the conventional pumps in terms of their symmetric design. The inlet and outlet ports are of the same geometry and have equal resistance to the flow in both directions. This gives the pumps the ability to operate in 4-quadrants. The "4-quadrant" stands for the 4 quarter of the differential pressure Δp versus flow q plane. Operation in 4-quadrant is an important property as the load locus is in 4-quadrants the pumps and the servomotor should be able to operate in 4-quadrants.

Operation in 4-quadrant means that the pump unit can both work as a hydraulic pump or a hydraulic motor that is both the high pressure port and the flow direction can change. Figure 3-6 represents on the pump how the high and low pressure ports and the flow direction changes in the 4-quadrant.

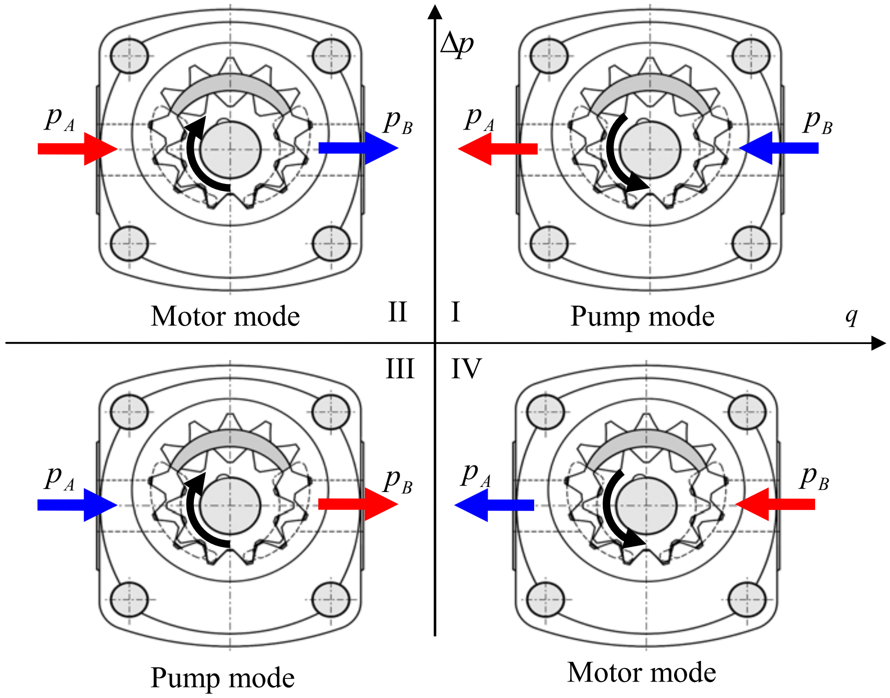

Figure 3-6 Hydraulic Pump Operation in 4 Quadrants

In Figure 3-6 the counter clockwise (CCW) rotation of the pump is assumed to be positive. The high pressure port is designated with red arrow and the low pressure port is designated with blue arrow. The A side (left side) of the pump is defined as the outlet and the B side (right side) of the pump is defined to be the inlet port.

- In the 1st quadrant the differential pressure between the inlet and the outlet ports of the pump is positive, $\Delta p = p_A - p_B > 0$ and the pump is running in positive direction, thus the power transmitted to the system is positive $\Delta p \cdot q > 0$ and the pump is working on the pump mode.
- In the 2nd quadrant the differential pressure between the inlet and the outlet ports of the pump is positive, $\Delta p = p_A - p_B > 0$ but the pump is running in negative direction, thus the power transmitted to the

system is negative $\Delta p \cdot q < 0$, in other words system is doing work on the pump and the pump is working on the motor mode.

- In the 3rd quadrant the differential pressure between the inlet and the outlet ports of the pump is negative, $\Delta p = p_A - p_B < 0$ and the pump is running in negative direction, thus the power transmitted to the system is positive $\Delta p \cdot q > 0$, and the pump is working on the pump mode.
- In the 4th quadrant the differential pressure between the inlet and the outlet ports of the pump is negative, $\Delta p = p_A - p_B < 0$ and the pump is running in positive direction, thus the power transmitted to the system is negative $\Delta p \cdot q < 0$, in other words system is doing work on the pump and the pump is working on the motor mode.

Flow Losses

There are factors like temperature, pressure, speed etc. affecting the leakage coefficients meaning that machine performance is almost impossible to define in general terms [28]. But, in literature, it is seen that simple linear terms may be adequate to model the flow losses for systems performance studies. As the flow rate of the leakage through its path is generally very small, the leakage flow can be assumed to be laminar, and then the leakage flow will only depend on the pressure differential.

The following assumptions are made for modeling the flow losses of a pump/motor unit.

- The flow losses of the pump/motor unit consists of the internal leakages, external leakages and the losses due to compressibility.
- The internal leak leakage of a pump/motor unit is proportional to the differential pressure between the inlet and outlet ports.
- The external leakage flow contains two components. One component of the external flow is from high pressure side to the pump casing and the remaining part of the external leakage is from

low pressure side of the pump to the pump casing. The pressure inside the casing is negligible.

According to the assumptions given above, the losses in a pump/motor unit can be expressed as below.

q_i : Internal (cross-port) leakage flow

q_{ea} , q_{eb} : External leakage flow losses from high and low pressure sides to the casing

q_{ca} , q_{cb} : Compressibility flow loss at the high and low pressure side

These loss terms are represented in Figure 3-7 on a hydraulic pump and a hydraulic motor separately. The q_t in the figure is the theoretical flow rate.

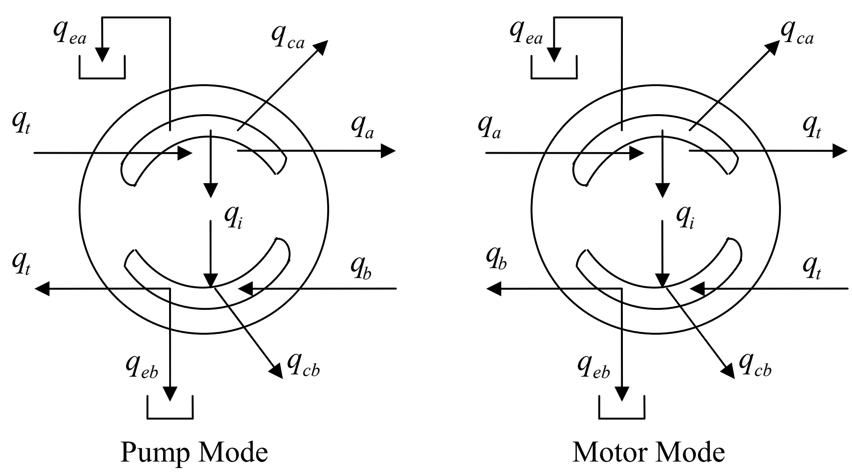

Figure 3-7 Representation of Flow Losses in Hydraulic Pumps and Motors [28]

From Figure 3-7 the flow continuity equations are written in terms of flow rates for the hydraulic pump at its outlet port

$$q_a = q_t - q_i - q_{ea} - q_{ca} \tag{3.5}$$

and at its inlet port

$$q_b = q_t - q_i + q_{eb} + q_{ca} \tag{3.6}$$

for the hydraulic motor at its inlet port

$$q_{a\_m} = q_t + q_i + q_{ea} + q_{ca} \tag{3.7}$$

and at its outlet port

$$q_{b\_m} = q_t + q_i - q_{eb} - q_{ca} \tag{3.8}$$

The theoretical or ideal flow q_t, is caused by gear displacement as defined by the ideal equation,

$$q_t = n_P D_p \tag{3.9}$$

It was assumed that the internal leakage is proportional to the differential pressure across the ports

$$q_i = C_i \left(p_a - p_b \right) \tag{3.10}$$

The external leakages will be proportional to inlet or outlet port pressure when the drain pressure is neglected.

$$q_{ea} = C_{ea} \cdot p_a \tag{3.11}$$

$$q_{eb} = C_{eb} \cdot p_b \tag{3.12}$$

The flow loss due to compressibility of the hydraulic fluid is modeled as follows.

$$q_{ca} = \frac{D_p}{E} \frac{dp_a}{dt} \tag{3.13}$$

$$q_{cb} = \frac{D_p}{E} \frac{dp_b}{dt} \tag{3.14}$$

Where D_p is the pump displacement; and since it is very small with respect to transmission lines and cylinder chamber volumes, the compressibility losses can be neglected and lumped into the transmission lines and the cylinder.

From the flow continuity Eqs. (3.5) to (3.8), written for the hydraulic pump and hydraulic motor, it seems that two different formulation should be written for the internal gear pump unit whether it is operating in pump mode or motor mode. However if the flow continuity equations are written in terms of port pressures, then the signs of the coefficients will automatically be corrected, regardless of pump mode or motor mode. Of course to do so, the inlet and the outlet ports of the pump unit should be defined and fixed.

As shown in Figure 3-5, the counter clockwise rotation of the pumps are assumed to be positive. Then, for pump 1, the port connected to the cap end of the hydraulic cylinder (chamber A) is defined as the inlet port and the port connected to the hydraulic tank is defined as outlet port and for pump 2, the port connected to the rod end of the hydraulic cylinder (chamber B) is defined as the inlet port and the port connected to the cap end of the hydraulic cylinder (chamber A) is defined as the outlet port.

Neglecting the compressibility losses in the pump displacement volume and assuming that the internal leakage flow coefficients of the pumps are the same, since the two pumps used in the test set up are identical; the flow continuity equations for the pump/motor units can be expressed as

for the outlet (A side) port of pump 2,

$$q_{p2A} = D_P n_p - C_i \left(p_A - p_B \right) - C_{ea} p_A \tag{3.15}$$

for the inlet port (B side) port of pump 2,

$$q_{p2B} = D_P n_p - C_i \left(p_A - p_B \right) + C_{eb} p_B \tag{3.16}$$

for the outlet (A side) port of pump 1,

$$q_{p1A} = D_P n_p - C_i p_A - C_{ea} p_A \tag{3.17}$$

Note that these equations from Eq. (3.15) to Eq. (3.17) are valid in 4-quadrants, the signs of the coefficients do not change according to the working mode pump or motor. The terms p_A and p_B represent the hydraulic cylinder cap end side and rod end side chamber pressures not the high and low pressure ports of the hydraulic pump/motor.

In Figure 3-8, a positive q_{p1A} stands for a flow rate delivered by the pump 1 to the cap end side of the hydraulic cylinder (chamber A). A positive q_{p2A} stands for a flow rate delivered by the pump 2 to the hydraulic cylinder chamber A, and a positive q_{p2B} stands for a flow rate sucked by the pump 2 from the hydraulic cylinder chamber B.

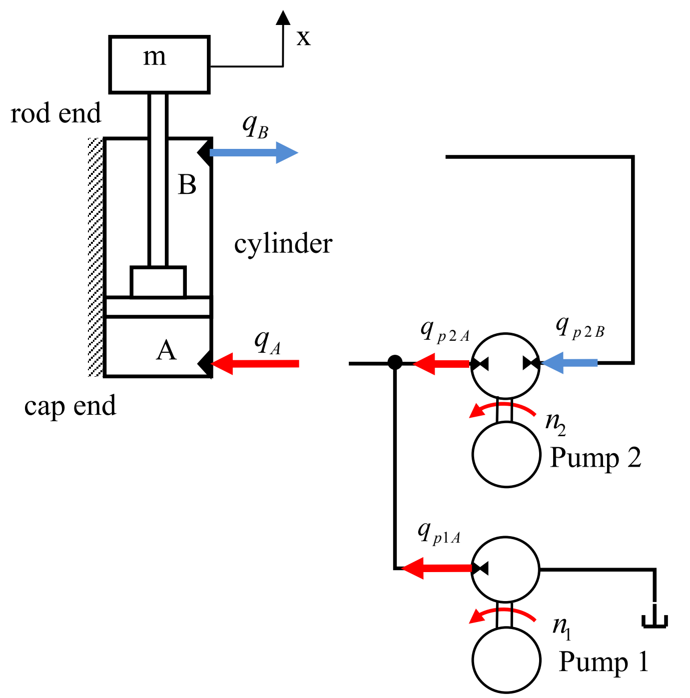

Figure 3-8 Flow Rates of the Hydraulic Cylinder and Pumps

According to the formulation defined from Eq. (3.15) to Eq.(3.17) , a linear model of the two pumps are formed in MATLAB Simulink environment. The model is shown in Figure 3-9.

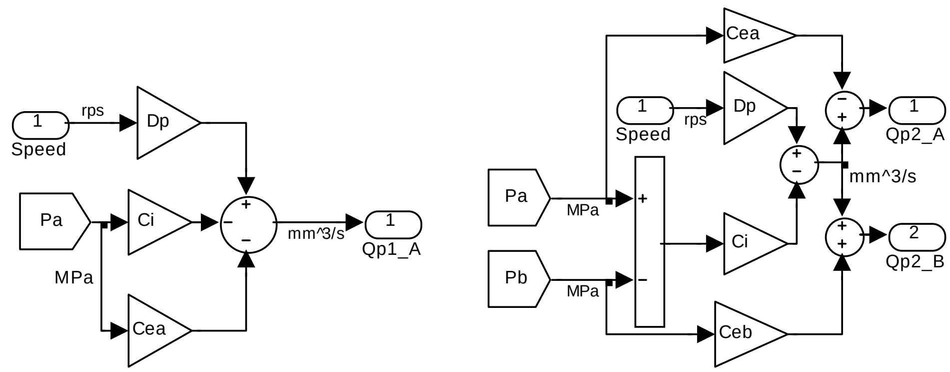

Figure 3-9 MATLAB Simulink Model of the Hydraulic Pump/Motor Unit

The input to this Simulink sub-system is the pump drive angular velocity in terms of revolution per second [rps] and the output is the pumps' inlet and outlet flow rates in terms of [mm^3/s]. Note that no torque losses are mentioned in the pump model because servomotors are assumed to be ideal angular velocity sources as they have an inner control loop.

The leakage coefficients of the pumps can be determined through an experimental study by measuring the inlet and outlet flow rates under a known pressure differential. In this study, due to the lack of flow meters, the leakage coefficients are not found experimentally and but their values on the manufacturer’s manual are used instead. However, in the open loop tests, it is seen that the real system response is not consistent with the modeled system response due to the incorrect values of the leakage coefficients. For this reason, the leakage coefficients are found indirectly by using the steady state chamber pressure response of the test set up.

3.2.2.2 Hydraulic Actuator Model

As there are a lot of hydraulic actuator models in literature, the hydraulic cylinder model is given below without going in its details.

The assumptions used to model the hydraulic cylinder are

- The leakage coefficient between the two chambers of the hydraulic cylinder is laminar flow and it is proportional with the differential pressure between them. Note that, in the mathematical model of the overall system, the cylinder leakage coefficient will be coupled with the pump internal leakage coefficient. As the pump leakage coefficient is expected to be much higher than the cylinder leakage coefficient, it can be neglected.
- The friction force between the hydraulic cylinder and the piston sealing is assumed to be proportional with the cylinder velocity. Only viscous friction is included in the system linear model. The frictional characteristics of the system are found experimentally.
- The hydraulic piston is assumed to be a distinct load and lumped into the mass which is connected to the hydraulic cylinder.
- The chamber volumes are assumed to be constant in linear mathematical model. However in the MATLAB Simulink model, the chamber volumes are changing proportional to the cylinder position.

In the hydraulic actuator model the hydraulic cylinder chamber A (cap-end) is assumed to be inlet and the hydraulic cylinder chamber B (rod-end) is assumed to be the outlet. Thus, the upward movement of the cylinder is assumed to be positive. In Figure 3-8, the positive flow rate q_A that is entering the chamber A, and the positive flow rate q_B that is leaving the chamber B are shown.

The continuity equations for the hydraulic cylinder chambers can be written as

$$q_A = A_A \dot{x} + \frac{V_A}{E} \cdot \frac{dp_A}{dt} \tag{3.18}$$

$$q_B = A_B \dot{x} - \frac{V_B}{E} \cdot \frac{dp_B}{dt} \tag{3.19}$$

and the load pressure is defined as

$$p_A A_A - p_B A_B = A_B \left(\gamma p_A - p_B \right) \tag{3.20}$$

$$p_L = \gamma p_A - p_B \tag{3.21}$$

Then, the force transmitted to the load will be expressed by the equation,

$$f_L = p_L \cdot A_B \tag{3.22}$$

The MATLAB Simulink model of the hydraulic actuator is represented in Figure 3-10. The inputs to this sub-system are the flow rates of the inlet and outlet ports of the pump 1 and pump 2 in terms of [mm^3/s] and the outputs of the sub-system are the chamber A and chamber B pressures p_A, p_B in terms of [MPa] and the load force f_L in terms of [N].

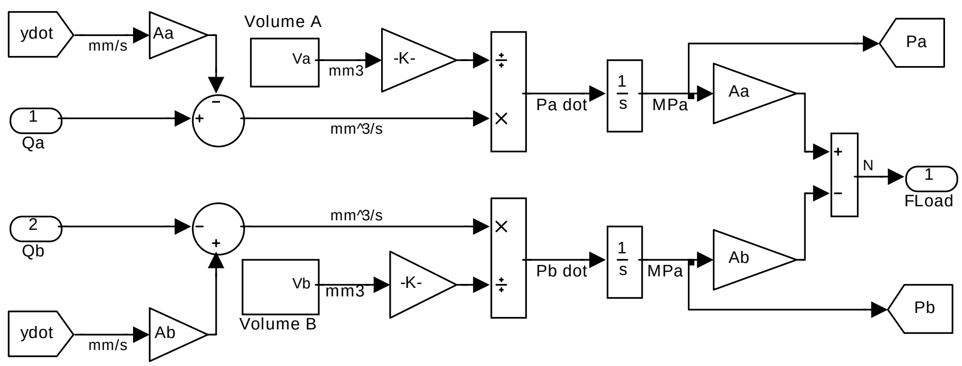

Figure 3-10 MATLAB Simulink Model of the Hydraulic Actuator

In the MATLAB Simulink model of the system, the hydraulic cylinder chamber volumes are not constant but changing with the hydraulic cylinder position. In fact, this does not affect the simulation results much as the dead volume due to the transmission lines are much more than the volume change due to the cylinder position. Hydraulic cylinder chamber volume models in MATLAB Simulink environment are given in Figure 3-11. The common input of both sub-systems is the hydraulic cylinder position, x, in terms of [mm], and the outputs of the sub-systems are the chamber volumes V_A, V_B in terms of [mm^3].

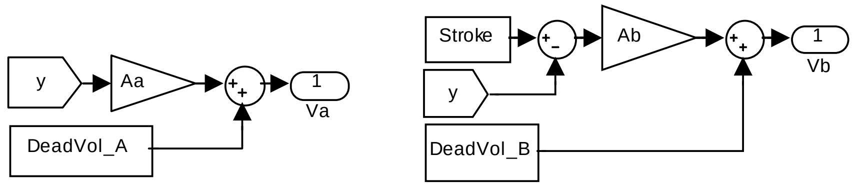

Figure 3-11 MATLAB Simulink Model of the Hydraulic Cylinder Chamber Volumes

3.2.2.3 Load Model

The test system load can simply be thought as a mass-damper system. The mass consists of the hydraulic piston and the steel plate attached to it, and represented by m . The friction force which is assumed to be viscous constitutes the damping part of the load and the viscous friction coefficient is represented by b .

The friction force acting on the load is highly non-linear. However to have a linear model, there assumed to be viscous friction between the hydraulic cylinder and piston sealing. The friction is not a parameter that can be measured directly or specified by manufacturer. In this thesis, the friction characteristics of the hydraulic cylinder is determined through an experimental procedure by measuring the hydraulic cylinder chamber pressures.

After modeling the system as a mass-damper system, the structural equation for the load by using the Newton's 2nd law, can be written as,

$$f_L = m\ddot{x} + b\dot{x} + mg \tag{3.23}$$

The mg term in Equation (3.23) represents the weight of the hydraulic load consisting of the steel plate and the hydraulic cylinder piston. It is not included in the dynamic analysis of the system.

The overall MATLAB Simulink model of the pump controlled hydraulic system is given in Figure 3-12. The inputs to the pump controlled hydraulic system are the pump 2 speed n_2, in terms of [rps] and the set pressure P_{set}, in terms of

[MPa], which is the desired sum of the chamber pressures. The output of the system is the cylinder position, y in terms of [mm].

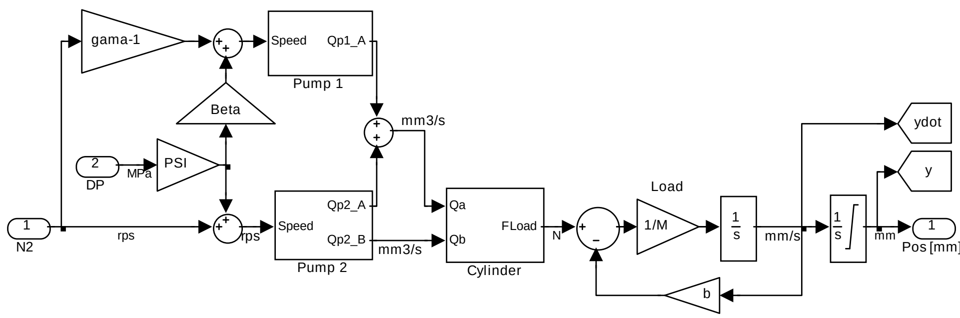

Figure 3-12 MATLAB Simulink Model of the Overall System

Note that there is a single control input to the system which is the pump 2 speed. The pump speed 1 is determined according to this speed. The relation between these two pump speeds will be explained in the following sections.

3.2.3 Steady State Characteristics of the System

In Section 3.2.1, it is explained that there should be offset pump speeds n_{1o}, n_{2o} to pressurize the cylinder chambers. The offset speeds of the pumps are adjusted to compensate the leakage flows; so that the hydraulic cylinder is not moving but is stationary. Thus, at steady state, the system can be thought as a simple resistance which is a function of the internal and external leakages coefficients, the input to the system is the ideal flow rate generated by the two pumps revolutions and the output is the chamber pressures of the hydraulic cylinder. This simple resistance analogy of the system is shown in Figure 3-13.

At steady state, the two chamber pressures p_A and p_B are not independent variables, for the zero loading case the from the Eqs. (3.20) (3.22) and (3.23), the relation between the chamber pressures is;

$$p_{L\_s} = \gamma p_{A\_ss} - p_{B\_ss} \tag{3.24}$$

where p_{L_s} term stand for the static load pressure which is caused by the mass of the hydraulic cylinder and the load. It is equal to;

$$p_{L\_s} = \frac{mg}{A_B} \tag{3.25}$$

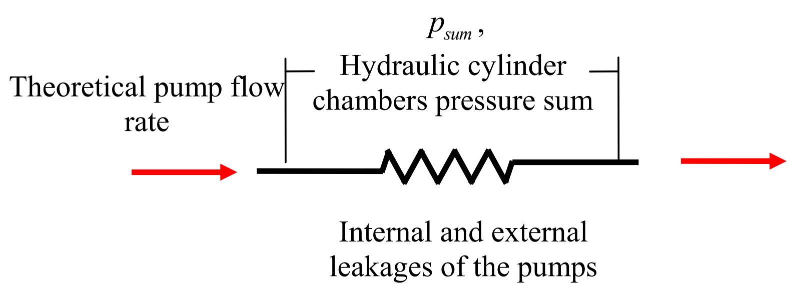

Figure 3-13 Electrical Analogy of the Pump Leakage Flow Rates

Note that, according to Eq. (3.24), as the chamber pressures are not independent at steady state, there should be a single pressure output of the resistance circuit shown in Figure 3-13 and it is selected as the sum of the chamber pressures. Sum pressure is expressed as.

$$p_{sum} = p_{A\_ss} + p_{B\_ss} \tag{3.26}$$

Likewise there should be a single input, that is the pumps speeds must be dependent otherwise the hydraulic cylinder will not be stationary and the flow rate supplied by the pumps will not only compensate the leakage flows, but moves the cylinder upwards or downwards.

From Eq. (3.24) and Eq. (3.25), the steady state chamber pressures can be written in terms of static load p_{L_s}, pressure and sum pressure p_{sum} as follows,

$$p_{A\_ss} = \frac{p_{sum} + p_{L\_s}}{\gamma + 1} \tag{3.27}$$

$$p_{B\_ss} = \frac{\gamma p_{sum} - p_{L\_s}}{\gamma + 1} \tag{3.28}$$

At steady state, the compressibility term in the flow continuity equation of the hydraulic cylinder chamber B drops and Eq. (3.19) becomes,

$$q_{B\_ss} = A_B \dot{x} - \frac{V_B}{E} \cdot \frac{dp_B}{dt} = 0 \tag{3.29}$$

From continuity, as there are no flow losses at the transmission lines the flow rate exiting the cylinder chamber B, is equal to the flow rate entering the hydraulic pump 2 which is defined by Eq. (3.16)

$$q_{B\_ss} = q_{p2B} \tag{3.30}$$

$$0 = D_P n_{2o} - C_i \left(p_{A\_ss} - p_{B\_ss} \right) + C_{eb} p_{B\_ss}$$

$$D_P n_{2o} = C_i p_{A\_ss} - \left(C_i + C_{eb} \right) p_{B\_ss} \tag{3.31}$$

Substituting Eq. (3.27) and Eq. (3.28) into Eq. (3.31), the relation between the pump 2 speed and the sum pressure becomes

$$n_{2o} = -\frac{(\gamma - 1) C_i + \gamma C_{eb}}{D_P (\gamma + 1)} p_{sum} + \frac{2C_i + C_{eb}}{D_p (\gamma + 1)} p_{L\_s} \tag{3.32}$$

For the hydraulic cylinder chamber A at steady state, the flow rate defined by Eq (3.18), the compressibility terms will drop and this equation becomes,

$$q_{A\_ss} = A_A \dot{x} + \frac{V_A}{E} \cdot \frac{dp_A}{dt} = 0 \tag{3.33}$$

From continuity, this flow is equal to the sum of the output flow rates of the pump 1 and the pump 2, defined by the equation,

$$q_{A\_ss} = q_{p1A} + q_{p2A} \tag{3.34}$$

$$0 = \left[D_P n_{1o} - \left(C_i + C_{ea} \right) p_{A\_ss} \right] + \left[D_P n_{20} - C_i \left(p_{A\_ss} - p_{B\_ss} \right) - C_{ea} p_{A\_ss} \right]$$

$$D_P n_{1o} + D_P n_{2o} = \left(2C_{ea} + 2C_i \right) p_{A\_ss} - C_i p_{B\_ss} \tag{3.35}$$

Substituting Eq. (3.27) and Eq. (3.28) and Eq. (3.31) into Eq. (3.35), the relation between the pump 1 speed and the sum pressure becomes

$$n_{1o} = \frac{2C_{ea} + \gamma C_{eb} + C_i}{D_P\left(\gamma+1\right)} p_{sum} + \frac{C_i + 2C_{ea} - C_{eb}}{D_p\left(\gamma+1\right)} p_{L\_s} \tag{3.36}$$

Note that if the static load pressure is neglected due to the low mass, then the ratio between these two offset speeds defined can be found by using Eq.(3.32) and Eq.(3.36) ,

$$\beta = \frac{n_{1o}}{n_{2o}} = -\frac{C_i + 2C_{ea} + \gamma C_{eb}}{\left(\gamma-1\right)C_i + \gamma C_{eb}} \tag{3.37}$$

Note that the constant β is a negative value that is the pumps rotate in opposite direction with respect to each other. To pressurize the cylinder chambers pump 2 turns in CW direction (negative), while the pump 1 turns in CCW direction (positive).

The relation between the desired sum pressure and the offset pump 2 speed is obtained from Eq. (3.32) as

$$n_{2o} = \Psi p_{sum} = -\frac{\left(\gamma-1\right)C_i + \gamma C_{eb}}{D_P\left(\gamma+1\right)} p_{sum} \tag{3.38}$$

$$\Psi = -\frac{\left(\gamma-1\right)C_i + \gamma C_{eb}}{D_P\left(\gamma+1\right)} \tag{3.39}$$

3.2.4 Dynamic Characteristics of the System

In this section, a general transfer function between the input pump 2 speed and the output cylinder position is obtained. The formulation is the same as the steady state analysis but this time, flows due to the rod movement and compressibility is added to the continuity equations defined by Eq. (3.30) and Eq. (3.34).

For the rod end side of the hydraulic cylinder if the continuity equation is written by using Eq. (3.19) and Eq. (3.16),

$$q_B = q_{p2B} \tag{3.40}$$

$$A_B \dot{x} - \frac{V_B}{E} \cdot \frac{dp_B}{dt} = D_P n_2 - C_i \left(p_A - p_B \right) + C_{eb} p_B \tag{3.41}$$

For the cap end side of the hydraulic cylinder if the continuity equation is written by using Eq. (3.15), Eq. (3.17) and Eq.(3.18),

$$q_A = q_{p1A} + q_{p2A} \tag{3.42}$$

$$A_A \dot{x} + \frac{V_A}{E} \cdot \frac{dp_A}{dt} = D_P n_1 - \left(C_i + C_{ea} \right) p_A + D_P n_2 - C_i \left(p_A - p_B \right) - C_{ea} p_A \tag{3.43}$$

Note that the pump speeds n_1 and n_2 written in Eq. (3.41)and Eq. (3.42) are the manipulated input speed signals generated from the position control loop. The offset speeds are not included to the formulation, because they are static and do not affect the dynamic behavior of the system. Also it should be pointed out that the pump speeds n_1 and n_2 are not independent; due to the area difference there should always be relation as explained in Eq. (3.4) in Section 0.

$$n_1 = \left(\gamma - 1 \right) n_2 \tag{3.44}$$

If Eq.(3.3) and Eq.(3.44) are substituted into Eq.(3.41) and Eq. (3.43), then rearranged the continuity equations can be written in s-domain as,

$$D_P N_2 \left(s \right) - A_B s X \left(s \right) = C_i P_A \left(s \right) - \left(\frac{V_B}{E} s + C_i + C_{eb} \right) P_B \left(s \right) \tag{3.45}$$

$$\gamma \left[D_P N_2 \left(s \right) - A_B s X \left(s \right) \right] = \left(2C_i + 2C_{ea} + \frac{V_A}{E} s \right) P_A \left(s \right) - C_i P_B \left(s \right) \tag{3.46}$$

From Eq. (3.20), Eq. (3.22) and Eq. (3.23) the force balance on the load gives,

$$\left[\gamma P_A \left(s \right) - P_B \left(s \right) \right] A_B = \left(ms + b \right) s X \left(s \right) \tag{3.47}$$

The two continuity and the one structural equations, Eq. (3.45), Eq. (3.46), Eq. (3.47), written above are the general equations that defines the overall variable speed pump controlled system dynamics. Arranging these three equations, the transfer function between the drive speed of pump 2 and the hydraulic cylinder rod velocity can be written as follows,

$$\frac{V(s)}{N_2(s)} = \frac{a_1 s + a_2}{b_1 s^3 + b_2 s^2 + b_3 s + b_4} \tag{3.48}$$

where

$$a_1 = \left(\gamma^2 + \alpha\right)\frac{V_B}{E} D_P A_B$$
$$a_2 = \left(\left(\gamma^2 - 2\gamma + 2\right)C_i + \gamma^2 C_{eb} + 2C_{ea}\right) D_P A_B$$
$$b_1 = m\frac{\alpha V_B^{\,2}}{E^2}$$
$$b_2 = m\left(\left(2+\alpha\right)C_i + 2C_{ea} + \alpha C_{eb}\right)\frac{V_B}{E} + b\frac{\alpha V_B^{\,2}}{E^2}$$
$$b_3 = m\left(C_i^2 + 2\left(C_{ea} + C_{eb}\right)C_i + 2C_{ea}C_{eb}\right) + b\left(\left(2+\alpha\right)C_i + 2C_{ea} + \alpha C_{eb}\right)\frac{V_B}{E} + \left(\gamma^2 + \alpha\right)\frac{V_B}{E} A_B^{\,2}$$
$$b_4 = b\left(C_i^2 + 2\left(C_{ea} + C_{eb}\right)C_i + 2C_{ea}C_{eb}\right) + \left(\left(\gamma^2 - 2\gamma + 2\right)C_i + \gamma^2 C_{eb} + 2C_{ea}\right) A_B^{\,2}$$

Here the term α represents the hydraulic cylinder chambers volume ratio for a predetermined fixed position,

$$\alpha = \frac{V_A}{V_B} \tag{3.49}$$

Since the order of the denominator is three and cannot be written in factored form, it is very hard to interpret how the system parameters affect the roots of the characteristic equation. However, if the numerical values of the system parameters are used in this transfer function it will be seen that the system has a zero and a pole next to each other. This is due to the chamber pressure relations. By writing an appropriate relationship between the dynamic pressures changes of the cylinder chambers the order of the system can be reduced by one.

Note the relationship between Eq. (3.45) and Eq. (3.46), it is seen that left hand sides of the equations are proportional with the area ratio γ. From these two equations if Eq. (3.45) is multiplied by γ and subtract from Eq. (3.46) the relation between the hydraulic cylinder chambers pressures can be written as follows,

$$P_A(s) = -\frac{(\gamma-1)C_i + \gamma C_{eb} + \gamma \dfrac{V_B}{E}s}{C_i(2-\gamma) + 2C_{ea} + \dfrac{V_A}{E}s} P_B(s) \tag{3.50}$$

It is strictly noted that in the above equation, P_A and P_B terms are the dynamic pressure changes of the hydraulic cylinder chambers under an applied load. It does not represent the magnitude of the real pressure in the cylinder chambers. The real pressure is the sum of the steady state pressures due to the offset pump speeds plus the dynamic pressure change due to loading.

Eq. (3.50) implies that for the specific volume ratio and leakage coefficients if the time constants of the numerator and the denominator are identical then the relation between the chamber pressure changes will be linearly dependent and can be represented as,

$$P_A(s) = -\varphi P_B(s) \tag{3.51}$$

where the dynamic pressure change ratio is,

$$\varphi = \frac{\gamma V_B}{V_A} = \frac{(\gamma-1)C_i + \gamma C_{eb}}{C_i(2-\gamma) + 2C_{ea}} \tag{3.52}$$

To satisfy this condition, the external and internal leakages of the pumps have to be adjusted, however this is practically impossible. For this reason one way to hold this condition is to add external leakage paths to the transmission lines. In Figure 3-14, the pump internal and external leakages paths are represented with the additional external leakage paths to the transmission lines.

As it can be understood from Figure 3-14 the additional external leakage paths are parallel to the external leakage paths of the pumps. Therefore, nothing will be changed if the following replacements defined by Eq. (3.53) are made in the formulations,

$$\begin{aligned} 2C_{ea} &\rightarrow 2C_{ea} + C_{Aext} \\ C_{eb} &\rightarrow C_{eb} + C_{Bext} \end{aligned} \tag{3.53}$$

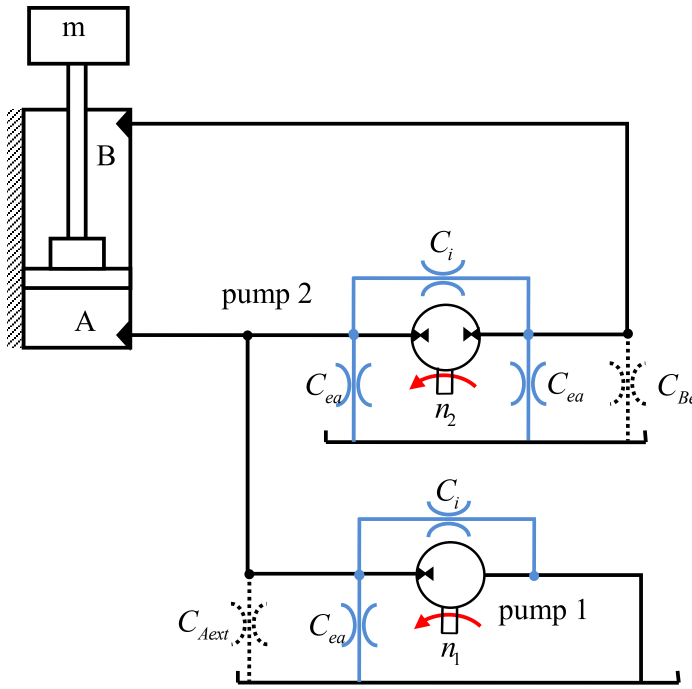

Figure 3-14 Representation of the Hydraulic Pump Leakages with Additional External Leakages

The desired values of the additional external leakage coefficients C_{Aext}, C_{Bext} , so that the condition defined by Eq. (3.51) holds, can be found by equating the time constants of the numerator and denominator of the transfer function defined by Eq. (3.50).

$$\frac{(\gamma-1)C_i + \gamma\left(C_{eb} + C_{Bext}\right)}{\gamma \dfrac{V_B}{E}} = \frac{C_i\left(2-\gamma\right) + 2C_{ea} + C_{Aext}}{\dfrac{V_A}{E}} \tag{3.54}$$

Taking the external leakage coefficient on line B, $C_{Bext} = 0$, the resulting C_{Aext} is,

$$C_{Aext} = \frac{V_A}{\gamma V_B}\left((\gamma - 1)C_i + \gamma C_{eb}\right) - C_i(2-\gamma) - 2C_{ea} \tag{3.55}$$

When the condition defined by Eq. (3.51) holds, and the order of the transfer function between the drive speed of pump 2 and hydraulic cylinder rod velocity reduces from 3 to 2, then a much simpler and understandable transfer function can be derived by using Eq. (3.45), Eq. (3.46), Eq. (3.47) and Eq. (3.51). The derivation of the reduced order transfer function between the drive speed of pump 2 and hydraulic cylinder rod velocity is given in the Appendix A in detail. Below, the second order transfer function defining the open loop velocity response of the hydraulic cylinder to the pump 2 speed is given,

$$\frac{V(s)}{N(s)} = \frac{\left(\gamma^2 + \alpha\right) D_P A_B}{m\frac{\alpha V_B}{E}s^2 + \left(b\frac{\alpha V_B}{E} + mC_{Leak}\right)s + bC_{Leak} + \left(\gamma^2 + \alpha\right)A_B{}^2} \tag{3.56}$$

where

$$C_{Leak} = \frac{\left(\varphi(2\gamma + \alpha) + (\alpha + \gamma)\right)C_i + \varphi 2\gamma C_{ea} + \alpha C_{eb}}{\gamma\varphi + 1} \tag{3.57}$$

stands for the equivalent leakage flow coefficient of the pump and the parameter φ represents the assumed dynamic pressure change ratios of the hydraulic cylinder chambers, defined by Eq. (3.52).

Note that the 2nd order transfer function defined by Eq. (3.56) is identical to the 3rd order transfer function defined by Eq. (3.48). Because after adding an external leakage to the system defined by Eq.(3.57), one of the roots of the denominator of the 3rd order transfer function becomes equal to the root of its numerator and reduces to a 2nd order transfer function.

The transfer function defined by Eq. (3.56) is more meaningful, than the transfer function defined by Eq. (3.48). This second order transfer function can be used to understand the dynamic behavior of the system. The natural frequency and the damping ratio of the variable speed pump controlled hydraulic system can be written as,

$$\omega_n = \sqrt{E \frac{bC_{Leak} + \left(\gamma^2 + \alpha\right) A_B{}^2}{m\alpha V_B}} \tag{3.58}$$

$$\xi = \frac{1}{2}\sqrt{\frac{E}{m\alpha V_B \left(bC_{Leak} + \left(\gamma^2 + \alpha\right) A_B{}^2\right)}} \left(\frac{b\alpha V_B}{E} + mC_{Leak}\right) \tag{3.59}$$

It is seen that the equivalent leakage resistance term C_{leak} increases the natural frequency and damping of the system. Then after adding external leakage paths on the transmission lines the system becomes faster as it will increases the equivalent leakage flow coefficient C_{leak} so that the natural frequency of the system. However, it should be remembered that the additional leakage paths decreases the efficiency of the system due to the throttling losses. Another important factor which determines the natural frequency of the system is the hydraulic cylinder chamber volumes. Different from the valve controlled hydraulic systems, where the valve is mounted next to the cylinder, in the pump controlled system there are transmission lines between the pump inlet/outlet and cylinder inlet/outlet. From the equations above, it is seen that the dead volume of these transmission lines decreases both the natural frequency and the damping ratio. Lastly, the term $\gamma^2 + \alpha$ appearing in the above equations indicate that increasing the area ratio and dead volume ratio, increases the natural frequency of the system while decreases the damping ratio.

The equivalent block diagram representation of the open loop position response of the variable speed pump controlled system is given below in Figure 3-15.

Mathematically adding an external leakage element to the system with a pre-determined value is simple, but practically this does not seems rational. Furthermore, this additional leakage element reduces the energy efficiency of the system.

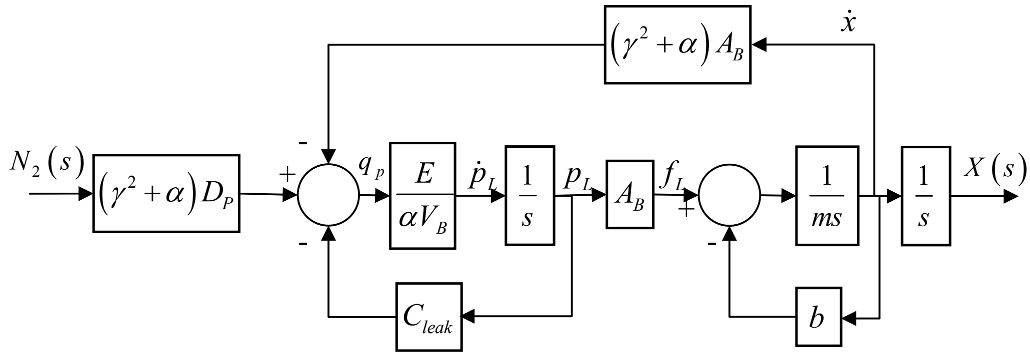

Figure 3-15 Block Diagram Representation of the Open Loop Position Response of the Variable Speed Pump Controlled System

If the frequency response of the transfer function between the dynamic pressure changes of the hydraulic cylinder chambers $P_A(s)/P_B(s)$, which is defined by Eq. (3.50) is plotted, it will be seen the relation is linear below and above some predetermined cut off (corner) frequencies. For simplicity, the dynamic pressure change relation is written in a standard first order transfer function form.

$$\frac{P_A(s)}{P_B(s)} = -\frac{\gamma \dfrac{V_B}{E} s + (\gamma-1)C_i + \gamma C_{eb}}{\dfrac{V_A}{E} s + C_i(2-\gamma) + 2C_{ea}} = -K\frac{T_1 s+1}{T_2 s+1} \tag{3.60}$$

where

$$\begin{aligned} K_{OL} &= \frac{(\gamma-1)C_i + \gamma C_{eb}}{C_i(2-\gamma)+2C_{ea}} \\ T_1 &= \frac{\gamma V_B}{E\left((\gamma-1)C_i+\gamma C_{eb}\right)} \\ T_2 &= \frac{V_A}{E\left(C_i(2-\gamma)+2C_{ea}\right)} \end{aligned} \tag{3.61}$$

If the frequency response of this first order transfer function defining the dynamic chamber pressure change relation is investigated, it is seen at low excitation frequencies ($\omega \to 0$) the dynamic pressure change ratio is equal to the open loop gain K_{OL} which is fully determined by the pump leakage coefficients. At higher excitation frequencies ($\omega \to \infty$), the dynamic pressure change ratio is equal to the ratio of time constants which is fully determined by the hydraulic cylinder volumes and area ratio. For the frequencies between the cut off frequencies, which are determined by T_1 and T_2, the dynamic pressure change ratio will be determined by both leakage flow coefficients and hydraulic cylinder volumes together with the area ratio.

From the investigation above, it can be concluded that, for low excitation frequencies the hydraulic oil tends to leak out and the leakage flow coefficients determines the change of chamber pressures, while for high excitation frequencies the hydraulic oil tends to compress and the hydraulic cylinder chamber volumes determines the change of chamber pressures. The frequency response of the dynamic pressure change ratio is plotted in Figure 3-16 by using the numerical values defined in Table 3-7.

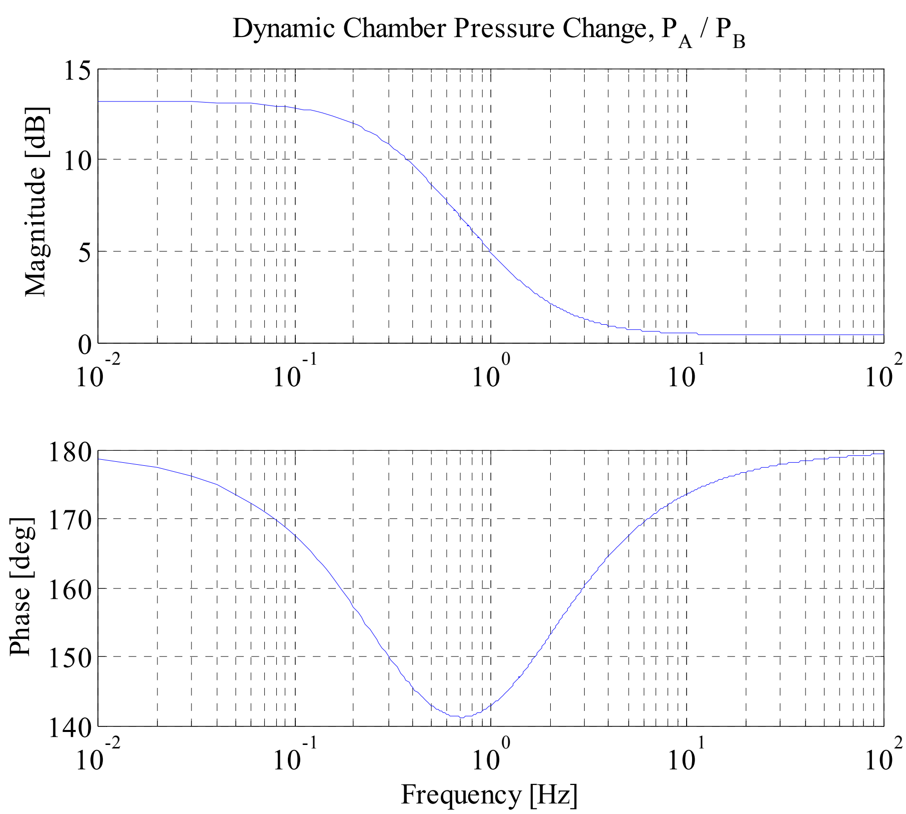

Figure 3-16 Pump Dynamic Chamber Pressure Change Relations

It is seen that at low excitation frequencies ($\omega \to 0$) the dynamic pressure changes ratios of the cylinder chambers are 13.17 dB (magnitude 4.55) which is equal to the gain K_{OL} of the transfer function (Eq.(3.61)), and at higher frequencies $(\omega \to \infty)$ that are larger than 3 Hz, the dynamic pressure change ratio drops to 0.39dB (magnitude 1.05) which is equal to the $\varphi = \gamma V_B / V_A = \gamma / \alpha$ value.

Practically this means that under a sinusoidal dynamic loading whose frequency is higher than 3 Hz, to compensate the dynamic load pressure, the chamber pressure p_B will reduce Δp value from its steady state value, while the chamber pressure p_A will increase $1.05\Delta p$ value from its steady state value. Thus the order of the position control system will reduce from 4 to 3 as the chamber pressures become linearly dependent.

Therefore, it will be a reasonable assumption to use the linear dynamic pressure change relation $p_A = -\varphi p_B$ instead of adding an additional leakage path to the system. Because, the inertial effects of the load on the chamber pressures are very small and negligible for low excitation frequencies, φ value should be calculated for higher excitation frequencies ($\omega \to \infty$). Then, the linearly dependent chamber pressure relation is equal to the ratio of time constants and written as follows,

$$\varphi = \frac{T_1}{T_2} = \frac{\gamma V_B}{V_A} \tag{3.62}$$

To verify the linear dynamic pressure change assumption the numerical values of the system defined in Table 3-7 will be used. Below in the first row of Table 3-5, the poles and zeros of the general 3rd order transfer function defined by Eq. (3.48) between the drive speed of pump 2 and hydraulic cylinder rod velocity are given. In the remaining rows, the poles of the reduced 2nd order transfer function defined in Eq.(3.56) between the drive speed of pump 2 and hydraulic cylinder rod velocity for different φ values are given.

Table 3-5 Pole and Zero Comparison of Reduced and Full Order Transfer Functions

	Poles	Zeros	Error Between the poles of 3^{rd} order TF and 2^{nd} order TF
General 3^{rd} order TF	-120.02 +1874.63i -120.02 -1874.63i -6.9582	-6.9588	
Reduced 2^{nd} order TF $\varphi = \frac{\gamma V_B}{V_A} = 1.047$	-120.02 +1874.63i -120.02 -1874.63i	0	0.00047+0.0030i
Reduced 2^{nd} order TF $\varphi = K = 4.555$	-119.21 +1874.59i -119.21 -1874.59i	0	0.81359+0.0368i
Reduced 2^{nd} order TF $\varphi = 2$	-119.58 +1874.61i -119.58 -1.874.61i	0	0.44623+0.01878i

From Table 3-5, it is seen that third pole and zero of the general 3^{rd} order transfer function are very close, canceling each other, and the remaining complex conjugate pole pairs are very close to the pole pair of the reduced second order system. Furthermore, the error between the third order transfer function poles and second order transfer function poles are much smaller if the dynamic chamber pressure change ratio, φ, is determined for higher excitation frequencies.

3.3 Valve Controlled System

In the valve controlled system, the load and the hydraulic actuator are the same with the pump controlled circuit. As the mathematical models for the hydraulic actuator and the load are derived in Section 3.2.2, they will not be modeled again. Additionally, the mathematical model of the valve used in the test set up is derived.

3.3.1 Mathematical Modeling of the System

As explained in Section 3.1, the valve driver has a spool position controller which takes spool position feedback from the LVDT on the valve. The bandwidth of the valve used in this study for 100% command input signal is around 70 Hz which is very high with respect to the hydraulic applications, and can be assumed to be an ideal flow rate source for a given reference spool position command. Therefore, of the valve controlled system the valve dynamics is neglected in the mathematical modeling given below and the servovalve opening is directly related to the reference spool position command.

3.3.1.1 Valve Model

Shown in Figure 3-17 is the schematic of representation of the valve controlled asymmetric cylinder. According to the defined direction for a given positive spool position u_v, the following cylinder movement is upwards, in positive direction.

The valve used in the test set up is a servo proportional close centered zero-lap valve; therefore, as there is no dead zone or initial opening, the valve orifice area is proportional to the spool displacement at any time. Thus, under constant pressure differential across the valve, the flow gain is constant and does not change with the spool position. The flow gain versus command signal graph is shown in Figure 3-4.

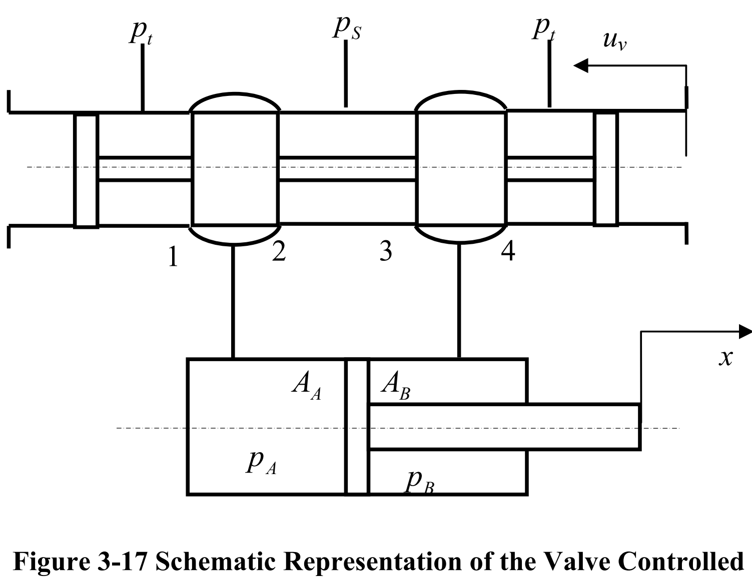

Figure 3-17 Schematic Representation of the Valve Controlled System

In the zero lap valve, only two of the arms are open at any time, therefore only two orifice equations can represent the valve dynamics. Assuming zero tank pressure, these expressions can be written as follows.

For positive spool position, $u_v > 0$

$$q_2 = C_d w_o u_v \sqrt{\frac{2}{\rho}\left(p_S - p_A\right)}$$
$$q_4 = C_d w_o u_v \sqrt{\frac{2}{\rho} p_B} \tag{3.63}$$

For negative spool position $u_v < 0$

$$q_1 = C_d w_o u_v \sqrt{\frac{2}{\rho} p_A}$$
$$q_3 = C_d w_o u_v \sqrt{\frac{2}{\rho}\left(p_S - p_B\right)} \tag{3.64}$$

Note that the valve and oil parameters C_d, w, and ρ are constants and generally not given in the manuals. Instead, they are represented by a flow gain, K_v, that can be obtained from the valve manual from the relation between the flow rate and valve input current u.

$$K_v = C_d w_o \sqrt{\frac{2}{\rho}} \tag{3.65}$$

Then the valve flow equations becomes,

$$\left.\begin{aligned} q_2 &= K_v u \sqrt{p_S - p_A} \\ q_4 &= K_v u \sqrt{p_B} \end{aligned}\right\} \quad u > 0$$
$$\left.\begin{aligned} q_1 &= K_v u \sqrt{p_A} \\ q_3 &= K_v u \sqrt{p_S - p_B} \end{aligned}\right\} \quad u < 0 \tag{3.66}$$

It is important to note that the parameter u is an electrical signal representing the reference spool position command of the driver not the spool position.

The MATLAB Simulink model of the valve is shown in Figure 3-18. Here the input to valve sub-system is the spool position signal in terms of Volt, and the output of the system is the flow rate in terms of mm^3/s.

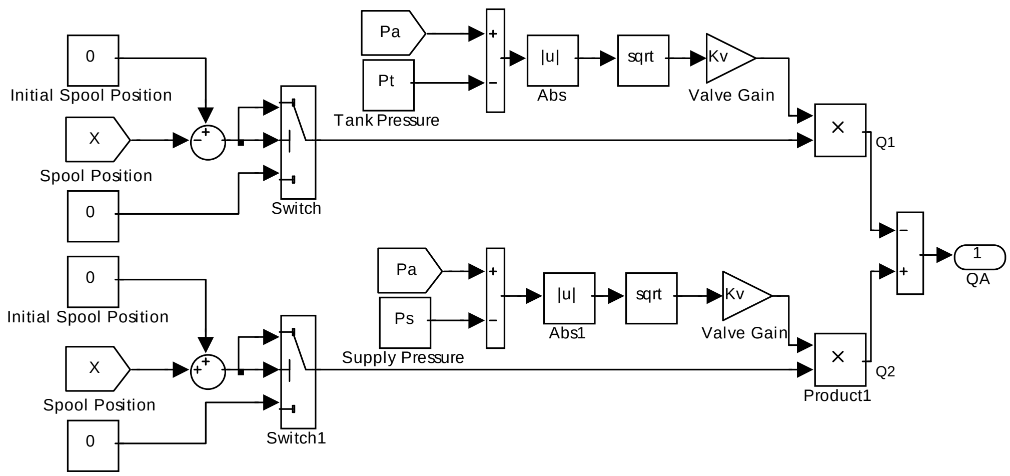

Figure 3-18 MATLAB Simulink Model of the Proportional Valve with Zero Lap

3.3.2 Steady State Characteristics of the System

The symmetric or single rod cylinders have different characteristics for extending and for retracting motions. This is due to the area difference between two faces of the hydraulic cylinder piston. The steady state chamber pressures p_A and p_B for a given valve spool position input is derived below for both extending and retracting case.

At steady state, the compressibility terms in the flow continuity equations of the hydraulic cylinder chambers A and B drop and Eq. (3.18) and Eq. (3.19) become,

$$q_{B\_ss} = A_B \dot{x} \tag{3.67}$$

$$q_{A\_ss} = A_A \dot{x} = \gamma A_B \dot{x} \tag{3.68}$$

From the equations above, the steady state relation between the flow rate entering the cylinder chamber A and leaving the cylinder chamber B is obtained as

$$q_{A\_ss} = \gamma q_{B\_ss} \tag{3.69}$$

Assuming that there exist no flow losses at the transmission lines, the continuity requires that the steady state inlet and outlet flow rates of the cylinder are equal to the valve flow rates.

Hence, for the extending case,

$$q_{A\_ss} = q_2 \tag{3.70}$$

$$q_{B\_ss} = q_4 \tag{3.71}$$

and for the retracting case,

$$q_{A\_ss} = q_1 \tag{3.72}$$

$$q_{B\_ss} = q_3 \tag{3.73}$$

Substituting Eq. (3.66), Eq. (3.70) and Eq. (3.71) into Eq. (3.69) the relation between the steady state chamber pressures can be found.

Hence, for extending case,

$$q_{A\_ss} = q_2 = K_v u \sqrt{p_S - p_{A\_ss}} = \gamma K_v u \sqrt{p_{B\_ss}} = \gamma q_4 = \gamma q_{B\_ss} \tag{3.74}$$

$$p_{A\_ss}{}^2 + \gamma^2 p_{B\_ss}{}^2 = p_S{}^2 \tag{3.75}$$

and for retracting case,

$$q_{A\_ss} = q_1 = K_v u \sqrt{p_{A\_ss}} = \gamma K_v u \sqrt{p_S - p_{B\_ss}} = \gamma q_3 = \gamma q_{B\_ss} \tag{3.76}$$

$$p_{A\_ss}{}^2 + \gamma^2 p_{B\_ss}{}^2 = \gamma^2 p_S{}^2 \tag{3.77}$$

For zero loading case, the static equilibrium is written as,

$$p_{A\_ss} - \gamma\, p_{B\_ss} = 0 \tag{3.78}$$

Then, the steady state chamber pressures for extracting and retracting in terms of supply pressure can be written by using Eq.(3.75), (3.77) and (3.78).

Hence, for extending case,

$$p_{A\_ss\_ext} = \frac{p_S}{\gamma^3 + 1} \tag{3.79}$$

$$p_{B\_ss\_ext} = \frac{\gamma\, p_S}{\gamma^3 + 1} \tag{3.80}$$

and for retracting case

$$p_{A\_ss\_ret} = \frac{\gamma^2 p_S}{\gamma^3 + 1} \tag{3.81}$$

$$p_{B\_ss\_ret} = \frac{\gamma^3 p_S}{\gamma^3 + 1} \tag{3.82}$$

3.3.3 Linearized Valve Coefficients

As the valve flow equation is highly non-linear, in order to obtain a linear relationship between the input spool position and output cylinder position, the characteristic flow equation of the valve should be linearized. Another non-linearity comes from the differential area of the cylinder, the chamber pressures shows different characteristics for extension and retraction. In this section, the characteristic valve flow equation is linearized both for extending and retracting cases.

To linearize the valve flow equation it is assumed that, under a dynamic loading, the chamber pressures are at steady state, and the dynamic pressure changes due to compensate the load pressure are small with respect to the steady state pressures. Then the flow continuity equations defined by Eq. (3.66) can be linearized at the steady state pressures defined by Eq. (3.79) through Eq. (3.82) for a given constant reference spool position input $u = u_o$.

3.3.3.1 Extension Case

For the extension case, the pressurized oil coming from the supply passes through the orifice 2 and goes to the chamber A and the oil in chamber B passes through orifice 4 and goes to the tank. Therefore, for the extension case, the linearization of the orifices 2 and 4 for a given spool input position u_o at steady state extension chamber pressures $p_{A\_ss\_ext}$ and $p_{B\_ss\_ext}$ should be performed.

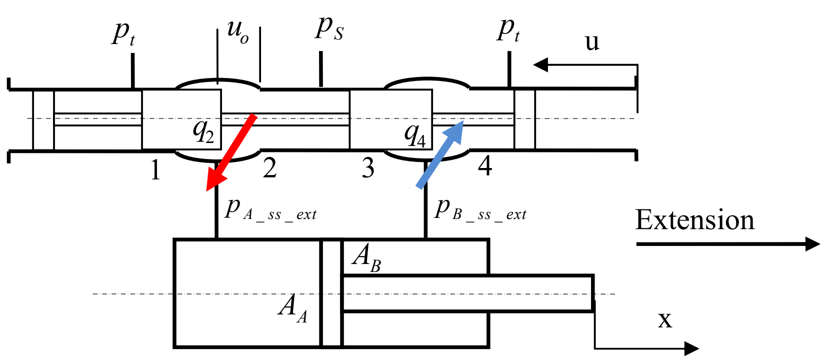

Figure 3-19 Schematic Representation of the Valve Spool Opening for Extension

Orifice 2

The flow rate passing through the orifice 2 can be linearized as follows,

$$q_2 = K_v u \sqrt{p_S - p_A} = K_{u2\_ext} u - K_{p2\_ext} p_A \tag{3.83}$$

Here the terms K_{u2_ext} is valve spool position gain of orifice 2 linearized at the spool position u_o and steady state chamber pressure $p_{A\_ss\_ext}$.

$$K_{u2\_ext} = \left.\frac{\partial q_2}{\partial u}\right|_{\substack{u=u_o \\ p_A = p_{A\_ss\_ext}}} = K_v\sqrt{p_S - p_{A\_ss\_ext}} = K_v\sqrt{P_s - \frac{p_s}{\gamma^3+1}}$$
$$K_{u2\_ext} = K_v\sqrt{\frac{\gamma^3 p_s}{\gamma^3+1}} \tag{3.84}$$

The term K_{p2_ext} is the valve pressure gain of orifice 2 which is also linearized at the spool position u_o and steady state chamber pressure $p_{A\_ss\_ext}$.

$$K_{p2\_ext} = -\left.\frac{\partial q_2}{\partial p_A}\right|_{\substack{u=u_o \\ p_A = p_{A\_ss\_ext}}} = \frac{K_v \cdot u_o}{2\sqrt{p_S - p_{A\_ss\_ext}}} = \frac{K_v \cdot u_o}{2\sqrt{p_S - \frac{p_S}{\gamma^3+1}}}$$
$$K_{p2\_ext} = \frac{K_v \cdot u_o}{2\sqrt{\frac{\gamma^3 p_S}{\gamma^3+1}}} \tag{3.85}$$

If a comparison is made with the variable speed pump controlled system, the valve spool position gain K_{u2_ext} defines the relation between the valve spool position and the flow generated. Therefore, it can be thought as the pump displacement D_P, which is the gain between pump drive speed and pump flow rate. The valve pressure gain K_{p2_ext} defining flow losses of the valve for a given spool position can be thought as the leakage flow coefficients of the pump.

Orifice 4

The flow rate passing through the orifice 2 can be linearized as follows,

$$q_4 = K_v u\sqrt{p_B} = K_{u4\_ext}u + K_{p4\_ext}p_B \tag{3.86}$$

Here the terms K_{u4_ext} is valve spool position gain of orifice 2 linearized at the spool position u_o and steady state chamber pressure $p_{B\_ss\_ext}$

$$K_{u4\_ext} = \left.\frac{\partial q_2}{\partial u}\right|_{\substack{u=u_o \\ p_B = p_{B\_ss\_ext}}} = K_v\sqrt{p_{B\_ss\_ext}} = K_v\sqrt{\frac{\gamma p_s}{\gamma^3+1}}$$
$$K_{u4\_ext} = K_v\sqrt{\frac{\gamma p_s}{\gamma^3+1}} \tag{3.87}$$

The term K_{p4_ext} is the valve pressure gain of orifice 2 which is also linearized at the spool position u_o and steady state chamber pressure $p_{B\_ss\_ext}$

$$K_{p4\_ext} = \left.\frac{\partial q_4}{\partial p_B}\right|_{\substack{u=u_o \\ p_B=p_{B\_ss\_ext}}} = \frac{K_v \cdot u_o}{2\sqrt{p_{B\_ss\_ext}}} = \frac{K_v \cdot u_o}{2\sqrt{\dfrac{\gamma p_s}{\gamma^3+1}}}$$

$$K_{p4\_ext} = \frac{K_v \cdot u_o}{2\sqrt{\dfrac{\gamma p_s}{\gamma^3+1}}} \tag{3.88}$$

Note that the valve spool position gain of the orifice 2 is γ times the valve spool position gain of orifice 4.

$$K_{u2\_ext} = \gamma K_{u4\_ext} \tag{3.89}$$

The valve pressure gain of the orifice 4 is γ times the valve pressure gain of orifice 2.

$$K_{p2\_ext} = \frac{K_{p4\_ext}}{\gamma} \tag{3.90}$$

3.3.3.2 Retraction Case

Shown in Figure 3-20, to retract the hydraulic cylinder, the pressurized oil coming from the supply passes through the orifice 3 and goes to the chamber B, the oil in chamber A passes through orifice 1 and goes to the tank. Therefore, for the retraction case, the linearization of the orifices 1 and 3 for a given spool input position u_o at steady state retraction chamber pressures $p_{A\_ss\_ret}$, $p_{B\_ss\_ret}$, should be performed.

Orifice 3

The flow rate passing through the orifice 3 can be linearized as follows,

$$q_3 = K_v u\sqrt{p_S - p_B} = K_{u3\_ret}u - K_{p3\_ret}p_B \tag{3.91}$$

Here the terms K_{u3_ret} is valve spool position gain of orifice 2 linearized at the spool position u_o and steady state chamber pressure $p_{B\_ss\_ext}$

$$K_{u3\_ext} = \left.\frac{\partial q_2}{\partial u}\right|_{\substack{u=u_o \\ p_B=p_{B\_ss\_ext}}} = K_v\sqrt{p_S - p_{B\_ss\_ext}} = K_v\sqrt{P_s - \frac{\gamma^3 p_s}{\gamma^3+1}}$$
$$K_{u3\_ext} = K_v\sqrt{\frac{p_s}{\gamma^3+1}} \tag{3.92}$$

The term K_{p3_ret} is the valve pressure gain of orifice 3 which is also linearized at the spool position u_o and steady state chamber pressure $p_{B\_ss\_ext}$

$$K_{p3\_ret} = -\left.\frac{\partial q_2}{\partial p_B}\right|_{\substack{u=u_o \\ p_B=p_{B\_ss\_ext}}} = \frac{K_v \cdot u_o}{2\sqrt{p_S - p_{B\_ss\_ext}}} = \frac{K_v \cdot u_o}{2\sqrt{p_S - \frac{\gamma^3 p_S}{\gamma^3+1}}}$$
$$K_{p3\_ret} = \frac{K_v \cdot u_o}{2\sqrt{\frac{p_S}{\gamma^3+1}}} \tag{3.93}$$

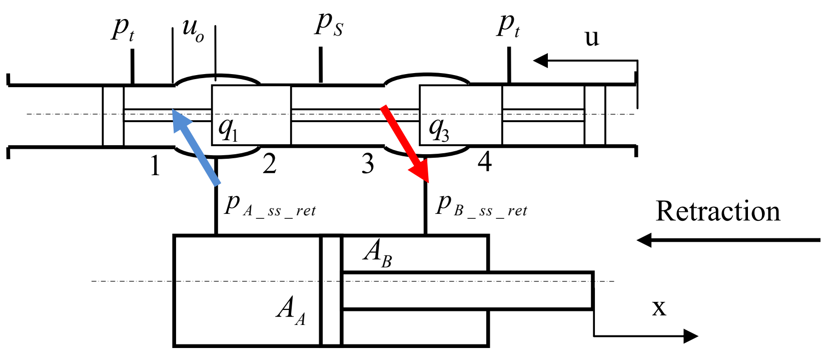

Figure 3-20 Schematic Representation of the Valve Spool Opening for Retraction

Orifice 1

The flow rate passing through the orifice 1 can be linearized as follows,

$$q_1 = K_v u\sqrt{p_A} = K_{u1\_ret}u + K_{p1\_ret}p_B \tag{3.94}$$

Here the terms K_{u1_ret} is valve spool position gain of orifice 1 linearized at the spool position u_o and steady state chamber pressure $p_{A\_ss\_ext}$

$$K_{u1\_ext} = \left.\frac{\partial q_1}{\partial u}\right|_{\substack{u=u_o \\ p_A=p_{A\_ss\_ext}}} = K_v \sqrt{p_{A\_ss\_ext}}$$
$$K_{u1\_ext} = K_v \sqrt{\frac{\gamma^2 p_s}{\gamma^3+1}} \tag{3.95}$$

The term K_{p1_ret} is the valve pressure gain of orifice 1 which is also linearized at the spool position u_o and steady state chamber pressure $p_{A\_ss\_ext}$

$$K_{p1\_ext} = \left.\frac{\partial q_1}{\partial p_A}\right|_{\substack{u=u_o \\ p_A=p_{A\_ss\_ext}}} = \frac{K_v \cdot u_o}{2\sqrt{p_{A\_ss\_ext}}} = \frac{K_v \cdot u_o}{2\sqrt{\frac{\gamma^2 p_s}{\gamma^3+1}}}$$
$$K_{p1\_ext} = \frac{K_v \cdot u_o}{2\sqrt{\frac{\gamma^2 p_s}{\gamma^3+1}}} \tag{3.96}$$

Note that the valve spool position gain of the orifice 1 is γ times the valve spool position gain of orifice 3.

$$K_{u1\_ext} = \gamma K_{u3\_ext} \tag{3.97}$$

The valve pressure gain of the orifice 3 is γ times the valve pressure gain of orifice 1.

$$K_{p1\_ext} = \frac{K_{p3\_ext}}{\gamma} \tag{3.98}$$

3.3.4 Dynamic Characteristics of the System

In this section, a transfer function between the input valve spool position and the output cylinder rod velocity is derived. In order to obtain a linear relationship, the linearized valve flow coefficients found in the previous sub-section are to be used. A dynamic analysis for the extending case is carried out below. Since the procedure is the same; the transfer function derivation for the retraction case is not explained.

Likewise in the pump controlled system, two flow continuity equations of the cylinder chambers and valve and one structural equation of the load define the system dynamics.

For the cap end of the hydraulic cylinder, the flow continuity equation can be written by using the linearized valve flow equation Eq. (3.83) and the flow continuity equation of the cylinder chamber Eq.(3.18),

$$q_2 = q_A \tag{3.99}$$

$$K_{u2\_ext}u - K_{p2\_ext}p_A = A_A\dot{x} + \frac{V_A}{E}\frac{dp_A}{dt} \tag{3.100}$$

For the rod end of the hydraulic cylinder, the flow continuity equation can be written by using the linearized valve flow equation Eq.(3.86) and the flow continuity equation of the cylinder chamber Eq.(3.19),

$$q_4 = q_B \tag{3.101}$$

$$K_{u4\_ext}u + K_{p4\_ext}p_B = A_B\dot{x} - \frac{V_B}{E}\frac{dp_B}{dt} \tag{3.102}$$

The structural equation of the load is the same with the pump controlled system given by Eq. (3.47) and it is repeated here as,

$$\left[\gamma P_A(s) - P_B(s)\right]A_B = (ms+b)sX(s) \tag{3.103}$$

These 3 equations, with one known control input u, and 3 unknowns which are cylinder chamber pressures p_A, p_B and cylinder rod velocity $\dot{x}$, can be solved to find the transfer function between the input spool position u, and output cylinder rod velocity $\dot{x}$. The derivation of the transfer function is explained in detail in Appendix B.

The transfer function between the reference input spool position command $U(s)$ and the cylinder rod velocity $V(s)$ for the extension case is as follows,

$$\frac{V(s)}{U(s)} = \frac{a_1 s + a_2}{b_1 s^3 + b_2 s^2 + b_3 s + b_4}$$

$$
\begin{aligned}
a_1 &= K_{u4\_ext} A_B \left(\gamma^2 + \alpha\right)\frac{V_B}{E} \\
a_2 &= K_{u4\_ext} A_B \left(\gamma^3 + 1\right) K_{p2\_ext} \\
b_1 &= m\frac{\alpha V_B{}^2}{E^2} \\
b_2 &= mK_{p2\_ext}\frac{V_B}{E}\left(\gamma\alpha + 1\right) + b\frac{\alpha V_B{}^2}{E^2} \\
b_3 &= m\gamma K_{p2\_ext}{}^2 + bK_{p2\_ext}\frac{V_B}{E}\left(\gamma\alpha + 1\right) + \left(\gamma^2 + \alpha\right)\frac{V_B}{E} A_B{}^2 \\
b_4 &= b\gamma K_{p2\_ext}{}^2 + \left(\gamma^3 + 1\right) K_{p2\_ext} A_B{}^2
\end{aligned}
\tag{3.104}
$$

The result is a 3rd order transfer function. Since the characteristic equation cannot be written in a factored form; it is very hard to interpret how the system parameters affect the roots of the characteristic equation. Therefore, likewise in the variable speed pump controlled system a relationship between the chamber pressures will be defined to reduce the order of the system.

By using Eq.(3.89), Eq.(3.90), Eq. (3.100) and Eq. (3.102) the relation between the chamber pressures can be written. Inserting Eq.(3.89) into Eq. (3.100), Eq.(3.90) into Eq. (3.102), multiplying Eq. (3.102) by γ and subtracting from Eq. (3.100) the relation between p_A and p_B in s-domain can be obtained as follows,

$$P_A(s) = -\frac{\gamma\frac{V_B}{E}s + \gamma^2 K_{p2\_ext}}{\frac{V_A}{E}s + K_{p2\_ext}} P_B(s) \tag{3.105}$$

This equation represents the dynamic pressure changes under an applied load. Likewise in the pump controlled system, if the frequency response of the transfer function between the dynamic chamber pressure changes is investigated, it will be seen the relation is linear below and above some predetermined frequencies. By this way a linear relationship between the dynamic pressure changes can be defined as follows,

$$P_A(s) = -\varphi P_B(s) \tag{3.106}$$

Similar to the variable speed pump control system case at high frequency excitations the chamber pressure change ratio will be determined by the chamber volumes and cylinder area ratio and will be equal to,

$$\varphi = \frac{\gamma V_B}{V_A} \tag{3.107}$$

For low frequency excitations the chamber pressure change ratio will be determined by the cylinder area ratio, and will be equal to

$$\varphi = \gamma^2 \tag{3.108}$$

Note that if the valve pressure coefficients are linearized for zero spool opening $u_o = 0$, then the valve pressure flow gain will be zero $K_{p2\_ext} = K_{p2\_ext} = 0$, and the dynamic pressure changes relation will be,

$$P_A(s) = -\frac{\gamma V_B}{V_A} P_B(s) \tag{3.109}$$

That is, for an applied loading independent of excitation frequency, the chamber pressure, p_A, will change $\gamma V_B / V_A$ times greater than the change of the chamber pressure, p_B.

The frequency response of the dynamic pressure change ratios are shown in Figure 3-21. Here the valve pressure coefficients are linearized at a spool position $u_o = 0.1V$ and for supply pressure $P_s = 12\,MPa$.

It is seen at low excitation frequencies that the dynamic pressure ratio of the cylinder chambers is 11.7 dB (magnitude 3.85) which is equal to γ^2. At higher frequencies larger than 1 Hz, the dynamic pressure change ratio drops to 4 dB (magnitude 1.047) which is equal to the $\varphi = \gamma V_B / V_A = \gamma / \alpha$ value. Practically, this means that under an oscillatory dynamic loading whose frequency is higher than 1 Hz, to compensate the dynamic load pressure, the chamber pressure p_B will reduce ΔP value from its steady state value, while the chamber pressure p_A will increase $1.047\Delta P$ value from its steady state value. Thus, the order of the open loop velocity response of the valve controlled system reduces by one, as the chamber pressures become linearly dependent.

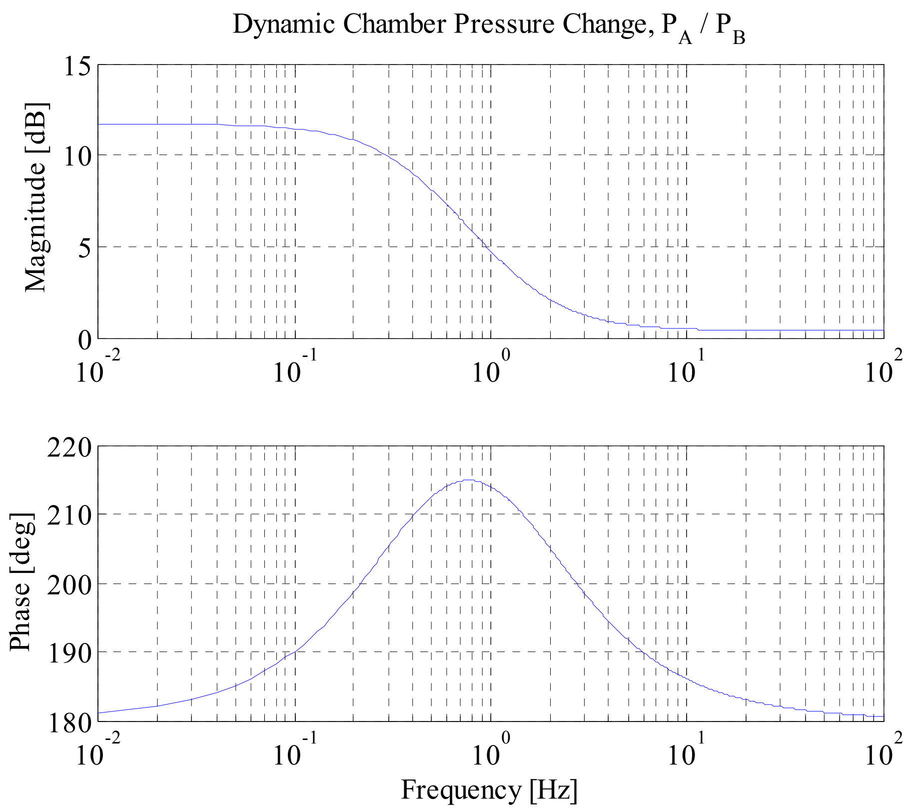

Figure 3-21 Dynamic Pressure Change Ratios

Of course, the valve pressure coefficient linearized at a higher spool position will increase the cut off frequency as it will increase the K_{p2_ext}, but it should be noted that in closed loop control applications the spool movement is not constant and always changing during the transient zone, and at steady state it becomes zero. Then assuming the spool position value as zero or a very small value will be reasonable rather than assuming spool position values like 1 or 2.

Practically it will be a reasonable assumption to use the linear dynamic pressure change relation Eq. (3.106) calculating the dynamic pressure change ratio φ, for higher excitation frequencies. That is,

$$\varphi = \frac{\gamma V_B}{V_A} \tag{3.110}$$

When the dynamic chamber pressure changes are linearly dependent, the order of the system reduces from 4 to 3. Then a much simpler and understandable transfer function can be derived by using the same continuity equations of the valve and cylinder chambers and structural equation of the load. The derivation of the transfer function is explained in detail in Appendix B.

The transfer function between the reference input spool position command $U(s)$ and the cylinder rod velocity $V(s)$ for the extension case is as follows,

$$\frac{V(s)}{U(s)} = \frac{\left(\gamma^2 + \alpha\right) K_{u4\_ext} A_B}{\frac{m\alpha V_B}{E} s^2 + \left(m\frac{\varphi + \alpha}{\gamma\varphi + 1}\gamma K_{p2\_ext} + \frac{b\alpha V_B}{E}\right) s + b\frac{\varphi + \alpha}{\gamma\varphi + 1}\gamma K_{p2\_ext} + \left(\gamma^2 + \alpha\right) A_B^{\,2}} \tag{3.111}$$

In Figure 3-22 the equivalent block diagram representation of this reduced order differential cylinder valve controlled system is given for the extension case. Note that it is very similar to the variable speed pump controlled system block diagram representation which is shown in Figure 3-22. The pump displacement term is replaced with the valve spool position gain and the pump leakage term is replaced with the valve pressure gain, as expected and explained in Section 3.3.3.1.

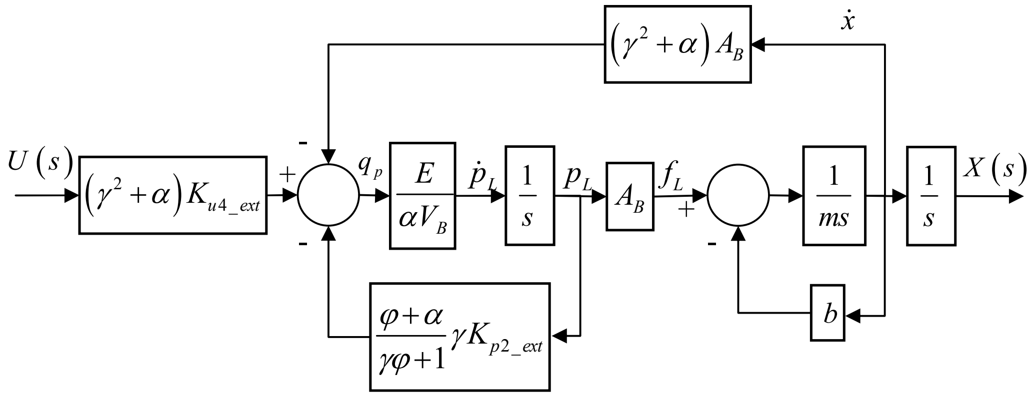

Figure 3-22 Block Diagram Representation of the Valve Controlled System for the Extension Case

Note that, for the retraction case, the following replacements for the linearized valve spool position and valve pressure coefficients, in Eq.(3.104), Eq. (3.111) and in Figure 3-22 should be made

$$\begin{aligned} K_{u4\_ext} &\rightarrow K_{u3\_ret} \\ K_{p2\_ext} &\rightarrow K_{p1\_ret} \end{aligned} \tag{3.112}$$

This second order transfer function can be used to understand the dynamic behavior of the system. The natural frequency and the damping ration of the valve controlled hydraulic system can be written as,

$$\omega_n = \sqrt{E\frac{b\dfrac{\varphi+\alpha}{\gamma\varphi+1}\gamma K_{p2\_ext} + \left(\gamma^2+\alpha\right)A_B{}^2}{m\alpha V_B}} \tag{3.113}$$

$$\xi = \frac{1}{2}\frac{\sqrt{E}\left(\dfrac{b\alpha V_B}{E} + m\dfrac{\varphi+\alpha}{\gamma\varphi+1}\gamma K_{p2\_ext}\right)}{\sqrt{m\alpha V_B\left(b\dfrac{\varphi+\alpha}{\gamma\varphi+1}\gamma K_{p2\_ext} + \left(\gamma^2+\alpha\right)A_B{}^2\right)}} \tag{3.114}$$

From the natural frequency and damping ratio equations defined above if a comparison is to be made with the pump controlled system it is seen that valve pressure gain K_{p2_ext}, which is found through the linearization of the valve flow equation around a fixed spool position and a constant supply pressure is similar to the equivalent leakage coefficient term C_{leak} of the pump controlled system.

Depending on the spool position where the linearization is performed, as the valve pressure gain decreases with the increasing supply pressure, it seems that the natural frequency of the open loop system will decrease with the increasing supply pressure. However it should be noted that as the valve spool position gain K_{u2_ext}, also depends on the supply pressure, the response of the closed loop system will increase by increasing the supply pressure as it will increase the valve spool position gain which is the open loop gain and shown in Figure 3-22.

Other important parameters which determine the natural frequency of the system is the hydraulic cylinder chamber volumes, bulk modulus of the hydraulic oil and cylinder area. The natural frequency of the system increases with the cylinder area and bulk modulus of the oil, whereas decreases with the hydraulic cylinder volume. Furthermore, the load mass decreases the natural frequency of the system as expected. Lastly, likewise in the pump controlled system, the term $\gamma^2 + \alpha$ appearing in the above equations indicate that increasing the area ratio and dead volume ratio, increases the natural frequency of the system while decreases the damping ratio.

Lastly the linear dynamic chamber pressure change assumption is checked. Table 3-6 gives the roots of the characteristic equations of the reduced second order transfer function defined by Eq. (3.111), and the third order transfer function defined by Eq. (3.104). The numerical values of the system parameters for the calculation of the transfer functions are taken from Table 3-7 and the valve flow coefficients are linearized at the spool position $u_o = 0.1V$ for supply pressure $p_s = 12\,MPa$.

Table 3-6 Pole and Zero Comparison of Reduced and Full Order Transfer Functions

	Poles	Zeros	Error between The poles of 3rd order TF and 2nd order TF
General 3rd order TF	-108.79 +1978.14 -108.79 -1978.14 -9.2330	-9.2339	
Reduced 2nd order TF $\varphi = \dfrac{\gamma V_B}{V_A} = 1.047$	-108.78 +1978.15 -108.78 -1978.15	0	0.00062+0.00431i
Reduced 2nd order TF $\varphi = \gamma^2 = 3.844$	-107.85 +1978.10 -107.85 -1978.10	0	0.92891+0.04406i
Reduced 2nd order TF $\varphi = 2$	-108.24 +1978.12 -108.24 -1978.12	0	0.05493+0.02422i

Likewise the pump controlled system, in valve controlled system it is seen in Table 3-6 that third pole and zero of the general 3rd order transfer function are very close, canceling each other, the remaining complex conjugate pole pairs are very close to the pole pair of the reduced second order system. Furthermore, the error between the real third order transfer function poles and second order transfer function poles are much smaller if the dynamic chamber pressure change ratio, φ, is determined for higher excitation frequencies

Table 3-7 Numerical Values of the System Parameters

Hydraulic Cylinder Parameters			
Cap side area	A_A	mm^2	1963.5
Rod Side area	A_B	mm^2	1001.4
Area ratio	γ	-	1.9608
Initial Cylinder Position	x_{in}	mm	50
Cylinder Stroke	$x_{\max}$	mm	100
Cap side chamber Volume (Pump System)	V_A	mm^3	172030
Rod Side Chamber Volume (Pump System)	V_B	mm^3	91842
Volume Ratio (Pump Sys)	α	-	1.8731
Cap side chamber Volume (Valve System)	V_A	mm^3	154387
Rod Side Chamber Volume (Valve System)	V_B	mm^3	82455
Volume Ratio (Valve Sys)	α	mm^3	1.8724
Load Parameters			
Mass	M	Ton	0.0123
Viscous friction coefficient	b	N s/mm	2.6
Pump Parameters			
Pump displacement	D_P	mm^3/rev	15600
Internal leakage coefficient	C_i	mm^3/(s.MPa)	1027
External leakage coefficient (cap side)	C_{e_a}	mm^3/(s.MPa)	120
External leakage coefficient (rod side)	C_{e_b}	mm^3/(s.MPa)	120
Hydraulic Oil Parameters			
Bulk Modulus	E	MPa	1300
Valve Parameter			
Valve Gain	K_v	mm^3/(s.V)	21380

CHAPTER 4

CONTROLLER DESIGN AND IMPLEMENTATION

This section is devoted to the controller and Kalman filter design for the variable speed pump and valve controlled systems. A state feedback control scheme is applied to both systems, as their performance is to be compared; the desired pole locations are chosen to be the same for the both systems. The linear state equations of the pump controlled system is used for pole placement in pump controlled system, whereas, the linearized state equations are used for the non-linear valve controlled system. As not all the states are measured directly and the measured ones are noisy, for filtering and estimation purposes a Kalman filter is designed. For the linear pump controlled system linear discrete time Kalman filter is designed, and for the non-linear valve controlled system a non-linear unscented Kalman filter is designed.

In this chapter the dynamic equations, which are already obtained in Chapter 3 for the pump controlled and valve controlled systems are expressed in state space form, the linear state feedback controller design and Kalman filter design are explained.

4.1 State Space Representation of Pump Controlled System

In order to design a state feedback controller and a Kalman filter, the systems should be defined in the form of state space. Thus, in this sub-section the state space representation of the variable speed pump controlled system will be obtained by using the dynamic equations defined in Section 3.2.4.

In Section 3.2.4, the order of the transfer function defining the speed response of the variable speed pump controlled system is found as 3. However, after showing that the hydraulic cylinder chamber pressures are linearly dependent below and above two prescribed cut off frequencies, it is concluded that the speed response can be represented by a 2nd order open loop transfer function. However if the position response is to be considered, then the order of the open loop transfer functions increases by one, due to the integration.

In this section, a general 4th order and a reduced 3rd order state space representation of the variable speed pump and valve controlled system are given. The reduced 3rd order state space representations of the systems will be used in the controller design. Because the cylinder chamber pressure changes are assumed to be dependent, the system can be defined and controlled by 3 states. The general 4th order state space representation will be used in Kalman filter design, because both of the hydraulic actuator chamber pressures are measured and filtered independently.

4.1.1 4th Order State Space Representation of Pump Controlled System

The system equations can be written in the standard state space form as,

$$\begin{aligned} \dot{\mathbf{x}} &= \mathbf{A}\mathbf{x} + \mathbf{B}\mathbf{u} \\ \mathbf{y} &= \mathbf{C}\mathbf{x} + \mathbf{D}\mathbf{u} \end{aligned} \tag{4.1}$$

where

$\mathbf{x}$: state vector

$\mathbf{y}$: output vector

$\mathbf{u}$: control input

$\mathbf{A}$: system matrix

$\mathbf{B}$: input matrix

$\mathbf{C}$: output matrix

D: feedforward matrix

The state variables, x_1, x_2, x_3 and x_4 are chosen as

$$\begin{aligned}
x_1 &= x && \text{Hydraulic cylinder position} \\
x_2 &= \dot{x} && \text{Hydraulic cylinde velocity} \\
x_3 &= p_A && \text{Hydraulic cylinder chamber A} \left(\text{cap end}\right) \text{pressure} \\
x_4 &= p_B && \text{Hydraulic cylinder chamber B} \left(\text{rod end}\right) \text{pressure}
\end{aligned} \tag{4.2}$$

Then from the definition of the state variables and Eq.(3.37), Eq. (3.38), Eq. (3.41), Eq. (3.43), Eq.(3.44) and Eq. (3.47) the state equations are obtained as,

$$\begin{aligned}
\dot{x}_1 &= x_2 \\
\dot{x}_2 &= \frac{-b}{m} x_2 + \frac{\gamma A_B}{m} x_3 - \frac{A_B}{m} x_4 \\
\dot{x}_3 &= -\gamma A_B \frac{E}{V_A} x_2 - \left(2C_i + 2C_{ea}\right) \frac{E}{V_A} x_3 + C_i \frac{E}{V_A} x_4 + \gamma D_p \frac{E}{V_A} n_2 + D_p \Psi \left(\beta + 1\right) \frac{E}{V_A} p_{sum} \\
\dot{x}_4 &= A_B \frac{E}{V_B} x_2 + C_i \frac{E}{V_B} x_3 - \left(C_i + C_{eb}\right) \frac{E}{V_B} x_4 - D_p \frac{E}{V_A} n_2 - D_p \Psi \frac{E}{V_A} p_{sum}
\end{aligned}$$

(4.3)

Note that in the pump control system, there are two control signals determining the total pump drive speed. One of them is the open loop pressure control signal n_{2o}, which is used to compensate the leakages and pressurize the cylinder chambers to a desired sum pressure value p_{sum}. This control input determines the static chamber pressures. The other control signal is the closed loop position control signal n_2. The position control signal determines the dynamic characteristics of the system that is the change of position, velocity and chamber pressures. To find the absolute value of the chamber pressures not only the position control signal n_2, but also the static pressure control signal n_{2o} is required. Thus the control inputs are defined as,

$$\mathbf{u} = \begin{bmatrix} n_2 \\ p_{sum} \end{bmatrix} \tag{4.4}$$

Then the state equations can be rewritten in standard vector matrix from as,

$$\begin{bmatrix} \dot{x}_1 \\ \dot{x}_2 \\ \dot{x}_3 \\ \dot{x}_4 \end{bmatrix} = \begin{bmatrix} 0 & 1 & 0 & 0 \\ 0 & \frac{-b}{m} & \frac{\gamma A_B}{m} & -\frac{A_B}{m} \\ 0 & -\frac{\gamma A_B E}{V_A} & -\frac{(2C_i + 2C_{ea})E}{V_A} & \frac{C_i E}{V_A} \\ 0 & \frac{A_B E}{V_B} & \frac{C_i E}{V_B} & -\frac{(C_i + C_{eb})E}{V_B} \end{bmatrix} \begin{bmatrix} x_1 \\ x_2 \\ x_3 \\ x_4 \end{bmatrix} + \begin{bmatrix} 0 & 0 \\ 0 & 0 \\ \frac{\gamma D_p E}{V_A} & \frac{D_p \Psi (\beta + 1) E}{V_A} \\ \frac{-D_p E}{V_B} & \frac{-D_p \Psi E}{V_B} \end{bmatrix} \begin{bmatrix} n_2 \\ p_{sum} \end{bmatrix}$$

(4.5)

In Kalman filter application, all the states are estimated. There is no feed through element as the control input does not affect the output directly. Then the output expression can be written in standard vector matrix form as,

$$\mathbf{y} = \begin{bmatrix} 1 & 0 & 0 & 0 \\ 0 & 1 & 0 & 0 \\ 0 & 0 & 1 & 0 \\ 0 & 0 & 0 & 1 \end{bmatrix} \begin{bmatrix} x_1 \\ x_2 \\ x_3 \\ x_4 \end{bmatrix} + \begin{bmatrix} 0 & 0 \\ 0 & 0 \\ 0 & 0 \\ 0 & 0 \end{bmatrix} \begin{bmatrix} n_2 \\ p_{sum} \end{bmatrix} \tag{4.6}$$

4.1.2 Reduced 3th Order State Space Representation of Pump Controlled System

The reduced order state space equations will be used to in controller design. To reduce the order of the system it is assumed that the dynamic changes of chamber pressures are linearly dependent, as it is explained in Section 3.2.4.

$$p_A = -\varphi \, p_B \tag{4.7}$$

Then the structural equation of the load can be written in terms of dynamic load pressure p_L instead of hydraulic cylinder chamber pressures p_A and p_B.

$$p_L = \gamma p_A - p_B \tag{4.8}$$

Then the states x_1, x_2 and x_3 of the system will be,

$$\begin{aligned} x_1 &= x && \text{Hydraulic cylinder position} \\ x_2 &= \dot{x} && \text{Hydraulic cylinder velocity} \\ x_3 &= p_L && \text{Dynamic load pressure change} \end{aligned} \tag{4.9}$$

and the state equations will be,

$$\begin{aligned}
\dot{x}_1 &= x_2 \\
\dot{x}_2 &= \frac{-b}{m}x_2 + \frac{A_B}{m}x_3 \\
\dot{x}_3 &= -\left(\gamma^2+\alpha\right)A_B\frac{E}{\alpha V_B}x_2 - C_{leak}\frac{E}{\alpha V_B}x_3 + \left(\gamma^2+\alpha\right)D_P\frac{E}{\alpha V_B}n_2
\end{aligned} \tag{4.10}$$

Note that only the position control signal n_2 appears as a control input in the state equations. Because the offset pressure control signal n_{2_o} does not affect the dynamics of the system, but only steady state chamber pressures, it is not included.

The output of the system is the hydraulic cylinder position which is to be controlled, and then the corresponding state equations and the output expressions can be written in standard matrix form as,

$$\begin{bmatrix}\dot{x}_1\\ \dot{x}_2\\ \dot{x}_3\end{bmatrix} = \begin{bmatrix} 0 & 1 & 0 \\ 0 & -\dfrac{b}{m} & \dfrac{A_B}{m} \\ 0 & -\dfrac{\left(\gamma^2+\alpha\right)A_B E}{\alpha V_B} & -C_{leak}\dfrac{E}{\alpha V_B}\end{bmatrix}\begin{bmatrix}x_1\\ x_2\\ x_3\end{bmatrix} + \begin{bmatrix}0\\ 0\\ \dfrac{\left(\gamma^2+\alpha\right)D_P E}{\alpha V_B}\end{bmatrix} n_2 \tag{4.11}$$

$$y = \begin{bmatrix}1 & 0 & 0\end{bmatrix}\begin{bmatrix}x_1\\ x_2\\ x_3\end{bmatrix} + \begin{bmatrix}0\end{bmatrix} n_2 \tag{4.12}$$

4.2 State Space Representation of Valve Controlled System

In Section 3.3 it is explained that, in valve controlled hydraulic circuit, there are two main non-linearities, affecting the system dynamics. The first one is the pressure flow relationship defined by Eq.(3.66). This non-linear flow equation is linearized around steady state chamber pressures and a prescribed spool position. Another main non-linearity is the result of the single rod cylinder with unequal piston areas, this result in unequal flow gains for the retracting and extraction of the hydraulic circuit. As a result, a piecewise linearized system is formed, the linearized dynamic equations are written both for extension and retraction cases.

4.2.1 4th Order State Space Representation of the Valve Controlled System

Likewise the pump control system, the valve controlled system is also defined fully by the same four states. Here, to be compatible with the pump controlled circuit, the state space representation of the 4th order system will be given by using the linearized valve dynamic equations. However different from the pump controlled system the 4th order state space representation of the valve system will not be used in Kalman filter design, as it is a non-linear filter.

The states of the system are,

$$\begin{aligned}
x_1 &= x && \text{Hydraulic cylinder position} \\
x_2 &= \dot{x} && \text{Hydraulic cylinde velocity} \\
x_3 &= p_A && \text{Hydraulic cylinder chamber A}\left(\text{cap end}\right)\text{pressure} \\
x_4 &= p_B && \text{Hydraulic cylinder chamber B}\left(\text{rod end}\right)\text{pressure}
\end{aligned} \tag{4.13}$$

Then from the definition of the state variables and Eq. (3.100), Eq. (3.102), Eq. (3.103) and Eq. (3.89), Eq. (3.90) the state equations for the extension case are obtained as

$$\begin{aligned}
\dot{x}_1 &= x_2 \\
\dot{x}_2 &= \frac{-b}{m}x_2 + \frac{\gamma A_B}{m}x_3 - \frac{A_B}{m}x_4 \\
\dot{x}_3 &= -\gamma A_B \frac{E}{V_A}x_2 - K_{p2_ext}\frac{E}{V_A}x_3 + \gamma K_{u4_ext}\frac{E}{V_A}u \\
\dot{x}_4 &= A_B \frac{E}{V_B}x_2 - \gamma K_{p2_ext}\frac{E}{V_B}x_4 - K_{u4_ext}\frac{E}{V_B}u
\end{aligned} \tag{4.14}$$

where the control input of the system is the valve spool position, u

$$u = \left[u\right] \tag{4.15}$$

Then the state equations can be rewritten in standard vector matrix from as,

$$
\begin{bmatrix} \dot{x}_1 \\ \dot{x}_2 \\ \dot{x}_3 \\ \dot{x}_4 \end{bmatrix} = \begin{bmatrix} 0 & 1 & 0 & 0 \\ 0 & \frac{-b}{m} & \frac{\gamma A_B}{m} & -\frac{A_B}{m} \\ 0 & -\frac{\gamma A_B E}{V_A} & -K_{p2\_ext}\frac{E}{V_A} & 0 \\ 0 & \frac{A_B E}{V_B} & 0 & -\gamma K_{p2\_ext}\frac{E}{V_B} \end{bmatrix} \begin{bmatrix} x_1 \\ x_2 \\ x_3 \\ x_4 \end{bmatrix} + \begin{bmatrix} 0 \\ 0 \\ \frac{\gamma K_{u4\_ext} E}{V_A} \\ -\frac{K_{u4\_ext} E}{V_B} \end{bmatrix} [u] \quad (4.16)
$$

Note that the state equations above are written for the extension case, for the retraction case the pressure flow gain, K_{p2_ext} should be replaced with K_{p1_ext} and the valve spool position flow gain K_{u4_ext} should be replaced by K_{u3_ext}. The output expression in standard vector matrix form is,

$$
y = \begin{bmatrix} 1 & 0 & 0 & 0 \\ 0 & 1 & 0 & 0 \\ 0 & 0 & 1 & 0 \\ 0 & 0 & 0 & 1 \end{bmatrix} \begin{bmatrix} x_1 \\ x_2 \\ x_3 \\ x_4 \end{bmatrix} + \begin{bmatrix} 0 \\ 0 \\ 0 \\ 0 \end{bmatrix} [u] \quad (4.17)
$$

4.2.2 Reduced 3th Order State Space Representation of Valve Controlled System

The reduced order state space equations will be used to in controller design. Likewise the pump controlled system, in valve controlled system, the order of the system can be reduced by assuming a linear relationship between the dynamic pressure changes of the hydraulic cylinder chambers and using dynamic load pressure p_L instead of hydraulic cylinder chamber pressures p_A and p_B.

$$
p_A = -\varphi\, p_B \quad (4.18)
$$

$$
p_L = \gamma\, p_A - p_B \quad (4.19)
$$

then the states x_1, x_2 and x_3 of the system will be,

$$
\begin{aligned}
x_1 &= x && \text{Hydraulic cylinder position} \\
x_2 &= \dot{x} && \text{Hydraulic cylinder velocity} \\
x_3 &= p_L && \text{Dynamic load pressure change}
\end{aligned} \quad (4.20)
$$

The corresponding state equations can be written if the assumed chamber pressure relations defined by Eq. (4.18) and Eq. (4.19) are substituted in the general form of state equations. The arrangement of the equations in more detail is given in Appendix B.

$$\begin{aligned}
\dot{x}_1 &= x_2 \\
\dot{x}_2 &= \frac{-b}{m}x_2 + \frac{A_B}{m}x_3 \\
\dot{x}_3 &= -\left(\gamma^2+\alpha\right)A_B\frac{E}{\alpha V_B}x_2 - \frac{\varphi+\alpha}{\gamma\varphi+1}\gamma K_{p2_ext}\frac{E}{\alpha V_B}x_3 + \left(\gamma^2+\alpha\right)K_{u4_ext}\frac{E}{\alpha V_B}u
\end{aligned} \tag{4.21}$$

The corresponding state equations and the output expressions for the extension case of the hydraulic cylinder can be written in standard matrix for as,

$$\begin{bmatrix}\dot{x}_1\\ \dot{x}_2\\ \dot{x}_3\end{bmatrix} = \begin{bmatrix} 0 & 1 & 0 \\ 0 & -\dfrac{b}{m} & \dfrac{A_B}{m} \\ 0 & -\dfrac{\left(\gamma^2+\alpha\right)A_B E}{\alpha V_B} & -\gamma K_{p2\_ext}\dfrac{\varphi+\alpha}{\gamma\varphi+1}\dfrac{E}{\alpha V_B}\end{bmatrix}\begin{bmatrix}x_1\\ x_2\\ x_3\end{bmatrix} + \begin{bmatrix}0\\ 0\\ \dfrac{\left(\gamma^2+\alpha\right)K_{u4\_ext}E}{\alpha V_B}\end{bmatrix}u \tag{4.22}$$

$$y = \begin{bmatrix}1 & 0 & 0\end{bmatrix}\begin{bmatrix}x_1\\ x_2\\ x_3\end{bmatrix} + \begin{bmatrix}0\end{bmatrix}u \tag{4.23}$$

Note that for the retraction case the pressure flow gain in the above the reduced order state equations, K_{p2_ext} should be replaced with K_{p1_ext} and the valve spool position flow gain K_{u4_ext} should be replaced by K_{u3_ext} .

4.3 Controller Design for the Pump System

In Table 3-5 the dominant open loop pole pairs of the transfer function defining the speed response of the pump controlled system is given as -120.02 ±1874.63i indicating a damping ratio of 0.064. Low damping is a drawback of the hydraulic systems, as it causes the system to oscillate; therefore, critical damping ratio is also a desired property to avoid overshoot as well as high bandwidth. From the transfer function given in Eq. (3.56) or the block diagram representation of the system given in Figure 3-15, it is obvious that the damping ratio of the system can be increased by increasing the equivalent leakage coefficient C_{leak}, meaning adding external leakage elements to the system resulting in additional energy losses. However the damping ratio of the system can be increased without conceding from energy efficiency, by control means.

To increase the damping of the hydraulic system, load pressure feedback or acceleration feedback can be applied. Because the load pressure feedback is directly proportional to the acceleration, they have the same effect on the closed loop system. In practical means, the load pressure feedback corresponds to an increase in the leakage coefficient. In Figure 4-1, if a block diagram reduction is made then the equivalent leakage coefficient will becomes $C_{leak} + K_{LP}\left(\gamma^2 + \alpha\right)D_P$. Then, the closed loop poles can be moved to desired locations by simply adjusting the gain of a proportional controller. However, in position control systems, in addition to complex conjugate pole pairs, there appears to be a pole at the origin pulling the root locus to the right half of the complex s-plane. Therefore, the desired closed loop pole locations are limited and the system will have a poor stability and even instability with the increasing gain value.

To have a critically damped system, that is dominant closed loop poles without imaginary parts, a compensator is necessary. For example if a second order compensator is utilized and the complex zero pair of the compensator are chosen such that they cancel the lightly damped pole pair of the plant, then the desired dominant closed loop pole locations can be specified by adjusting the pole pair of the compensator.

Another way is the pole placement, where not only the dominant closed loop pole locations, as in the conventional design approached discussed above, but all the closed loop pole locations are specified. If the system is fully state controllable and all the states are available then the closed loop pole locations can be chosen freely only limited by the saturation of the control element. By this way the dynamic characteristics of the system can be specified easily.

In this thesis study, the controller is designed through a pole placement via linear state feedback for the position control of the variable speed pump controlled system. The control system is designed using the linear set of reduced order system equations defined in Section 4.1.2.

The system is defined by three states which are

- cylinder position,
- cylinder velocity,
- load pressure.

The block diagram representation of the closed loop position control of the variable speed pump controlled system with the defined states is given in Figure 4-1. The parameters K_{pos}, K_{vel}, K_{PL} represent the state feedback gains of the position, velocity, and the load pressure signals.

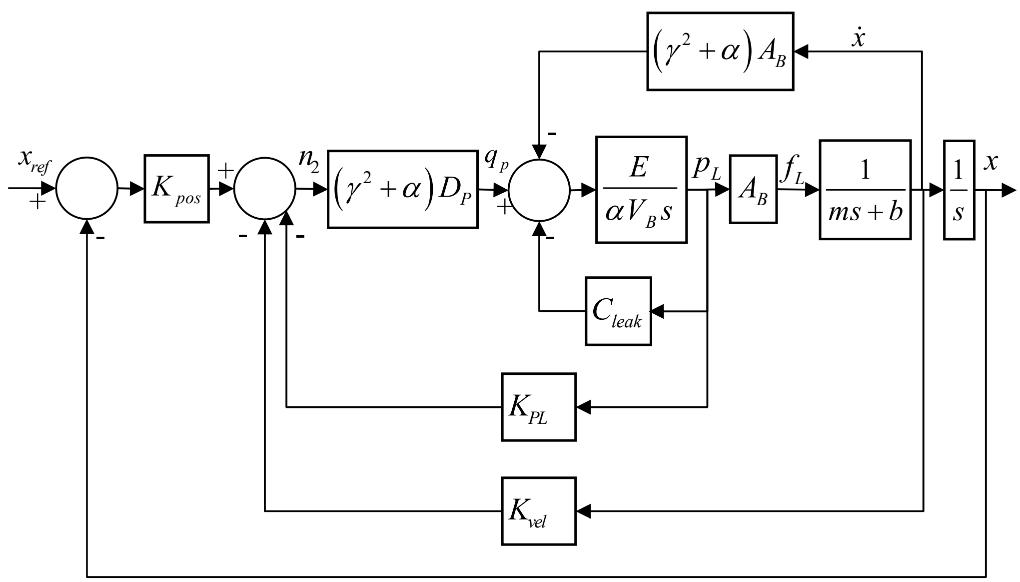

Figure 4-1 Block Diagram Representation of the Close Loop Pump Controlled System

After applying state feedback, the closed loop transfer function of the position control system becomes,

$$\frac{X(s)}{X_{ref}(s)} = \frac{(\gamma^2+\alpha)D_P A_B K_{pos}}{a_1 s^3 + a_2 s^2 + a_3 s + a_4}$$

$$\begin{aligned}
a_1 &= m\frac{\alpha V_B}{E} \\
a_2 &= m\left(C_{leak} + K_{LP}(\gamma^2+\alpha)D_P\right) + b\frac{\alpha V_B}{E} \\
a_3 &= b\left(C_{leak} + K_{LP}(\gamma^2+\alpha)D_P\right) + (\gamma^2+\alpha)(A_B + K_{vel}D_P)A_B \\
a_4 &= (\gamma^2+\alpha)D_P A_B K_{pos}
\end{aligned} \tag{4.24}$$

While designing the controller, it is assumed that all the state variables are available for feedback. The position and chamber pressures are measured and filtered through the Kalman filter, and the cylinder velocity is estimated by the Kalman filter.

The state equations and output expression derived in Section 4.1.2 is repeated below.

$$\begin{bmatrix}\dot{x}_1\\ \dot{x}_2\\ \dot{x}_3\end{bmatrix} = \begin{bmatrix} 0 & 1 & 0 \\ 0 & -\frac{b}{m} & \frac{A_B}{m} \\ 0 & -\frac{(\gamma^2+\alpha)A_B E}{\alpha V_B} & -C_{leak}\frac{E}{\alpha V_B}\end{bmatrix}\begin{bmatrix}x_1\\ x_2\\ x_3\end{bmatrix} + \begin{bmatrix}0\\ 0\\ \frac{(\gamma^2+\alpha)D_P E}{\alpha V_B}\end{bmatrix} n_2 \tag{4.25}$$

$$y = \begin{bmatrix}1 & 0 & 0\end{bmatrix}\begin{bmatrix}x_1\\ x_2\\ x_3\end{bmatrix} + [0]n_2 \tag{4.26}$$

In order to apply a state feedback, the control signal is chosen to be

$$u = -\mathbf{K}\mathbf{x} \tag{4.27}$$

where

$$\mathbf{K} = \begin{bmatrix}k_1 & k_2 & k_3\end{bmatrix} \tag{4.28}$$

$\mathbf{K}$ is the state feedback gain vector.

All the closed loop poles of the system can be placed at any arbitrary locations in the complex s-plane if the system is fully state controllable, requiring that the rank of the controllability matrix $\mathbf{M}$, is equal to number of states, that is 3.

The controllability matrix is defined by

$$\mathbf{M} = \left[\mathbf{B} \;\vdots\; \mathbf{AB} \;\vdots\; \mathbf{A}^2\mathbf{B}\right] \tag{4.29}$$

Since $\mathbf{M}$ is a 3x3 square matrix, the controllability condition reduces to

$$\det(\mathbf{M}) = -\left(\frac{\left(\gamma^2 + \alpha\right) D_P E}{\alpha V_B}\right)^3 \cdot \left(\frac{A_B}{m}\right)^2 \neq 0 \tag{4.30}$$

which is automatically satisfied, indicating that the system is fully state controllable.

The numerical values of $\mathbf{A}$, $\mathbf{B}$, $\mathbf{M}$ and $\det(\mathbf{M})$ are given below by using the numerical values of the hydraulic system parameters defined in Table 3-7.

$$\mathbf{A} = \begin{bmatrix} 0 & 1 & 0 \\ 0 & -211.38 & 81413.22 \\ 0 & -43.27 & -28.66 \end{bmatrix} \tag{4.31}$$

$$\mathbf{B} = \begin{bmatrix} 0 \\ 0 \\ 674.04 \end{bmatrix} \tag{4.32}$$

$$\mathbf{M} = \begin{bmatrix} 0 & 0 & 5.48 \cdot 10^7 \\ 0 & 5.48 \cdot 10^7 & -1.32 \cdot 10^{10} \\ 6.74 \cdot 10^2 & -1.93 \cdot 10^4 & -2.37 \cdot 10^9 \end{bmatrix} \tag{4.33}$$

$$\det(\mathbf{M}) = -2.03 \cdot 10^{18} \tag{4.34}$$

The characteristic equation of the system is obtained as

$$\left|s\mathbf{I} - \mathbf{A}\right| = s^3 + 240.04 s^2 + 3.53 \cdot 10^6 s + 0 \tag{4.35}$$

with the following coefficients of the characteristic equation

$$a_1 = 240.04 \qquad a_2 = 3.53 \cdot 10^6 \quad a_3 = 0 \tag{4.36}$$

It is seen that since there is a free s term in characteristic equation, the open loop system for position output behaves as an integrator. For the speed output system, the order reduces to two and the system is stable, as all the coefficients are of the same sign (positive).

In this thesis study, the performance of the system is determined through a sine sweep test, from their frequency responses. Therefore an m-file script is written which is calculating the state feedback gains for desired bandwidths, and then the system is tested for these gains and compared with the mathematical model results. The calculation of the controller gains for 5 Hz bandwidth is illustrated below.

For the closed loop position control system, in order to have a 5 Hz bandwidth, the desired closes loop poles are chosen as

$$\mu_1 = -5 \cdot (2\pi) \quad \mu_2 = -600 \qquad \mu_3 = -700 \tag{4.37}$$

The locations of the last two of the desired poles are chosen far away from the origin compared to the location of the first pole, which is the dominant one. The last two poles will decay very quickly, so that the fist pole, closer to the origin, will dominate in system response and determine the bandwidth of the system.

As a result the desired characteristic equation becomes,

$$(s-\mu_1)(s-\mu_2)(s-\mu_3) = s^3 + 1.33 \cdot 10^3 s^2 + 4.61 \cdot 10^5 s + 1.32 \cdot 10^7 \tag{4.38}$$

yielding the following coefficients of the desired characteristic equation,

$$b_1 = 1.33 \cdot 10^3 \quad b_2 = 4.61 \cdot 10^5 \quad b_3 = 1.32 \cdot 10^7 \tag{4.39}$$

Then the state feedback matrix can be obtained by the flowing equation [29].

$$\mathbf{K} = \begin{bmatrix} b_3 - a_3 & b_2 - a_2 & b_1 - a_1 \end{bmatrix} \mathbf{T}^{-1} \tag{4.40}$$

where the transformation matrix $\mathbf{T}$ is given by

$$\mathbf{T} = \mathbf{MW} \tag{4.41}$$

where $\mathbf{M}$ is the controllability matrix derived previously, and $\mathbf{W}$ is given by

$$\mathbf{W} = \begin{bmatrix} a_2 & a_1 & 1 \\ a_1 & 1 & 0 \\ 1 & 0 & 0 \end{bmatrix} = \begin{bmatrix} 3.53 \cdot 10^6 & 240.04 & 1 \\ 240.04 & 1 & 0 \\ 1 & 0 & 0 \end{bmatrix} \tag{4.42}$$

thus **T** is calculated to be

$$\mathbf{T} = \begin{bmatrix} 5.49 \cdot 10^7 & 0 & 0 \\ 0 & 5.49 \cdot 10^7 & 0 \\ -9.54 \cdot 10^{-7} & 1.42 \cdot 10^5 & 6.74 \cdot 10^2 \end{bmatrix} \tag{4.43}$$

Finally the desired feedback gain vector $\mathbf{K}$, obtained by use of the Eq.(4.40), is calculated to be,

$$\mathbf{K} = \begin{bmatrix} 0.2404 & -0.0601 & 1.6191 \end{bmatrix} \tag{4.44}$$

The feedback gain vector $\mathbf{K}$ is used to control the linear variable speed pump controlled hydraulic system. The MATLAB Simulink model of the closed loop position control system is shown in Figure 4-2.

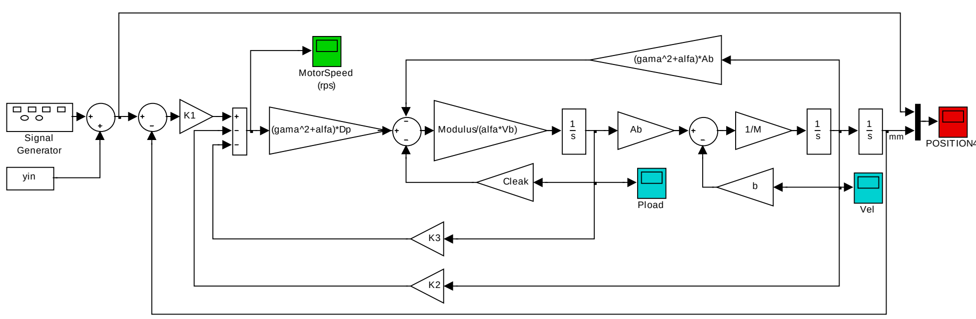

Figure 4-2 MATLAB Simulink Model of the Closed Loop Pump Controlled Position Control System

4.4 Controller Design for the Valve System

The same procedure applied in the pumped controlled system will be repeated here for the valve controlled system. Because of the inherent property that different extending and retracting dynamic characteristics of the single rod cylinder, unlike from the pump controlled system, here two set of controller gains are calculated one set for extension and another for retraction.

Similar to the variable speed pump controlled system, the valve control system is designed using the linearized set of reduced order system equations defined in Section 4.2.2 through pole placement via linear state feedback. The system is defined by three states which are

- cylinder position,
- cylinder velocity,
- load pressure.

The block diagram representation of the closed loop position control of the valve controlled system with the defined states is given in Figure 4-3.

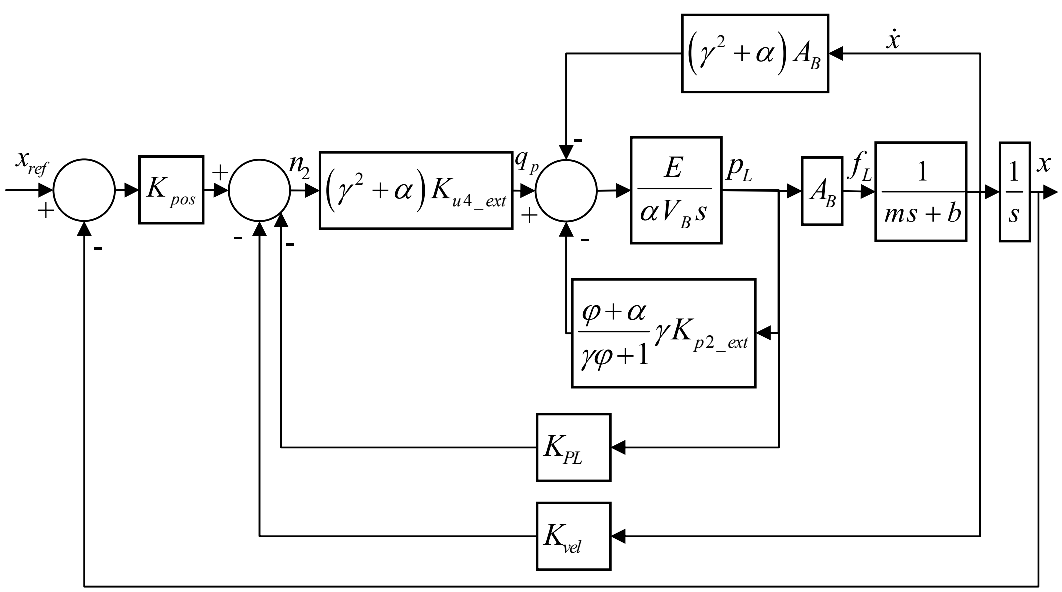

Figure 4-3 Block Diagram Representation of the Closed Loop Valve Controlled System

In Figure 4-3, the parameters K_{pos}, K_{vel}, K_{PL} represent the state feedback gains of the position, velocity and the load pressure signals.

Note that this block diagram representation is for the extension of the hydraulic actuator, for the retraction it will be the same if the replacement of valve gains defined in Eq. (3.112) are made.

After adding state feedback the closed loop transfer function of the position control system becomes

$$\frac{X(s)}{X_{ref}(s)} = \frac{\left(\gamma^2+\alpha\right)K_{u4\_ext}A_B K_{pos}}{a_1 s^3 + a_2 s^2 + a_3 s + a_4} \tag{4.45}$$

$$a_1 = m\frac{\alpha V_B}{E}$$
$$a_2 = m\left(\frac{\varphi+\alpha}{\gamma\varphi+1}\gamma K_{p2\_ext} + K_{LP}\left(\gamma^2+\alpha\right)K_{u4\_ext}\right) + b\frac{\alpha V_B}{E}$$
$$a_3 = b\left(\frac{\varphi+\alpha}{\gamma\varphi+1}\gamma K_{p2\_ext} + K_{LP}\left(\gamma^2+\alpha\right)K_{u4\_ext}\right) + \left(\gamma^2+\alpha\right)\left(A_B + K_{vel}K_{u4\_ext}\right)A_B$$
$$a_4 = \left(\gamma^2+\alpha\right)K_{u4\_ext}A_B K_{pos}$$

In the controller designs, it is assumed that all the state variables are available for feedback. The position and chamber pressures are measured and filtered through the unscented Kalman filter while the cylinder velocity is estimated through the unscented Kalman filter.

The state equations and output expression derived in Section 4.2 is repeated below for extension

$$\begin{bmatrix} \dot{x}_{1\_ext} \\ \dot{x}_{2\_ext} \\ \dot{x}_{3\_ext} \end{bmatrix} = \begin{bmatrix} 0 & 1 & 0 \\ 0 & -\frac{b}{m} & \frac{A_B}{m} \\ 0 & -\frac{\left(\gamma^2+\alpha\right)A_B E}{\alpha V_B} & -\gamma K_{p2\_ext}\frac{\varphi+\alpha}{\gamma\varphi+1}\frac{E}{\alpha V_B} \end{bmatrix} \begin{bmatrix} x_1 \\ x_2 \\ x_3 \end{bmatrix} + \begin{bmatrix} 0 \\ 0 \\ \frac{\left(\gamma^2+\alpha\right)K_{u4\_ext}E}{\alpha V_B} \end{bmatrix} n_2 \tag{4.46}$$

for retraction

$$\begin{bmatrix} \dot{x}_{1\_ret} \\ \dot{x}_{2\_ret} \\ \dot{x}_{3\_ret} \end{bmatrix} = \begin{bmatrix} 0 & 1 & 0 \\ 0 & -\dfrac{b}{m} & \dfrac{A_B}{m} \\ 0 & -\dfrac{\left(\gamma^2+\alpha\right)A_B E}{\alpha V_B} & -\gamma K_{p1\_ext}\dfrac{\varphi+\alpha}{\gamma\varphi+1}\dfrac{E}{\alpha V_B} \end{bmatrix} \begin{bmatrix} x_1 \\ x_2 \\ x_3 \end{bmatrix} + \begin{bmatrix} 0 \\ 0 \\ \dfrac{\left(\gamma^2+\alpha\right)K_{u3\_ext}E}{\alpha V_B} \end{bmatrix} n_2 \quad (4.47)$$

$$y = \begin{bmatrix} 1 & 0 & 0 \end{bmatrix} \begin{bmatrix} x_1 \\ x_2 \\ x_3 \end{bmatrix} + \begin{bmatrix} 0 \end{bmatrix} n_2 \quad (4.48)$$

In the state feedback control algorithm of the valve controlled system, two different control signals are generated, one for extension and another for retraction.

$$\begin{aligned} u_{ext} &= -\mathbf{K}_{ext}\,\mathbf{x}_{ext} \\ u_{ret} &= -\mathbf{K}_{ret}\,\mathbf{x}_{ret} \end{aligned} \quad (4.49)$$

where

$$\begin{aligned} \mathbf{K}_{ext} &= \begin{bmatrix} k_{1\_ext} & k_{2\_ext} & k_{3\_ext} \end{bmatrix} \\ \mathbf{K}_{ret} &= \begin{bmatrix} k_{1\_ret} & k_{2\_ret} & k_{3\_ret} \end{bmatrix} \end{aligned} \quad (4.50)$$

where $\mathbf{K}_{ext}$ is the state feedback gain vector for the extension of the hydraulic cylinder and $\mathbf{K}_{ret}$ is the state feedback gain vector for the retraction of the hydraulic cylinder.

All the closed loop poles of the system can be replaced at any arbitrary locations in the complex plane if the system is fully state controllable, requiring that the rank of the controllability matrix $\mathbf{M}$, is equal to number of states, that is 3.

The controllability matrix is defined by

$$\mathbf{M} = \begin{bmatrix} \mathbf{B} & \vdots\ \mathbf{AB} & \vdots\ \mathbf{A}^2\mathbf{B} \end{bmatrix} \quad (4.51)$$

Since $\mathbf{M}$ is a 3x3 square matrix, the controllability condition reduces to

$$\det(\mathbf{M}) = -\left(\frac{\left(\gamma^2+\alpha\right)K_{u3\_ext}E}{\alpha V_B}\right)^3 \cdot \left(\frac{A_B}{m}\right)^2 \neq 0 \tag{4.52}$$

which is automatically satisfied, indicating that the system is fully state controllable.

The valve system is linearized at a spool position corresponding to $u_o = 0.1V$ and for a supply pressure of $P_s = 8.3\,MPa$. The numerical values of $\mathbf{A}$, $\mathbf{B}$, $\mathbf{M}$ and $\det(\mathbf{M})$ are given below by using the numerical values of the hydraulic system parameters defined in Table 3-7.

$$\mathbf{A}_{ext} = \begin{bmatrix} 0 & 1 & 0 \\ 0 & -211.38 & 81413.22 \\ 0 & -48.21 & -5.68 \end{bmatrix}$$

$$\mathbf{A}_{ret} = \begin{bmatrix} 0 & 1 & 0 \\ 0 & -211.38 & 81413.22 \\ 0 & -48.21 & -7.96 \end{bmatrix} \tag{4.53}$$

$$\mathbf{B}_{ext} = \begin{bmatrix} 0 \\ 0 \\ 1295.98 \end{bmatrix} \qquad \mathbf{B}_{ret} = \begin{bmatrix} 0 \\ 0 \\ 925.52 \end{bmatrix} \tag{4.54}$$

$$\mathbf{M}_{ext} = \begin{bmatrix} 0 & 0 & 1.05\cdot 10^{8} \\ 0 & 1.05\cdot 10^{8} & -2.29\cdot 10^{10} \\ 1296 & -7.37\cdot 10^{3} & -5.09\cdot 10^{9} \end{bmatrix}$$

$$\mathbf{M}_{ret} = \begin{bmatrix} 0 & 0 & 7.53\cdot 10^{7} \\ 0 & 7.53\cdot 10^{7} & -1.65\cdot 10^{10} \\ 925 & -7.37\cdot 10^{3} & -3.63\cdot 10^{9} \end{bmatrix} \tag{4.55}$$

$$\det(\mathbf{M}_{ext}) = -1.44\cdot 10^{19}$$

$$\det(\mathbf{M}_{ret}) = -5.25\cdot 10^{18} \tag{4.56}$$

The characteristic equation of the system is obtained as for extension

$$\left|s\mathbf{I}-\mathbf{A}_{ext}\right| = s^3 + 217.07s^2 + 3.93\cdot10^6 s + 0 \tag{4.57}$$

and for retraction

$$\left|s\mathbf{I}-\mathbf{A}_{ret}\right| = s^3 + 219.34s^2 + 3.93\cdot10^6 s + 0 \tag{4.58}$$

with the following coefficients of the characteristic equationfor extension

$$a_{1\_ext} = 217.07 \; a_{2\_ext} = 3.93\cdot10^6 \qquad a_{3\_ext} = 0 \tag{4.59}$$

and for retraction

$$a_{1\_ret} = 219.34 \; a_{2\_ret} = 3.93\cdot10^6 \qquad a_{3\_ret} = 0 \tag{4.60}$$

It is seen that, for the speed output, the system is stable, as all the coefficients are of the same sign (positive).

In order to be compatible with the pump controlled system, the state feedback gains will be calculated for the same desired closed loop pole locations.

$$\mu_1 = -5\cdot\left(2\pi\right) \; \mu_2 = -600 \qquad \mu_3 = -700 \tag{4.61}$$

The desired characteristic equation is the same with the variable speed pump controlled system,

$$\left(s-\mu_1\right)\left(s-\mu_2\right)\left(s-\mu_3\right) = s^3 + 1.33\cdot10^3 s^2 + 4.61\cdot10^5 s + 1.32\cdot10^7 \tag{4.62}$$

yielding the following coefficients of the desired characteristic equation,

$$b_1 = 1.33\cdot10^3 \quad b_2 = 4.61\cdot10^5 \quad b_3 = 1.32\cdot10^7 \tag{4.63}$$

Then the state feedback matrix sets both for extension and retraction can be obtained by the flowing equation [29].

$$\begin{aligned} \mathbf{K}_{ext} &= \left[b_3 - a_{3\_ext} \quad b_2 - a_{2\_ext} \quad b_1 - a_{1\_ext}\right]\mathbf{T}_{ext}^{-1} \\ \mathbf{K}_{ret} &= \left[b_3 - a_{3\_ret} \quad b_2 - a_{2\_ret} \quad b_1 - a_{1\_ret}\right]\mathbf{T}_{ret}^{-1} \end{aligned} \tag{4.64}$$

where the transformation matrix $\mathbf{T}$ is given by

$$\mathbf{T}_{ext} = \mathbf{M}_{ext}\mathbf{W}_{ext}$$
$$\mathbf{T}_{ret} = \mathbf{M}_{ret}\mathbf{W}_{ret} \tag{4.65}$$

where **M** is the controllability matrix derived previously, and **W** is given by

$$\mathbf{W}_{ext} = \begin{bmatrix} a_2 & a_1 & 1 \\ a_1 & 1 & 0 \\ 1 & 0 & 0 \end{bmatrix} = \begin{bmatrix} 3.93\cdot 10^6 & 217.07 & 1 \\ 217.07 & 1 & 0 \\ 1 & 0 & 0 \end{bmatrix}$$
$$\mathbf{W}_{ret} = \begin{bmatrix} a_2 & a_1 & 1 \\ a_1 & 1 & 0 \\ 1 & 0 & 0 \end{bmatrix} = \begin{bmatrix} 3.93\cdot 10^6 & 219.34 & 1 \\ 219.34 & 1 & 0 \\ 1 & 0 & 0 \end{bmatrix} \tag{4.66}$$

thus **T** is calculated to be

$$\mathbf{T}_{ext} = \begin{bmatrix} 1.05\cdot 10^8 & 0 & 0 \\ 3.81\cdot 10^{-6} & 1.05\cdot 10^8 & 0 \\ -1.91\cdot 10^{-6} & 2.74\cdot 10^5 & 1.29\cdot 10^3 \end{bmatrix}$$
$$\mathbf{T}_{ret} = \begin{bmatrix} 7.53\cdot 10^7 & 0 & 0 \\ -3.31\cdot 10^{-6} & 7.53\cdot 10^7 & 0 \\ 0 & 1.96\cdot 10^5 & 9.25\cdot 10^2 \end{bmatrix} \tag{4.67}$$

Finally the desired feedback gain vector sets $\mathbf{K}_{ext}$ and $\mathbf{K}_{ret}$ are obtained by use of the Eq.(4.40), is calculated to be,

$$\mathbf{K}_{ext} = \begin{bmatrix} 0.1251 & -0.0351 & 0.8598 \end{bmatrix}$$
$$\mathbf{K}_{ret} = \begin{bmatrix} 0.1751 & -0.0491 & 1.2015 \end{bmatrix} \tag{4.68}$$

The feedback gain vector sets $\mathbf{K}_{ext}$ and $\mathbf{K}_{ret}$ are used to control the linearized vale controlled hydraulic system. According to the spool position at the previous time step u_{k-1}, the control signal at time step k, u_k is chosen as follows,

$$\begin{aligned} u_{k-1} &\geq 0 \qquad \Rightarrow \qquad u_k = -K_{ext}x_{ext} \\ u_{k-1} &< 0 \qquad \Rightarrow \qquad u_k = -K_{ret}x_{ret} \end{aligned} \tag{4.69}$$

The MATLAB Simulink model of the closed loop position control system is shown in Figure 4-4.

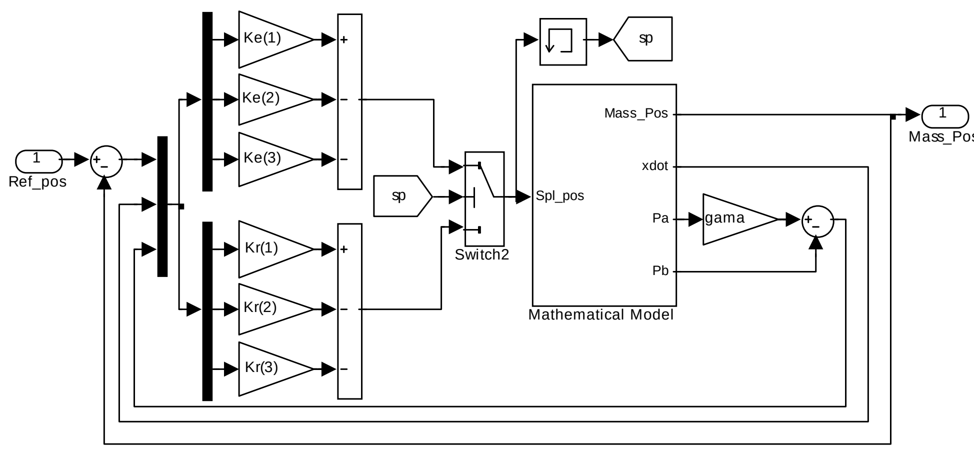

Figure 4-4 MATLAB Simulink Model of the Closed Loop Valve Controlled Position Control System

4.5 Kalman Filter Theory and Design

In this thesis study, Kalman filter is used both for filtering and estimation purposes. The measured states cannot be used directly as feedback signals to the controller, because the noise on the measurements disturbs the control signal resulting in chattering of the actuator (servomotor for the pump controlled case and solenoid valve for the valve controlled case). Therefore, the noise on the measured signals should be attenuated and the signal should be smoothed before feedingback to the controller. Both in the variable speed pump controlled and valve controlled systems, three states are measured, which are hydraulic actuator position (x) and hydraulic actuator chamber pressures (p_A, p_B). The noisy measured states are smoothed via Kalman filter and send to the controller. However, the controller needs another state, which is the hydraulic actuator velocity ($\dot{x}$); this state is estimated via Kalman filter.

In this section, a conventional discrete Kalman filter is designed and explained for the variable speed pump controlled system. However for the valve controlled system, an unscented Kalman filter is designed and explained.

4.5.1 Discrete Kalman Filter

A Kalman filter is a set of mathematical equations that provides an efficient way to estimate the state of the process; it minimizes the mean of the squared error between the measured and estimated state. The filter is powerful in estimation of past, present and even future states [30].

In order to use a Kalman filter to remove noise from a signal, the process that is measured must be describable by a linear system [31]. A general linear discrete time system is simply a process that can be described by the following two difference equations; namely,

state equation,

$$\mathbf{q}_k = \mathbf{\Phi}\,\mathbf{q}_{k-1} + \mathbf{G}\mathbf{q}_{k-1} + \mathbf{w}_{k-1} \tag{4.70}$$

and measurement equation

$$\mathbf{z}_k = \mathbf{H}\,\mathbf{q}_k + \mathbf{v}_k \tag{4.71}$$

where $\mathbf{\Phi}$ is the (nxn) state transition matrix, **G** is the (nxr) input matrix, **H** is the (mxn) measurement matrix, $\mathbf{q}_k$ is the (nx1) state vector, $\mathbf{z}_k$ is the system output, $\mathbf{u}_{k-1}$ is the (rx1) control input, $\mathbf{w}_k$ is the (nx1) process noise and $\mathbf{v}_k$ is the (mx1) measurement noise.

Both process and measurement noise ($\mathbf{w}_k$, $\mathbf{v}_k$) are assumed to have zero mean and Gaussian distribution. The covariances of these noise vectors are represented by **R** and **Q** covariance matrices in Kalman filter equations.

The (nxn) covariance matrix **Q** of the process noise $\mathbf{w}_k$ is defined by

$$\mathbf{Q} = E\left[\mathbf{w}\,\mathbf{w}^T\right] \tag{4.72}$$

The (mxm) covariance matrix $\mathbf{R}$ of the measurement noise $\mathbf{v}_k$ is defined by

$$\mathbf{R} = E\left[\mathbf{v}\,\mathbf{v}^T\right] \tag{4.73}$$

The $\mathbf{R}$ and $\mathbf{Q}$ matrices depend on the noise level of the measurements together with the accuracy of the sensors, and the modeling uncertainties.

The Kalman filter uses a predictor corrector algorithm to perform the estimation of states. Using the system model, a priori state estimate vector at time state k is predicted by using the previous state estimate at time state k-1. Then this predicted priori estimate is corrected by the actual measurements. To be more understandable a block diagram representation of the filter is drawn in Figure 4-5.

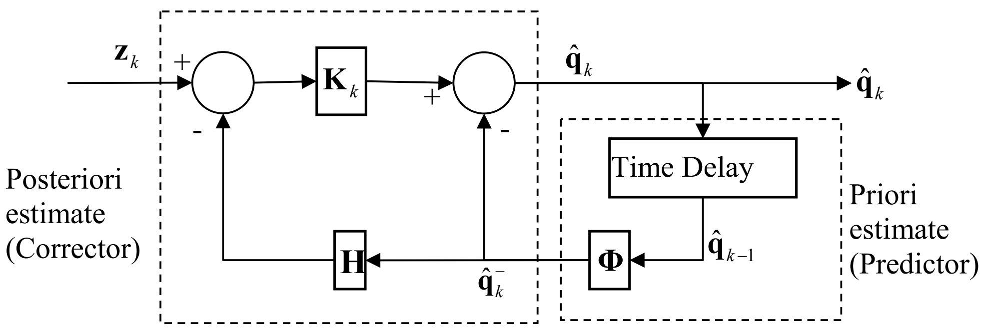

Figure 4-5 Kalman Filter Block Diagram

Here $\mathbf{z}_k$ is the actual measurement, $\hat{\mathbf{q}}_k^-$ is the priori estimate, which is an estimate at step k given the knowledge of the process at step k-1 and $\hat{\mathbf{q}}_k$ is the posteriori state estimate which is the corrected value of the measurement prediction $\mathbf{H}\,\hat{\mathbf{q}}_k^-$ with the actual measurements.

For the predictor-corrector algorithm of the Kalman filter defined in Figure 4-5, two estimate errors can be defined. One is the error between the actual state values and priori estimates, and the other is the error between the actual state values and posteriori state estimates as expressed below.

$$\mathbf{e}^-{}_k = \mathbf{q}_k - \hat{\mathbf{q}}_k^- \tag{4.74}$$

$$\mathbf{e}_k = \mathbf{q}_k - \hat{\mathbf{q}}_k \tag{4.75}$$

The nxn covariance matrices of the priori and posteriori estimate errors are defined as

$$\mathbf{P}_k^- = E\left[\mathbf{e}^-_k \, \mathbf{e}^{-T}_k\right] \tag{4.76}$$

$$\mathbf{P}_k = E\left[\mathbf{e}_k \, \mathbf{e}_k^T\right] \tag{4.77}$$

Returning to the Figure 4-5 again, the mathematical formulation of the block diagram can be written as,

$$\hat{\mathbf{q}}_k = \hat{\mathbf{q}}_k^- + \mathbf{K}_k\left(\mathbf{z}_k - \mathbf{H}\,\hat{\mathbf{q}}_k^-\right) \tag{4.78}$$

The main goal of the filter here is to find the nxm Kalman gain matrix $\mathbf{K}_k$ which will minimize posteriori estimate error covariance, which is defined as Eq. (4.77). This minimization can be accomplished by first substituting Eq. (4.78) into the above definition for $\mathbf{e}_k$, substituting that into Eq. (4.77), performing the indicated expectations, taking the derivative of the trace of the result with respect to $\mathbf{K}_k$, setting that equal to zero and then solving for $\mathbf{K}_k$. The details of these calculations can be found in literature [30].

The resulting Kalman gain matrix $\mathbf{K}$ that minimizes the posteriori state estimate error covariance Eq. (4.77) is found as,

$$\mathbf{K}_k = \frac{\mathbf{P}_k^-\mathbf{H}^T}{\mathbf{H}\mathbf{P}_k^-\mathbf{H}^T + \mathbf{R}} \tag{4.79}$$

From the Eq. (4.79) it is seen that as the measurement error covariance goes to zero, the Kalman gain weights the residual $\left(\mathbf{z}_k - \mathbf{H}\hat{\mathbf{q}}_k^-\right)$ defined in Eq.(4.78).

$$\lim_{\mathbf{R}\to 0}\mathbf{K}_k = \mathbf{H}^{-1} \tag{4.80}$$

As the priori estimate error covariance $\mathbf{P}_k^-$ goes to zero, the Kalman gain weights the residual $\left(\mathbf{z}_k - \mathbf{H}\,\hat{\mathbf{q}}_k^-\right)$ less heavily.

$$\lim_{P_k^- \to 0} \mathbf{K}_k = 0 \tag{4.81}$$

In other words, if the measurement error covariance $\mathbf{R}$ goes to zero, that is using high accuracy sensors in a noise-free environment, the Kalman filter trusts more on the actual measurements $\mathbf{z}_k$, while the predicted measurement $\mathbf{H}\,\hat{\mathbf{q}}_k^-$ are trusted less. If the priori estimate error covariance $\mathbf{P}_k^-$ goes to zero the Kalman filter trusts less on the actual measurements $\mathbf{z}_k$, and trusts more on the system model, which is the predicted measurement $\mathbf{H}\,\hat{\mathbf{q}}_k^-$.

Kalman Filter Algorithm

The equations of the Kalman filter fall into two groups, time update equations and measurement update equations. Time update equations can also be considered as predictor equations, while measurement equations can be considered as corrector equations.

Time update equations are responsible for projecting the current state and error covariance estimates at time step k-1 to obtain the priori estimates for the time step k.

$$\hat{\mathbf{q}}_k^- = \mathbf{\Phi}\,\hat{\mathbf{q}}_{k-1} + \mathbf{G}\mathbf{u}_{k-1} \tag{4.82}$$

$$\mathbf{P}_k^- = \mathbf{\Phi}\,\mathbf{P}_{k-1}\mathbf{\Phi}^T + \mathbf{Q} \tag{4.83}$$

In Eq. (4.82) a priori (predicted) state estimate vector, $\hat{\mathbf{q}}_k^-$, at time step k is defined from the posteriori (corrected) state estimate, $\hat{\mathbf{q}}_{k-1}$, at the previous time step k-1, by using the given system model and the control input $\mathbf{u}_{k-1}$. Likewise, in the Eq. (4.83) a priori estimate error covariance $\mathbf{P}_k^-$ at time step k is defined from the posteriori estimate error covariance $\mathbf{P}_{k-1}$ at the previous time step k-1.

The measurement update equations are responsible for incorporating new measurements into the priori estimate to obtain an improved posteriori estimate

$$\mathbf{K}_k = \mathbf{P}_k^-\,\mathbf{H}^T\left(\mathbf{H}\,\mathbf{P}_k^-\,\mathbf{H}^T + \mathbf{R}\right)^{-1} \tag{4.84}$$

$$\hat{\mathbf{q}}_k = \hat{\mathbf{q}}_k^- + \mathbf{K}\left(\mathbf{z}_k - \mathbf{H}\,\hat{\mathbf{q}}_k^-\right) \tag{4.85}$$

$$\mathbf{P}_k = \left(\mathbf{I} - \mathbf{K}_k \mathbf{H}\right)\mathbf{P}_k^- \tag{4.86}$$

In Eq. (4.84) the (nxm) Kalman gain $\mathbf{K}_k$ at time step k is calculated. As explained above this equation is the result of the minimization operation of the posteriori estimate error covariance. In other words, if the Kalman gain $\mathbf{K}_k$ is written in the way defined in Eq. (4.84), the error covariance between the actual measured states and the output estimated states will be minimized.

In Eq. (4.85) a posteriori state estimate $\hat{\mathbf{q}}_k$ is obtained as a linear combination of the priori estimate $\hat{\mathbf{q}}_k^-$ and a weighted difference between the actual measurements $\mathbf{z}_k$ and a measurement prediction $\mathbf{H}\,\hat{\mathbf{q}}_k^-$. Lastly in Equation (4.86) a posteriori estimate error covariance is obtained.

After each time and measurement update pair, the process is repeated with the previous a posteriori estimates used to project or predict the new a priori estimates. This recursive predictor corrector structure of the Kalman filter defined by the Equations (4.82), (4.83), (4.84), (4.85), (4.86).is represented in the Figure 4-6.

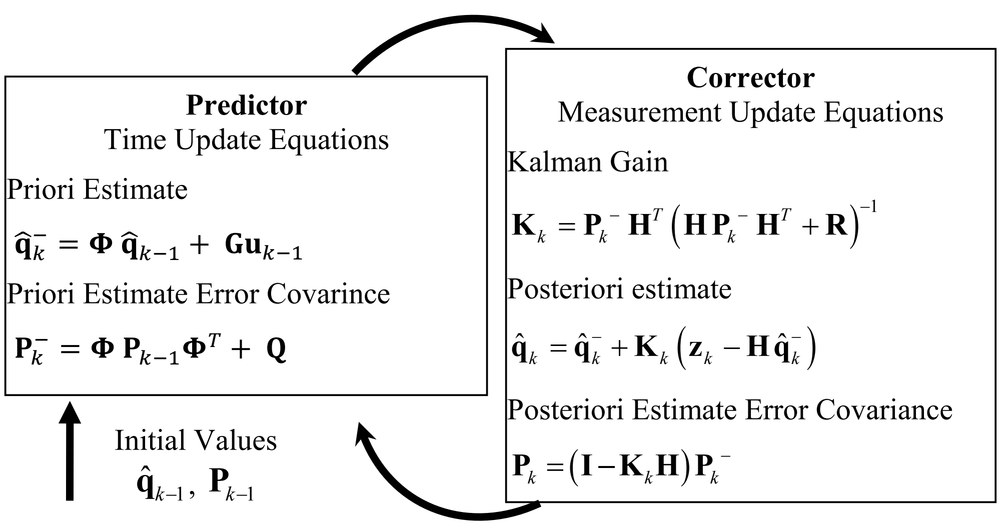

Figure 4-6 Kalman Filter Algorithm

4.5.2 Application in Pump Controlled System

Since the Kalman filter is a discrete time process and to be compatible with the real time digital computing, the state space equations defining the pump controlled systems are discretized.

Instead of writing analytical expressions for the discrete time state space equations MATLAB software is used to convert the continuous time states space equations which, are defined by Eq. (4.5), to discrete time state space equations. The MATLAB function used for this conversion is "`c2dm`".

The state space equations are discretized by using forward difference method for the sampling frequency of 1000 Hz. The resulting, system matrix, input matrix and output matrix are given below.

$$\mathbf{A}_d = \begin{bmatrix} 1 & 0.0005 & 0.0548 & -0.0279 \\ 0 & -0.3069 & 72.1932 & -36.6187 \\ 0 & -0.0067 & 0.1762 & 0.4178 \\ 0 & -0.0067 & 0.7826 & 0.5927 \end{bmatrix} \tag{4.87}$$

$$\mathbf{B}_d = \begin{bmatrix} 0.0072 & 0.0001 \\ 18.8356 & -0.1223 \\ 0.1213 & 0.0015 \\ -0.1153 & 0.0054 \end{bmatrix} \tag{4.88}$$

$$\mathbf{C}_d = \begin{bmatrix} 1 & 0 & 0 & 0 \\ 0 & 1 & 0 & 0 \\ 0 & 0 & 1 & 0 \\ 0 & 0 & 0 & 1 \end{bmatrix} \tag{4.89}$$

MATLAB Simulink model of the Kalman filter is shown in Figure 4-7. The model is formed by using the Eq. (4.82) to (4.86).

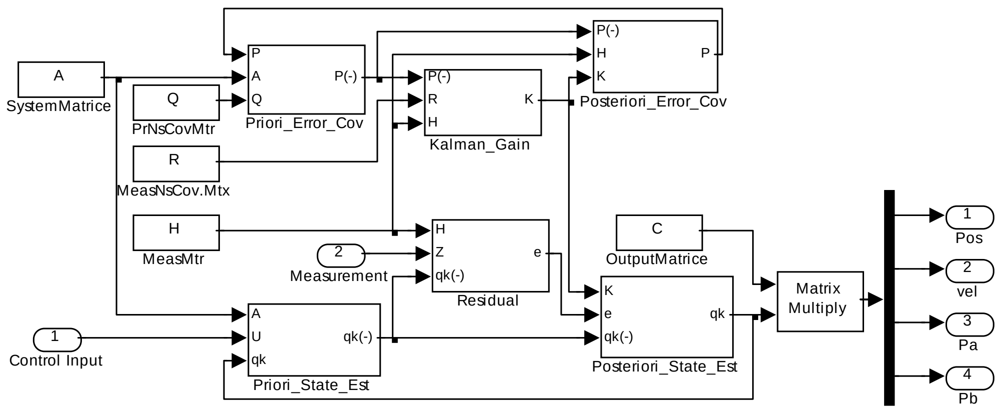

Figure 4-7 MATLAB Simulink Kalman Filter Model for the Variable Speed Pump Controlled System

4.5.3 Unscented Kalman Filter

Application of Kalman filters to non-linear systems is difficult, for this reason an extension of linear Kalman filter which is called extended Kalman filter (EKF) is developed to apply the Kalman filter algorithm in non-linear systems. EKF linearize all the non-linear system equations around the last states so that the traditional linear Kalman filter algorithm can be applied to non-linear systems. However, although it has common use, in literature a number of drawbacks of EKF algorithm is given, such as possibility of unstable filter, dependence on time interval, and especially unreliable estimates for highly non-linear systems.

In this thesis study a new approach, called unscented Kalman filter (UKF), is employed for the filtering and estimation purposes of the states of the valve controlled hydraulic system.

The unscented Kalman filter has the same structure with the linear discrete Kalman filter. Linear Kalman filter utilize linear transformation to predict the mean and covariance of the estimated states, Eq.(4.82) and Eq. (4.83), as the state transition matrix and the measurement matrix are linear, however UKF uses a transformation called unscented transform to calculate the mean and covariance of the states undergoing a non-linear transform. The details of this transformation can be found in the papers of Julier and Uhlmann [32]. Here the procedure will be summarized.

The problem of the unscented transformation is to predict the mean $\underline{\mathbf{y}}$ and the covariance $\mathbf{P}_{yy}$ of a m-dimensional vector random variable $\mathbf{y}$ from the n-dimensional random variable $\mathbf{x}$ with mean $\underline{\mathbf{x}}$ and covariance $\mathbf{P}_{xx}$, where the $\mathbf{y}$ is related to $\mathbf{x}$ by the non-linear transformation,

$$\mathbf{y} = f\left[\mathbf{x}\right] \tag{4.90}$$

The unscented transformation procedure can be summarized as below,

- Compute a 2n dimensional vector of sigma points, $\tilde{\mathbf{x}}$. The mean of the set of the sigma points are zero and all the sigma points have the same covariance $\mathbf{P}_{xx}$ with the random variable $\mathbf{x}$.

  $$\tilde{\mathbf{x}}_i = \underline{\mathbf{x}} + \left(\sqrt{n\,\mathbf{P}_{xx}}\right)_i \qquad i = 1 \ldots n \tag{4.91}$$

  $$\tilde{\mathbf{x}}_{i+n} = \underline{\mathbf{x}} - \left(\sqrt{n\,\mathbf{P}_{xx}}\right)_i \qquad i = 1 \ldots n \tag{4.92}$$

  where $\left(\sqrt{n\,\mathbf{P}_{xx}}\right)_i$ is the i^{th} row or column of the matrix square root of

- Transform each point.

  $$\tilde{\mathbf{y}}_i = f\left[\tilde{\mathbf{x}}_i\right] \tag{4.93}$$

- Compute the mean $\underline{\mathbf{y}}$ and covariance $\mathbf{P}_{yy}$ by computing the average of the transformed sigma points,

  $$\underline{\mathbf{y}} = \frac{1}{2n}\sum_{i=1}^{2n} \tilde{\mathbf{y}}_i \tag{4.94}$$

  $$\mathbf{P}_{yy} = \frac{1}{2n}\sum_{i=1}^{2n} \left(\tilde{\mathbf{y}}_i - \underline{\mathbf{y}}\right)\left(\tilde{\mathbf{y}}_i - \underline{\mathbf{y}}\right)^T \tag{4.95}$$

Unscented Kalman Filter Algorithm

A non-linear discrete time process is simply described by the following two difference equations; namely,

discrete time non-linear state transition equation,

$$\mathbf{q}_k = \mathbf{f}\left[\mathbf{q}_{k-1}, \mathbf{u}_{k-1}, \mathbf{w}_{k-1}\right] \tag{4.96}$$

and measurement equation

$$\mathbf{z}_k = \mathbf{h}\left[\mathbf{q}_k, \mathbf{v}_k\right] \tag{4.97}$$

where $\mathbf{f}\left[\ldots\right]$ is the non-linear process mode, $\mathbf{h}\left[\ldots\right]$ is the non-linear measurement model, $\mathbf{q}_k$ is the (nx1) state vector, $\mathbf{z}_k$ is the system output, $\mathbf{u}_{k-1}$ is the (rx1) control input, $\mathbf{w}_k$ is the (nx1) process noise and $\mathbf{v}_k$ is the (mx1) measurement noise. Both process noise and measurement noise ($\mathbf{w}_k$, $\mathbf{v}_k$) are assumed to have zero mean Gaussian distribution and uncorrelated. The covariances of the noise vectors are represented by **R** and **Q** covariance matrices in unscented Kalman filter equations.

The structure of the UKF algorithm is the same as Kalman filter. Likewise the Kalman filter, the equations of the UKF fall into two main groups, time update equations and measurement update equations.

Time update equations are responsible for transforming the current state and the error covariance estimates at time step k-1 to obtain the priori estimates for the time step k. Different from the Kalman filter where linear transformation is applied, unscented transformation is applied in UKF to find the priori estimates and their covariance.

The algorithm for time updating states are supplied below.

Compute the sigma points $\tilde{\mathbf{q}}_{k-1}^{i}$ at time k-1, by using the posteriori (corrected) state estimate $\hat{\mathbf{q}}_{k-1}$ at time step k-1 and the posteriori (corrected) estimate error covariance $\mathbf{P}_{k-1}$.

$$\tilde{\mathbf{q}}_{k-1}^{i} = \hat{\mathbf{q}}_{k-1} + \left(\sqrt{n\mathbf{P}_{k-1}}\right)_i \qquad i = 1 \ldots n \tag{4.98}$$

$$\tilde{\mathbf{q}}_{k-1}^{i+n} = \hat{\mathbf{q}}_{k-1} - \left(\sqrt{n\mathbf{P}_{xx}}\right)_i \quad i = 1 \ldots n \tag{4.99}$$

Transform the sigma points $\tilde{\mathbf{q}}_{k-1}^{i}$ at time step k-1, to time step k, by using the given non-linear system model and the control input u_{k-1}.

$$\hat{\mathbf{q}}_k^i = \mathbf{f}\left[\tilde{\mathbf{q}}_{k-1}^i, u_{k-1}, t_k\right] \tag{4.100}$$

Compute the priori state estimate $\hat{\mathbf{q}}_k^-$ at time step k, by averaging the 2n dimensional transformed sigma points $\hat{\mathbf{q}}_k^i$.

$$\hat{\mathbf{q}}_k^- = \frac{1}{2n}\sum_{i=1}^{2n}\hat{\mathbf{q}}_k^i \tag{4.101}$$

Compute the priori estimate error covariance $\mathbf{P}_k^-$ at time step k-1.

$$\mathbf{P}_k^- = \frac{1}{2n}\sum_{i=1}^{2n}\left(\hat{\mathbf{q}}_k^i - \hat{\mathbf{q}}_k^-\right)\left(\hat{\mathbf{q}}_k^i - \hat{\mathbf{q}}_k^-\right)^T + \mathbf{Q}_{k-1} \tag{4.102}$$

Similarly the observation vector and the observation error covariance is calculated as,

$$\hat{\mathbf{z}}_k^i = \mathbf{h}\left[\hat{\mathbf{z}}_k^i, t_k\right] \tag{4.103}$$

$$\hat{\mathbf{z}}_k = \frac{1}{2n}\sum_{i=1}^{2n}\hat{\mathbf{z}}_k^i \tag{4.104}$$

$$\mathbf{P}_z = \frac{1}{2n}\sum_{i=1}^{2n}\left(\hat{\mathbf{z}}_k^i - \hat{\mathbf{z}}_k\right)\left(\hat{\mathbf{z}}_k^i - \hat{\mathbf{z}}_k\right)^T + \mathbf{R}_k \tag{4.105}$$

and the cross covariance matrix between the priori state estimates and observation is calculates as,

$$\mathbf{P}_{qz} = \frac{1}{2n}\sum_{i=1}^{2n}\left(\hat{\mathbf{q}}_k^i - \hat{\mathbf{q}}_k^-\right)\left(\hat{\mathbf{z}}_k^i - \hat{\mathbf{z}}_k\right)^T \tag{4.106}$$

Likewise in the Kalman filter, the measurement update equations are responsible for incorporating new measurements into the priori estimate to obtain an improved posteriori estimate.

The algorithm for time updating measurements are supplied below.

First calculate the Kalman filter gain $\mathbf{K}_k$ at time step k

$$\mathbf{K}_k = \mathbf{P}_{qz}\mathbf{P}_z^{-1} \tag{4.107}$$

Calculate the posteriori (corrected) state estimate $\hat{\mathbf{q}}_k$ as a linear combination of the priori state estimate $\hat{\mathbf{q}}_k^-$ and a weighted difference between the actual measurement $\mathbf{z}_k$ and measurement prediction which is the predicted observation vector $\hat{\mathbf{z}}_k$.

$$\hat{\mathbf{q}}_k = \hat{\mathbf{q}}_k^- + \mathbf{K}_k\left(\mathbf{z}_k - \hat{\mathbf{z}}_k\right) \tag{4.108}$$

Lastly calculate the posteriori (corrected) estimate error covariance at time step k

$$\mathbf{P}_k = \mathbf{P}_k^- - \mathbf{K}_k\mathbf{P}_z\mathbf{K}_k^T \tag{4.109}$$

Likewise in the linear Kalman filter, after each time and measurement update pair, the process is repeated with the previous posteriori estimates used to predict the new priori estimates. This recursive predictor corrector structure of the Kalman filter defined through Eq.(4.98) to Eq.(4.109) is represented in the Figure 4-8.

Predictor

Time Update Equations

CalculaSigma Points

$$\tilde{\mathbf{q}}_{k-1}^{i} = \hat{\mathbf{q}}_{k-1} + \left(\sqrt{n\mathbf{P}_{k-1}}\right)_i \quad i = 1 \ldots n$$

$$\tilde{\mathbf{q}}_{k-1}^{i+n} = \hat{\mathbf{q}}_{k-1} - \left(\sqrt{n\mathbf{P}_{xx}}\right)_i \quad i = 1 \ldots n$$

Transform the sigma points

$$\hat{\mathbf{q}}_{k}^{i} = f\left[\tilde{\mathbf{q}}_{k-1}^{i}, u_{k-1}, t_k\right]$$

Compute the priori estimate

$$\hat{\mathbf{q}}_{k}^{-} = \frac{1}{2n}\sum_{i=1}^{2n}\hat{\mathbf{q}}_{k}^{i}$$

Priori estimate error covariance

$$\mathbf{P}_{k}^{-} = \frac{1}{2n}\sum_{i=1}^{2n}\left(\hat{\mathbf{q}}_{k}^{i} - \hat{\mathbf{q}}_{k}^{-}\right)\left(\hat{\mathbf{q}}_{k}^{i} - \hat{\mathbf{q}}_{k}^{-}\right)^{T} + \mathbf{Q}_{k-1}$$

Compute the observation vector

$$\hat{\mathbf{z}}_{k}^{i} = h\left[\hat{\mathbf{z}}_{k}^{i}, t_k\right]$$

$$\hat{\mathbf{z}}_{k} = \frac{1}{2n}\sum_{i=1}^{2n}\hat{\mathbf{z}}_{k}^{i}$$

Compute cross covariance matrix

$$\mathbf{P}_{qz} = \frac{1}{2n}\sum_{i=1}^{2n}\left(\hat{\mathbf{q}}_{k}^{i} - \hat{\mathbf{q}}_{k}^{-}\right)\left(\hat{\mathbf{z}}_{k}^{i} - \hat{\mathbf{z}}_{k}\right)^{T}$$

Corrector

Measurement Update Equations

Kalman filter gain

$$\mathbf{K}_k = \mathbf{P}_{qz}\mathbf{P}_{z}^{-1}$$

Posteriori state estimate

$$\hat{\mathbf{q}}_k = \hat{\mathbf{q}}_k^{-} + \mathbf{K}_k\left(\mathbf{z}_k - \hat{\mathbf{z}}_k\right)$$

Posteriori estimate error covariance

$$\mathbf{P}_k = \mathbf{P}_k^{-} - \mathbf{K}_k\mathbf{P}_z\mathbf{K}_k^{T}$$

Initial Values

$\hat{\mathbf{q}}_{k-1}$, $\mathbf{P}_{k-1}$

Figure 4-8 Unscented Kalman Filter Algorithm

4.5.4 Application in Valve Controlled System

For the real time control of the valve controlled hydraulic cylinder a MATLAB embedded function is written, implementing Eq.(4.98) to Eq.(4.109) in discrete time. The MATLAB m-file script is given in Appendix C. The sampling time of all the real time application is selected to be 1000 Hz that is measurements (observations) are taken every 1 ms.

Likewise in the pump controlled system, to be compatible with real time digital computing the non-linear state equations represented by $\mathbf{f}[\ldots]$ in Eq. (4.96) are discretized by forward difference method, and the measurement model represented by $\mathbf{h}[\ldots]$ in Eq.(4.97) is not discretized, as it is linear and equal to the measurement matrix **H** appearing in the pump controlled system.

However, during the offline tests, it is seen that, for time steps smaller than 1 ms, while transforming the sigma points from time step k-1 to time step k, the process defined by Eq. (4.100), the non-linear discrete state equations diverge resulting in a failure of the UKF. Therefore to be on the safe side, a 4^{th} order Runge Kutta scheme with 4 steps between each sample time is employed for the numerical integration process defined by Eq. (4.100). The 4^{th} order Runge Kutta algorithm can be seen in the UKF m-file script given in Appendix C with the name "`ffunc`".

The remaining UKF equations are written directly in the m-file script.

4.5.5 Filter Tuning

In this sub-section, the selection of the measurement noise and process noise covariance matrices (**R** & **Q**) that are introduced in Section 4.5.1 is explained.

The measurement noise matrix, **R**, represents the accuracy of the measurement. It is the covariance of the measurement noise $\mathbf{v}_k$ that appears in Eq. (4.71). As it is measurable and depends on the quality of the measurement device it is possible to determine the **R** matrix from a sample off-line measurement.

The diagonal terms of the **R** matrix are found directly by taking the covariance of the measured data from the sensors of systems. The diagonal elements of the **R** matrix are written below.

$$\begin{aligned}
\mathbf{R}_{11} &= \operatorname{cov}(x\,Measurement) \\
\mathbf{R}_{22} &= \operatorname{cov}(P_A\,Measurement) \\
\mathbf{R}_{33} &= \operatorname{cov}(P_B\,Measurement)
\end{aligned} \tag{4.110}$$

It should be noted that $\mathbf{R}$ is a 3x3 matrix, as there are 3 measured states, which are hydraulic cylinder position x and hydraulic cylinder chamber pressures p_A, p_B.

The off-diagonal elements of the measurement noise matrix represent the covariances between the measurements. These elements can be set to any value between 0 and $\sqrt{\mathbf{R}_{ii}\,\mathbf{R}_{jj}}$ [33]. Since no appreciable amount of covariance between the measurements is expected due to independent measurements, the off-diagonal elements are set to zero.

$$\mathbf{R}_{ij} = 0 \tag{4.111}$$

Note that, using a diagonal matrix as the measurement noise covariance so that using independent scalar measurements rather than a vector measurement is more advantages in terms of reduced computation time and improved numerical accuracy [34].

The process noise matrix, $\mathbf{Q}$, represents the accuracy of the mathematical model of the system. It is the covariance matrix of errors in the state variables represented by $\mathbf{w}_k$ in Eq.(4.70) that have been caused by $\mathbf{\Phi}$ not being truly representative of the system. Unlike the measurement noise matrix $\mathbf{R}$, the determination of $\mathbf{Q}$ matrix is not easy as it is not a measurable quantity.

However it should be noted that the Kalman filter performance does not depend on the absolute values of $\mathbf{Q}$ and $\mathbf{R}$ matrices but on their relative relationship [35]. This relation was investigated in Eq. (4.79). Therefore first fixing the measurement noise covariance matrix $\mathbf{R}$, which can be determined from measurements and then tuning the process noise matrix $\mathbf{Q}$ through an offline procedure is a reasonable way.

Likewise the measurement noise covariance matrix $\mathbf{R}$, the off-diagonal elements of the nxn $\mathbf{Q}$ matrix can be taken any value between 0 and $\sqrt{\mathbf{Q}_{ii}\mathbf{Q}_{jj}}$. These elements represent the covariance between the uncertainty of the states of the system and taking them as zero reduces the computation time and numerical accuracy. Therefore the off-diagonal elements are taken as zero.

$$\mathbf{Q}_{ij} = 0 \tag{4.112}$$

The diagonal elements of the $\mathbf{Q}$ matrix are written below.

$$\begin{aligned}
\mathbf{Q}_{11} &= \operatorname{cov}(x \text{ uncertainty of model}) \\
\mathbf{Q}_{22} &= \operatorname{cov}(\dot{x} \text{ uncertainty of model}) \\
\mathbf{Q}_{33} &= \operatorname{cov}(P_A \text{ uncertainty of model}) \\
\mathbf{Q}_{44} &= \operatorname{cov}(P_B \text{ uncertainty of model})
\end{aligned} \tag{4.113}$$

It should be noted that the $\mathbf{Q}$ is a 4x4 dimensional matrix, as the system is defined by 4 states, hydraulic cylinder position x, hydraulic cylinder velocity $\dot{x}$ and hydraulic cylinder chamber pressures p_A, p_B.

4.5.5.1 Pump Controlled System

To find the diagonal elements of the measurement noise matrix **R** the position and pressure data is acquired from the sensors while sending zero reference signals to the servomotors. By this way the only data collected by the sensors are the environment noise.

The Figure 4-9 shows the noise of the position transducer. The covariance of position data is calculated by MATLAB built in "`cov`" function and written as the first diagonal element of the measurement covariance matrix.

The Figure 4-10 and Figure 4-11 show the noise on the pressure transducers at the hydraulic cylinder chambers A and B. Likewise in the position transducer, the covariance of these data are calculated and written as the second and third diagonal elements of the measurement noise matrix **R**.

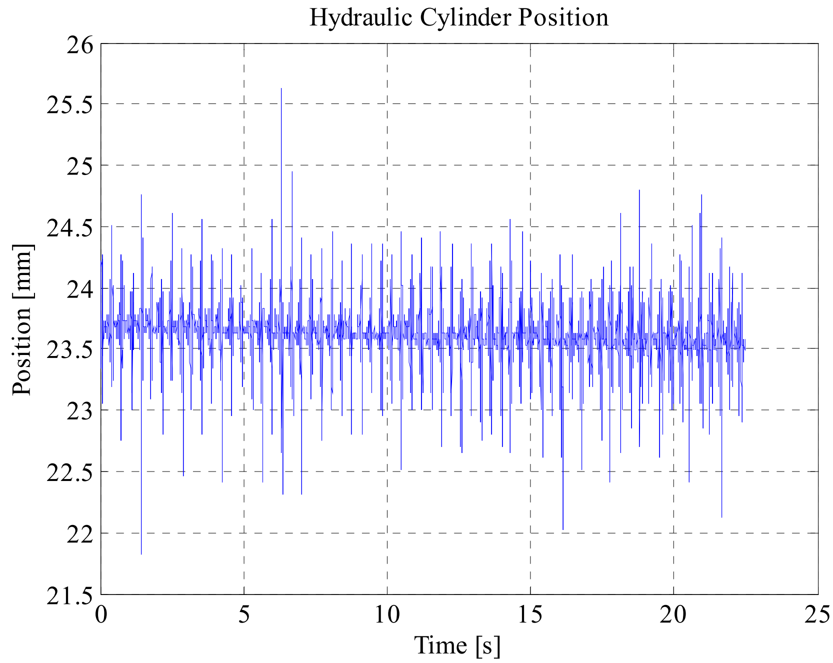

Figure 4-9 Position Transducer Measurement for Zero Reference Input

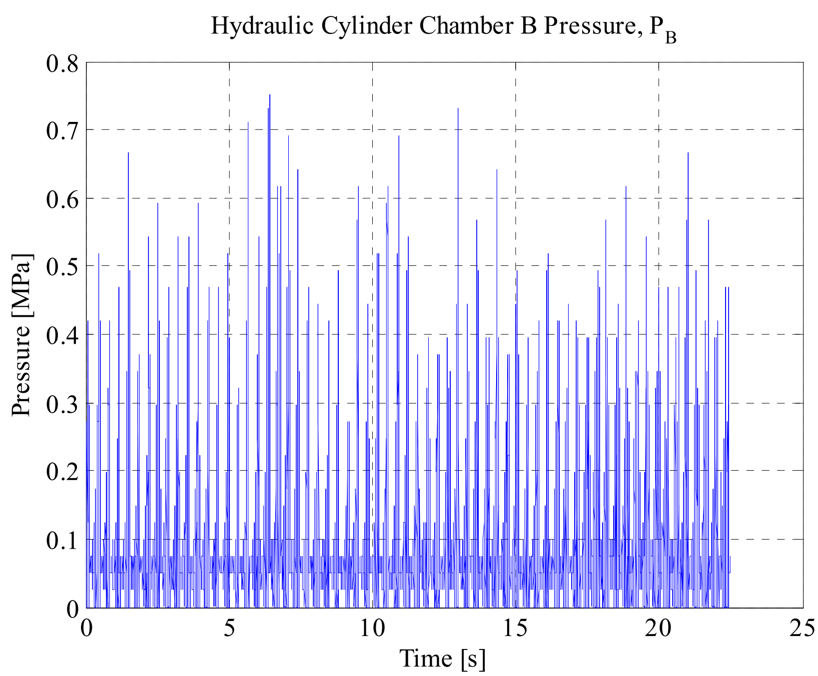

Figure 4-10 Hydraulic Cylinder Chamber B Pressure Transducer Measurement for Zero Speed

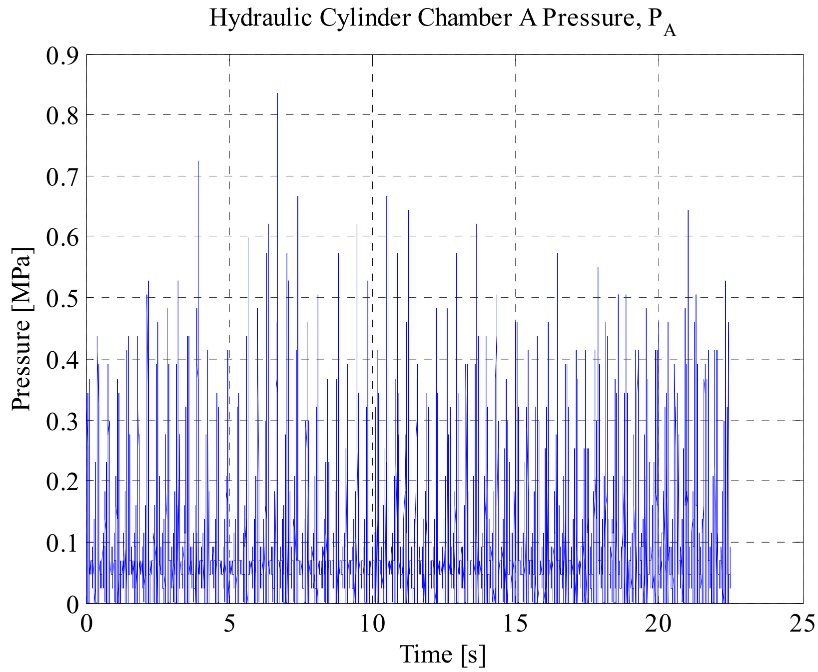

Figure 4-11 Hydraulic Cylinder Chamber A Pressure Transducer Measurement for Zero Reference Signal

Then the measurement noise covariance matrix is found as,

$$\mathbf{R} = \begin{bmatrix} 2.3635 \cdot 10^{-2} & 0 & 0 \\ 0 & 5.7700 \cdot 10^{-3} & 0 \\ 0 & 0 & 6.5500 \cdot 10^{-3} \end{bmatrix} \tag{4.114}$$

As it was explained in the above section, the Kalman filter performance does not depends on the absolute values of the **R** and **Q** matrix but their relative relationship.

Therefore the process noise covariance matrix **Q** is found through an offline iterative procedure. For tuning purposes a **R**/**Q** ratio is defined for each diagonal element of the process noise covariance matrix. If the **R**/**Q** ratio increases the Kalman filter trusts on the measurement more heavily, while if the **R**/**Q** ratio decreases the Kalman filter trusts on the model more heavily.

For the position estimation **R**/**Q** ratio is decreased till the noise on the position measurement is attenuated. A lower$_{\mathrm{r}}$ **R**/**Q** ratio means a smoother position signal. But, as the Kalman filter trusts more on the model than the measurement, at higher frequencies the filtered signal differs from the actual measured signal. For the velocity and pressure estimation **R**/**Q** ratio is decreased more to thrust on the model, rather than the measurement.

The resulting process noise covariance matrix found throughout the offline trial and error iterative process is given below,

$$\mathbf{Q} = \begin{bmatrix} 2.36 \cdot 10^{-5} & 0 & 0 & 0 \\ 0 & 2.36 \cdot 10^{-9} & 0 & 0 \\ 0 & 0 & 5.77 \cdot 10^{-7} & 0 \\ 0 & 0 & 0 & 6.55 \cdot 10^{-7} \end{bmatrix} \tag{4.115}$$

According to the selected process noise matrix **Q**, and the measurement noise matrix R, the Kalman filter performance tested on the variable speed hydraulic test set up with proportional controller. The proportional gain is 1 while the reference input signal is a 1 Hz sinusoidal signal with 5 mm amplitude.

Figure 4-12 shows the performance of the designed Kalman filter for position estimate. The covariance of the error between the measured and filtered position signal is 0.229 with standard deviation 0.15 mm.

Figure 4-13 shows the pressure filtering performance of the Kalman filter. The noisy blue data is the actual measurement data, the red one is the filtered pressure data, and the magenta data is the linear MATLAB Simulink model response. Note that the actual pressure measurements seem different from the model response. This is due to the static friction of the hydraulic cylinder which is not taken into account in the linear model of the system. The effect of static friction can be seen more clearly in Figure 4-14.

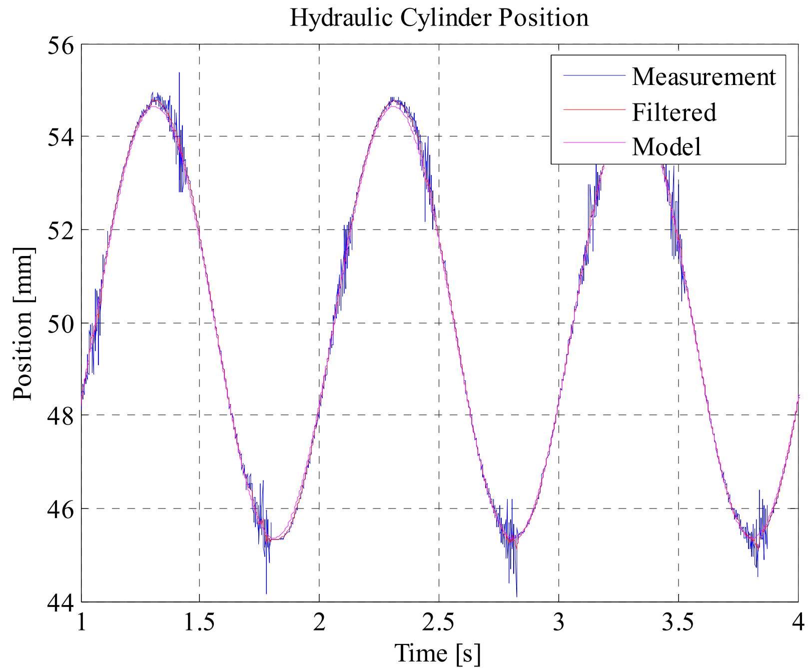

Figure 4-12 Kalman Filter Position Filtering Performance

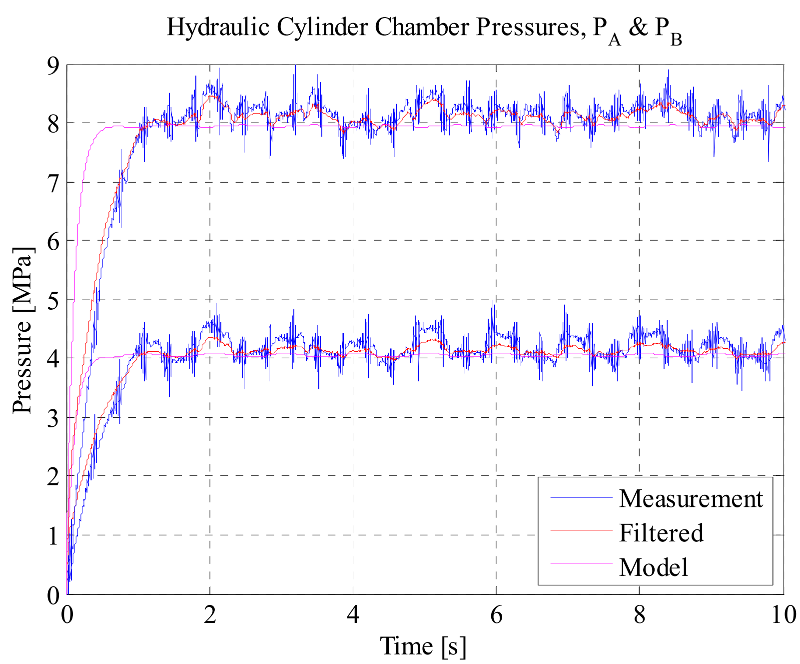

Figure 4-13 Kalman Filter Pressure Filtering Performance

In Figure 4-14 it is seen that the measured load pressure response of the system is a square wave like signal, although the reference input of the system is a sinusoidal position signal. This is due to the static friction on the hydraulic cylinder, which becomes dominant at low cylinder speeds. However, despite the real square wave like load pressure, Kalman filter estimated the load pressure as a sinusoidal signal, which is similar to the linear MATLAB Simulink model response. This is done intentionally. Because the load pressure is one of the feedback elements of the linear state feedback controller, the **Q** matrix is tuned such that the filter thrusts on the model more heavily and do not reflect the non-linear system properties on the linear controller, as it may result in the instability of the system.

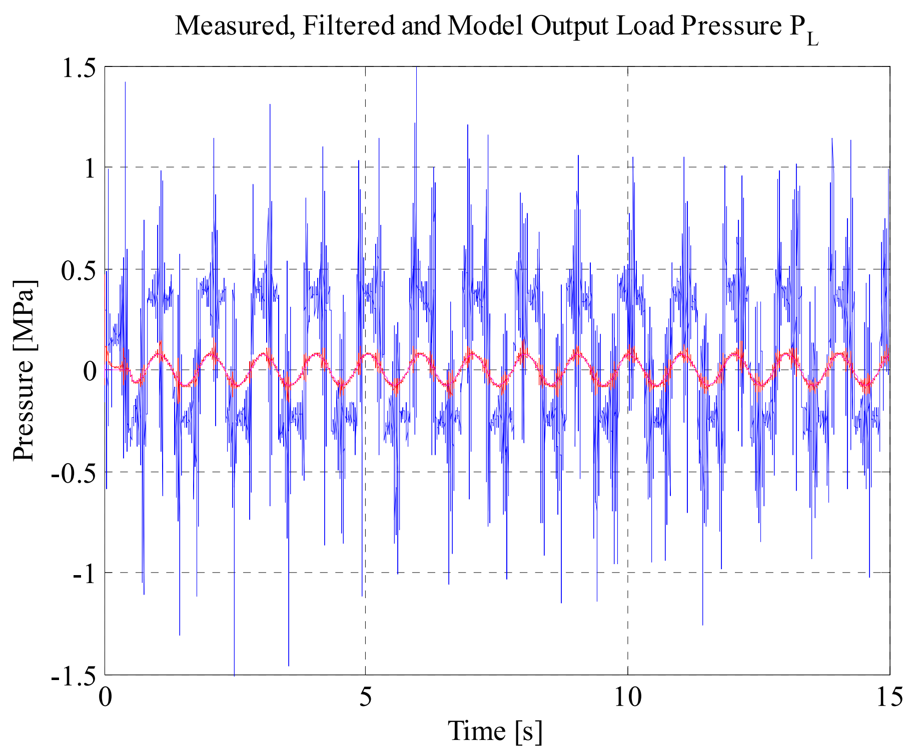

Figure 4-14 Kalman Filter Performance Load Pressure

4.5.5.2 Valve Controlled System

The same sensors are used in the valve controlled system as in the variable speed controlled system. Therefore the measurement noise covariance matrix $\mathbf{R}$, is taken to be the same in the variable speed pump controlled system. However, as the two system models are different, the process noise covariance matrix $\mathbf{Q}$, is different.

Likewise in the variable speed pump controlled system, the process noise covariance matrix is tuned offline through a trial and error procedure, by defining $\mathbf{R}/\mathbf{Q}$ ratio for each diagonal element.

The numerical values of $\mathbf{R}$ and $\mathbf{Q}$ used throughout all the valve controlled system tests are given below

Measurement noise matrix covariance,

$$\mathbf{R} = \begin{bmatrix} 2.3635 \cdot 10^{-2} & 0 & 0 \\ 0 & 5.7700 \cdot 10^{-3} & 0 \\ 0 & 0 & 6.5500 \cdot 10^{-3} \end{bmatrix} \tag{4.116}$$

Process noise matrix covariance

$$\mathbf{Q} = \begin{bmatrix} 2.36 \cdot 10^{-6} & 0 & 0 & 0 \\ 0 & 2.36 \cdot 10^{-11} & 0 & 0 \\ 0 & 0 & 5.77 \cdot 10^{-12} & 0 \\ 0 & 0 & 0 & 6.55 \cdot 10^{-12} \end{bmatrix} \tag{4.117}$$

CHAPTER 5

PERFORMANCE TESTS OF THE SYSTEM

In this chapter, real time test results of the valve controlled and pump controlled system are given. In Section 5.1, the test procedure to find the pump leakage coefficients and hydraulic cylinder friction are explained. In Section 5.2 and 5.3, step responses of pump controlled and valve controlled system are illustrated. In Section 5.4, frequency responses of valve controlled and pump controlled systems are given for 5 Hz desired dominant closed loop pole location. In Section 5.5, a comparison of two systems is made in terms of dynamic performance.

All the tests are conducted on the MATLAB Simulink Real Time Windows Target environment. For the entire control applications, a discrete fixed step size solver with 1000 Hz sampling frequency is used.

Figure 5-1 shows the MATLAB Simulink Real Time Windows Target model of the pump controlled system. The inputs of the model measured via data acquisition card are: actuator position, the hydraulic cylinder chamber pressures, and the servomotor speeds. Through a look up table, the measured signals in terms of Volts are converted to mm, MPa, and rps, respectively. Then, the position and pressure signals are feed through the Kalman filter. The Kalman filter attenuates the noise on the position and pressure signals and estimates the velocity. Then, the smoothed position signal is compared with the reference position signal, and sent through the controller accompanying with the other two states. The controller generates the manipulated input signal that is the speed of the servomotor 2. After adding the offset speeds determined according to the desired sum of the chamber pressures, the signal is converted to Volts from rps through a look up table and sent to the servomotor 2 driver, meanwhile the reference speed of the servomotor 1 is adjusted according to the servomotor 2 speed.

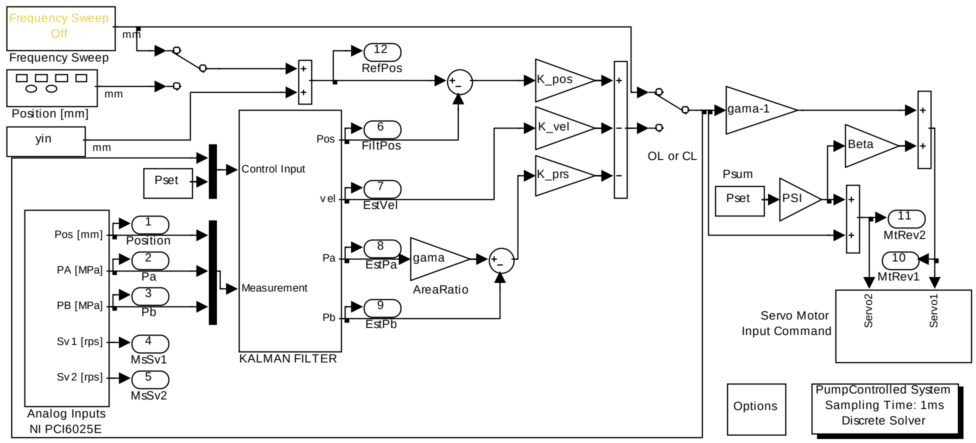

Figure 5-1 MATLAB Simulink RTWT Controller of the Pump Controlled System

Figure 5-2 shows the MATLAB Simulink Real Time Windows Target model of the valve controlled system. All the procedure is the same in the pump controlled case, differently in the controller, two manipulated input signals are generated, and according to the spool position one of them is selected and send to the valve driver. The second output of the system is the servomotors' speed command which is constant and determined manually according to the frequency and amplitude of the test signal. The servomotor speeds should be chosen such that the pumps always deliver excess flow to the system so that the pressure relief valve is always open fixing the supply pressure.

The magnitude and frequency of test signals are selected such that no saturation occurs in servomotors or valve driver. For this reason, each test signal is run on the MATLAB Simulink models of the systems before conducting real time tests.

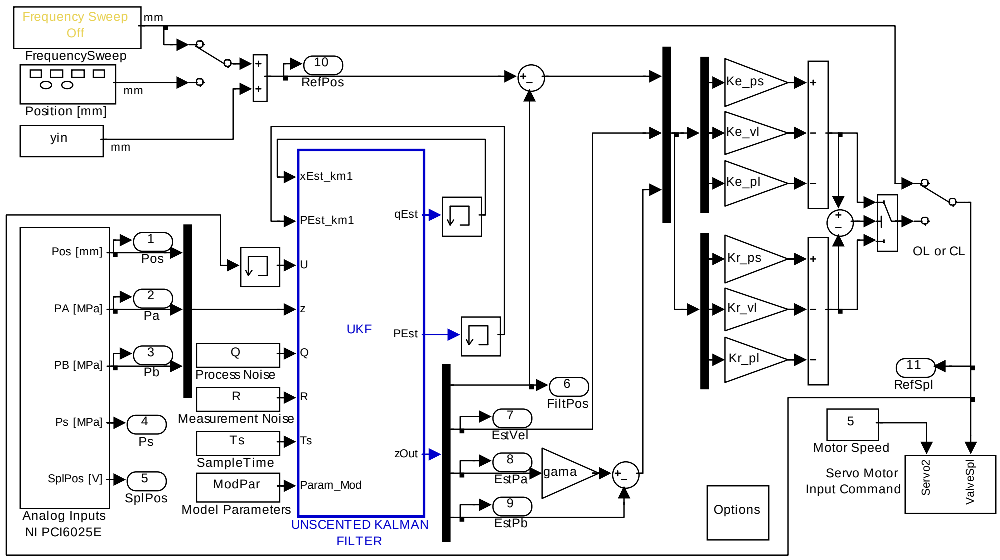

Figure 5-2 MATLAB Simulink RTWT Controller of the Valve Controlled System

5.1 System Identification

In this sub-section, the test procedures are explained in order to determine those parameters which are not measurable. The unknown parameters to be found are pump leakage coefficients and hydraulic actuator friction force. The leakage coefficients are found throughout the steady state pressure response of the system, the friction force is found by applying a low frequency chirp signal to the system and measuring the chamber pressures.

5.1.1 Hydraulic Pump Leakage Coefficients

In Section 3.2.2.1, it is explained that the flow losses of a hydraulic pump / motor unit can be expressed by internal and external leakage coefficients. In Section 3.2.3, it is shown that these coefficients determine the characteristics of the steady state behavior of the pump controlled system. The steady state pressures of the hydraulic cylinder chambers are determined mainly by the leakage coefficients and pump flow rate.

Remembering the electrical analogy of the pump controlled system represented by Figure 3-13, if the voltage difference across a resistance and the current through it are known, then the value of the resistance can be obtained. Thus, in this sub-section the internal and external leakage coefficients are obtained by using the steady state sum pressure of the hydraulic cylinder chambers due to steady state flow rate generated by a known pump speed command.

The relation between the pump offset speeds and the relation between the hydraulic cylinder chambers pressure sum and pump 2 speed, expressed in Section 3.2.3, are repeated here for convenience.

$$\beta = \frac{n_{1o}}{n_{2o}} = -\frac{C_i + 2C_{ea} + \gamma C_{eb}}{(\gamma - 1)C_i + \gamma C_{eb}} \tag{5.1}$$

$$n_{2o} = \Psi p_{sum} = -\frac{(\gamma - 1)C_i + \gamma C_{eb}}{D_P(\gamma + 1)} p_{sum} \tag{5.2}$$

Note that as the two pumps used in the system are identical and there is no external leakage paths added to the system, the leakage coefficients C_{ea} and C_{eb} are assumed to be the same and will be represented by C_e.

From the Eq. (5.1), a ratio between the internal and external leakages can be found as,

$$C_{ie_{Ratio}} = \frac{C_i}{C_e} = -\left(\frac{1 + \beta\gamma}{1 + \beta(\gamma + 1)}\right) \tag{5.3}$$

In Eq. (5.3), because the β constant has always a negative value and both β and γ are greater than unity, $C_{ie_{Ratio}}$ is a positive constant. If the Eq. (5.3) is substituted in Eq. (5.2) then the external leakage coefficient is expressed as

$$C_e = \frac{-n_{20} D_p(\gamma + 1)}{\left((\gamma - 1)C_{ie_{Ratio}} + \gamma\right) p_{sum}} \tag{5.4}$$

To find the pump internal coefficients an open loop test procedure is applied. Pumps are driven with two independent speed inputs, n_{10} ,and n_{20} . It is important to remember that the above equations are valid for zero hydraulic cylinder movement. Thus, through a trial and error process the right speed ratio which makes the hydraulic cylinder velocity zero is found.

Shown in Figure 5-3 is the steady state chamber pressures, for a given two independent pump speeds $n_{10} = 0.5$ rps and $n_{20} = -0.42$ rps. The mean value of the measured chamber pressure is $P_{A\_ss} = 5.05$ MPa and the mean value of the chamber B pressure is $P_{B\_ss} = 9.74$ MPa.

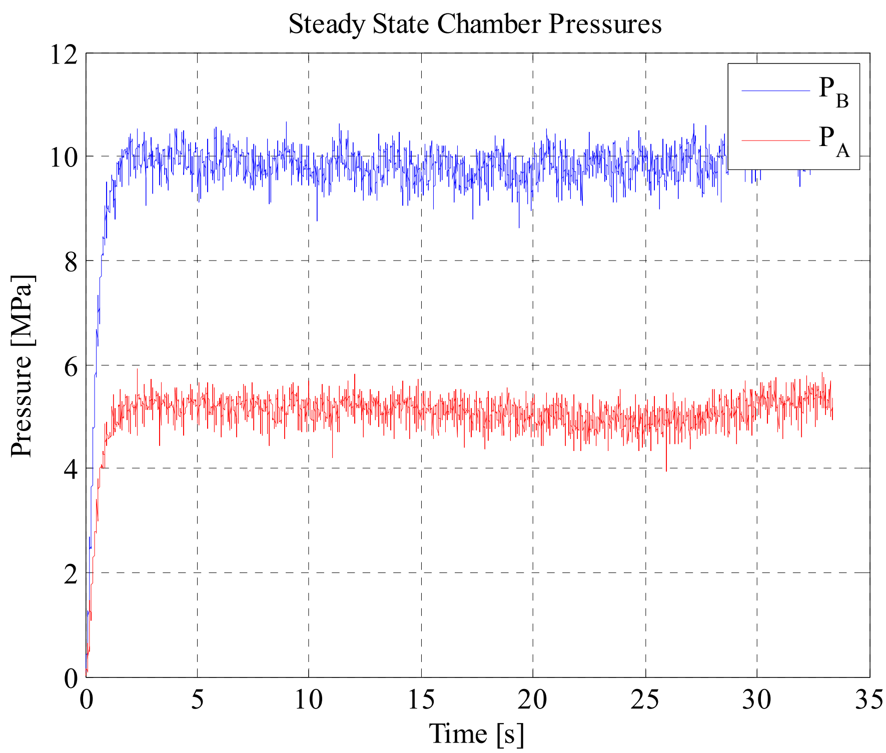

Figure 5-3 Steady State Chamber Pressures

If the steady state chamber pressure values and the motor speeds are inserted into Eq. (5.3) and Eq. (5.4), the internal and external leakage coefficients of the pumps will be found as,

$$C_e = C_{ea} = C_{eb} = 120\, mm^3 \,/\, s.MPa \tag{5.5}$$

$$C_i = 1097\, mm^3 \,/\, s.MPa \tag{5.6}$$

Figure 5-4 shows the steady state cylinder position due to the applied offset speeds. Because this is an open loop process, it is very hard to fix the hydraulic cylinder without position feedback. However as can be seen from the Figure 5-4, during 33 seconds the actuator moves only 2 mm and can be assumed to be motionless. Then, the flow rates delivered by the pumps directly used to compensate the leakages, while pressurizing the hydraulic cylinder chambers.

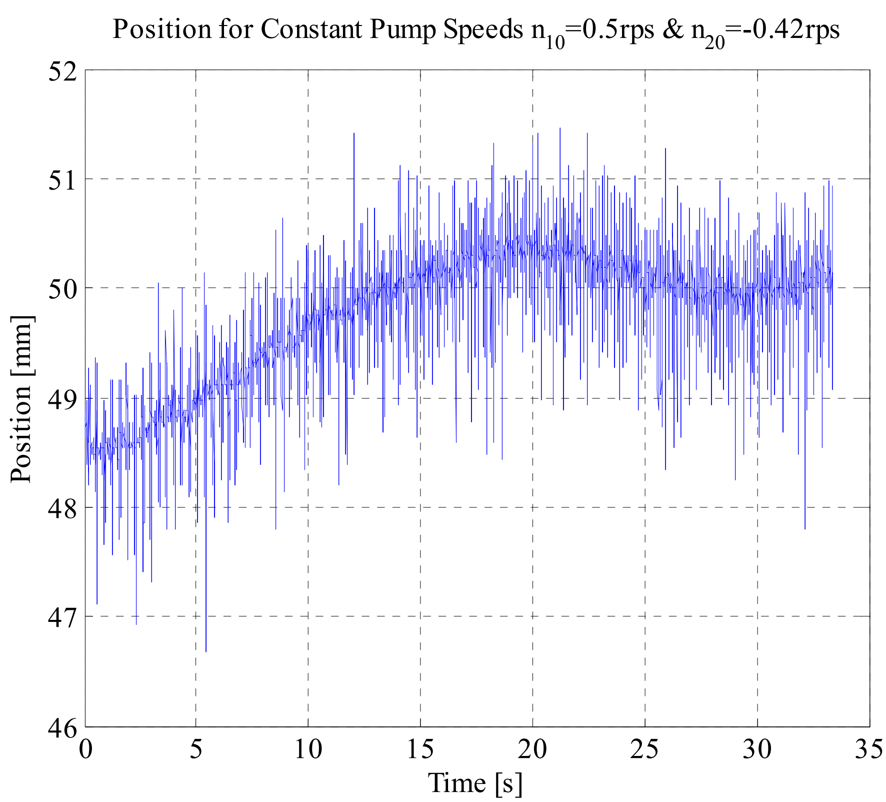

Figure 5-4 Steady State Cylinder Position for the Given Offset Pump Speeds

5.1.2 Hydraulic Cylinder Friction

In Section 3.2.2.3 in load model, it is assumed that the friction force is viscous. In this sub-section, the experimental study to find the viscous friction coefficient is explained.

The friction in the experimental test set-up is mainly due to the sliding surfaces between the hydraulic piston seals and the hydraulic cylinder. Furthermore another friction force exists between the steel plate and the two sliders due to the misalignment of the two sliders.

To find the friction force acting on the system, a reference position signal is sent to the closed loop hydraulic position control system. The reference signal is chosen to be a low frequency sinusoidal signal, to minimize the inertial effects on the hydraulic cylinder chamber pressures. Throughout the test the hydraulic cylinder chamber pressures and cylinder position are measured and the hydraulic cylinder velocity is estimated by use of a Kalman filter. After calculating the friction force defined by Eq.(5.7), the friction force versus cylinder velocity is plotted. The acceleration represented by $\ddot{x}$ in Eq.(5.7) is neither measured nor estimated from the Kalman filter. The acceleration data is obtained off-line by using the MATLAB Simulink model of the system.

$$f_f = p_A A_A - p_B A_B - m\left(g + \ddot{x}\right) \tag{5.7}$$

Note that friction is a highly non-linear process that depends on many physical parameters and environmental conditions. When two sliding materials are lubricated, different sliding speeds cause different film thicknesses of the lubricant and therefore friction characteristics may change. Another factor affecting the friction is the hydraulic cylinder chamber pressures as it will affect the surface area of the sealing in contact with the hydraulic cylinder wall. Also it is observed that the hydraulic cylinder location and thus the amplitude of the reference test signal effects the friction force characteristics.

To find the friction characteristics of the hydraulic actuator, a chirp signal, which has an increasing frequency from 0.1 Hz to 4 Hz is used as a test signal. The signal frequency increases linearly in time. The total duration of the signal is 66 seconds. As the hydraulic cylinder location affects the friction characteristics the amplitude of the chirp signal is chosen as 5 mm with a 50 mm offset cylinder stroke. Because the chamber pressures affect the friction force the desired chamber pressure sum is set to 12 MPa, which will be the same in the closed loop position control system. Figure 5-5 shows the test signal used to determine the friction characteristics of the hydraulic cylinder.

In Figure 5-5 the blue signal is the reference position signal and the red signal is the response of the close loop hydraulic system. The position response of the system is filtered by the Kalman filter. In the close loop hydraulic position control system a proportional controller with gain $K_p = 1$ is used.

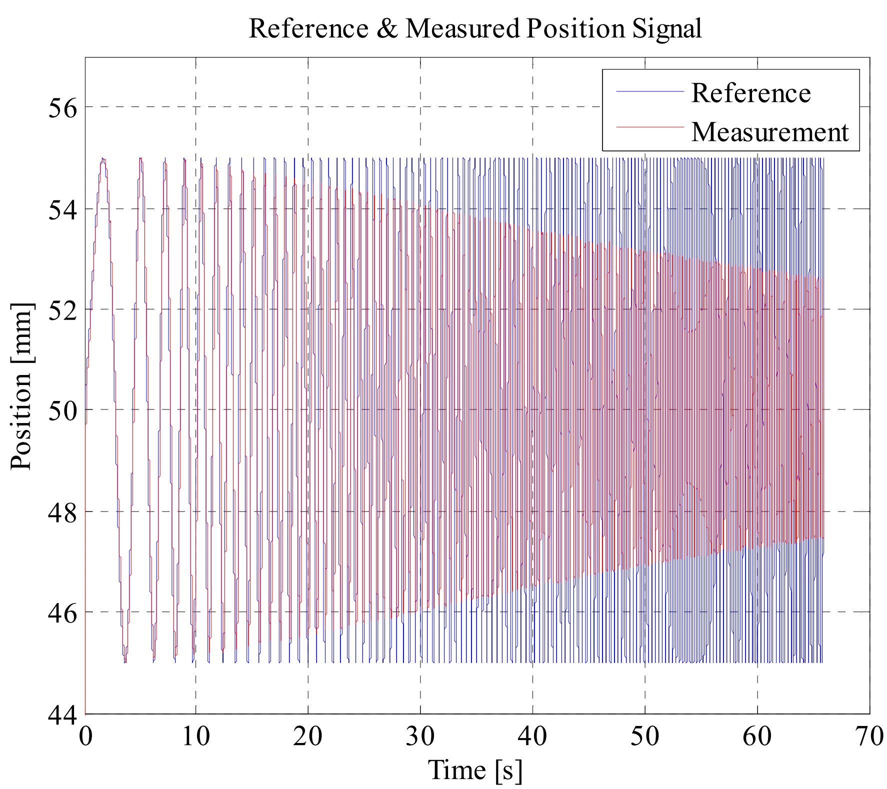

Figure 5-5 Friction Test Signal and System Response

Figure 5-6 shows the friction force versus velocity graph. The friction force is calculated by using Eq. (5.7). The chamber pressures used for the friction force calculation are not filtered. However to reduce the noise level, the pressure data which have a 1000 Hz sampling frequency is averaged at every 10 data interval. The velocity data which is the x axes of the graph is not measured but estimated by using the designed Kalman filter for pump controlled system.

Furthermore, the acceleration data to find the inertial forces is calculated by using the mathematical model of the system. Figure 5-8 shows the inertial forces. Note that when the chirp signal frequency becomes greater than 2 Hz the inertial forces seems to be important nevertheless its maximum value is around 17 N which may be negligible with respect to the friction force.

The friction force data in Figure 5-6 seems very scattered. This is not due to the noisy pressure measurement but due to the different friction force characteristics for different cylinder speeds. The friction force resulting from the low frequency components of the chirp signal dominates the static friction around zero, while the friction force resulting from the high frequency components of the chirp signal dominates dynamic friction at higher velocities. Furthermore it seems there exist a large hysteresis between the extending and retracting friction forces at low velocity region. However at high velocity region, that is for the velocities greater than 20 mm/s the friction force for the extracting and retracting seems to be the same and proportional with velocity.

From the data represented in Figure 5-6 it is very hard to approximate a viscous friction coefficient. Thus the velocity data is divided into 40 equal velocity intervals between the maximum and minimum cylinder velocity. An equivalent friction force is calculated by taking the mean of the friction forces at each velocity interval. The resulting friction force versus cylinder velocity is represented in Figure 5-7. The red line in Figure 5-6 is formed by connecting these points.

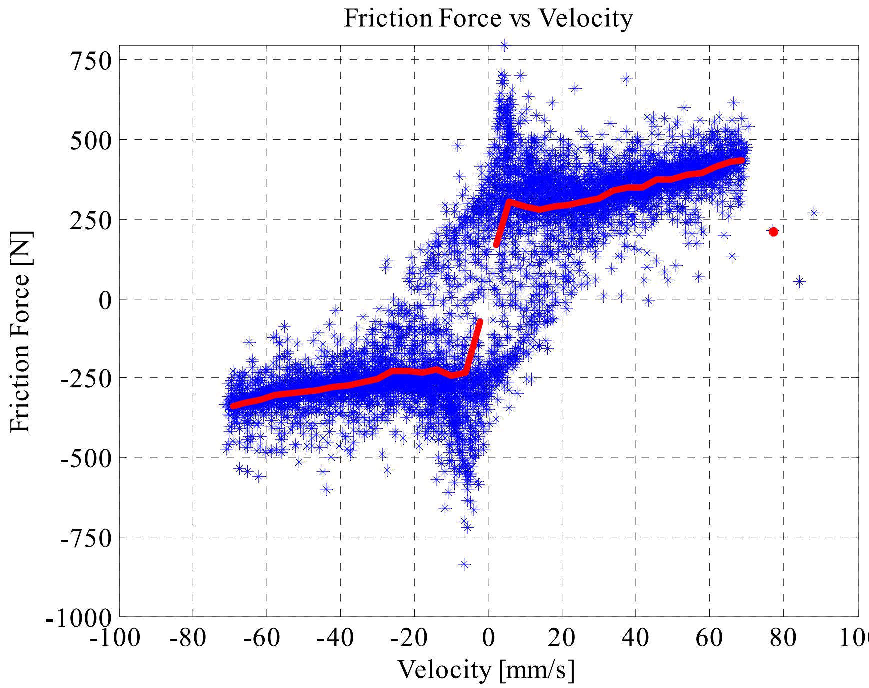

Figure 5-6 Friction Force vs Cylinder Velocity

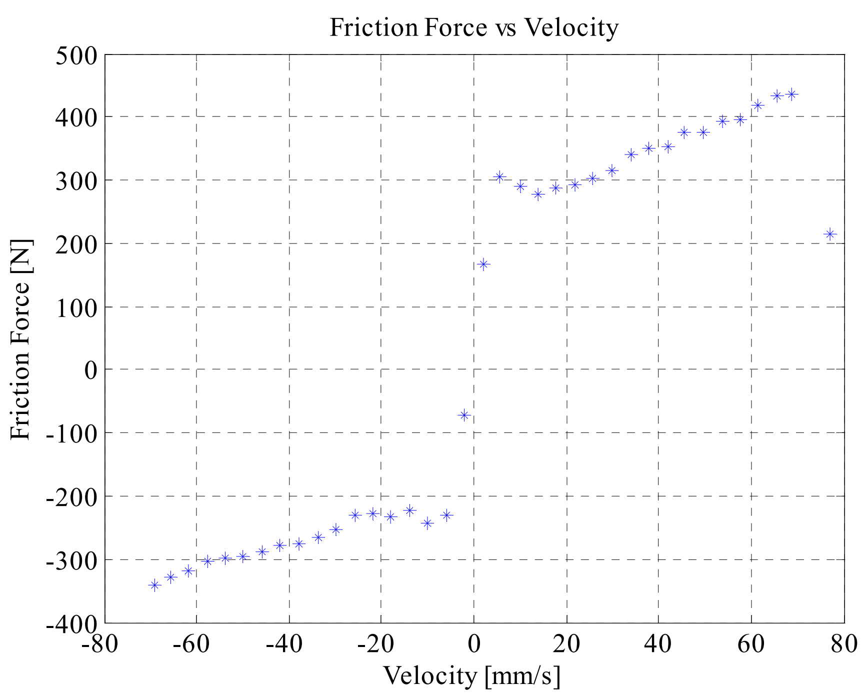

Figure 5-7 Mean Friction Force vs Cylinder Velocity

The friction force characteristics represented in Figure 5-7 is more understandable. There seems to be a non-linearity around zero velocity, causing a stick-slip motion while moving the cylinder. After the cylinder is moved the friction force decreases. This type of friction can be modeled with Karnopp's friction model if the friction at low velocity is considered. However, in this thesis study, the both hydraulic control systems are modeled as linear systems, therefore, the friction is assumed to be viscous.

From the higher velocity region of the Figure 5-7, the viscous friction force coefficient of the system both for extending and retracting is taken to be,

$$b = 2.6 \ N.s / mm$$

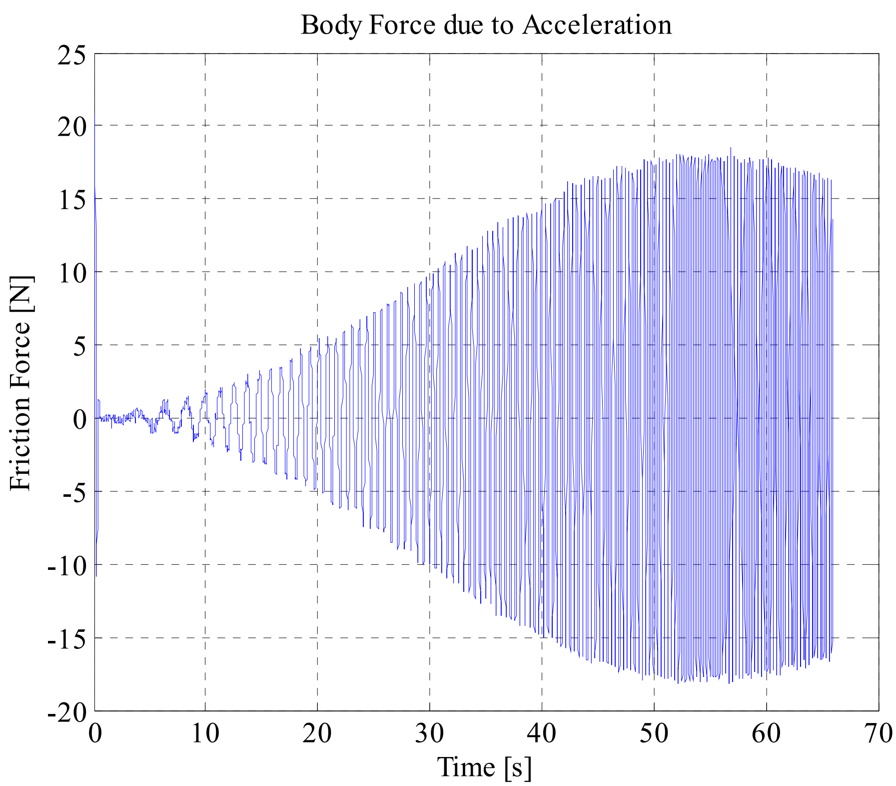

Figure 5-8 Body Force due to Acceleration

5.2 Step Response of Pump Controlled System

In this sub-section, the step response of the pump controlled system is given. A step signal with 10 mm amplitude and 0.5 Hz frequency is chosen as the reference position signal. The system is controlled with linear state feedback control algorithm as explained in Section 4.3. The bandwidth of the closed loop system is chosen to be 2 Hz and therefore the dominant desired closed loop pole of the system is located at -2.2π rad/s. The desired poles of the closed loop position control system and the corresponding controller gains are given in Table 5-1 with the accompanying test signal properties.

Table 5-1 Pump Controlled System Step Response Test-1 Data

Reference Step Signal	Magnitude	10 mm
	Frequency	0.5 Hz
Desired Closed Loop Poles	$[-2.2\pi, -600, -700]$	
State Feedback Gains	$[0.0962, -0.0604, 1.5912]$	

Figure 5-9 shows the step response of the closed loop pump controlled system. The black signal is the reference position signal, while the blue one is the measured position signal, the red one is the filtered signal, which is the output of the Kalman filter and used as the feedback signal, and lastly the magenta signal is the position response of the linear MATLAB Simulink model. It is seen that the linear model response and the real system response are consistent.

Note that the desired closed loop pole that dominates the system behavior is located at -2.2π rad/s. Because the other two poles (-600 rad/s,-700 rad/s) are located very far to the left of the desired closed loop pole, their effects on the response can be assumed to be negligible, so that the closed loop position control system can be thought as a first order system with the following transfer function.

$$\frac{X(s)}{X_r(s)} = \frac{1}{Ts+1} \tag{5.8}$$

and the time constant T is equal to

$$T = \frac{1}{2 \cdot 2\pi} = 0.0795\,s \tag{5.9}$$

Time constant T is an important parameter of first order systems, because at time t=T, the response of the system reaches 63.2% of its total change. This can be verified from the system response, at time t= 10.08 s the hydraulic cylinder position is 52.3 mm which is 61.5% of its total change.

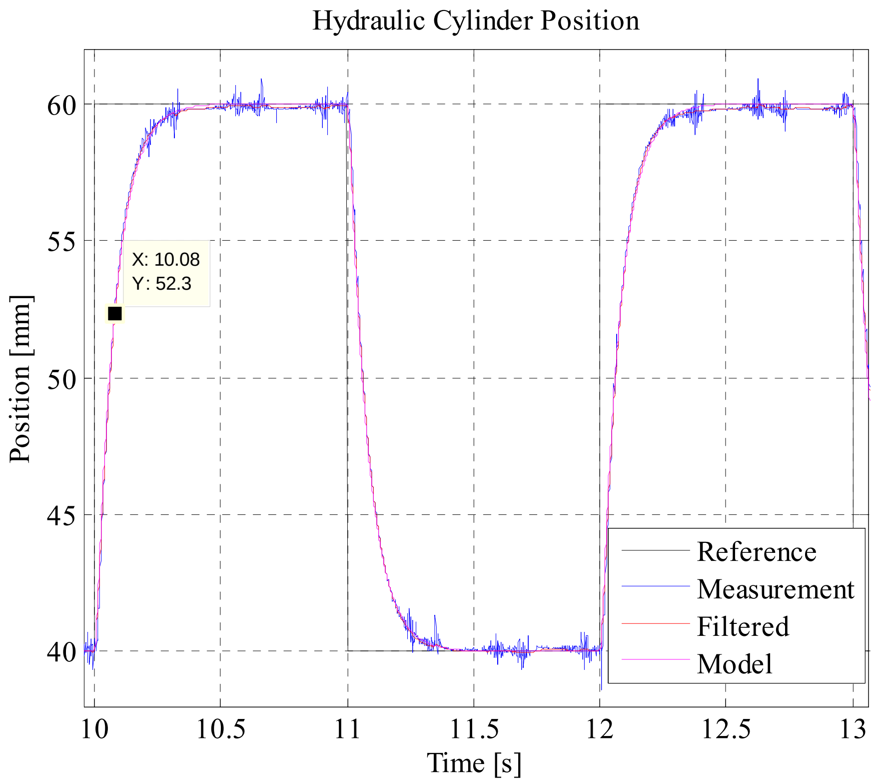

Figure 5-9 Step Response of the Pump Controlled System with Dominant Desired Closed Loop Pole Located at -2.2π rad/s

In Figure 5-9 at steady state there seems a 0.15 mm steady state error corresponding to 0.75% of the 20 mm step input magnitude. However, in Section 3.2.4, the open loop position response of the system was found to be of type 1, with a free "s" term in the denominator. Because the system acts as an integrator, the steady state error in the response is not expected.

The static friction of the hydraulic cylinder and the dead band of the servomotor and the pump may be the reason of this steady state error.

To decrease the steady state error, the state feedback gains of the system are increased, the dominant desired closed loop pole of the system is located at -10.2π rad/s while the location of the other closed loop poles are remained unchanged. The test signal properties, the desired closed loop poles and the corresponding state feedback gains are given in Table 5-2.

Table 5-2 Pump Controlled System Step Response Test-2 Data

Reference Step Signal	Magnitude	2.5 mm
	Frequency	0.5 Hz
Desired Closed Loop Poles	$[-10.2\pi, -600, -700]$	
State Feedback Gains	$[0.4809, -0.0595, \ 1.6657]$	

Figure 5-10 shows the step response of the closed loop pump controlled system with the dominant desired closed loop located at -10.2π rad/s. Again, the model response and the real system response are consistent. For the dominant desired closed loop pole located at -10.2π rad/s, the time constant of the equivalent first order system is 0.016 seconds. In Figure 5-10, it is seen that the system reaches 63.2% of its total change at this time as expected. Different from the model response there occur a 5.4% overshoot of the real system response indicating that the closed loop system tends to be oscillatory if a high bandwidth is desired.

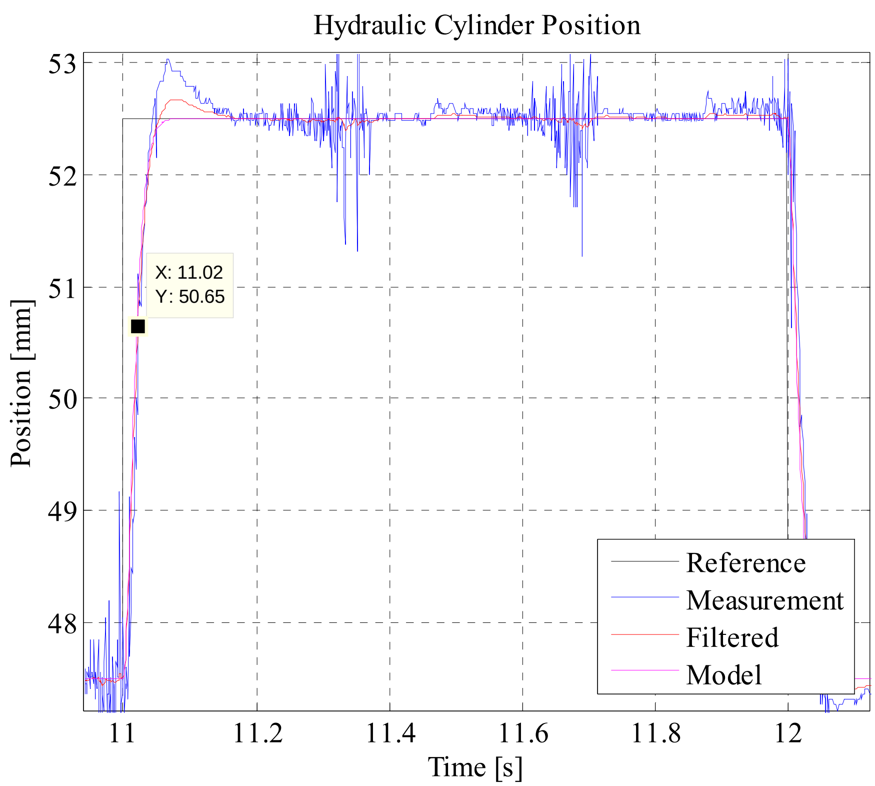

Figure 5-10 Step Response of the Pump Controlled System with Dominant Desired Closed Loop Pole Located at -10.2π rad/s

5.3 Step Response of Valve Controlled System

The same test signal with the same desired closed loop pole locations utilized in the pump controlled system, are also applied on the valve controlled system. The corresponding linear state feedback gains of the valve controlled system are determined through the linearized system equations defined in Section 4.2. Because the single rod cylinder has inherently different characteristics for extension and retraction, two set of linear state feedback gains are calculated.

The test signal properties, the desired closed loop poles and the corresponding state feedback gains are listed in Table 5-3.

Table 5-3 Valve Controlled System Step Response Test-1 Data

Reference Step Signal	Magnitude	10 mm
	Frequency	0.5 Hz
Desired Closed Loop Poles		$[-2.2\pi, -600, -700]$
State Feedback Gains	Extension	$[0.0449, -0.0317, -0.7588]$
	Retraction	$[0.0629, -0.0443, -1.0602]$
Linearized at	Supply Pressure	8.3 MPa
	Spool Position	0.1 V

Figure 5-11 shows the step response of the closed loop valve controlled system. The black signal is the reference position signal, while the blue one is measured position signal and the red one is the filtered signal, which is the output of the unscented Kalman filter and used as the feedback signal, and lastly the magenta signal is the position response of the non-linear MATLAB Simulink Model.

Different from the pump controlled system, the non-linear model behavior and the real system behavior are not the same at transient zone. When the non-linear model reaches 63.2% of its total change, which corresponds to the cylinder position of 52.64 mm, the total time passed is 87 ms, this is consistent with the linearized closed loop system model with the dominant closed loop pole located at -2.2π rad/s with the corresponding time constant of 80 ms. However from the graph it is seen that the real system response reaches this position with a 50 ms delay. The same behavior is valid for the settling time; the real system reaches 96% of its total change after 250 ms from the non-linear model.

It should be noted that there seems a difference between the real measurement and the Kalman filter output. This is because the filter trusts on the model rather than the real position measurement. Thrusting on the model is a necessary strategy for this type of controller. Because the controller gains switch at zero spool position, any noise in the feedback position signal causes chattering of the valve.

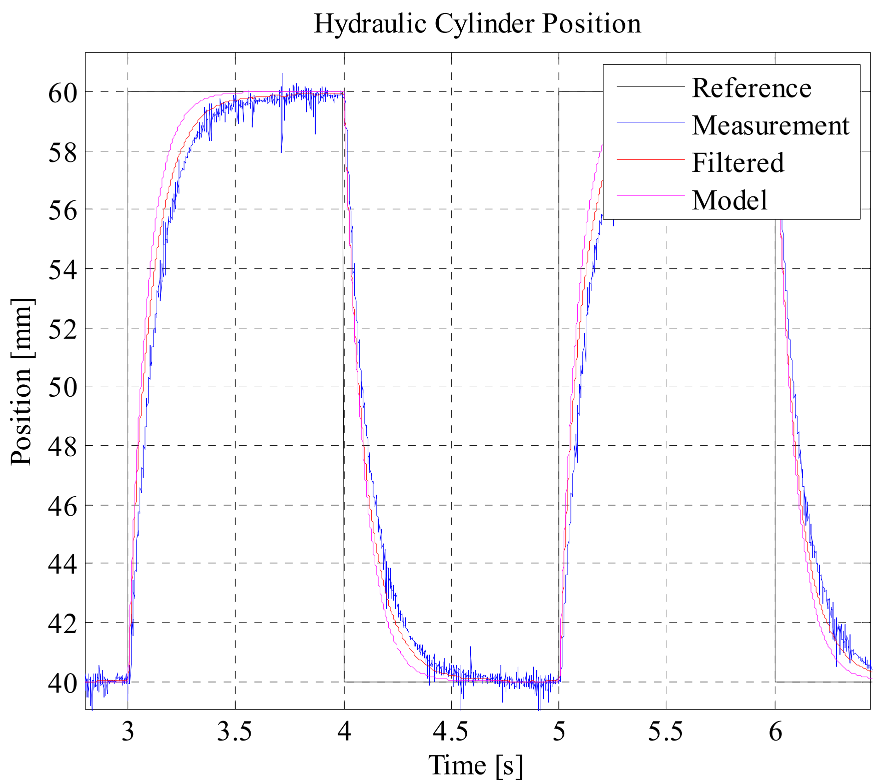

Figure 5-11 Step Response of the Valve Controlled System with Dominant Desired Closed Loop Pole Located at -2.2π rad/s

To be compatible with the pump controlled system tests, a second step response test is performed with the increased state feedback gains. In the second case, the dominant desired closed loop pole is located at -10.2π rad/s, while the location of the other closed loop poles are remained unchanged. The test signal properties, the desired closed loop poles and the corresponding state feedback gains are listed in Table 5-4.

As the dominant closed loop pole moves away from the origin, the response of the closed loop system becomes faster as seen in Figure 5-12. When the desired dominant closed loop pole moves from -2.2π rad/s to -10.2π rad/s, the time constant of the real system decreases from 130 ms to 35 ms.

Table 5-4 Valve Controlled System Step Response Test-2 Data

<table>
<tr><td rowspan="2">Reference Step Signal</td><td>Magnitude</td><td>2.5 mm</td></tr>
<tr><td>Frequency</td><td>0.5 Hz</td></tr>
<tr><td colspan="2">Desired Closed Loop Poles</td><td>$[-10.2\pi, -600, -700]$</td></tr>
<tr><td rowspan="2">State Feedback Gains</td><td>Extension</td><td>$[0.2246, -0.0312, 0.7936]$</td></tr>
<tr><td>Retraction</td><td>$[0.3145, -0.0437, 1.1090]$</td></tr>
<tr><td rowspan="2">Linearized at</td><td>Supply Pressure</td><td>8.3 MPa</td></tr>
<tr><td>Spool Position</td><td>0.1 V</td></tr>
</table>

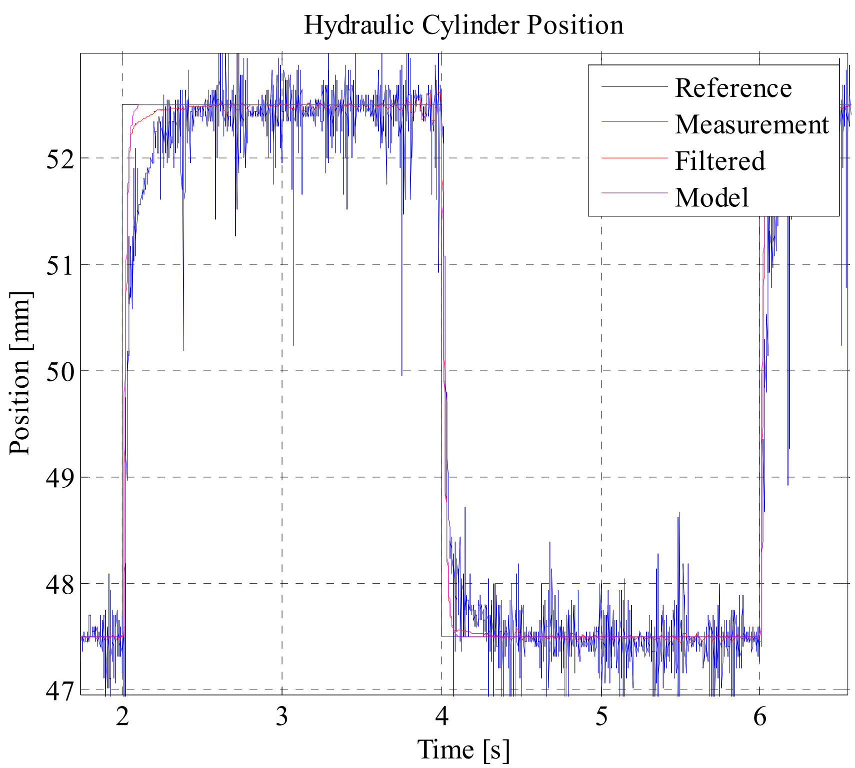

Figure 5-12 Step Response of the Valve Controlled System with Dominant Desired Closed Loop Pole Located at -10.2π rad/s

Despite the high dynamics, it is seen that increasing gains causes stability problems. At steady state the hydraulic cylinder tends to make random oscillations. Increasing the state feedback gains make the control signal more sensitive to noise as seen in Figure 5-13. In this figure, the reference valve spool position command sent to the valve driver is compared with the valve spool position command of the non-linear MATLAB Simulink model of the valve controlled system. It is seen that, in the real system, the spool position command makes oscillations around zero, whereas in the Simulink model the spool position is constant and equal to zero at steady state.

In order to overcome this problem, a dead band can be defined in the controller instead of switching immediately at zero spool position.

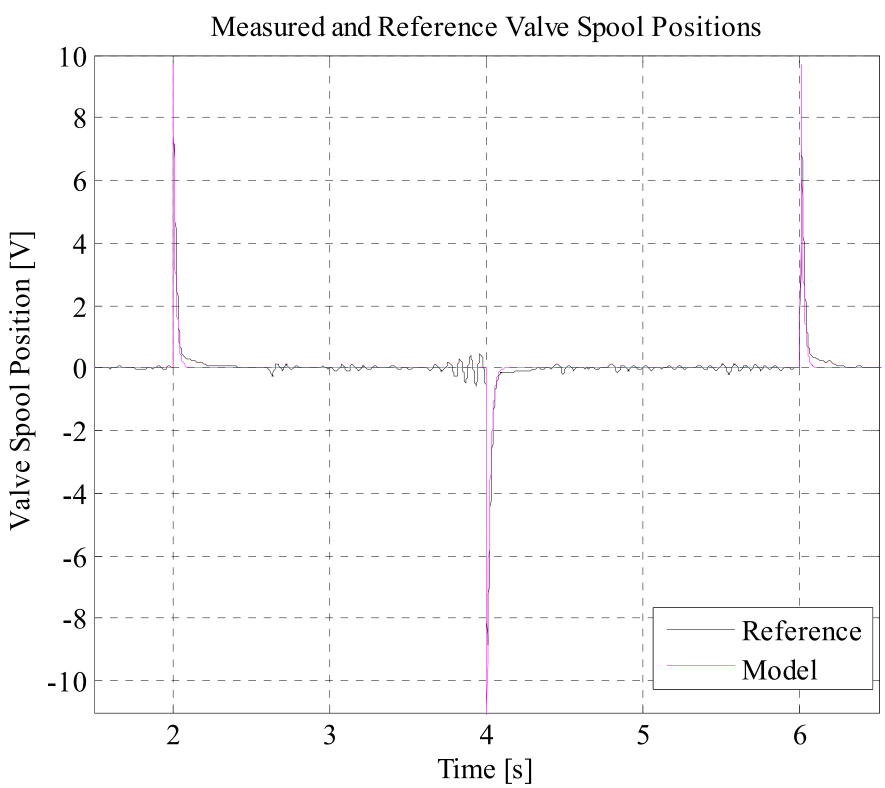

Figure 5-13 Real System Valve Spool Position Command and Simulink Model Spool Position Command

Next to increasing the controller gains, another way to increase the dynamics of the closed loop valve controlled systems is to increase the supply pressure. This can be seen clearly when the block diagram of the valve controlled system, Figure 3-22, is investigated. The valve spool position gain K_{u4_ext} is proportional to the square root of the supply pressure as defined in Eq. (3.87). Theoretically, doubling the supply pressure will increase the valve spool position gain 1.414 times, which is equivalent to increasing all the state feedback gains 1.414 times while remaining the supply pressure unchanged. Of course increasing the supply pressure will decrease the energy efficiency of the system.

5.4 Frequency Response Test

In this sub-section the frequency of a sinusoidal signal is varied over a certain range and the resulting system response is studied. The open loop and closed loop frequency responses of the system are obtained throughout an experimental procedure and compared with the modeled system response.

The dominant closed loop poles are chosen to determine the bandwidth of the closed loop position control hydraulic system. The desired bandwidth is 5 Hz. The linear state feedback controller gains corresponding to the desired closed loop pole locations are determined by following the procedure explained in Section 4.3.

The experimental data in the time domain is transformed into frequency domain by using MATLAB built in functions. To find the frequency response of the system Fast Fourier Transforms (FFT) of the input signal and the system output are taken to determine the amplitudes of the constituting harmonics and their frequencies. FFT's are taken with MATLAB "`fft`" command. The m-file script written for this purposes is given in Appendix C.

5.4.1 Test Signal

In this experimental study, a MATLAB m-file script is written for generating the reference sine sweep signal.

For the open loop tests the written m-file generates a sinusoidal signal with exponentially decaying amplitude and linearly decreasing frequency with time. In the open loop test in order to prevent the saturation of the hydraulic actuator, that is, to prevent the piston rod to reach the end of the stroke at low frequencies, this type of signal is generated.

For the closed loop tests, constant amplitude sinusoidal test signals are generated with linearly increasing frequencies. This signal is the same as the MATLAB Simulink Chirp signal.

Note that the amplitude and frequency range of the input signals are selected by considering the saturation limits of the servomotor and valve drivers.

5.4.2 Open Loop Frequency Response of Pump Controlled Hydraulic System

In the open loop frequency response test, a sinusoidal signal with an exponentially decaying magnitude is applied. The amplitude of the test signal starts from 10 V decreases to zero in 70 seconds with a time constant of 13.77 s, while its frequency starts with 10 Hz and decreases linearly in time down to 0.1 Hz. In Figure 5-14 the open loop test signal which is the reference signal of the servomotor 2 and its response is shown.

Figure 5-15 shows the experimental and the theoretical open loop frequency responses of the system. Since the type number of the transfer function defining the position response of the open loop system is one, the system acts as an integrator and the slope of the Bode diagram at the low frequency region is –20 dB/dec as expected.

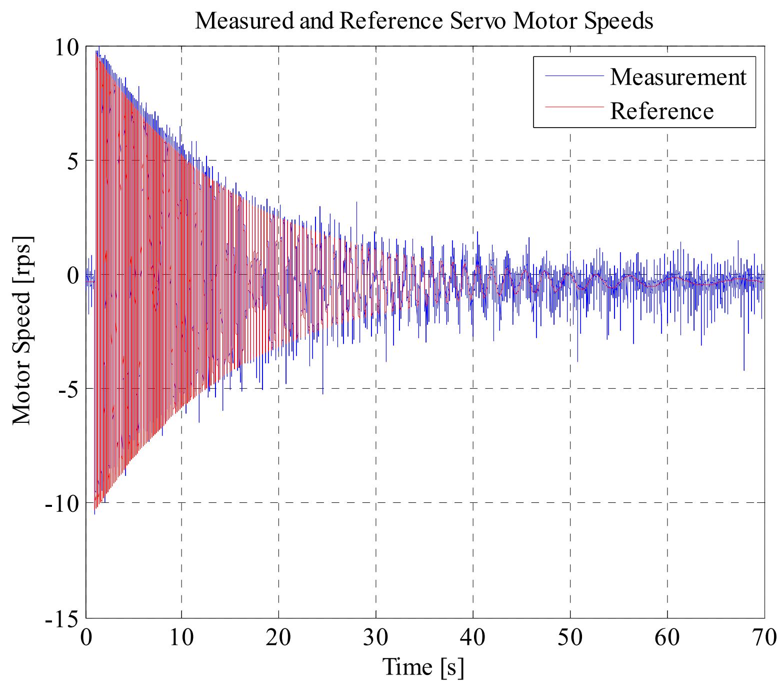

Figure 5-14 Pump Controlled System Open Loop Frequency Response Test Signal

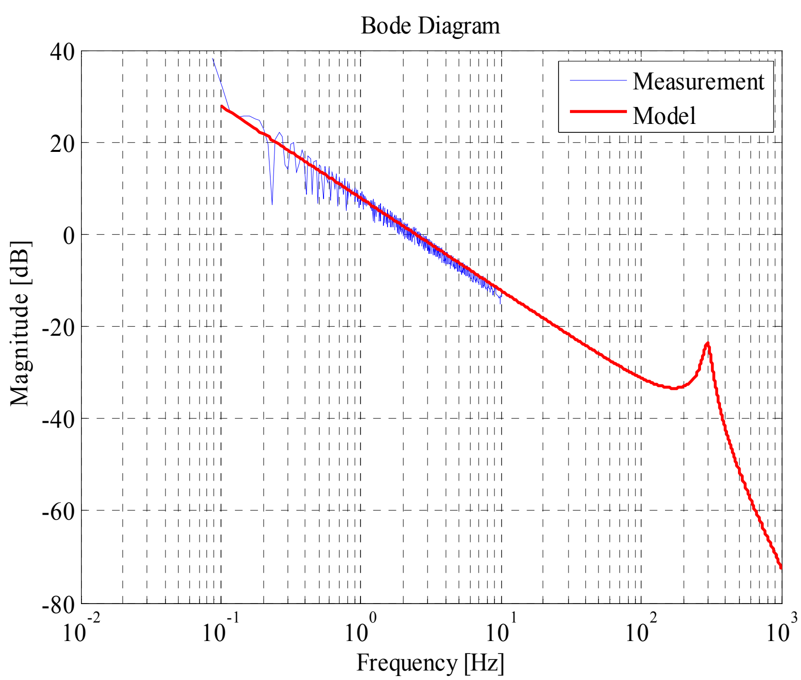

Figure 5-15 Experimental and Theoretical Open Loop Frequency Response of the Pump Controlled System

It is seen from the Bode diagram that the theoretical resonance frequency of the system is around 295 Hz. Only in the neighborhood of this frequency, damping dominates the dynamic behavior and some time should pass for the system to reach steady state. However, at low frequency region the system rapidly responses to the input signal and there is no need to wait for the system to reach steady state. Thus continuously changing the test signal frequency is not a problem for this frequency response tests.

Figure 5-16 shows the hydraulic cylinder position response and illustrates why an exponentially decaying amplitude sinusoidal signal is chosen as the test signal. By decreasing the amplitude and frequency with time saturation of the hydraulic cylinder is prevented.

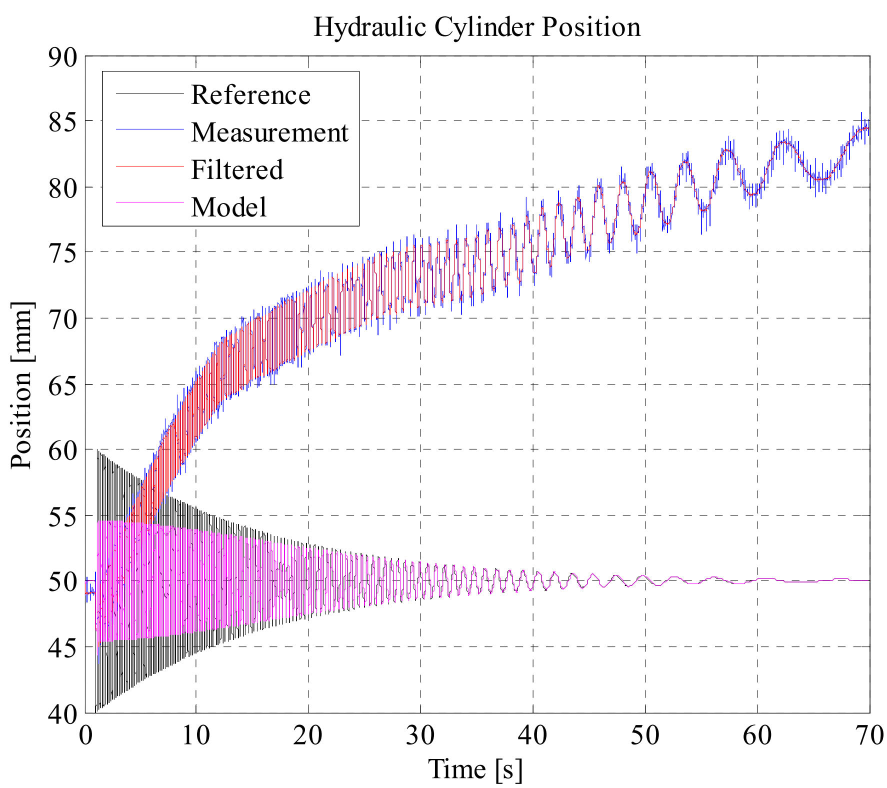

Figure 5-16 Hydraulic Cylinder Position in Open Loop Tests

Theoretically the cylinder is expected to make oscillations without moving upwards or downwards movement. However in the open loop frequency response test it is seen that the cylinder is continuously moving upwards while making oscillations. This is due to the leakage coefficients found in Section 5.1.1 not truly representing the real system leakage characteristics. While modeling the system, the leakage flow is assumed to be linear, however it is known that the volumetric efficiency of the pump, which is the representative of the pump flow losses changes with the pump drive speed. Furthermore, the pump excitation frequency also affects the pump leakage characteristics. Because the pump leakage coefficients in Section 5.1.1 are found for constant pump speeds it is not an unexpected result to see that the model and the real system behaves differently. However despite the sharp slope of the upwards movement at high frequency region, this slope decreases at low frequency region showing that the real system leakage characteristics are much similar to the assumed ones.

5.4.3 Close Loop Frequency Response of Pump Controlled Hydraulic System

In the closed loop frequency response test, a sinusoidal signal with 4 mm amplitude is chosen with a frequency starting from 0.1 Hz and linearly increasing to 10 Hz in 100 seconds. The maximum motor speed corresponding to maximum frequency is 8 rps (480 rpm), eliminating the risk of the saturation of the servomotor speeds. The desired bandwidth of this closed loop position control system is 5 Hz, therefore the desired closed loop poles are selected as $[-5.2\pi, -600, -700]$. Note that the last two poles, $[-600, -700]$, are located far away from the origin with respect to the first pole, so that their dynamics can be neglected and the closed loop system dynamics is determined by the first pole located at -5.2π rad/s.

The linear state feedback controller gains are determined by following the procedure explained in Section 4.3. The test signal properties, the desired closed loop poles and the corresponding state feedback gains are listed in Table 5-5.

Table 5-5 Pump Controlled System Frequency Response Test Data

Reference Chirp Signal			
Magnitude	Start Frequency	Stop Frequency	Duration
4 mm	0.1 Hz	10 Hz	100 s
Desired Closed Loop Poles		$[-5.2\pi, -600, -700]$	
State Feedback Gains		$[0.2405, -0.0601, -1.6191]$	

Figure 5-17 shows the response to sine sweep input of the variable speed pump controlled hydraulic system. The black signal is the reference position signal, while the blue one is measured position signal and the red one is the filtered signal, which is the output of the Kalman filter and used as the feedback signal, and lastly the magenta signal is the position response of the linear MATLAB Simulink model. In Figure 5-17, the general behaviors of the closed loop systems seem to be consistent with the model, however it is hard to see the performance of the system therefore a detailed view is given in Figure 5-18.

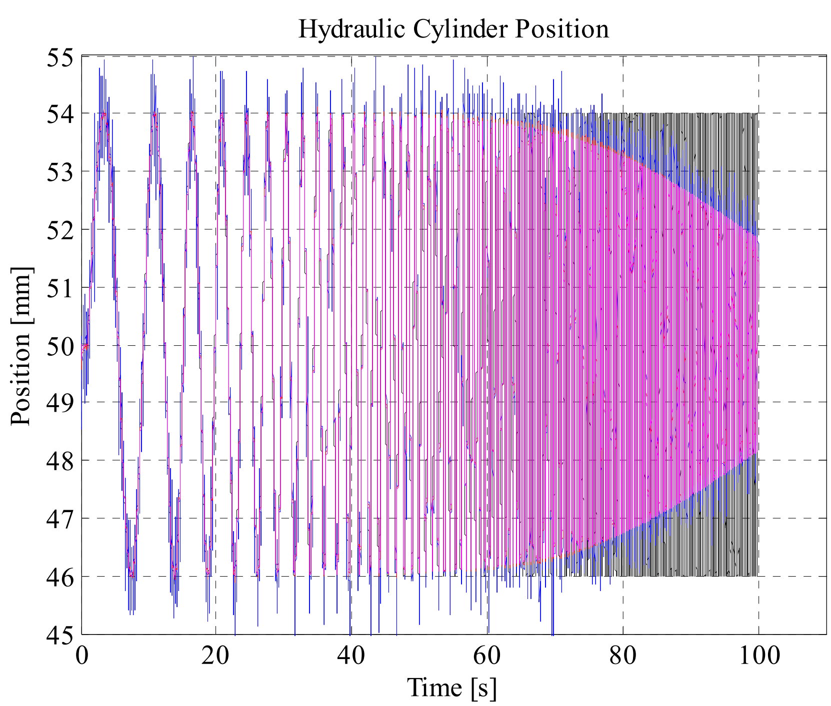

Figure 5-17 Position Response of Pump Controlled System

The upper plot of the Figure 5-18 shows the response of the closed loop pump speed controlled system at low frequency range. The excitation frequency is around 1 Hz. It is seen that, at low frequency region, the Kalman filter works well and the closed loop model response is similar to the measured real system response. In low frequency range, the affect of noise on the position signal is substantial. If the measured signal is to be used directly as the feedback position signal, then it will cause noise and chattering in the servomotors.

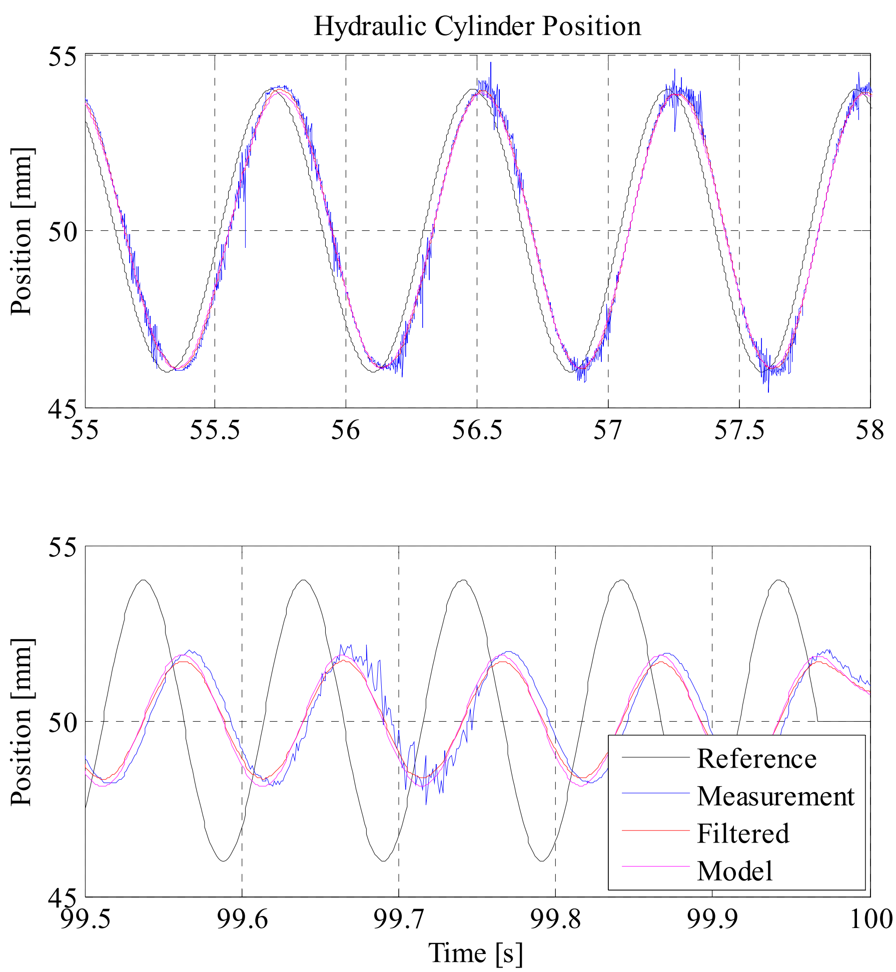

Figure 5-18 Detailed View of Position Response of Pump Controlled System

The bottom plot of the Figure 5-18 shows the response of the system around 10 Hz. It is seen that the model response and the measured real system response are consistent. However, at high frequency range, the performance of Kalman filter begins to deteriorate, there occurs a small phase difference between the measured and estimated position signal. This is an expected result since the filter thrusts more on the model than the measurement, when the model uncertainties becomes effective at high frequencies the error between the measurement and model increases. Note that, different form the conventional low pass, band pass etc. filters, where the filtered signal lags the measured signal, the Kalman filter output signal leads the measured signal.

In Figure 5-19 the performance of Kalman filter is illustrated by plotting the error between the measured and filtered position signals.

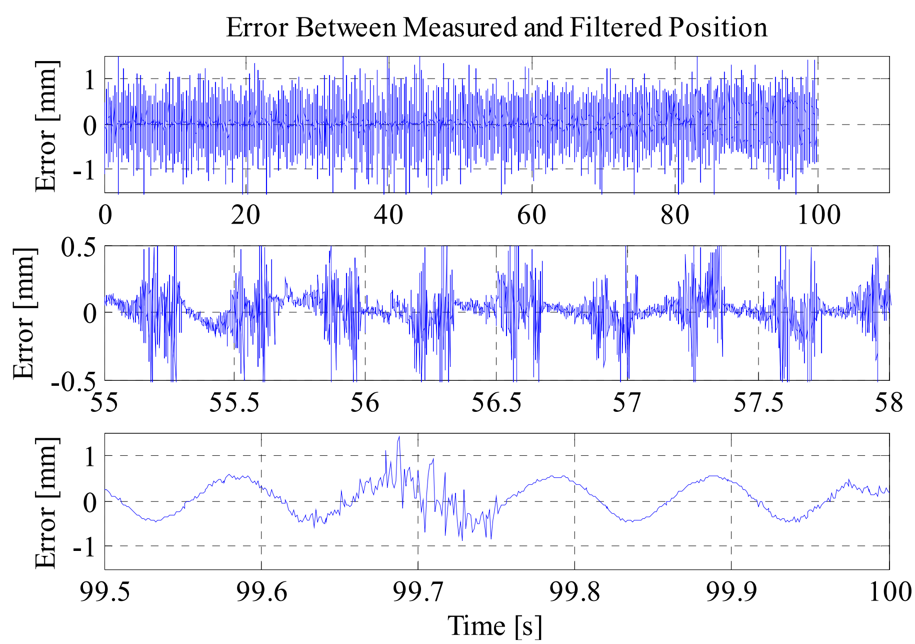

Figure 5-19 Error Between the Measured and Filtered Position Signal

From the detailed view of Figure 5-19, it is seen that at high frequency region, that is exictation frequency of 10 Hz, the error between the real measurement and the filtered output increases to 0.5 mm, where it is around

0.2 mm at around 1 Hz excitation frequency. However, it should be noted that the increasing error is mainly due to the phase shift at higher frequencies.

Furthermore, from the position response, it is useful to look at the pressure response as they are feedback signals and are used to manipulated input command. Figure 5-20 shows the pressure response of the hydraulic cylinder chambers during the sine sweep test. The blue signal is the measured signal, the red one is the filtered, and the magenta is the linear MATLAB Simulink model response. The pressure signal with higher amplitude, around 8 MPa, is the rod side chamber pressure (Chamber B with smaller cylinder piston area), and the signal with lower amplitude, around 4 MPa, is the cap side chamber pressure (Chamber A bigger cylinder piston area).

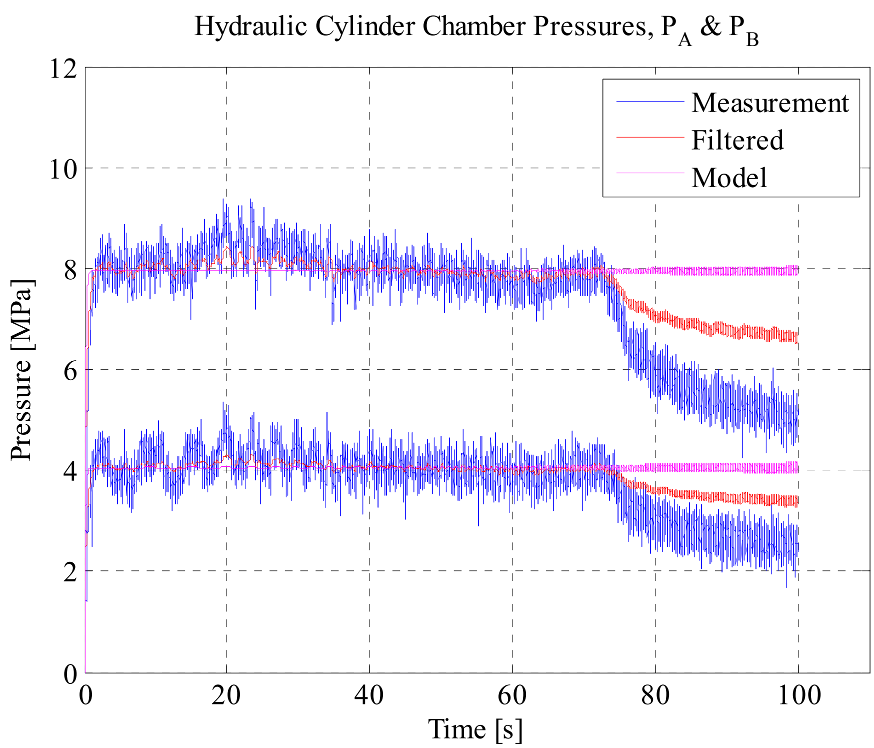

Figure 5-20 Pressure Response

It is seen that the model response is consistent with the measured ones at low frequency region. The resulting chamber pressures for a desired 12 MPa chamber pressure sum are 4 MPa and 8MPa, showing that the open loop pressure control works well. This also confirms the internal and external leakages coefficients found experimentally in Section 5.1.1, as they determine the open loop pressure control coefficients β and Ψ. Although the open loop sum pressure control works well at low frequency region, the chamber pressures begin to differ from the model response around time $t = 75\,s$ at high frequency region. This is mainly due to the changing leakage characteristics at higher frequencies. Also it should be noted that at these frequencies the servomotors which were assumed to be ideal angular velocity sources with zero dynamics do not respond to the desired velocity command. This can be clearly seen in Figure 5-21 where the reference and measured servomotor 2 speeds are plotted. It is seen that after time $t = 75\,s$ at higher frequencies, the measured velocity signal, the blue one, differs from reference velocity signal, the red one.

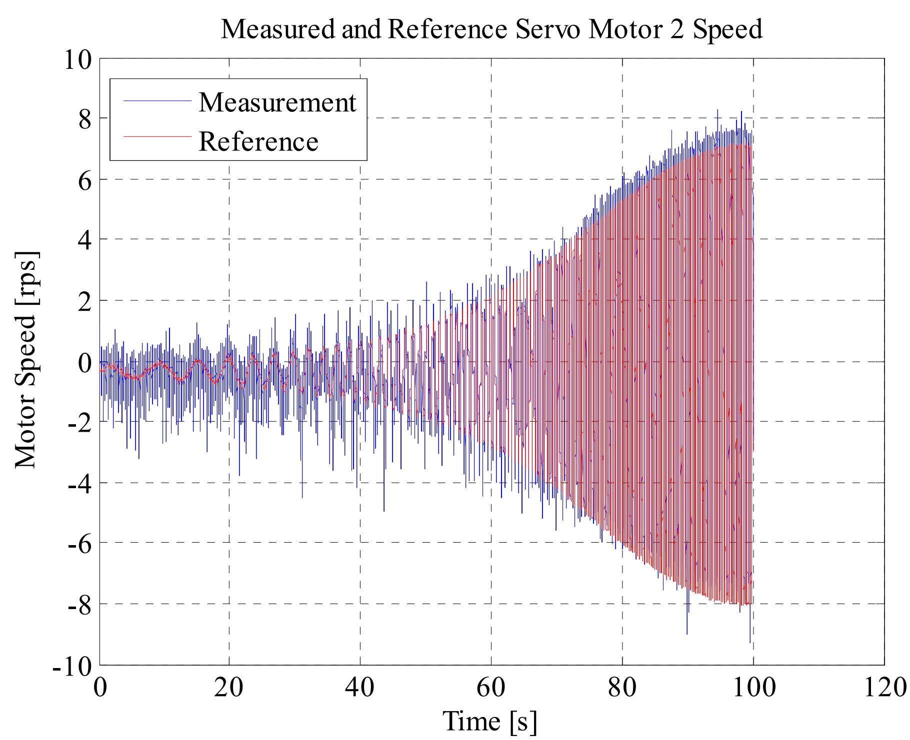

Figure 5-21 Servomotor Response

In Figure 5-20, it is seen that when the unexpected decrease of the chamber pressure at higher frequencies occurs, the filtered signals tracks the measured ones. However, the filtered pressure signals are not truly representative of the real chamber pressures. In Kalman filter, the measurement and process noise covariance matrices (**R** and **Q**) are tuned such that the filter trusts more and more on the model rather than the measurement. This is to prevent the effects of the non-linear real system properties on the linear controller.

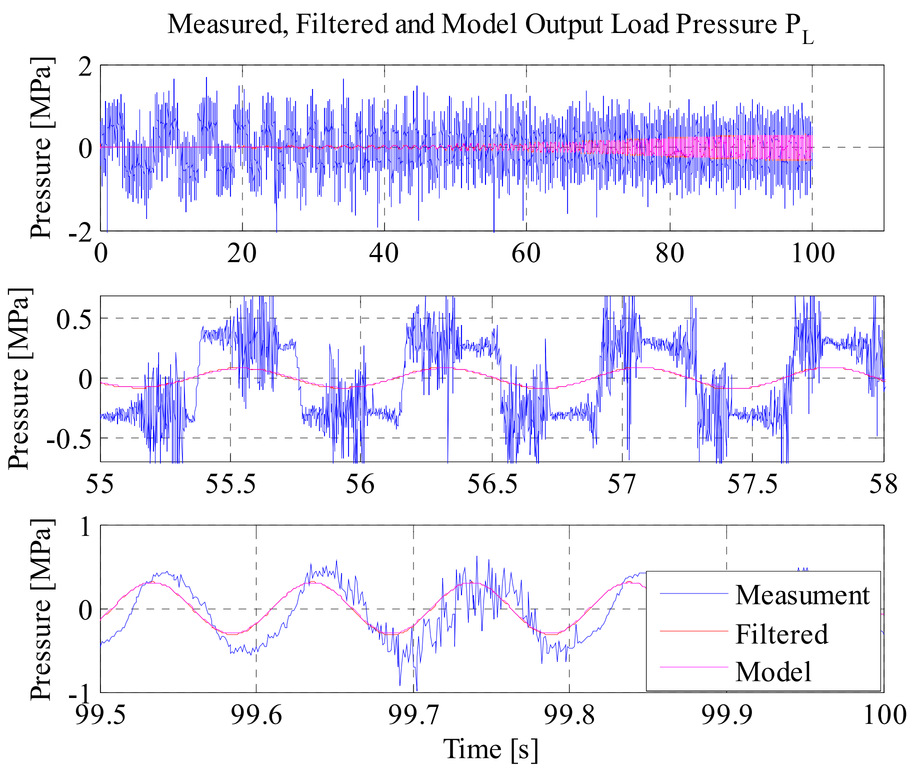

Figure 5-22 Load Pressure

In the controller, not the absolute chamber pressures itself but the load pressure, that is the dynamic change of pressure, is chosen as the state variable. If the measurements are to be trusted more, then the static friction, which is effective at low frequency region, will dominate the control signals send through the servomotors and may result in stability problem of the system. This can be seen in

Figure 5-22, where the measured and estimated load pressures are plotted. It is seen that despite the sinusoidal excitation, the load pressure at low frequency region resembles a square wave. This is due to the static friction on the sealing of the hydraulic cylinder, whereas the filtered signal is sinusoidal as expected and is similar to the model response. By this way, the feedback load pressure signal, which is calculated with the Kalman filter output chamber pressures, does not reflect the effect of static friction. At high frequency region the effect of static friction on the load pressure decreases due to increased effect of the inertial forces. The model pressure response and filtered pressure signals become consistent with the real load pressure for higher excitation frequency.

In Figure 5-23 and Figure 5-24, the frequency response of the real system and the model are compared on frequency domain.

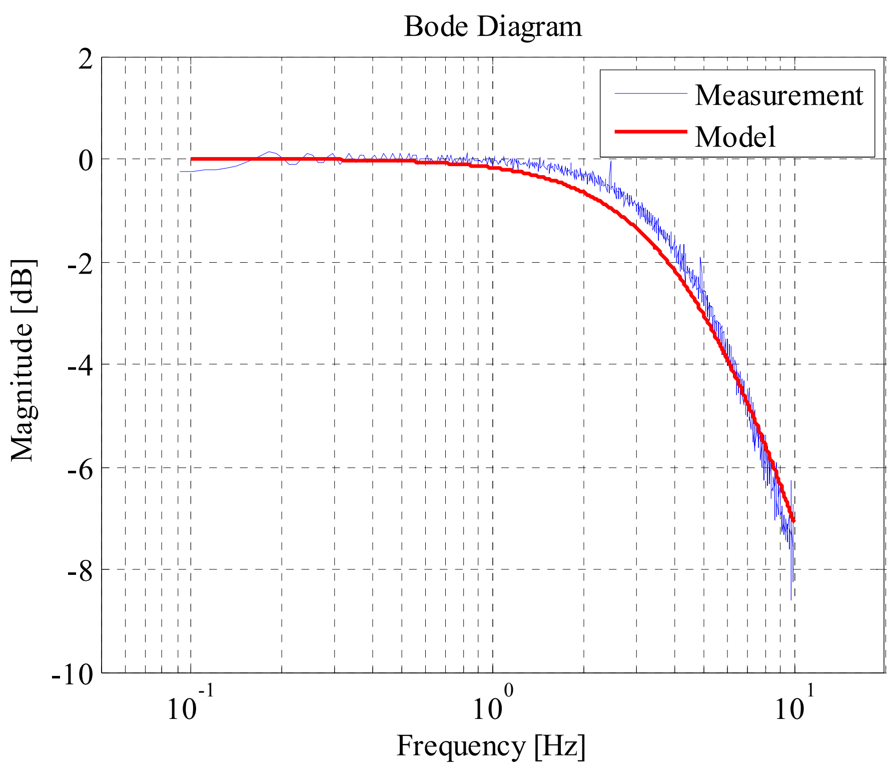

Figure 5-23 Magnitude Plot of the Experimental and Theoretical Frequency Response of Pump Controlled System with Desired Dominant Pole Located at -5.2π rad/s

The red signal shows the frequency response of the closed loop transfer function given in Eq. (4.24). The frequency response of the transfer function is drawn by the MATLAB built in "`bode`" command. The frequency response of the experimental data is converted from time domain to frequency domain by using MATLAB built in "`fft`" function. The MATLAB m-file script written for this purposes is given in Appendix C. It is seen that the real system response and the model response are consistent. The magnitude of the closed loop frequency response is -3 dB at 5 Hz excitation frequency, indicating the bandwidth of the system. This is an expected result, because the desired closed loop poles were located at $[-5.2\pi, -600, -700]$. Because the last two poles are far away from the imaginary axes with respect to the first pole, the pole located at -5.2π rad/s dominates the system characteristics, and resulting in a 5 Hz bandwidth of the closed loop system.

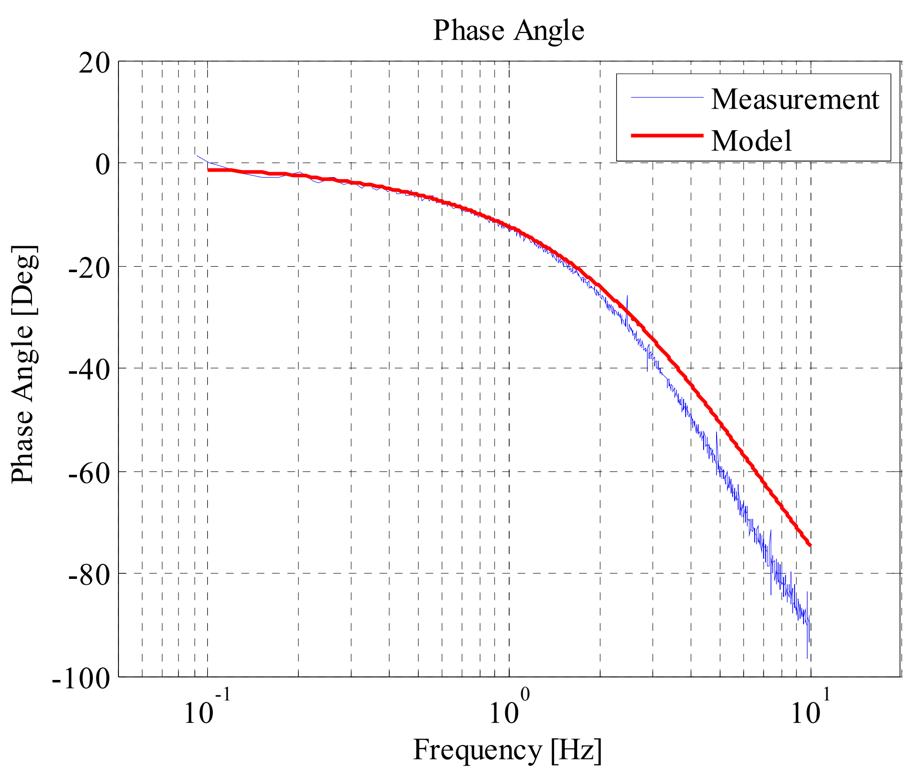

Figure 5-24 Phase Plot of the Experimental and Theoretical Frequency Response of Pump Controlled System with Desired Dominant Pole Located at -5.2π rad/s

5.4.4 Open Loop Frequency Response of Valve Controlled Hydraulic System

For the open loop test of the valve controlled system a sinusoidal signal with 1 V amplitude and -0.1 V offset is chosen. The frequency of the test signals starts from 0.1 Hz and linearly increases to 10 Hz in 100 seconds. The test signal used in the open loop test of the valve controlled system is shown in Figure 5-25.

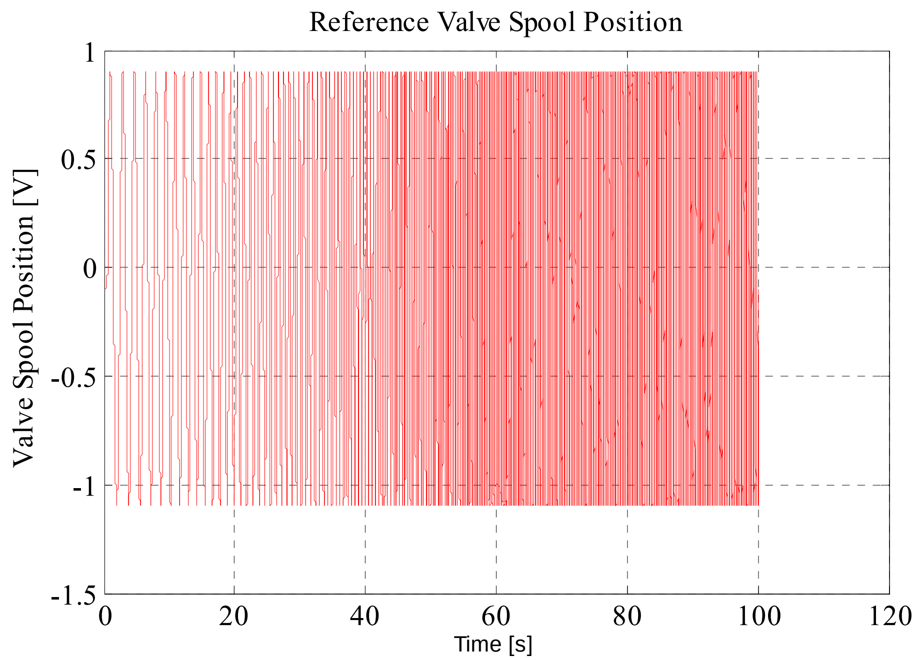

Figure 5-25 Test Signal for Valve Controlled System Open Loop Frequency Response

Figure 5-26 shows the experimental and the theoretical open loop frequency responses of the system. Since the type number of the transfer function defining the open loop position response of the system is one like in the pump controlled system, the slope of the Bode diagram at the low frequency region is –20 dB/dec. The system behaves like an integrator as expected. It is seen from the Bode diagram that the theoretical resonance frequency of the system is around 316 Hz. Likewise in the pump controlled case, at low frequency region, the system rapidly responses to the input signal and there is no need to wait for the system to reach steady state. Thus continuously changing the test signal frequency is not a problem for this frequency response tests.

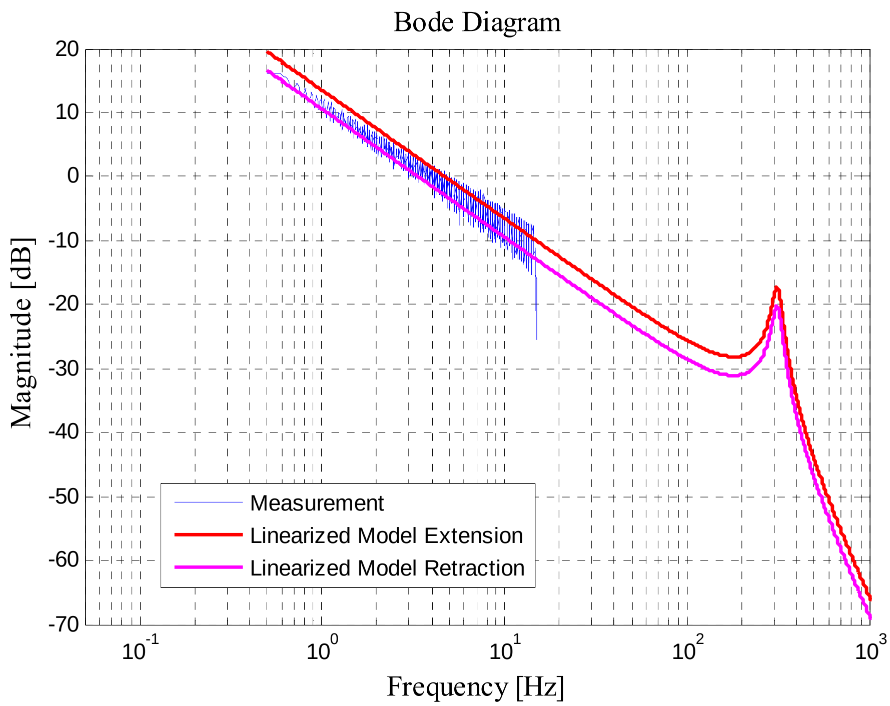

Figure 5-26 Magnitude Plot of the Experimental and Theoretical Open Loop Frequency Response of the Valve Controlled System

Different from the pump controlled system, two different open loop frequency response graphs are drawn for the linearized mathematical model of the valve controlled system. This is due to the inherent property of the single rod cylinders that different extending and retracting speed exist. It is seen that at low frequency region the measured frequency response is consistent with the linearized frequency response for retraction.

Figure 5-27 shows the experimental and the theoretical phase plots of the open loop frequency response of valve controlled system. Due to the free s term in the open loop transfer function between the valve spool position and hydraulic cylinder position, there occurs a 90 degrees phase shift at low frequency region. Note that there exist two different curves representing the phase plot of the open loop valve controlled system. However, as the roots of the characteristic equation defining the dynamics for retraction and extension is very closer, it is seen as a single curve.

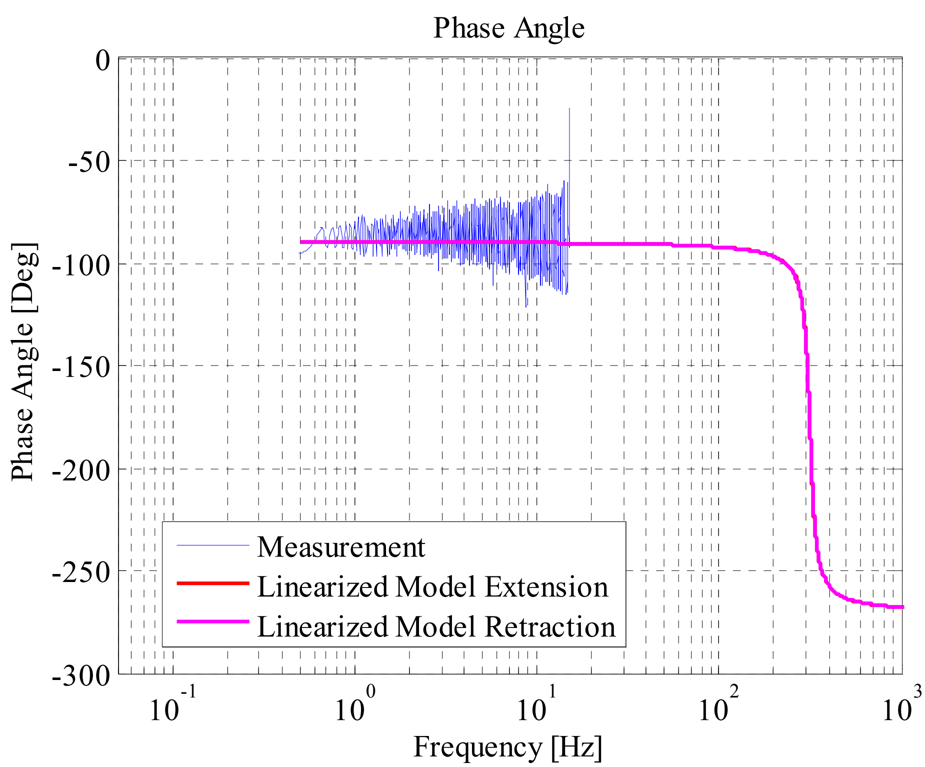

Figure 5-27 Phase Plot of the Experimental and Theoretical Open Loop Frequency Response of the Valve Controlled System

5.4.5 Closed Loop Frequency Response of Valve Controlled Hydraulic System

To be compatible with the pump controlled system, the same test signal is applied to valve controlled system. Also the desired closed loop pole locations are chosen to be the same with the pump controlled system. The linear state feedback gains corresponding to desired closed loop pole locations are determined by following the procedure explained in Section 4.4. Throughout all the frequency response tests the supply pressure of the servo solenoid valve is fixed by setting the set pressure of the relief valve to 8.3 MPa. The test signal properties, the desired closed loop poles and the corresponding state feedback gains are listed in Table 5-6.

Table 5-6 Valve Controlled System Frequency Response Test Data

<table>
<tr><td colspan="4">Reference Chirp Signal</td></tr>
<tr><td>Magnitude</td><td>Start Frequency</td><td>Stop Frequency</td><td>Duration</td></tr>
<tr><td>4 mm</td><td>0.1 Hz</td><td>10 Hz</td><td>100 s</td></tr>
<tr><td colspan="2">Desired Closed Loop Poles</td><td colspan="2">$[-5.2\pi, -600, -700]$</td></tr>
<tr><td rowspan="2">State Feedback Gains</td><td>Extension</td><td colspan="2">$[0.1132, -0.0315, 0.7719]$</td></tr>
<tr><td>Retraction</td><td colspan="2">$[0.1573, -0.0441, 1.0784]$</td></tr>
<tr><td rowspan="2">Linearized at</td><td>Supply Pressure</td><td colspan="2">8.3 MPa</td></tr>
<tr><td>Spool Position</td><td colspan="2">0.1 V</td></tr>
</table>

Figure 5-28 shows the response of the valve controlled hydraulic system. The black signal is the reference position signal, while the blue one is measured position signal and the red one is the filtered signal, which is the output of the unscented Kalman filter and used as the feedback signal, and lastly the magenta signal is the position response of the non-linear MATLAB Simulink model.

The second plot of the Figure 5-28 shows the detailed view of the response of the closed loop valve controlled system at low frequency range. The excitation frequency is around 1 Hz. It is seen that at low frequency region unscented Kalman filter works well, the filtered signal and the measured signal are the same without any phase difference. In low frequency region, it is seen that the effect of noise is substantial as in the case of pump controlled system. If the measured signal is not smoothed and directly used as feedback signal then the noise will cause chattering in the servo solenoid valve.

In the second plot of Figure 5-28, it is seen that the sinusoidal position response is rugged just after the peaks, for example at time 55 seconds or 57 seconds. This oscillatory behavior is due to the switching of the controller gains, at this time, the linear state feedback gains for extension is replaced with the controller gains for retraction. Because the gains are switched exactly at zero spool position command, there occurs oscillations, this is nothing to do with the noise, in non-linear MATLAB Simulink model response there also occur oscillations. To get rid of this response with unwanted property, the controller should be modified. However this is out of the scope of the thesis, as the aim is just to make performance comparison with the pump controlled system.

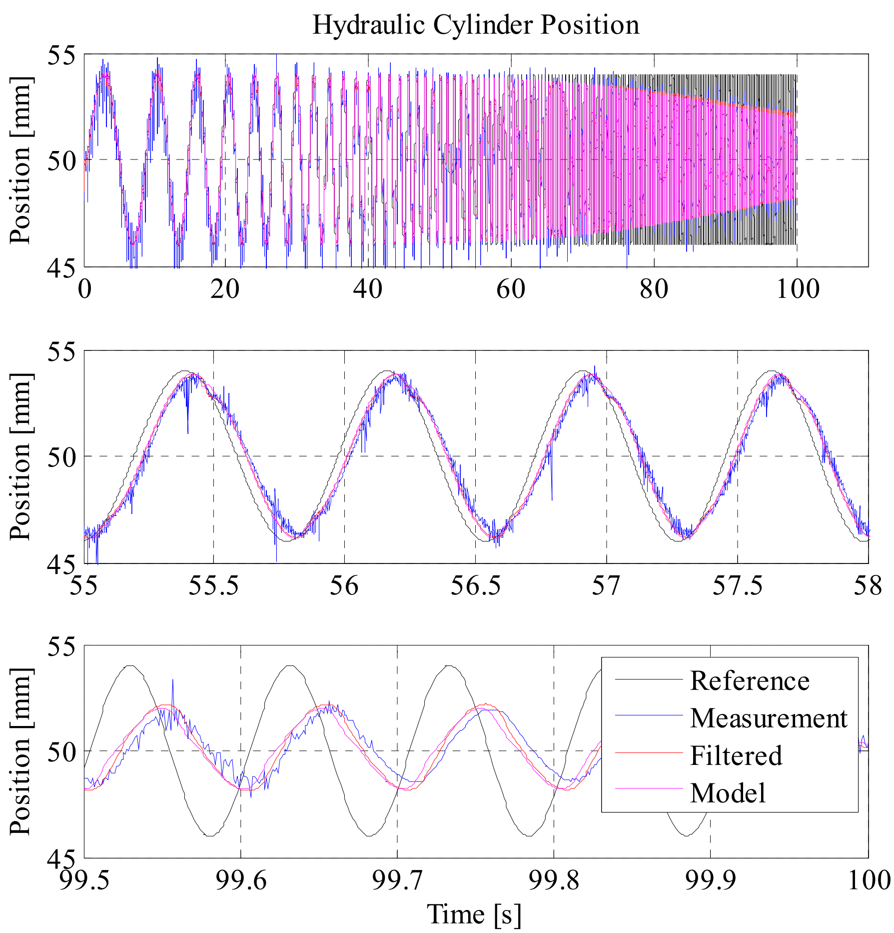

Figure 5-28 Valve Controlled System Position Response

The third plot of Figure 5-28 is the detailed view at higher frequencies. The excitation frequency is around 10 Hz. It is seen that the non-linear model response and the real system response are consistent. However, the performance of unscented Kalman filter begins to deteriorate and a small phase shift occurs between the real and measured signals. This is an inevitable property as the filter trusts more on the model.

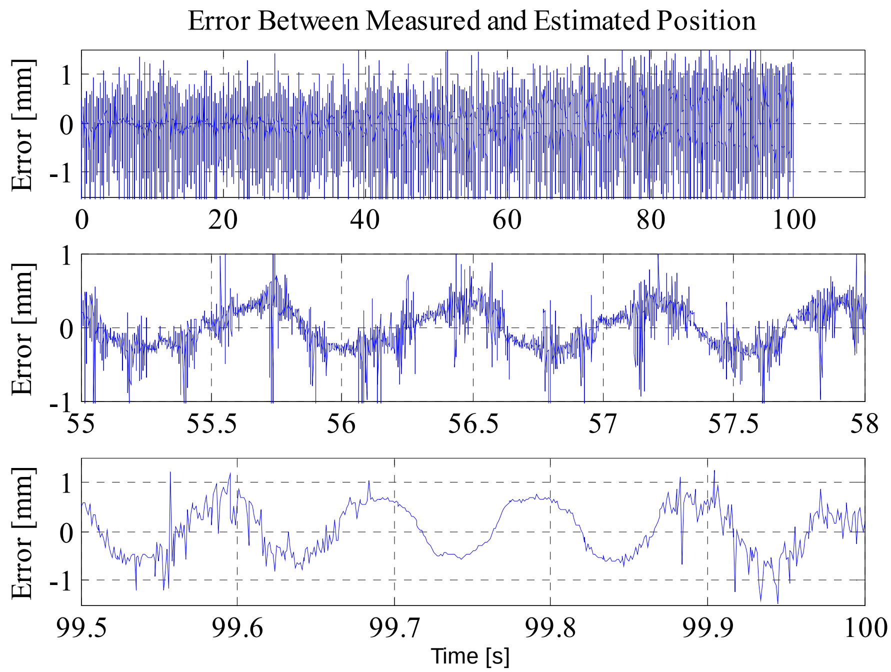

Figure 5-29 Valve Controlled System Error Between the Measured and Filtered Position Signal

In Figure 5-29, the error between the measured and filtered position signal is plotted. From the detailed views it is seen that the error increases to 0.5 mm around 10 Hz excitation frequency, where it is 0.3 mm at around 1 Hz excitation frequency. However this error is mainly due to the phase shift, as the filter output leads the measured signal.

In the third plot of Figure 5-28, at higher frequencies, it is seen that the real system and the non-linear model responses seem to track not an exact sinusoidal profile, but rather a ramp like profile. This the result of switching type controller strategy with the gains calculated according to the linearized system equations, if the same controller is to be applied on the linearized model, it will be seen that the response profile is exactly sinusoidal.

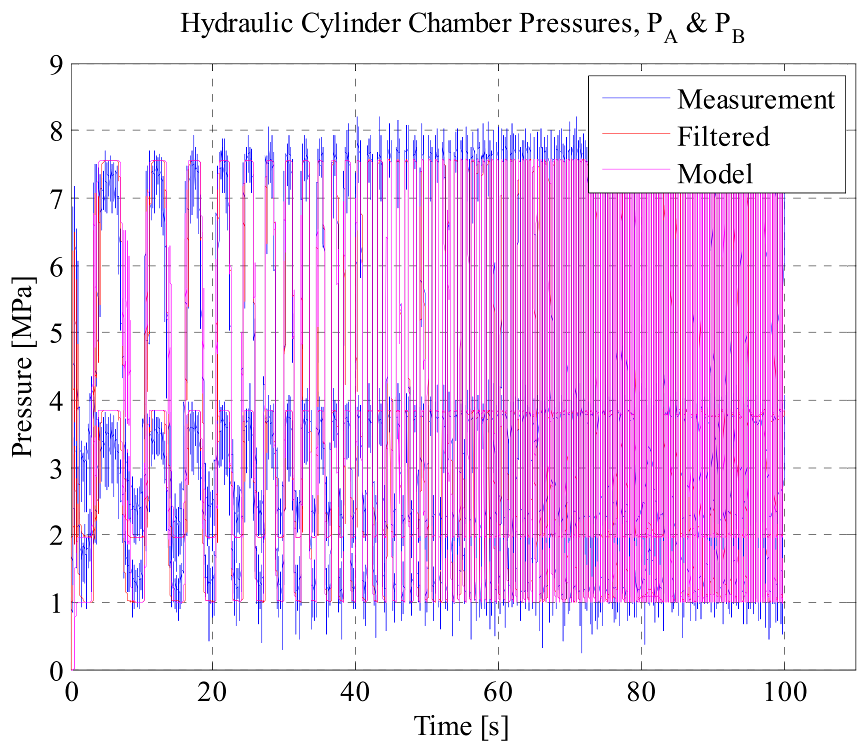

Figure 5-30 Valve Controlled System Hydraulic Cylinder Chamber Pressure Response

In Figure 5-30, the pressure response of the hydraulic cylinder chambers during the sine sweep test is plotted. The blue signal is the measured signal while the red one is the filtered, and the magenta is the non-linear MATLAB Simulink model response. It is validated that there exist two different steady state chamber pressures for extension and for retraction; this can be clearly seen at low frequency region. Likewise in the pumped controlled system the filtered pressure response signals are similar to the non-linear model response rather than the measurement, as the filters trusts more on more on the model. Consequently, the effects of the non-linear friction on the load pressure are eliminated. This can be seen in Figure 5-31**.**

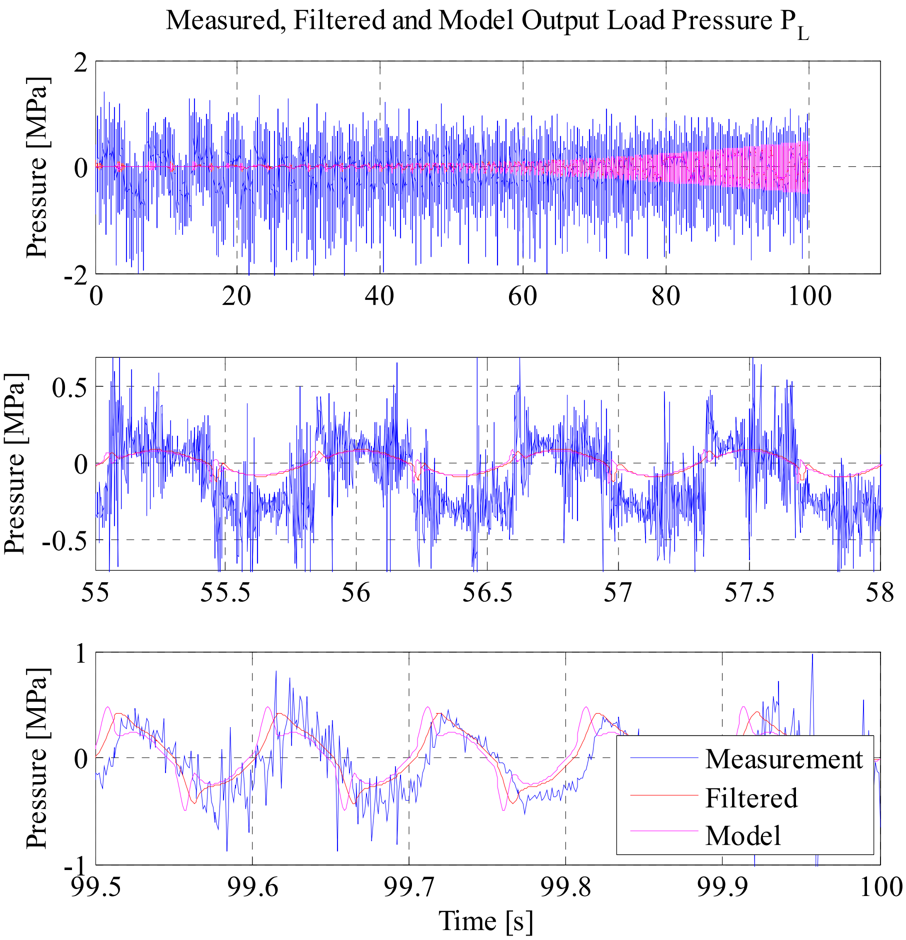

Figure 5-31 Valve Controlled System Load Pressure Response

Figure 5-31 shows the load pressure response of the system, during the sine sweep test. In the detailed view at lower frequency region, which is the second plot, it is seen that the load pressure tracks a square wave like profile. This is due to the static friction of the hydraulic cylinder. However, this non-linear load pressure characteristics is not reflected to the generated manipulated input signal sent to the servovalve drives. The filtered signal which is very similar to the model response is fedback to the controller. In the third plot of the Figure 5-31 the detailed view of the load pressure responses at higher excitation frequency is shown, it is seen that the effects of the static friction on the load pressure is reduced and the real load pressure is consistent with the model response.

In Figure 5-32 the frequency response of the real system and the model are compared. The red signal shows the frequency response of the linearized closed loop transfer function obtained by the Eq.(3.111). It is drawn by the MATLAB built in "bode" command.

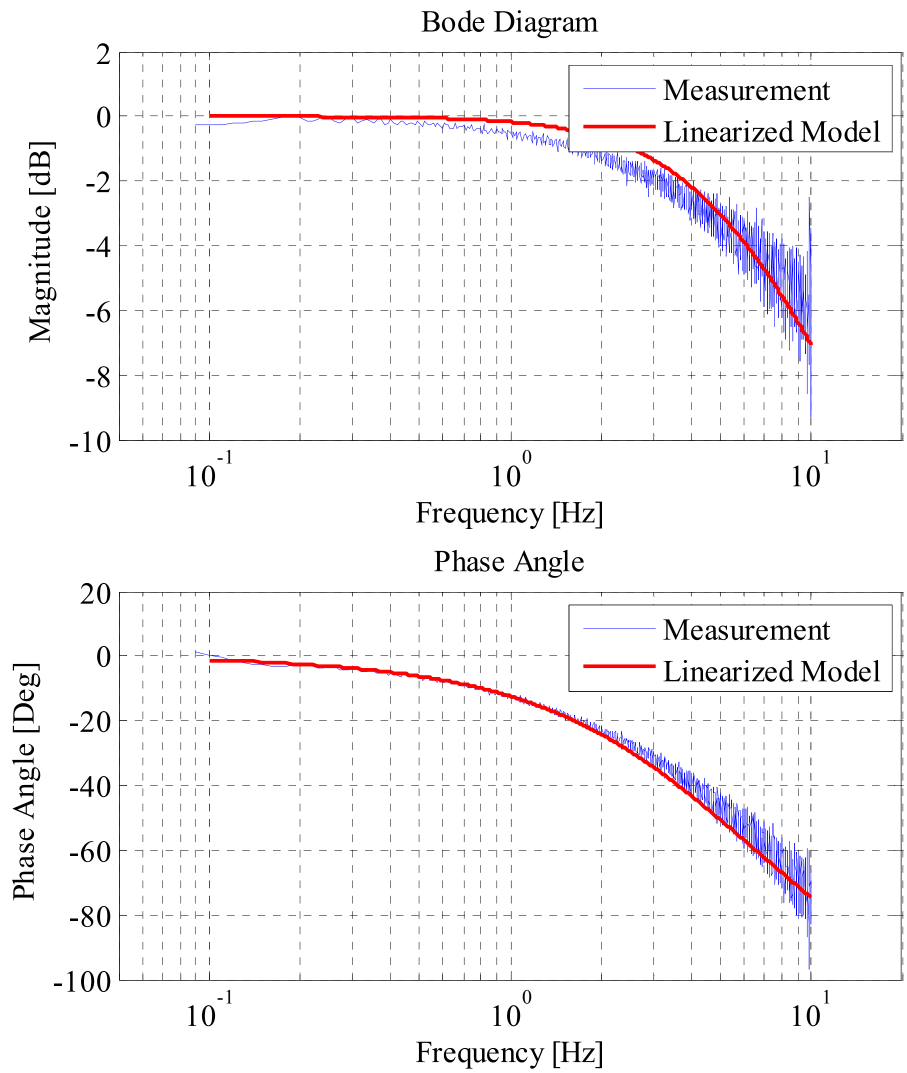

Figure 5-32 Experimental and Theoretical Frequency Response of Valve Controlled System with Desired Dominant Pole Located at -5.2π rad/s

Note that because the desired closed loop pole locations for extension and retraction are the same, the dynamic response of the closed loop system for extension and retraction are identical, therefore unlike from the open loop frequency response graph, there exists only one frequency response curve defining the closed loop system characteristics.

In Figure 5-32 it is seen that, the magnitude plot of the real system response reflects the desired closed loop system behavior. The magnitude of the closed loop frequency response is -3 dB at 5 Hz excitation frequency, indicating the bandwidth of the system. This is an expected result, because the desired closed loop poles are located at $[-5.2\pi, -600, -700]$. Because the last two poles are far away from the imaginary axis with respect to the first pole, the pole located at -5.2π rad/s dominates the system characteristics, and resulting in a 5 Hz bandwidth of the closed loop system. However, the real system response is not consistent with the linearized model response at higher frequencies. This is the result of linearization, with the increasing excitation frequency the operating points where the linearization is performed changes. For example, the valve gains are linearized at steady state operating pressures both for extension and retraction, the steady state chamber pressure values are constant and do not change with the spool position, but the spool direction. However, with the increased excitation frequency when the valve spool changes direction the time passed in transient period dominates the total excitation frequency period, resulting in a different system behavior than the linearized one.

5.5 Comparison of Two Systems

Throughout the performance tests the closed loop position control of a single rod asymmetric cylinder is performed by utilizing the conventional valve control and variable speed pump control techniques independently.

Due to the inherent property of the single rod hydraulic actuator with unequal cylinder areas, the flow rate entering the cap end side chamber is not equal to the flow rate exiting from the rod end side.

In valve controlled systems the asymmetric flow rate of the hydraulic actuator results in such a non-linearity that different steady state chamber pressures exists according to the valve spool position; causing different valve spool position gains and different extension and retraction speeds.

The different dynamics characteristics of the valve controlled system for extension and retraction brings about the necessity to use different controller gains for extension and retraction. However switching the controller gains according to spool position causes somewhat oscillatory-rugged behavior on the hydraulic actuator position response at switching times. Of course, this unwanted property can be eliminated by modifying the control strategy, but this brings another complexity.

However, in pump controlled system, there exist two servo pumps, which can be actuated and controlled independently. This brings the edge of compensating the unequal flow rate of the single rod asymmetric hydraulic actuator. In the constructed variable speed pump control circuit, the pump 1 is utilized to compensate the leakage flows and the unequal flow rate of the hydraulic actuator, and the pump 2 is left with the position and direction control of the hydraulic actuator. Because pump 1 is always compensating the unequal flow rate pump 2 can be thought as a control element regulating the flow rate of a symmetric double rod cylinder. Thus the dynamic characteristic defined between the pump 2 drive speed and the hydraulic actuator position remains the same for extension and retraction.

The same dynamic characteristics for extension and retraction brings the superiority of the two pump controlled circuit, over the valve control circuit. The position of the single rod actuator can be controlled with only one set of state feedback gains thus eliminating the controller complexity and its unwanted results on the system response.

In addition to the simpler controller requirement the pump controlled circuit is superior to the valve controlled circuit, due to its linear nature. If the non-linear friction characteristic of hydraulic actuator is neglected, it is seen that the total system dynamics can be defined fully by linear set of differential equations. As a result, the desired system response and the real system response are consistent. However in the valve controlled circuit, unlike from the pumped controlled circuit where the flow rate is proportional to the drive speed but it is proportional to the square root of the valve pressure differential. This non-linear valve flow characteristics brings the necessity of linearization to define a transfer function representing the system dynamics. From the experimental test results it is seen that the real system response designed according to the linearized system equations, performs well at low frequency region. Nevertheless, at high frequency region the response characteristics of the real system differ from the linearized system, as the operating points, where the linearization is performed, changes suddenly.

As a result, in terms of dynamic performance, controller simplicity due to same dynamic characteristics for extension and retraction and the consistency with the desired system response due to its linear nature are the superiorities of the variable speed pumped controlled system over the valve controlled system.

Besides the dynamic performance, if the energy efficiency of the two circuits is to be compared, it is seen that the pump controlled circuit is by far advantageous over the valve controlled circuit. Because the flow rate is regulated by adjusting the pump drive speed there exist no throttling losses in the pump controlled circuit. In valve controlled circuit most of the energy loss is due to throttling losses. However, if the Figure 2-4, where the power losses of a conventional valve controlled circuit is illustrated, is to be remembered, it is understood that most of the power losses is not due to regulate the flow rate through the hydraulic actuator but to supply a constant pressure for the servo solenoid valve intake. Most of the flow delivered by the pump to the system passes through the relief valve to the oil tank, accompanying with a pressure drop equivalent to the valve supply pressure. One way to reduce the power loss on the relief valve is to decrease the pump drive speed, thus to decrease the amount of oil delivered to the system. However, this will result in the fluctuations of the supply pressure, and affect the dynamic behavior adversely. Another alternative is to use a pressure compensated pump, where the flow rate is adjusted according to the system requirements by changing pump displacement, while maintaining a constant supply pressure for the flow control valve intake. However it should be noted that this will increase the total cost of the hydraulic drive system.

It should be remembered that the fluid power energy lost on the servo solenoid valve and the relief valve transforms into heat energy, warming up the hydraulic oil. Hydraulic oil characteristics change with the increasing oil temperature, thus necessitate for cooling of the hydraulic oil arises in the valve controlled system. This should be accounted for another additional energy loss. Furthermore, the oil used in the pump controlled system is not heated up fewer amount of hydraulic oil is used with respect to the valve controlled system, thus decreasing the bulky oil reservoir volume.

The hydraulic systems are famous as drive systems, due to their high power to weight ratio, this is the biggest advantage of the valve controlled circuit. For example a valve mounted directly on the hydraulic actuator of a robot arm will not increase the total inertia however if a pumped controlled circuit is utilized, the mass of the two pumps and the two servomotors, will increase the inertia of the robot arm considerably. A solution to this may be using long transmission lines and mounting the pump motor assembly on the ground, but this time the dead volumes due to long transmission line will decrease the dynamic performance of the hydraulic system. For this reason in manipulator like applications, where the power to mass ratio is important, the valve controlled systems seems to be favorable.

In variable speed pump control technique the drive speed of the pumps are adjusted via servomotors powered from an AC electric supply. In the valve controlled circuit, the pumps are also driven with electric motors; however, as the drive speed is constant, an internal combustion engine can also be utilized as the power source. This brings another superiority of the valve controlled system, which is the ability to be used in mobile application.

At last, in most of the engineering applications, cost is by far the most important criteria. Of course, using only a servovalve accompanied with a standard power supply seems to be reasonable rather than using two special pumps and two servomotors. But despite the investment cost, if the operating cost is to be considered, pump controlled systems may be advantageous. The energy savings of the pump controlled circuit, the reduced amount of hydraulic fluid, accompanying with the increased oil change period are considerable costs in a hydraulic system. Despite the energy point of view, the maintenance cost of the pump controlled circuit is another advantage over valve controlled systems, as the pump controlled hydraulic circuit is simpler than the valve controlled one with less number of components. Another important factor that determines the cost of a hydraulic system is the oil contaminations level. It should be noted that because the pump controlled system is less sensitive to oil contamination, rather than the valve controlled system the filtering cost will also decrease the operating cost.

CHAPTER 6

DISCUSSIONS, CONCLUSIONS AND RECOMMENDATIONS

6.1 Outline of the Study and Discussions

The tasks accomplished within the scope of this thesis study include

- modeling of the valve controlled and pump controlled systems in MATLAB Simulink environment;
- derivation of linear and linearized reduced order differential equations defining the system dynamics;
- linear state feedback controller design by using the reduced order linear and linearized system equations;
- design of linear and non-linear unscented Kalman filters for filtering and estimation purposes;
- construction of the experimental test set up where the two control techniques can be applied on the same actuator;
- system identification and finding the unmeasurable quantities experimentally;
- conducting the performance tests;
- comparison of the two hydraulic control techniques.

At the beginning of the study, detailed mathematical models of pump controlled systems and valve controlled systems are developed. For simplification purposes, the dynamics of the valve actuator and the pump actuator are considered to be ideal elements with no dynamics assuming that they have a high bandwidth controller inside. A non-linear model of the valve controlled system and a linear model for the pump controlled system consisting of the hydraulic actuator and the load dynamics are developed in the MATLAB Simulink environment.

Next to numerical methods used in computer environment, both systems are also modeled analytically to understand their system dynamics fully. The cylinder dynamics accompanied with the load dynamics results in a 3rd order differential equation between the actuator input and the hydraulic cylinder velocity response. However when the relation between the dynamic change of hydraulic cylinder chamber pressures is investigated, it is seen that dynamic pressure changes in the hydraulic cylinder chambers become linearly dependent above and below some prescribed cut off frequencies. Thus, assuming linearly dependent chamber pressure response, the order of the dynamic equations defining the system dynamics is reduced, resulting in a 2nd order transfer function between the actuator input and the hydraulic cylinder velocity. By this way, the parameters affecting the system dynamics of the system are explained clearly. Different from the pump controlled system, the valve flow characteristic equation is linearized at steady state chamber pressures for extension and retraction at a given spool position to derive a transfer function for the valve controlled system. From the block diagram representations drawn for the open loop response of the two systems Figure 3-15 and Figure 3-22 it is concluded that the system dynamics of the two control techniques are the same except for the actuator gains between the control input and the flow rate delivered to the system and the load pressure feedback gain, which is determined by pump leakages in the pump controlled circuit and determined by the valve pressure gain in the valve controlled circuit.

For the position control of the single rod hydraulic actuator, it is decided to use a linear state feedback control scheme. In the pump controlled system the state feedback gains are determined by using the linear reduced order system equations, and in valve controlled system the linearized reduced order system equations are used. Unlike from the pump controlled system, there exist only one control element in the valve controlled system. Therefore, the unequal flow rate of the single rod cylinder is not compensated, resulting in two different system dynamics for extension and for retraction. For this reason, two different state feedback gain sets are determined in the valve controlled system for extension and for retraction. In the applied control algorithm the state feedback gains are switched according to the valve spool position command.

Because the measured position and the pressure signals are noisy and should be smoothed in order to be used as the feedback signal through the controller, and there exist an unknown state which is the actuator velocity and should be estimated to be used in state feedback control algorithm, Kalman filters are utilized both for the filtering and estimation purposes. For the pump controlled system due to its linear nature a conventional discrete linear Kalman filter is designed, however for the valve controlled system due to its non-linear characteristics an unscented Kalman filter is designed. The two Kalman filters are tuned such that the filtered pressure responses and the velocity estimations thrust on the system model rather than the measurement. By this way the undesirable properties of the real systems, which are not modeled like the static friction of the hydraulic cylinder, are prevented to affect the controller performance. Another outcome of this filtering strategy is that the hydraulic cylinder position can also be controlled with the same state feedback controller algorithm by only using the position transducer.

In both systems, the unknown parameters, which are the pump leakage characteristics and the hydraulic cylinder friction characteristics, are found indirectly through a test procedure as they are not measurable quantities. The internal and external leakage coefficients are found from the steady state chamber pressures and the hydraulic cylinder friction characteristics is found by applying a chirp signal and measuring effective load pressure acting on the hydraulic cylinder.

To test the performance of the valve controlled and pump controlled hydraulic systems, step response and open loop and closed loop frequency response tests are conducted on the constructed experimental test set up. For control purposes, the MATLAB Simulink Real Time Windows Target module is utilized. The magnitude and frequency of the test signals are chosen such that valve or servomotor actuators will not saturate. Therefore, the test signals are pre-tested on the MATLAB Simulink system models, before running real time tests. Step response and frequency response tests are repeated for different closed loop pole locations. The test signal properties, and the desired closed loop pole locations are selected to be the same in the pump and valve controlled circuit. The test results revealed that the dynamic performance of variable speed pump controlled system is superior to the servo solenoid valve controlled circuit, in terms of controller simplicity and consistency with the model response. For the both control systems, it is seen that the bandwidth of the closed loop system can be adjusted via linear state feedback control algorithm. However in the valve controlled system the performance of the closed loop system degrades at higher frequencies.

At last a comparison of the variable speed pump controlled and valve controlled system are made, in terms of dynamic performance, application and cost.

At the end of this thesis study a hydraulic test set up is constructed, this set up may be used for different linear or non-linear control applications, with educational purposes.

6.2 Conclusions

Variable speed pump control technique is a recently developed research area in hydraulic control systems. In this thesis study, this recent method is investigated in depth with theoretical and experimental analyses and compared with the conventional valve controlled hydraulic systems.

It is shown that the maximum efficiency of a conventional valve controlled circuit is 38.5%, and noted that this is valid for only at an instant of time when the maximum power requirement is equal to the maximum power input of the valve, if the total duty cycle of the load is considered, the efficiency of the hydraulic circuit will be lower than this figure. If this low efficiency of the conventional valve controlled circuits is considered, then the importance of pump controlled systems will be well understood where there exist no throttling losses. In the variable speed pump controlled circuit constructed and analyzed throughout the thesis study, two variable speed pumps are utilized to regulate the flow rate going through the hydraulic actuator and eliminating throttling losses. Thus, all the throttling losses are eliminated and the only energy loss in this new circuit concept is the losses due to pump leakages, motor drives and transmission lines.

Besides the elimination of throttling losses, in this thesis study, it is also revealed that the two pump control principle is superior to the valve control technique due to the ability to compensate for the asymmetric flow rate of the single rod cylinder. Thus different from the valve controlled circuit, where two different dynamic characteristics exist for extension and retraction, the dynamic response of the pumped controlled system is the same both for extension and retraction. This property makes the variable speed pump controlled circuit superior to the valve controlled circuit in terms of controller simplicity. The different characteristics of the valve controlled circuit for extension and retraction necessitates a complex controller than in the pumped controlled case. In this thesis study two different state feedback gains are calculated for extension and retraction of the valve controlled circuit. These gains are switched between each other for the zero spool position command and it is observed that this results in a rugged response at the switching times. However in the variable speed pump controlled system, a smooth response is obtained by using a simple linear state feedback control algorithm.

Besides the controller simplicity, due to the linear nature of the variable speed pump controlled circuit, from the test results it is seen that the linear model responses are completely in accordance with the test results. Thus a high performance closed loop variable speed pump control system can be designed just by using the linear system equations with the conventional analytical controller design methods. However in valve controlled system the linearized model response differs from the real system at high frequency excitations, thus to design a high performance closed loop valve controlled circuit not the linearized system equations but the non-linear system equations should be used.

Except the dynamic performance and the energy consumption if the two systems are compared in terms of cost, then it is seen that the investment cost of the pump controlled system is higher than the valve controlled one, however if the operation and maintenance cost is considered the pump controlled system can amortize the investment cost depending on the duty cycle of the system.

The main drawbacks of the variable speed controlled systems are the low power to mass ratio with respect to valve controlled systems and requirement for an electrical power supplies. Besides, the long transmission lines between the pumps and actuator is another drawback decreasing the dynamic performance in variable speed pump controlled system. All these factors oppose to apply variable speed pump control technique in mobile and robotic, manipulator like applications. However, for stationary applications, like industrial presses, where power to mass ratio is not important and a electrical supply is available, the variable speed pump control principle seem to be favorable.

6.3 Recommendations for Future Work

In this thesis study, motor dynamics is neglected completely and servomotors are assumed to be angular velocity resources as they have a high bandwidth controller inside. However, during the tests it is seen that motor dynamics has an effect on the system performance. Especially at high frequency excitations, the motor does not respond well, there occur a shift both in phase and magnitude level resulting in a decrease of the chamber pressures. To model the system more accurately not only the servomotor model dynamics should be added to system dynamic equations, but also the non-linear behavior of the servomotor should be taken into account. Because, the system is controlled by regulating the servomotor speed, especially at steady state where the servomotor speed is very low or near to zero, the dead band of the servomotor becomes more of issue and should be investigated.

In this thesis study, the pumps are also assumed as ideal transformation elements, with linear internal and external leakage coefficients, transforming the input shaft speed to the flow rate delivered to the system. The pump characteristics are not investigated. However, it is known that the pump volumetric efficiency changes with the motor speed implying that the leakage coefficients are not the same for high speed and low speed excitations. In variable speed pump controlled systems, the pumps are required to work under high pressures with very low drive speeds. Therefore, to increase the system performance, pump characteristics at low drive speeds should be investigated. The dead band in the pump drive speeds and non-linear leakage flow coefficients may be found experimentally.

Considering the effects of the servomotor dynamics, non-linear pump characteristics, and of course designing and tuning an appropriate controller, the steady state behavior of the variable speed pump controlled system could further be improved.

In this thesis study, the parameters like bulk modulus of the oil, leakage coefficients of the pump and the friction characteristics of the hydraulic cylinder are found through an experimental procedure. However, there are some studies in literature utilizing Kalman filters for monitoring system parameters which are not measurable directly. In this study, Kalman filters are used for only filtering and estimation purposes, the unknown parameters may also be estimated from the Kalman filters by adding these parameters as auxiliary states. By this way, the non-linear characteristics of these parameters can be obtained without any need for excess measurement devices. For example, pump leakage flow coefficients are important parameters affecting the system dynamic and static behavior. To find these coefficients for variable drive speed a flow meter is required. If such a device is not available as in in this study, these coefficients can be estimated at different drive speeds with the help of a Kalman filter.

In Chapter 3, the operation in 4-quadrants is explained, it is said that the pumps are able to operate as a hydraulic motor. In the pump controlled system while operating in motor mode the energy transmitted from the system through the hydraulic pumps to the servomotor drives are dissipated as heat energy on the servomotor resistances. To increase the energy efficiency of the system, an energy storage element like a hydraulic accumulator could be added to the system.

Different from the valve controlled system, in pump controlled systems, pumps are not positioned next to the hydraulic actuator, they are mounted directly on the power source. This arrangement results in long transmission lines, decreasing the dynamic performance of the system. In the modeling section of the thesis study, the transmission line volumes are lumped into the hydraulic cylinder volumes, and the lines are assumed to be lossless. Modeling the lines as conductive elements and neglecting the resistance is a valid assumption especially when the lines are short. However when long transmission lines are required as in the pump controlled case, their resistances may affect the system dynamics. As a future work in line dynamics, the pressure loss in the lines may be added to the system dynamic equations, and the effect of the transmission lines on the system performance may be investigated in more detail.

In Chapter 3 in modeling section, it is explained that for high excitation frequencies, the dynamic pressure changes of the hydraulic cylinder chambers become linearly dependent. The state feedback controllers are designed, by using this property; however the cylinder chamber pressures are measured and filtered through Kalman filter. As a future work, the state feedback control algorithm for the position control of the hydraulic cylinder may be applied with reduced number of transducers.

REFERENCES

1. Burrow, C.R., "Fluid Power Systems - Some Research Issues", Proceedings of the Institution of Mechanical Engineers, Vol. 214, Part C, pp. 203-220, 2000.
2. Edge, K.A., "The control of fluid power systems-responding to the challenges", Proceedings of the Institution of Mechanical Engineers, Vol. 211, Issue 1, pp. 91-110, 1997.
3. Habibi, S., Goldenberg A., "Design of a New High-Performance Electrohydraulic Actuator", IEEE/ASME Transactions on Mechatronics, Vol. 5, Issue 2, pp. 158-164, 2000.
4. Sepasi, M., "Fault Monitoring in Hydraulic Systems using Unscented Kalman Filter", M.Sc. Thesis, The University of British Columbia, Mechanical Engineering Department, Nov. 2007.
5. Yao, D., DeBoer, C., "Energy-Saving Adaptive Robust Motion Control of Single-Rod Hydraulic Cylinders with Programmable Valves", Proceedings of the American Control Conference, Anchorage, AK, USA, pp. 4819-4824, May 2002.
6. Çalışkan, H., Balkan, T., Platin, B.E., "Hydraulic Position Control System with Variable Speed Pump", ASME Dynamic Systems and Control Conference and Bath/ASME Symposium on Fluid Power & Motion Control, Hollywood, CA, USA, Oct. 2009.
7. Rahmfeld, R., Ivantysynova, M., "Displacement Controlled Linear Actuator with Differential Cylinder - A Way to Save Primary Energy in Mobile Machines", 5^{th} International Conference on Fluid Power Transmission and Control, Hangzhou, China, pp. 316-322, 2001.

8. Manasek, R., "Simulation of an Electrohydraulic Load-Sensing System with AC Motor and Frequency Changer", Proc. of 1st FPNI-PhD Symp., Hamburg, Germany, pp. 311-324, 2000.

9. Lovrec, D., Kastrevc, M., Ulaga, S., "Electro-Hydraulic Load Sensing with Speed-Controlled Hydraulic Supply System on Forming Machines", International Journal Advanced Manufacturing Technology, Vol. 41, pp. 1066-1075, 2008.

10. Yuan, Q., Lew, J.Y., "Modeling and Control of Two Stage Twin Spool Servo-Valve for Energy-Saving", Proceedings of the American Control Conference, Portland, OR, USA, Vol. 6, pp. 4363-2368, Jun. 2005.

11. Blackburn, J.F., Reethof, G., and Shearer, J.L., Fluid Power Control, 1st Ed., MIT Press and John Wiley & Sons Inc., New York & London, 1960.

12. Cho, S.H., Racklebe, S., Helduser, S., "Position Tracking Control of a Clamp-Cylinder For Energy-Saving Injection Moulding Machines with Electric-Hydrostatic Drives", Proceedings of the Institution of Mechanical Engineers, Part 1, Journal of Systems and Control Engineering, Vol. 223, Number 4, pp. 479-491, 2009.

13. INNAS. Hydraulic Transformers, http://www.innas.com/IHT.html, 2009-Last accessed on 19.08.2009.

14. Heybroek, K., "Saving Energy in Construction Machinery Using Displacement Control Hydraulics - Concept Realization and Validation", M.Sc. Thesis, Linköping University, Mechanical Engineering Department, Jun. 2008.

15. Hewett, A.J., Hydraulic Circuit Flow Control, US, Patent No 5,329,767, 1994

16. Ahn, K.K., Chau, N.H.T., "Design of a Robust Force Controller For The New Mini Motion Package Using Quantitative Feedback Theory", Journal of Mechatronics, Vol. 17, pp. 542-550, 2007.

17. Helduser, S., "Electric–Hydrostatic Drive - An Innovative Energy-Saving Power And Motion Control System", Proceedings of the Institution of Mechanical Engineers, Vol. 213, pp. 427-437, 1999.

18. Long, Q., "Differential Cylinder Servo System Based on Speed Variable Pump and Sum Pressure Control Principle", 5th International Conference on Fluid Power, Hangzhou, China, pp. 69-73, 2001.

19. Neubert, T., "Untersuchungen von drehzahlveranderbaren Pumpen", Doktoringenieur angenommene Dissertation, Technishen Universitat Dresden, Fakultat Maschinenwesen, Germany, 2001.

20. Long, Q., Neubert, T., Helduser, S., "Principle to Closed Loop Control Differential Cylinder with Double Speed Variable Pumps and Single Loop Control Signal", Chinese Journal of Mechanical Engineering, Vol. 17, No. 1, pp. 85-88, 2004.

21. Çalışkan H., Balkan, T., Platin, B.E., Demirer, S. "Değişken Devirli Pompa ile Servo Hidrolik Konum Kontrolu", Proc. of V. National Hydraulic and Pneumatics Congress, İzmir, Turkey, pp. 359-375, 2008; also published in Mühendis ve Makina, Vol.50, No. 587, pp. 1-12.

22. Merritt, H.E., Hydraulic Control Systems, John Wiley & Sons Inc., New York, London, Sydney, 1967.

23. Shang, T., "Improving Performance of an Energy Efficient Hydraulic Circuit", M.Sc. Thesis, University of Saskatchewan, Mechanical Engineering Department, 2004.

24. Eriksson, B., "Control Strategy for Energy Efficient Fluid Power Actuators Utilizing Individual Metering", M.Sc. Thesis, Linköping University, Mechanical Engineering Department, 2007.

25. Sampson, E.B., "Fuzzy Control of the Electrohydraulic Actuator", M.Sc. Thesis, University of Saskatchewan, Mechanical Engineering Department, May 2005.

26. Johnson, J.L., "Summarizing Two Pump Control", Hydraulics & Pneumatics, pp. 22-25, Jun. 2007.

27. Rexroth Bosch Group, "Servo solenoid valves with electrical feedback Type 4WRPH6", RE 29028/01.05.

28. Watton, J., Fluid Power Systems Modeling, Simulation, Analog and Microcomputer Control, Prentice Hall Inernational (UK) Ltd., Hempstead, 1989.

29. Ogata, K., Modern Control Engineering, 4th Ed., Prentice Hall, 2002.

30. Welch, G., Bishop, G., "An Introduction to the Kalman Filter", University of North Carolina at Chapel Hill, TR 95-041, Jul. 2006.

31. Simon, D., "Kalman Filtering", Embedded Systems Programming, pp. 72-79, Jun. 2001.

32. Julier S. J., Uhlman, J.K., "A New Extension of the Kalman Filter to Nonlinear Systems", Proc. SPIE, Vol. 3068, pp. 182-193, Signal Processing, Sensor Fusion, and Target Recognition VI, 1997.

33. Dean, G.C., "An Introduction to Kalman Filters", Measurement and Control, Vol. 19, pp. 69-73, Mar. 1986.

34. Grewal, M.S., Andrews, P.A., Kalman Filtering Theory and Practice Using MATLAB, 2nd Ed., John Wiley & Sons, Hoboken, NJ, USA, 2001.

35. Wang, J.J., Ding, J, Wang, J., "Improving Adaptive Kalman Filter in GPS/SDINS Integration with Neural Network", Proceedings of the 20th International Technical Meeting of the Satellite Division of the Institute of Navigation, Fort Worth, Texas, USA, pp. 571-578, 2007.

APPENDIX A

TRANSFER FUNCTION DERIVATION FOR PUMP CONTROLLED SYSTEM

To be uniform and perceptible all the dynamic equations that define the pump controlled system are repeated below.

The flow continuity equations of the pump/motor unit,

For the outlet (A side) port of Pump 2,

$$q_{p2A} = D_P n_2 - C_i \left(p_A - p_B \right) - C_{ea} p_A \tag{7.1}$$

For the inlet port (B side) port of Pump 2,

$$q_{p2B} = D_P n_2 - C_i \left(p_A - p_B \right) + C_{eb} p_B \tag{7.2}$$

For the outlet (A side) port of Pump 1,

$$q_{p1A} = D_P n_1 - C_i p_A - C_{ea} p_A \tag{7.3}$$

The flow continuity equations of the hydraulic cylinder:

$$q_A = A_A \dot{x} + \frac{V_A}{E} \cdot \frac{dp_A}{dt} \tag{7.4}$$

$$q_B = A_B \dot{x} - \frac{V_B}{E} \cdot \frac{dp_B}{dt} \tag{7.5}$$

Load Pressure:

$$p_L = \gamma p_A - p_B \tag{7.6}$$

Structural equation of the load:

$$p_L A_B = m\ddot{x} + b\dot{x} \tag{7.7}$$

Continuity equations:

$$q_{B\_ss} = q_{p2B} \tag{1.39 (7.8)}$$

$$q_{A\_ss} = q_{p1A} + q_{p2A} \tag{1.41 (7.9)}$$

Substituting Eq. (7.2) and Eq. (7.5) into Eq. (7.8), and Eq.(7.1), Eq.(7.3) and Eq.(7.4) into Eq.(7.9),

$$A_B \dot{x} - \frac{V_B}{E} \cdot \frac{dp_B}{dt} = D_P n_2 - C_i \left(p_A - p_B \right) + C_{eb} p_B \tag{7.10}$$

$$A_A \dot{x} + \frac{V_A}{E} \cdot \frac{dp_A}{dt} = \left[D_P n_1 - \left(C_i + C_{ea} \right) p_A \right] + \left[D_P n_2 - C_i \left(p_A - p_B \right) - C_{ea} p_A \right] \tag{7.11}$$

and making the substitution defined below

$$n_1 = \left(\gamma - 1 \right) n_2 \tag{7.12}$$

$$A_A = \gamma A_B \tag{7.13}$$

$$V_A = \alpha V_B \tag{7.14}$$

the continuity equations can be rewritten as

$$\frac{\alpha V_B}{E} \cdot \frac{dp_A}{dt} = \gamma D_P n_2 + C_i p_B - \left(2C_i + 2C_{ea} \right) p_A - \gamma A_B \dot{x} \tag{7.15}$$

$$-\frac{V_B}{E} \cdot \frac{dp_B}{dt} = D_P n_2 - C_i p_A + \left(C_i + C_{eb} \right) p_B - A_B \dot{x} \tag{7.16}$$

Taking the Laplace transformation, with zero initial conditions gives

$$\gamma D_P N_2 \left(s \right) - \gamma A_B s X \left(s \right) = \left(\frac{\alpha V_B}{E} s + 2C_i + 2C_{ea} \right) P_A \left(s \right) - C_i P_B \left(s \right) \tag{7.17}$$

$$D_P N_2 \left(s \right) - A_B s X \left(s \right) = C_i P_A \left(s \right) - \left(\frac{V_B}{E} s + C_i + C_{eb} \right) P_B \left(s \right) \tag{7.18}$$

$$\left(\gamma P_A \left(s \right) - P_B \left(s \right) \right) = P_L \left(s \right) A_B = \left(m s^2 + b s \right) X \left(s \right) \tag{7.19}$$

From the load pressure equation (Eq.6), the chamber pressures can be written as

$$P_B(s) = \gamma P_A(s) - P_L(s) \tag{7.20}$$

$$P_A(s) = \frac{P_L(s) + P_B(s)}{\gamma} \tag{7.21}$$

Inserting Eq. (7.20) into Eq.(7.17), and inserting the Eq.(7.21) into Eq.(7.18) give

$$\gamma\left(D_P N_2(s) - A_B sX(s)\right) = \left(\frac{\alpha V_B}{E}s + (2-\gamma)C_i + 2C_{ea}\right)P_A(s) + C_i P_L(s) \tag{7.22}$$

$$D_P N_2(s) - A_B sX(s) = \frac{C_i}{\gamma}P_L(s) - \left(\frac{V_B}{E}s + \frac{\gamma-1}{\gamma}C_i + C_{eb}\right)P_B(s) \tag{7.23}$$

Multiplying Eq. (7.22) with $\gamma\left(\frac{V_B}{E}s + \frac{\gamma-1}{\gamma}C_i + C_{eb}\right)$ and multiplying Eq. (7.23) with $\left(\frac{\alpha V_B}{E}s + (2-\gamma)C_i + 2C_{ea}\right)$, then summing these two equations give

$$\begin{aligned}
&\left[\gamma^2\left(\frac{V_B}{E}s + \frac{\gamma-1}{\gamma}C_i + C_{eb}\right) + \left(\frac{\alpha V_B}{E}s + (2-\gamma)C_i + 2C_{ea}\right)\right]\left(D_P N_2(s) - A_B sX(s)\right) \\
&\quad = \left[\gamma^2\left(\frac{V_B}{E}s + \frac{\gamma-1}{\gamma}C_i + C_{eb}\right) + \left(\frac{\alpha V_B}{E}s + (2-\gamma)C_i + 2C_{ea}\right)\right]\frac{C_i}{\gamma}P_L(s) \\
&\quad + \left(\frac{V_B}{E}s + \frac{\gamma-1}{\gamma}C_i + C_{eb}\right)\left(\frac{\alpha V_B}{E}s + (2-\gamma)C_i + 2C_{ea}\right)P_L(s)
\end{aligned} \tag{7.24}$$

After rearranging, it becomes

$$\begin{aligned}
&\left[\left(\gamma^2+\alpha\right)\frac{V_B}{E}s + \left(\gamma^2 - 2\gamma + 2\right)C_i + \gamma^2 C_{eb} + 2C_{ea}\right]\left(D_P N_2(s) - A_B sX(s)\right) \\
&\quad = \left(\left(\gamma^2+\alpha\right)C_i\frac{V_B}{E}s + \left(\gamma^2 - 2\gamma + 2\right)C_i^2 + \gamma^2 C_{eb}C_i + 2C_{ea}C_i\right)\frac{P_L(s)}{\gamma} \\
&\quad + \left[\begin{aligned}&\frac{\alpha {V_B}^2}{E^2}s^2 + \left(\frac{2\gamma - \gamma^2 + \gamma\alpha - \alpha}{\gamma}C_i + 2C_{ea} + \alpha C_{eb}\right)\frac{V_B}{E}s \\ &\quad + \frac{\gamma-1}{\gamma}(2-\gamma)C_i^2 + 2\frac{\gamma-1}{\gamma}C_iC_{ea} + (2-\gamma)C_iC_{eb} + 2C_{ea}C_{eb}\end{aligned}\right]P_L(s)
\end{aligned} \tag{7.25}$$

Rearranging again, one obtains

$$\begin{aligned}&\left[\left(\gamma^2+\alpha\right)\frac{V_B}{E}s+\left(\gamma^2-2\gamma+2\right)C_i+\gamma^2C_{eb}+2C_{ea}\right]\left(D_PN_2\left(s\right)-A_BsX\left(s\right)\right)\\&=\left[\frac{\alpha V_B{}^2}{E^2}s^2+\left(\left(2+\alpha\right)C_i+2C_{ea}+\alpha C_{eb}\right)\frac{V_B}{E}s+C_i^2+2\left(C_{ea}+C_{eb}\right)C_i+2C_{ea}C_{eb}\right]P_L\left(s\right)\end{aligned} \tag{7.26}$$

Inserting Eq. (7.26) into Eq.(7.19) gives

$$\begin{aligned}&\left[\left(\gamma^2+\alpha\right)\frac{V_B}{E}s+\left(\gamma^2-2\gamma+2\right)C_i+\gamma^2C_{eb}+2C_{ea}\right]\left(D_PN_2\left(s\right)-A_BsX\left(s\right)\right)\\&\quad=\left[\begin{array}{l}\dfrac{\alpha V_B{}^2}{E^2}s^2+\left(\left(2+\alpha\right)C_i+2C_{ea}+\alpha C_{eb}\right)\dfrac{V_B}{E}s\\ \qquad\qquad+\left(C_i^2+2\left(C_{ea}+C_{eb}\right)C_i+2C_{ea}C_{eb}\right)\end{array}\right]\frac{ms^2+bs}{A_B}X\left(s\right)\end{aligned} \tag{7.27}$$

Then the transfer function between the input pump 2 speed and the output hydraulic actuator velocity becomes,

$$\frac{V\left(s\right)}{N_2\left(s\right)}=\frac{a_1s+a_2}{b_1s^3+b_2s^2+b_3s+b_4} \tag{7.28}$$

where

$$\begin{aligned}a_1&=\left(\gamma^2+\alpha\right)\frac{V_B}{E}D_PA_B\\a_2&=\left(\left(\gamma^2-2\gamma+2\right)C_i+\gamma^2C_{eb}+2C_{ea}\right)D_PA_B\\b_1&=m\frac{\alpha V_B{}^2}{E^2}\\b_2&=m\left(\left(2+\alpha\right)C_i+2C_{ea}+\alpha C_{eb}\right)\frac{V_B}{E}+b\frac{\alpha V_B{}^2}{E^2}\\b_3&=m\left(C_i^2+2\left(C_{ea}+C_{eb}\right)C_i+2C_{ea}C_{eb}\right)+b\left(\left(2+\alpha\right)C_i+2C_{ea}+\alpha C_{eb}\right)\frac{V_B}{E}+\left(\gamma^2+\alpha\right)\frac{V_B}{E}A_B{}^2\\b_4&=b\left(C_i^2+2\left(C_{ea}+C_{eb}\right)C_i+2C_{ea}C_{eb}\right)+\left(\left(\gamma^2-2\gamma+2\right)C_i+\gamma^2C_{eb}+2C_{ea}\right)A_B{}^2\end{aligned}$$

Reduced Order Transfer Function Derivation is explained below.

Multiplying Eq.(7.15) with the area ratio γ, and multiplying Eq.(7.16) with the volume ratio α.

$$\gamma\left[\frac{\alpha V_B}{E}\cdot\frac{dp_A}{dt}\right]=\gamma\left[\gamma D_P n_2 + C_i p_B - \left(2C_i + 2C_{ea}\right)p_A - \gamma A_B \dot{x}\right] \tag{7.29}$$

$$-\alpha\left[\frac{V_B}{E}\cdot\frac{dp_B}{dt}\right]=\alpha\left[D_P n_2 - C_i p_A + \left(C_i + C_{eb}\right)p_B - A_B \dot{x}\right] \tag{7.30}$$

and summing the resulting expressions give the rate of the change of the load pressure $\dot{p}_L$ as

$$\begin{aligned}\frac{\alpha V_B}{E}\dot{p}_L &= \left(\gamma^2+\alpha\right)D_P n_2 - \left(\left(2\gamma+\alpha\right)C_i + 2\gamma C_{ea}\right)p_A \\ &\quad + \left(\left(\alpha+\gamma\right)C_i + \alpha C_{eb}\right)p_B - \left(\gamma^2+\alpha\right)A_B\dot{x}\end{aligned} \tag{7.31}$$

Assuming that the dynamic chamber pressure changes p_A and p_B are linearly dependent and defined by

$$p_A = -\varphi p_B \tag{7.32}$$

and through Eq.(7.6) and Eq.(7.32) writing the dynamic chamber pressure changes p_A and p_B in terms of load pressure p_L as

$$p_A = \frac{\varphi p_L}{\gamma\varphi + 1} \tag{7.33}$$

$$p_B = \frac{-p_L}{\gamma\varphi + 1} \tag{7.34}$$

and substituting Eq.(7.33) and Eq.(7.34) into the Eq.(7.31) give

$$\begin{aligned}\frac{\alpha V_B}{E}\dot{p}_L &= \left(\gamma^2+\alpha\right)D_P n_2 - \left(\left(2\gamma+\alpha\right)C_i + 2\gamma C_{ea}\right)\frac{\varphi p_L}{\gamma\varphi+1} \\ &\quad - \left(\left(\alpha+\gamma\right)C_i + \alpha C_{eb}\right)\frac{p_L}{\gamma\varphi+1} - \left(\gamma^2+\alpha\right)A_B\dot{x}\end{aligned} \tag{7.35}$$

Rearranging and taking the Laplace transform assuming zero initial conditions give

$$\left(\frac{\alpha V_B}{E}s+\frac{\left(\varphi\left(2\gamma+\alpha\right)+\left(\alpha+\gamma\right)\right)C_i+\varphi 2\gamma C_{ea}+\alpha C_{eb}}{\gamma\varphi+1}\right)P_L\left(s\right)$$
$$=\left(\gamma^2+\alpha\right)D_P N_2\left(s\right)-\left(\gamma^2+\alpha\right)A_B sX\left(s\right) \tag{7.36}$$

Defining

$$C_{Leak}=\frac{\left(\varphi\left(2\gamma+\alpha\right)+\alpha+\gamma\right)C_i+\varphi 2\gamma C_{ea}+\alpha C_{eb}}{\gamma\varphi+1} \tag{7.37}$$

and insert the Eq.(7.19) into Eq.(7.36) give

$$\left(\frac{\alpha V_B}{E}s+C_{Leak}\right)\frac{ms+b}{A_B}sX\left(s\right)+\left(\gamma^2+\alpha\right)A_B sX\left(s\right)=\left(\gamma^2+\alpha\right)D_P N_2\left(s\right) \tag{7.38}$$

Then the reduced order transfer function between the input pump 2 speed and the output hydraulic velocity is obtained as

$$\frac{V\left(s\right)}{N_2\left(s\right)}=\frac{\left(\gamma^2+\alpha\right)D_P A_B}{m\frac{\alpha V_B}{E}s^2+\left(b\frac{\alpha V_B}{E}+mC_{Leak}\right)s+bC_{Leak}+\left(\gamma^2+\alpha\right)A_B{}^2} \tag{7.39}$$

APPENDIX B

TRANSFER FUNCTION DERIVATION FOR VALVE CONTROLLED SYSTEM

To be uniform and perceptible all the dynamic equations that define the pump controlled system are repeated below. Because the procedure is the same, the transfer function is derived only for the extension of the hydraulic actuator.

The linearized valve flow characteristic equations:

$$q_2 = K_v u\sqrt{p_S - p_A} = K_{u2\_ext}u - K_{p2\_ext}\,p_A \tag{7.1}$$

$$q_4 = K_v u\sqrt{p_B} = K_{u4\_ext}u + K_{p4\_ext}\,p_B \tag{7.2}$$

The flow continuity equations of the hydraulic cylinder:

$$q_A = A_A\dot{x} + \frac{V_A}{E}\cdot\frac{dp_A}{dt} \tag{7.3}$$

$$q_B = A_B\dot{x} - \frac{V_B}{E}\cdot\frac{dp_B}{dt} \tag{7.4}$$

Load Pressure:

$$p_L = \gamma\, p_A - p_B \tag{7.5}$$

Structural equation of the load:

$$p_L A_B = m\ddot{x} + b\dot{x} \tag{7.6}$$

Continuity equations:

$$q_2 = q_A \tag{7.7}$$

$$q_4 = q_B \tag{7.8}$$

Substituting Eq. (7.1)and Eq. (7.3)into Eq. (7.7), and Eq. (7.2) and Eq. (7.4) into Eq. (7.8),

$$K_{u2\_ext}u - K_{p2\_ext}p_A = A_A\dot{x} + \frac{V_A}{E}\cdot\frac{dp_A}{dt} \tag{7.9}$$

$$K_{u4\_ext}u + K_{p4\_ext}p_B = A_B\dot{x} - \frac{V_B}{E}\cdot\frac{dp_B}{dt} \tag{7.10}$$

and making the substitution defined below

$$A_A = \gamma A_B \tag{7.11}$$

$$K_{u2\_ext} = \gamma K_{u4\_ext} \tag{7.12}$$

$$K_{p4\_ext} = \gamma K_{u2\_ext} \tag{7.13}$$

$$V_A = \alpha V_B \tag{7.14}$$

and rearranging Eq. (7.9) and Eq. (7.10)

$$\gamma K_{u4\_ext}u - \gamma A_B\dot{x} - K_{p2\_ext}p_A = \frac{\alpha V_B}{E}\cdot\frac{dp_A}{dt} \tag{7.15}$$

$$K_{u4\_ext}u - A_B\dot{x} + \gamma K_{p2\_ext}p_B = -\frac{V_B}{E}\cdot\frac{dp_B}{dt} \tag{7.16}$$

Taking the Laplace transform, and rearranging

$$\frac{\gamma K_{u4\_ext}}{K_{p2\_ext} + \frac{\alpha V_B}{E}s}u(s) - \frac{\gamma A_B}{K_{p2\_ext} + \frac{\alpha V_B}{E}s}sX(s) = P_A(s) \tag{7.17}$$

$$\frac{K_{u4\_ext}}{\gamma K_{p2\_ext} + \frac{V_B}{E}s}u(s) - \frac{A_B}{\gamma K_{p2\_ext} + \frac{V_B}{E}s}sX(s) = -P_B(s) \tag{7.18}$$

Multiplying the Eq. (7.17) by the area ratio γ and summing with the Eq. (7.18) give

$$\frac{\gamma^2 K_{u4\_ext}\left(\gamma K_{p2\_ext}+\frac{V_B}{E}s\right)+K_{u4\_ext}\left(K_{p2\_ext}+\frac{\alpha V_B}{E}s\right)}{\left(K_{p2\_ext}+\frac{\alpha V_B}{E}s\right)\left(\gamma K_{p2\_ext}+\frac{V_B}{E}s\right)}U(s)$$
$$-\frac{\gamma^2 A_B\left(\gamma K_{p2\_ext}+\frac{V_B}{E}s\right)+A_B\left(K_{p2\_ext}+\frac{\alpha V_B}{E}s\right)}{\left(K_{p2\_ext}+\frac{\alpha V_B}{E}s\right)\left(\gamma K_{p2\_ext}+\frac{V_B}{E}s\right)}sX(s)=\gamma P_A(s)-P_B(s) \tag{7.19}$$

Inserting Eq.(7.5) and Eq. (7.6) into Eq. (7.19) and rearranging give

$$\frac{\left(\gamma^3+1\right)K_{p2\_ext}+\left(\gamma^2+\alpha\right)\frac{V_B}{E}s}{\frac{\alpha V_B{}^2}{E^2}s^2+K_{p2\_ext}\frac{V_B}{E}(\gamma\alpha+1)s+\gamma K_{p2\_ext}{}^2}K_{u4\_ext}U(s)$$
$$-\frac{\left(\gamma^3+1\right)K_{p2\_ext}+\left(\gamma^2+\alpha\right)\frac{V_B}{E}s}{\frac{\alpha V_B{}^2}{E^2}s^2+K_{p2\_ext}\frac{V_B}{E}(\gamma\alpha+1)s+\gamma K_{p2\_ext}{}^2}A_B sX(s)=\frac{ms^2+bs}{A_B}X(s) \tag{7.20}$$

Arranging Eq. (7.20) again, the transfer function between the valve spool position and the hydraulic actuator velocity is given as

$$\frac{V(s)}{U(s)}=\frac{a_1 s+a_2}{b_1 s^3+b_2 s^2+b_3 s+b_4}$$

$$\begin{aligned}
a_1 &= K_{u4_ext}A_B\left(\gamma^2+\alpha\right)\frac{V_B}{E}\\
a_2 &= K_{u4_ext}A_B\left(\gamma^3+1\right)K_{p2_ext}\\
b_1 &= m\frac{\alpha V_B{}^2}{E^2}\\
b_2 &= mK_{p2_ext}\frac{V_B}{E}(\gamma\alpha+1)+b\frac{\alpha V_B{}^2}{E^2}\\
b_3 &= m\gamma K_{p2_ext}{}^2+bK_{p2_ext}\frac{V_B}{E}(\gamma\alpha+1)+\left(\gamma^2+\alpha\right)\frac{V_B}{E}A_B{}^2\\
b_4 &= b\gamma K_{p2_ext}{}^2+\left(\gamma^3+1\right)K_{p2_ext}A_B{}^2
\end{aligned} \tag{7.21}$$

Reduced Order Transfer Function Derivation for Valve Controlled System for Extension is explained below.

Multiplying Eq.(7.15) with the area ratio γ and multiplying Eq.(7.16) with the volume ratio α,

$$\gamma^2 K_{u4\_ext} u - \gamma^2 A_B \dot{x} - \gamma K_{p2\_ext} p_A = \frac{\alpha V_B}{E} \cdot \frac{\gamma dp_A}{dt} \tag{7.22}$$

$$\alpha K_{u4\_ext} u - \alpha A_B \dot{x} + \gamma\alpha K_{p2\_ext} p_B = -\frac{\alpha V_B}{E} \cdot \frac{dp_B}{dt} \tag{7.23}$$

and summing the resulting expressions give the rate of the change of the load pressure $\dot{p}_L$ as

$$\left(\gamma^2 + \alpha\right) K_{u4\_ext} u - \left(\gamma^2 + \alpha\right) A_B \dot{x} - \gamma K_{p2\_ext} p_A + \gamma\alpha K_{p2\_ext} p_B = \frac{\alpha V_B}{E} \cdot \dot{p}_L \tag{7.24}$$

Assuming that the dynamic chamber pressure changes p_A and p_B are linearly dependent and defined by

$$p_A = -\varphi p_B \tag{7.25}$$

and through Eq.(7.5) and Eq.(7.25) writing the dynamic chamber pressure changes p_A and p_B in terms of load pressure p_L as

$$p_A = \frac{\varphi p_L}{\gamma\varphi + 1} \tag{7.26}$$

$$p_B = \frac{-p_L}{\gamma\varphi + 1} \tag{7.27}$$

and substituting Eq.(7.26) and Eq.(7.27) into the Eq.(7.24) give

$$\left(\gamma^2 + \alpha\right) K_{u4\_ext} u - \left(\gamma^2 + \alpha\right) A_B \dot{x} - \frac{\varphi + \alpha}{\gamma\varphi + 1} \gamma K_{p2\_ext} p_L = \frac{\alpha V_B}{E} \cdot \dot{p}_L \tag{7.28}$$

Rearranging and taking the Laplace transform of above expression, assuming zero initial condition give

$$\left(\gamma^2 + \alpha\right) K_{u4\_ext} U(s) - \left(\gamma^2 + \alpha\right) A_B s X(s) = \left(\frac{\alpha V_B}{E} s + \frac{\varphi + \alpha}{\gamma\varphi + 1} \gamma K_{p2\_ext}\right) \cdot P_L(s) \tag{7.29}$$

Taking the Laplace transform of Eq.(7.6) and inserting into Eq. (7.29) give

$$
\begin{aligned}
&\left(\gamma^2+\alpha\right)K_{u4\_ext}A_B U(s)-\left(\gamma^2+\alpha\right)A_B{}^2 sX(s)= \\
&\qquad\qquad \left(\frac{\alpha V_B}{E}s+\frac{\varphi+\alpha}{\gamma\varphi+1}\gamma K_{p2\_ext}\right)\cdot\left(ms+b\right)sX(s)
\end{aligned} \tag{7.30}
$$

Simplifying the above expression, the transfer function between the valve spool position and hydraulic actuator is obtained as

$$
\frac{V(s)}{U(s)}=\frac{\left(\gamma^2+\alpha\right)K_{u4\_ext}A_B}{\frac{m\alpha V_B}{E}s^2+\left(m\frac{\varphi+\alpha}{\gamma\varphi+1}\gamma K_{p2\_ext}+\frac{b\alpha V_B}{E}\right)s+b\frac{\varphi+\alpha}{\gamma\varphi+1}\gamma K_{p2\_ext}+\left(\gamma^2+\alpha\right)A_B{}^2} \tag{7.31}
$$

APPENDIX C

MATLAB FILES

UNSCENTED KALMAN FILTER ALGORITHM

```
function [xEst_k1,PEst_k1,yOut]=UKF(xEst,PEst,U,z,Q,R,Ts,Param_Mod)
% This function performs one complete step of the unscented Kalman
filter.
% INPUTS
%   - xEst            : state mean estimate at time k-1
%   - PEst            : state covariance at time k-1
%   - U               : control input (spool position) at time k-1
%   - z               : measurement vector at time k
%   - Q               : process noise covariance at time k-1
%   - R               : measurement noise covariance at timek
%   - Ts              : time step
%   - Param_Mod       : vector containing model paramter
% OUTPUTS  :
%   - xEst_k1         : updated estimate of state mean at time k+1
%   - PEst_k1         : updated state covariance at time k+1
%   - yOut            : Output States
% SUB FUNCTIONS:
%   - ffunc           : process model function
%   - hfunc           : measurement model function
%   - CalcSigmaPoints : sigma point calculation function
%   - StateMatrix     : non-linear state matrix

% The dimension of the vectors
states       = 4; % 1 number of rows, 2 number of columns
observations = 3;
vNoise       = 4;
wNoise       = 3;
noises       = vNoise+wNoise;

% Augment the state vector with the noise vectors.
N=[Q zeros(vNoise,wNoise); zeros(wNoise,vNoise) R];
PQ=[PEst zeros(states,noises);zeros(noises,states) N];
xQ=[xEst;zeros(noises,1)];

%   TIME UPDATE EQUATIONS
% Calculate the sigma points and there corresponding weights using
the Scaled Unscented
% Transformation
[xSigmaPts, nsp] = CalcSigmaPoints(xQ, PQ);
nsp=23;

% Project the sigma points and their means
```

```
xPredSigmaPts =
ffunc(xSigmaPts(1:states,:),repmat(U(:),1,nsp),xSigmaPts(states+1:s
tates+vNoise,:),Ts,Param_Mod); %evaluate the function ffunc
zPredSigmaPts =
hfunc(xPredSigmaPts,xSigmaPts(states+vNoise+1:states+noises,:));

% Calculate the mean
xPred = sum((xPredSigmaPts(:,2:nsp) -
repmat(xPredSigmaPts(:,1),1,nsp-1)),2);
zPred = sum((zPredSigmaPts(:,2:nsp) -
repmat(zPredSigmaPts(:,1),1,nsp-1)),2);
xPred=xPred+xPredSigmaPts(:,1);
zPred=zPred+zPredSigmaPts(:,1);

% Work out the covariances and the cross correlations. Note that
% the weight on the 0th point is different from the mean
% calculation due to the scaled unscented algorithm.

exSigmaPt = xPredSigmaPts(:,1)-xPred;
ezSigmaPt = zPredSigmaPts(:,1)-zPred;

PPred   = exSigmaPt*exSigmaPt';
PxzPred = exSigmaPt*ezSigmaPt';
S       = ezSigmaPt*ezSigmaPt';

exSigmaPt1 = xPredSigmaPts(:,2:nsp) - repmat(xPred,1,nsp-1);
ezSigmaPt1 = zPredSigmaPts(:,2:nsp) - repmat(zPred,1,nsp-1);
PPred     = PPred + exSigmaPt1 * exSigmaPt1';
S         = S + ezSigmaPt1 * ezSigmaPt1';
PxzPred   = PxzPred + exSigmaPt1 * ezSigmaPt1';


% MEASUREMENT UPDATE
% Calculate Kalman gain
K  = PxzPred / S;
% Calculate Innovation
inovation = z - zPred;
% Update mean
xEst_k1 = xPred + K*inovation;
%   Output States
C=[1 0 0 0;0 1 0 0; 0 0 1 0; 0 0 0 1];
yOut=C*xEst_k1;
% Update covariance
PEst_k1 = PPred - K*S*K';

function [xPts,nPts] = CalcSigmaPoints(x,P)
% Inputs:
%        x            mean
%        P            covariance
% Outputs:
%        xPts    The sigma points
%        nPts    The number of points

% Number of sigma points and scaling terms
n    = size(x(:),1);
nPts = 2*n+1;

% Allocate space
```

```
xPts=zeros(n,nPts);

% Calculate matrix square root of weighted covariance matrix
Psqrtm=(chol(n*P))';
% Array of the sigma points
xPts=[zeros(size(P,1),1) -Psqrtm Psqrtm];
% Add mean back in
xPts = xPts + repmat(x,1,nPts);


function xout = ffunc(x,u,v,Ts,Param_Mod)
% This function performs Runge Kutta Integration at 4 times in
% each time step
k1=StateMatrix(x,u,Param_Mod);
k2=StateMatrix(x+0.5*k1*Ts,u,Param_Mod);
k3=StateMatrix(x+0.5*k2*Ts,u,Param_Mod);
k4=StateMatrix(x+k3*Ts,u,Param_Mod);
x_delta=1/6.*(k1+2*k2+2*k3+k4)*Ts;
%   Calculate New State
xout=x+x_delta+v;


function x_dot=StateMatrix(x,u,Prm)
%%   Define the system Parameters
%   Number of States
n=size(x,1);
%   Number of Sigma Points
nSig=size(x,2);
%   Define the parameters
% Parameters=[M,Aa,Ab,Modulus,Kv,xin,xmax,Ps,Vo,b];
%   Mass
M=Prm(1);
%   Piston A and B Side Area
Aa=Prm(2);
Ab=Prm(3);
%   Bulk Modulus
Modulus=Prm(4);
%   Valve Constant
Kv=Prm(5);
%   Minimum and the maximum stroke of the cylinder
xin=repmat(Prm(6),1,nSig);
xmax=repmat(Prm(7),1,nSig);
%   Supply Pressure
Ps=repmat(Prm(8),1,nSig);
%   Initial Volume
Va=repmat(Prm(9),1,nSig);
Vb=repmat(Prm(10),1,nSig);
%   Damping Ratio
b=Prm(11);

%%  State Matrix
x_dot=zeros(n,nSig);  %   Since output must be column vector
x_dot(1,:)=x(2,:);
x_dot(2,:)=1/M*(Aa*x(3,:)-Ab*x(4,:)-b*x(2,:));
if (u(1,1)>=0)  %As all the other control signalas are the same
    x_dot(3,:)=Modulus./(Va+Aa*(x(1,:))).*(Kv*u(1,:).*sqrt(abs(Ps-
x(3,:)))-Aa*x(2,:));
```

```
    x_dot(4,:)=Modulus./(Vb+Ab*(xmax-x(1,:))).*(-
Kv*u(1,:).*sqrt(abs(x(4,:)))+Ab*x(2,:));
else

x_dot(3,:)=Modulus./(Va+Aa*x(1,:)).*(Kv*u(1,:).*sqrt(abs(x(3,:)))-
Aa*x(2,:));
    x_dot(4,:)=Modulus./(Vb+Ab*(xmax-x(1,:))).*(-
Kv*u(1,:).*sqrt(abs(Ps-x(4,:)))+Ab*x(2,:));
end


function y = hfunc(x,n)
% Measurement model for UKF
%  INPUT
%         x    :  state vetor at time k
%         n    :  measurement noise vector at time k
%  OUTPUT
%         y    :  state observation vector at time k
H=[1 0 0 0; 0 0 1 0; 0 0 0 1];
y = H*x+n;
```

CALCULATION OF THE FFT OF THE MEASURED DATA

```
function [x,y_mag,y_phase]= DrawBode(dat)
%%   Load the mat files and read the data
load(dat);
%   Read the input from the Position Scope
FlPos(:,1)=FiltPos;   %   Filtered position output
RfPos(:,1)=RefPos;   %   Reference Position
%%
fs=1/Ts; %   Sampling Rate [Hz]
tstart=T_step; %   Start Time [s]
tend=Tsim;   %   End Time    [s]
FreqMin=fr_start;    %   Minimum Frequency [Hz]
FreqMax=fr_stop;  %   Maximum Frequncy    [Hz]
Freq_Inc=.01;   %   Frequency Increment [Hz]
%%
%   Take the necessary Data
for i=1:1
    out(:,i)=FlPos(tstart*fs:tend*fs,i);
%     in(:,i)=input(tstart*fs:tend*fs,i);
    %   Remove the 'linear' trend of the output
    out(:,i)=detrend(out(:,i));
    %   Calculate the FFT of the input and the Output
%     in_fft(:,i)=fft(in(:,i));
    out_fft(:,i)=fft(out(:,i));
end
%   Input sabit
in(:,1)=RfPos(tstart*fs:tend*fs,1);
in_fft(:,1)=fft(in(:,1));

%   Take the Avarage FFT
for i=1:length(out_fft)
```

```
    out_fft_mean(i,1)=mean(out_fft(i,:));
%      in_fft_mean(i)=mean(in_fft(i,:));
end
%   Time Array
t=0:1/fs:(tend-tstart);
%   Frequency Array
FreqArray=0:fs/(length(in_fft)-1):fs;
%%   Bode Plot
Mag=20*log10(abs(out_fft_mean)./abs(in_fft));
PhsAngle=(-angle(in_fft)+angle(out_fft_mean))*180/pi;
f=FreqMin;
j=1;
for i=1:(length(Mag)-1)
    %
    if PhsAngle(i+1,1)-PhsAngle(i,1)>200
        PhsAngle(i+1,1)=PhsAngle(i+1,1)-360;
    end
    if PhsAngle(i+1,1)-PhsAngle(i,1)<-200
         PhsAngle(i+1,1)=PhsAngle(i+1,1)+360;
    end
    %
    if FreqArray(i)<FreqMax
        if FreqArray(i)>f
            x(j)=FreqArray(i-1);
            y_mag(j)=Mag(i-1);
            y_phase(j)=PhsAngle(i-1);
            f=f+Freq_Inc;
            j=j+1;
        end
    end
end
```

APPENDIX D

DRIVERS AND DAQ CARD CONNECTIONS

Servo Proportional Valve Driver Connections

0 V	b2	Power Zero	BOSCH SERVO-PROPORTIONAL VALVE DRIVER	Supply 24V	z2	24 V
	b4				z4	
SLND-2	b6	Solenoid output			z6	
SLND-1	b8	Solenoid output			z8	
	b10				z10	
0 V	b12	Control Zero			z12	
	b14				z14	
	b16			Enable 10 V	z16	Switch
	b18				z18	
DAQ-23	b20	Signal Input Ref		Signal Input	z20	DAQ-20
DAQ-15	b22	LVDT Feedback Signal			z22	
DAQ-1	b24	LVDT Feedback Ref.			z24	
	b26				z26	
	b28			Ground	z28	0 V
LVDT-1	b30	LVDT Supply -15 V		LVDT Supply +15 V	z30	LVDT-3
	b32			Supply of pot. 10 V	z32	Switch

Connect power zero b2 and control zero b12, b14 or z28 separately to central ground (neutral point)

Valve Controlled System NI 6025E Data Acquisition Card Connections

Connection	Signal	Pin	Pin	Signal
All Transducers	AIGND	1	51	PC7
	AIGND	2	52	GND
	ACH0	3	53	PC6
	ACH8	4	54	GND
Press. Trns. A	ACH1	5	55	PC5
	ACH9	6	56	GND
Press. Trns. B	ACH2	7	57	PC4
	ACH10	8	58	GND
Press. Trns. S	ACH3	9	59	PC3
	ACH11	10	60	GND
	ACH4	11	61	PC2
	ACH12	12	62	GND
	ACH5	13	63	PC1
	ACH13	14	64	GND
Valve Sp. Pos	ACH6	15	65	PC0
	ACH14	16	66	GND
	ACH7	17	67	PB7
Position Trns	ACH15	18	68	GND
	AISENSE	19	69	PB6
Valve Sp. z20	DAC0OUT	20	70	GND
Servo Mt. 1-2	DAC1OUT	21	71	PB5
	RESERVED	22	72	GND
Srv. Mts. Gnd Valve Gnd z20	AOGND	23	73	PB4
	DGND	24	74	GND
	DIO0	25	75	PB3
	DIO4	26	76	GND
	DIO1	27	77	PB2
	DIO5	28	78	GND
	DIO2	29	79	PB1
	DIO6	30	80	GND
	DIO3	31	81	PB0
	DIO7	32	82	GND
	DGND	33	83	PA7
	+5 V	34	84	GND
	+5 V	35	85	PA6
	SCANCLK	36	86	GND
	EXTSTROBE*	37	87	PA5
	PFI0/TRIG1	38	88	GND
	PFI1/TRIG2	39	89	PA4
	PFI2/CONVERT*	40	90	GND
	PFI3/GPCTR1_SOURCE	41	91	PA3
	PFI4/GPCTR1_GATE	42	92	GND
	GPCTR1_OUT	43	93	PA2
	PFI5/UPDATE*	44	94	GND
	PFI6/WFTRIG	45	95	PA1
	PFI7/STARTSCAN	46	96	GND
	PFI8/GPCTR0_SOURCE	47	97	PA0
	PFI9/GPCTR0_GATE	48	98	GND
	GPCTR0_OUT	49	99	+5 V
	FREQ_OUT	50	100	GND

Pump Controlled System NI 6025E Data Acquisition Card Connections